Transcriptional regulation of the Mouse PAC1 receptor gene

By

Walid El Bestawy

Thesis submitted for the Degree of Doctor of Philosophy

Strathclyde Institute of Pharmacy and Biomedical Sciences

University of Strathclyde

September 2013

This thesis is the result of the author's original research. It has been composed by the author and has not been previously submitted for examination which has led to the award of a degree.

Signed:

Date:

Acknowledgements

I would like to thank my supervisors, I cannot thank you enough Dr Ellis you have encouraged me and supported this project from the start. I would not have finished it if it weren't for you and thank you for being a great friend. I also thank you for the huge amount of patience you have shown, after all you did have to read the first draft of this and it would have remained strange hieroglyphs without your input. The late Dr Lutz started me on this project her wisdom and insight I sorely am grateful for, most of what I learned I learned from you. I sincerely hope Eve wherever you are that I have fulfilled your wishes for this project and that I have not disappointed you. I would also like to thank Dr Herron, for helping me with all the microbiology work and for taking me 'adopting' me in the microbiology group.

To my wonderful Hannele you've helped me many times when im down and I couldn't have done it without your encouragement. To my parents specially my father thank you dad you been a role model and thank you for supporting me on this path so many years ago you can finally tell your friends my son is a mad scientist.

I would also like to thank many people in SIPBS particularly the Micro group, Dr Hossikisson and Dr Tucker thanks for all the conversations and advice you'd given, I even appreciate you introducing me to Quiz night even though we always come last. I would love to thank my 'fan club' Alison, Kirsty and Jana and Dr john Tiong for helping me out when I got stuck on my cloning and allowing me to be a general nuisance. I still think Micro is horrible.

Finally I would like to thank everyone at SIPBS for being an awesome friendly group, The University of Strathclyde and the Scottish funding council for funding me through those 4 years.

Abstract

The G-protein coupled receptor PAC_1 has been implicated in playing a role in neural growth, development and stress-protection, cognition, homeostasis, immunomodulation and anti-inflammatory effects. Previously, an investigation of PAC_1 gene (mADCYAP1r1) revealed a minimum promoter region -113bp to +206 relative to the transcriptional start site. Binding of the Zac1 transcription factor has been investigated but no detailed analysis has been carried out of the region downstream or upstream of -2598bp from exon 1 and a full characterisation of the Transcription Factors (TF) that govern expression of the receptor has not been performed.

The aim of this study was to characterise the promoter of the *mAdcyap1r1* gene and to identify transcription factor binding sites, explore their role in controlling expression. Since the *mAdcyap1r1* gene is well conserved across vertebrate species, a cross-species DNA comparison was performed to detect evolutionary conserved regions. Mouse, rat, human and chimpanzee sequences were aligned, and several cross-species conserved regions rich in transcription factor binding sites have been identified and reported. 3 upstream regions AdU1, AdU2 and AdU3; 2 downstream AdD1 and AdD2; and a new minimum promoter region Ad1 -80 and including most of exon 1 to +353. 279 transcription factor binding sites were found in these regions.

Luciferase reporter gene assays of these regions was performed in Neuro-2a cell lines, α-T3 neuroendocrine models and Cos-7 cells as a negative control that don't express PAC1. Results indicated a functional new basal promoter region, Ad1, that was expressed in Neuro-2a. Upstream and downstream regions showed Neuro-2a specificity but were 20 fold lower than expression from Ad1. Hydrogen peroxide treatment gave increased expression via the AdU1, Ad1 and AdD2 regions mainly in Neuro-2a cells. Electrophoretic Mobility Shift Assays indicated binding of nuclear extracts to most promoter regions.

Promoter Expression data gave functional insight to the bioinformatic analysis, and transcription factor binding sites indicate further roles to be investigated in future studies.

Table of Contents

Chapter 1

Introduction

1. Introduction

1.1 Overview

The pituitary adenylate cyclase-activating polypeptide type I receptor or PAC1 Receptor is a G-protein coupled receptor that binds Pituitary adenylate cyclase-activating polypeptide (PACAP). PAC1r is activated by several neuropeptides, including the pituitary adenylate cyclase-activating polypeptides PACAP-38, PACAP-27 and VIP (vasoactive intestinal peptide). It mediates the actions of PACAP through two routes, one of which is via adenylate cyclase and cAMP, and the other via phospholipase C (PLC).

The PAC1 receptor is expressed in various tissues including the adrenal medulla, pancreas, uterus and brain. It is also expressed during early development in the mouse, as early as E9.5, and in stem cells, neuronal precursor cells, during neuronal cell differentiation, astrogenesis, migration, and is known to be induced by fear conditioning in mice.

PAC1 has had several roles ascribed to it and is thought to be neurotrophic, neuroprotective, it can act as a neurotransmitter, it has a role in neuronal development, and in survival and differentiation of neuroblasts. It is thought to coordinate normal physiological stress reactions, and may also play a role in anxiety, post-traumatic stress disorder, fear. More recently a role in Parkinsons and Alzheimers Disease have been investigated.

Given its central role in mediating a range of important neuronal function, an understanding of how the PAC1r receptor gene is regulated is needed. Much of the regulation is thought to be transcriptional and mediated through the effects of the PAC1r promoter. This thesis aims to uncover those aspects of the PAC1r promoter that are important for regulating expression of the gene. In this chapter, the importance of the PAC1 receptor is described along with information on what is known about the regulation of its promoter.

1.2 The PACAP receptor, a Group II G Protein-coupled receptor

1.2.1 PAC1 Structure and activation

The PAC1 receptor belongs to the group II (GpII) G protein-coupled receptors (GPCR). This group includes receptors for peptides related to PACAP, such as secretin, glucagon and VIP (Sherwood et al. 2000). This group of receptors is characterised by 7 transmembrane domains and coupling to heterotrimeric G-proteins (guanine nucleotide binding proteins) (Nussdorfer et al. 2000; Sherwood et al. 2000; Harmar 2001). Activation of the receptors causes the activation of various signal transduction mechanisms, for example, PAC1 couples to the activation of Adenyl Cyclase (AC) signalling pathway through G protein Gs (McCulloch et al. 2000; McCulloch et al. 2002). Activated AC produces cyclic adenosine monophosphate (cAMP), which then activates protein kinase A (PKA) and exchange factor directly activated by cAMP (Epac) (Vaudry et al. 1998) this is known as the cAMP/PKA pathway(*Figure 1.1*). PAC1r has been shown to couple to the activation of phospholipase C (PLC) through G protein Gq/11(Spengler et al. 1993). PLC activation produces Diacyl glycerol (DAG) and Inositol 1,4,5-triphosphate (IP_3)(Spengler et al. 1997; McCulloch et al. 2000; McCulloch et al. 2002; Vaudry et al. 2009), IP_3 causes release of Ca^{2+} from intracellular stores by binding to the IP_3 receptor located in endoplasmic reticulum (Berridge 1993; Rawlings et al. 1994; Rawlings et al. 1995; Mustafa et al. 2007) while DAG activates PKC (IP3/DAG pathway) (*Figure 1.1*) (Nishizuka 1992; Watanabe et al. 2006).
Other signal transduction mechanisms that are activated by PAC1r include phospholipase D (PLD) (McCulloch et al. 2000; McCulloch et al. 2001; McCulloch et al. 2002) and the mitogen-activated protein Kinase/extracellular signal-regulated kinases (MAPK/ERK) system (Vaudry et al. 2000a; Botia et al. 2008), which can be activated in a PKC and PKA independent manner (Moroo et al. 1998; Monaghan et al. 2008a). There are other signalling consequences of PAC1 activation like the induction of gene expression, for example the VIP gene in NB-1 neuroblastoma cells. This seems to involve PKA and PKC signalling as it was blocked using PKA and PKC antagonists, H-89 and Bisindolylmaleimide I respectively (Falktoft et al. 2009).

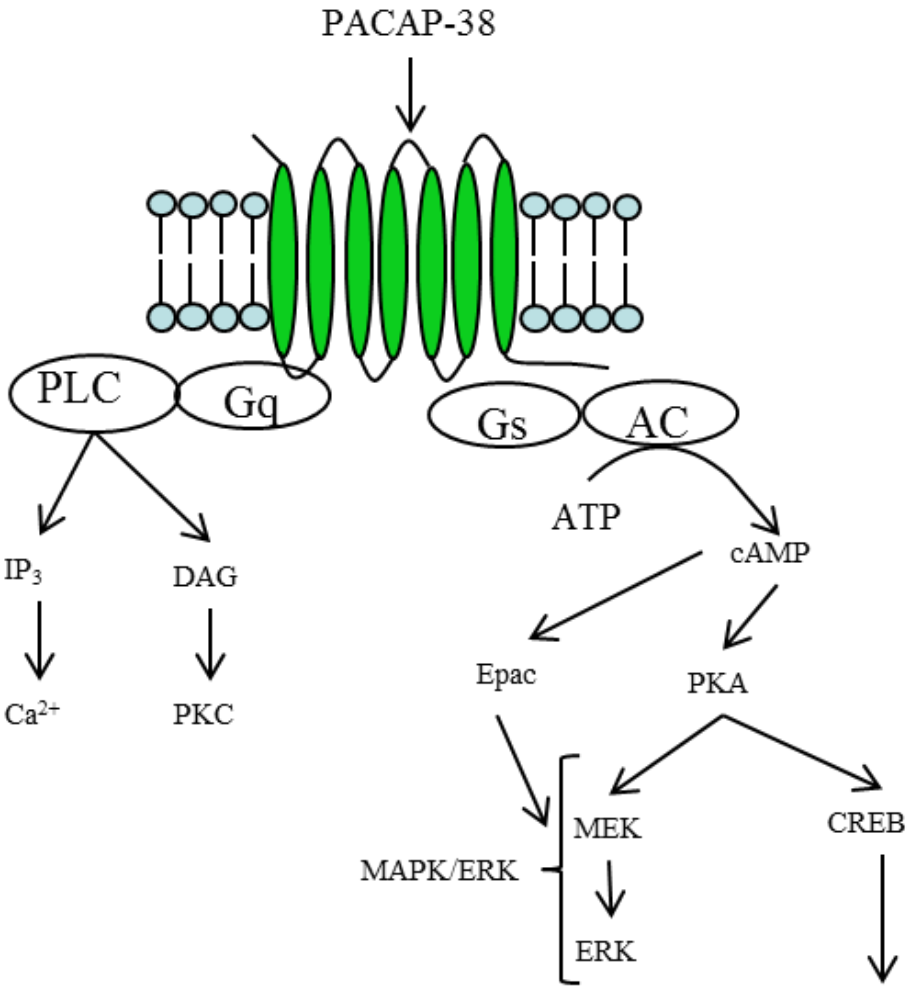

Figure 1.1:

Simplified diagram of PAC1 G-protein coupled receptor and intracellular signalling on activation of the receptor. Epac, exchange factor directly activated by cAMP; CREB, cAMP response element; ERK,extracellular signal-regulated kinase;MEK, mitogen-activated protein kinase.

1.2.2 PAC1 receptor function

In order to better understand the functions of the PAC1 receptor its expression pattern and PAC1 receptor knockout models provide a useful guide. The PAC1 receptor is expressed mainly in neuronal and neuroendocrine tissue as well as in immune cells like macrophages (Martinez et al. 2002; Mazzocchi et al. 2002; Vaudry et al. 2009) and some peripheral organs like the heart, lung and testis (Otto et al. 2004; Hautmann et al. 2007; Vaudry et al. 2009). The receptor is expressed early in development in embryonic stem cells (Hirose et al. 2005) as early as embryonic day 9.5 in mouse embryos (Sheward et al. 1998) and is present in germinative areas of the CNS (Sheward et al. 1998; Falluel-Morel et al. 2008; Vaudry et al. 2009). As mentioned earlier, the PAC1 receptor also shows differential expression during differentiation of neuronal cells (Hirose et al. 2005) and different temporal expression in the developing brain (Watanabe et al. 2007; Vaudry et al. 2009).

Studies on PAC1 receptor knockout mice seem to confirm a neuroprotective, neurodevelopmental and behavioural role in the CNS. PAC1 $^{-/-}$ mice showed decreased survival of neuronal cells migrating from the external granule layer (EGL) to Internal granule layer (IGL) due to increased apoptosis (Falluel-Morel et al. 2008) The migration of granule cells from the EGL to the IGL is an important part of postnatal development of the cerebellum, where about half the migrating cells will die due to apoptosis (Raff et al. 1993). PAC1$^{-/-}$ mice showed altered behaviour and mild memory deficits exhibiting reduced aggression to intruder males, reduced anxiety levels and increased spontaneous locomoter activity (Sauvage et al. 2000; Otto et al. 2001b; Nicot et al. 2004). It is important to note that the numbers used in the behavioural studies were very low (2 in one experiment) and the differences between the wild type and PAC1$^{-/-}$ mice in memory and learning studies were small, mainly the return of PAC1$^{-/-}$ to baseline activity faster after contextual fear conditioning (via footshock) (Sauvage et al. 2000). This information taken together would suggest that PAC1 has some effect on memory, learning and behaviour though the differences are not very pronounced. It is clear however that PAC1 plays an important role in neuronal development. It would therefore be plausible to assume a

developmental component to the expression of PAC1 which is consistent with the role of PACAP in neuroprotection and neurodevelopment.

The PAC1 receptor also plays a role in the immune system where it mediates a decrease in the production of pro inflammatory cytokines and decreases inflammation and it also plays a role in leukocytes recruitment (Martínez et al. 2005). $PAC1^{-/-}$ mice had a higher mortality rate than wild type mice in lipopolysacharide (LPS) induced septic shock the PAC1 agonist maxadilan increased survival rate by 25-30%. The $PAC1^{-/-}$ mice also showed impaired PACAP induced inhibition of expression of proinflammatory cytokine Il-6 (Martinez et al. 2002) and the reduction of the expression of intercellular adhesion molecule-1 (ICAM-1) and vascular cell adhesion molecule-1 (VCAM-1) which play a role in leukocyte recruitment during inflammation (Martínez et al. 2005). This role in immune-modulation makes it plausible to suggest, that there might be an inducible component to PAC1 receptor regulation, which would be beneficial in an inflammatory process.

PAC1 receptor functions aren't restricted to the neural and immune systems it plays a role in homeostasis and is also has functions in some peripheral organs. For example PACAP induced renin release was inhibited in $PAC1^{-/-}$ deficient mice compared to wild type. The release of renin is important in blood pressure regulation indicating the cardiovascular role of PAC1 receptor (Hautmann et al. 2007). PAC1 is also highly expressed in adrenal glands where it plays a role in catecholamine release (Mazzocchi et al. 2002). $PAC1^{-/-}$ mice also showed impaired glucagon response to insulin induced hypoglycaemia (Persson and Ahrén 2002). In a separate study $PAC1^{-/-}$ showed reduced glucose tolerance with glucose induced insulin secretion reduced by 55% *in vitro* and about 25% *in vivo* (Jamen et al. 2000). The PAC1 receptor also appears to have functions in the periphera in the heart, lungs and testis (Otto et al. 2004; Vaudry et al. 2009) an example of a this was a knockout study showed that $PAC1^{-/-}$ mice developed pulmonary hypertension, a higher rate of mortality and cardiac hypertrophy (Otto et al. 2004).

1.3. Peptides activating the PAC1 Receptor

1.3.1 PACAP

The 38 amino acid neuropeptide, Pituitary adenylate cyclase-activating polypeptide (PACAP-38) has many important and pleiotropic functions. It was first isolated from ovine hypothalamic extracts and its amino acid sequence showed 68% homology with ovine vasoactive intestinal polypeptide (VIP) at the amino-terminal (NT) sequence (1-28) 1. PACAP also exists as a carboxy-terminal truncated, 27 amino acid form known as PACAP-27 (*Figure 1.2*). Both PACAP-38 and PACAP-27 are amidated on the carboxyl-terminus (Miyata et al. 1989; Miyata et al. 1990). PACAP is derived from a large amino acid precursor known as preproPACAP (Vaudry et al. 2009), which is cleaved with Prohormone convertase (PC) into PACAP-38 and PACAP-27 (Vaudry et al. 2009). PACAP-38 is found distributed in many species including species of fish: lungfish, salmon (Parker et al. 1997; Lee et al. 2009) mammals like human, mouse, rat (Okazaki et al. 1995; Vaudry et al. 2009) as well as sea squirts (McRory 1997). The amino acid sequence of PACAP is completely conserved in mammals and is very well conserved across non-mammalian species. When compared to human PACAP-38 the different species have a very close % identity, for example chicken 97%, frog 97% and catfish 89% (Sherwood et al. 2000). This cross species distribution and homology shows it is a very well evolutionarily conserved peptide suggesting its biological importance.

PACAP38 **HSDGIFTDSYSRYRKQMAVKKYLAAVLGKRYKQRVKNK-NH2**
PACAP27 **HSDGIFTDSYSRYRKQMAVKKYLAAVL-NH2**
VIP **HSDAVFTDNYTRLRKQMAVKKYLNSILN-NH2**

Figure 2.2:

PACAP-38, PACAP-27 and VIP amino acid sequences. The underlined amino acids in the VIP sequence are those different from PACAP.

1.3.2 VIP and related peptides

PACAP belongs to a family of structurally related peptides that include secretin, glucagon like peptide 1 and 2(GLP1, 2), parathyroid hormone (PTH), glucagon, growth hormone releasing hormone (GHRH) and VIP (Nussdorfer et al. 2000; Harmar 2001; Jolivel et al. 2009). VIP/PACAP are widely distributed throughout the body (Fahrenkrug and Hannibal 2004; Vaudry et al. 2009; Dickson and Finlayson 2009; Jolivel et al. 2009) and are co-expressed in the same nerve fibres in the peripheral organs (Dickson and Finlayson 2009). However, they have different distribution patterns in the brain (Dickson and Finlayson 2009) as well as different temporal brain expression patterns during postnatal development (Girard et al. 2006). VIP and PACAP, are also co-expressed in neuroendocrine derived tumours like pheochromocytoma, ganglioneuroma and neuroblastoma (Fahrenkrug et al. 1995). This wide distribution of the peptides is linked with a wide range of different effects throughout the body and its systems.

VIP also shares its receptors with PACAP. These are the PACAP specific receptor PAC1 and the VIP/PACAP receptors VPAC1 and VPAC2 which show similar affinity to both PACAP-38 and VIP (Ishihara et al. 1992; Morrow et al. 1993; Lutz et al. 1993).

1.3.3 PACAP and VIP functions

PACAP and its receptors are widely distributed throughout the CNS and peripheral organs (Vaudry et al. 2009; Dickson and Finlayson 2009). PACAP was found to have many effects in the nervous system such as neurotrophic and neuroprotective effects (Vaudry et al. 2000b; Hirose et al. 2005; Shintani et al. 2005; Masmoudi-Kouki et al. 2007; Monaghan et al. 2008a; Monaghan et al. 2008b; Vaudry et al. 2009). Though PACAP shares receptors with VIP, they have complementary but distinct effects. This may be because of the difference in temporal and tissue distribution in the brain of VIP and PACAP and their receptors (Girard et al. 2006; Vaudry et al. 2009; Dickson and Finlayson 2009). Another reason why this occurs, would be the observation that mRNA levels, measured by semiquantitative RT-PCR, of PACAP-38, PAC1 VPAC1 and VPAC2 receptor are different during the different

stages of neuronal development (Hirose et al. 2005). Mouse neural cultures of EB5 embryonic stem (ES) cells were grown to induce 5 stages of cell differentiation into glial cells. PACAP mRNA levels gradually increased reaching a peak in stage 5 (differentiated), VIP mRNA levels however where only expressed in stage 4 and 5. PAC1 and VPAC2 receptor had a similar level and pattern of mRNA expression to PACAP, gradually increasing and showing the highest expression in stage 5. The VPAC1 was slightly expressed in stage 1, undifferentiated ES cells, showed the highest level of mRNA expression in stage 2, embryoid bodies (EB), then gradually decreased in stages 3-5 (Hirose et al. 2005). The PAC1 receptor and PACAP are also expressed in most germinative neuroepithelia (Vaudry et al. 2009) further highlighting their importance in neuronal development.

1.3.3.1 PACAP in CNS development and function

PACAP-38 and its PAC1receptor show distinct temporal distribution patterns in the brain during development (Hirose et al. 2005; Watanabe et al. 2007; Dickson and Finlayson 2009). PACAP has a well-documented role in the early development and growth of neuronal cells, this effect appears mainly through 2 means; a neurotrophic effect on neuronal tissue causing ES cells and neuroblast cell differentiation to neuronal cells (Cazillis et al. 2004; Monaghan et al. 2008a; Monaghan et al. 2008b); and a neuroprotective effect against apoptosis and harmful conditions for neuronal cells (Shintani et al. 2005; Monaghan et al. 2008b). Exposure of ES cells to PACAP caused an 80% increase in cells bearing neuronal phenotypes (Cazillis et al. 2004). In other studies exposure to PACAP-38 caused differentiation of SH-SY5Y neuroblastoma cells (Monaghan et al. 2008a; Monaghan et al. 2008b), a 4 day exposure of human SH-SY5Y neuroblastoma cells to 100nM PACAP-38 caused a 5.5 fold increase in neurite bearing SH-SY5Y cells when compared to cells grown in low serum medium (Monaghan et al. 2008b). The second role of PACAP in neural development is through a neuroprotective role protecting developing cells from apoptosis, during migration from EGL to IGL mentioned in 1.2.2, for example. In PACAP knockout mice ($PACAP^{-/-}$) a thinner IGL was apparent when compared to wild type, as well as increased apoptosis (Allais et al. 2007) mirroring results of

PAC1 $^{-/-}$ mice mentioned earlier (Falluel-Morel et al. 2008). This was also demonstrated *in vitro* in cortical neuron cultures extracted from 17 day old foetal rats, where the PAC1 receptor antagonist PACAP(6-38) decreased cell viability in a dose-dependant manner (Shintani et al. 2005). PACAP also increased the survivability of SH-SY5Y neuroblastoma cells, rat cortical neurons and rat cortical astrocytes after exposure to stressful conditions like glutamate, H_2O_2 and tumour necrosis factor- α (TNF-α) (Shintani et al. 2005; Monaghan et al. 2008b). This neuroprotective effect is exerted through affecting apoptosis directly through the MAPK/ERK pathway (Vaudry et al. 2000a; Gutiérrez-Cañas et al. 2003; Allais et al. 2007; Monaghan et al. 2008a; Monaghan et al. 2008b; Masmoudi-Kouki et al. 2011) or indirectly through antioxidant enzymes or the release of neurotrophic factors like brain-derived neurotrophic factor (BDNF) (Shintani et al. 2005; Botia et al. 2008). The PACAP-38 induced expression of antioxidant enzymes such as peroxiredoxin 2 was via a cAMP, PKC and MAPK dependant mechanism, which then decreased the activity of caspase-3 induced apoptosis (Botia et al. 2008; Masmoudi-Kouki et al. 2011).

PACAP has other important CNS functions such as its role in behaviour, learning and memory (Sauvage et al. 2000; Otto et al. 2001a; Otto et al. 2001b; Hashimoto et al. 2001; Vaudry et al. 2009). PAC1 deficient mice showed lower anxiety levels and higher locomoter activity than wild type (Otto et al. 2001b; Hashimoto et al. 2001). They also showed impaired contextual fear conditioning, delivered via footshock, 24hrs after training. Long term cued fear conditioning however was similar to wild type mice (Otto et al. 2001a).

1.3.3.2 PACAP immune system functions

PACAP also has immuno-modulatory effects for instance $PACAP^{-/-}$ mice showed higher mortality and increased cytokine production in DSS-(dextran sodium sulphate) induced colitis. Rescue with recombinant PACAP-38 resulted in decreased mortality (Azuma et al. 2008). PACAP-38 also decreased the severity of collagen induced arthiritis (Abad et al. 2001). These effects are through immuno-modulatory, antinflammatory actions decreasing proinflammatory cytokine production such as IL-12 (Delgado and Ganea 1999) IL-6 and TNF-α in macrophages (Martínez et al. 1998; Delgado et al. 1999).

1.3.3.3 PACAP's role in Homeostasis

The role of PACAP is also found in many neuronal cell bodies and fibres innervating peripheral organs, as well in peripheral non-neuronal tissue (Dickson and Finlayson 2009). It has cardiac, endocrine, urogenital, homeostasis and gastrointestinal tract (GIT) functions (Yamaguchi 2001; Adams et al. 2008; Vaudry et al. 2009). For example, $PACAP^{-/-}$ null mice have shown impaired metabolism and thermoregulation resulting in higher mortality, showing decreased thyrotropin-releasing hormone (TRH) and thermogenic gene mRNA levels and increased insulin sensitivity (Adams et al. 2008). PACAP also has endocrine functions acting as a secretagogue, for example, it stimulates insulin secretion from the pancreas (Filipsson et al. 2001), catecholamines and glucocorticoids from the adrenal medulla and cortex respectively (Nussdorfer and Malendowicz 1998; Vaudry et al. 2009). It also appears that PACAP is essential in the stress-induced corticosterone release demonstrated in PACAP-/- mice (Tsukiyama et al. 2011). PACAP also affects circadian rhythm regulation which is controlled by the biological clock in the hypothalamic suprachiasmatic nucleus (SCN). Light signals reach the SCN via a population of retinal ganglion cells from the retinohypothalmic tract (RHT) which express PACAP (Hannibal et al. 2002; Fahrenkrug et al. 2005). In a study, PAC1 knockout mice ($PAC1^{-/-}$) showed down regulation of light induced mRNA expression of 'clock genes' mPer1, mPer2 and c-Fos (Hannibal et al. 2001). There was also a delay in early night, light induced phase delay of circadian rhythm in $PAC1^{-/-}$ mice.

The effect of PACAP on circadian rhythm is also mediated though the VPAC2 receptor. VPAC2$^{-/-}$ mice showed a lack of circadian rhythm and when kept in total darkness the mRNA expression of the 'clock genes' was arrhythmic (Harmar 2003).

1.3.3.4 VIP functions

The 28 amino acid VIP was initially isolated and identified by its gastro intestinal tract (GIT) effects, affecting gastric acid secretion inhibition, pancreatic and biliary secretion and relaxation of smooth muscle (Fahrenkrug and Emson 1982). It is now known to have many other effects throughout the body. VIP has immune functions modulating production of macrophages, T cells and inflammatory cytokines, chemokines and their receptors such as IL-1 and TNF-α (Delgado et al. 2004; Gomariz et al. 2006; Yadav and Goetzl 2008) and modulating oxidative stress and TNF- α induced apoptosis(Gutiérrez-Cañas et al. 2003; Koh et al. 2009; Calafat et al. 2009) . VIP also has well documented CNS functions (Glowa et al. 1992; Takashima et al. 1993a; Takashima et al. 1993b; Chaudhury et al. 2008) such as memory and learning, for example, VIP knockout mice showed impaired recall of fear conditioning 48 hours or longer after training (Chaudhury et al. 2008). In another study of VIP learning effects, chronic intracerebroventricular administration of 10ng/day for 13 days resulted in increased learning times in a Morris water pool test and showed increased time to find the platform every time compared to saline controls. VIP antagonist cerulein restored learning time to control levels (Takashima et al. 1993a). VIP also has neurotrophic and neuroprotective functions acting as a neurotrophic factor secretagogue and an astrocyte mitogen (Brenneman et al. 1990; Brenneman 2007; Masmoudi-Kouki et al. 2007).

1.4. *mAdcyap1r1* gene and its Expression

1.4.1 Structure of the *mAdcyap1r1* gene

The PAC1 receptor in mouse is encoded by the *mAdcyap1r1* gene, which contains 18 exons with the transcriptional start site (TSS) in exon 1 and the open reading frame encoded within exons 2-18. Several isoforms of the receptor exist caused by the alternative splicing of two regions of the gene, exons 4-6 in the NT domain and exons 14 and 15 encoding extra amino acid cassettes inserted into the intracellular loop 3 (ic3) domain, called hip and hop respectively (*Figure 1.3*). This gives rise to multiple PAC1 receptor isoforms with inclusion/exclusion of short amino acid cassettes in these regions NT and ic3 (Spengler et al. 1993; Lutz et al. 2006). A splice variant missing cassettes encoded by exons 5, 14 and 15 from human would be called hPAC1 $_{\delta 5\text{ -null}}$ for example. mPAC1 $_{\delta 5\text{ -hiphop}}$ would be a mouse splice variant missing amino acid cassette encoded by exon 5 (Lutz et al. 2006). Different splice variants have been shown to have different temporal and tissue distribution, ligand affinity and signal transduction (Spengler et al. 1993; Basille et al. 2000; Lutz et al. 2006; Basille et al. 2006; Ushiyama et al. 2007). For example VIP but not PACAP-38, showed >55 fold greater potency stimulating cAMP response in hPAC1 $_{\delta 5,6\text{ -null}}$ and hPAC1 $_{\delta 5,6\text{ -hop}}$ splice variants compared to full or δ5 NT variants when expressed in COS 7 cells. In another example PACAP and VIP showed similar potency stimulating cAMP response in hPAC1$_{\text{-hip}}$ and hPAC1 $_{\delta 5\text{-hip}}$ splice variants (Lutz et al. 2006). Splice variants may also show different signal transduction mechanisms. For example, the PAC1-$_{\text{null}}$ variant showed adenosine diphosphate-ribosylation factor (ARF) independent PLD activation compared to PAC1$_{\text{-hop}}$ that was dependant on ARF (McCulloch et al. 2000; Ronaldson et al. 2002). There are also species differences between splice variants that may be species specific. For example, the bovine bPAC1$_{\text{-hop}}$ splice variant when expressed in rat PC12-G and NG108-15 neuronal cell lines showed that was essential for Ca^{2+} mobilisation and influx while the bPAC1$_{\text{-null}}$ variants lacked this effect (Mustafa et al. 2007).

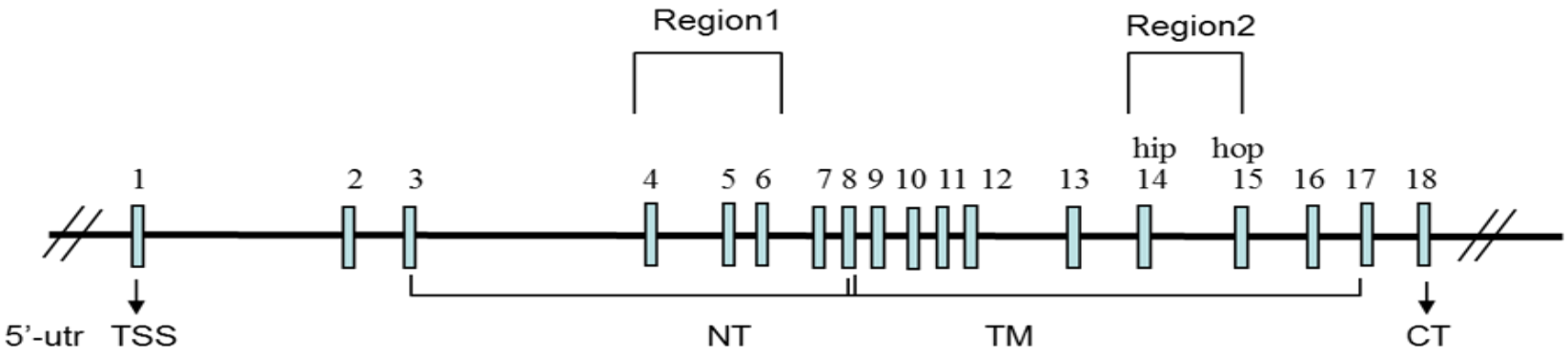

Figure 1.3:

PAC1 receptor gene *Adcyap1r1*. The TSS (transcription start site) starts at exon 1, where the translational start site at exon 2. The alternative splicing regions are shown region 1: exons 4,5 and 6 ; region 2: exon 14 and 15. The carboxy terminal, (CT) is at exon 18. Exons 3-17 code for the amino terminal domain (NT) and the transmembrane region (TM).

1.4.2 Control of *mAdcyap1r1* Gene expression

mAdcyap1r1 is expressed in a specific organised manner showing different tissue and developmental expression patterns. There is also growing strong evidence for inducible expression.

The expression of a gene involves turning the DNA code into an amino acid sequence through transcription then translation. Transcription is the act of copying a DNA sequence into its complementary mRNA, carried out by RNA polymerases. This mRNA is then translated into an amino acid sequence by the ribosomes (Brown 1999). Eukaryotic genes are divided into coding regions called exons and non-coding regions called introns. Some exons are non-coding as in Exon 1 in *Adcyap1r1*, for example (Spengler et al. 1993; Mazzocchi et al. 2002). The transcription start site (TSS) is followed by exons and introns. The ATG start codon is the location of the translational start site (*Figure 1.4*) (Latchman 1998; Brown 1999).

Upstream of the TSS is the promoter region. In the classic model the promoter has what is called a TATA box (5'-TATAA-3' sequence) where transcription is initiated. The TATA box is located about 30bp upstream of the TSS. In addition to the TATA box are other regulatory elements, like CCAAT and Sp1 for example. RNA polymerase is recruited to this basal promoter to initiate transcription. During transcription a preinitiation complex of various TFs like TFIIA, TFIID, TFIIF and RNA polymerase II bind to the TATA box and also bind to other promoter regions, to initiate transcription (Latchman 1998; Brown 1999).

Other upstream transcription control elements known as Enhancers or regulatory elements (Brown 1999) also affect the transcription of the gene. TF bind to these control sequences, which can be grouped in 3 classifications: 1.Tissue specific 2. Inducible, 3. Developmental.

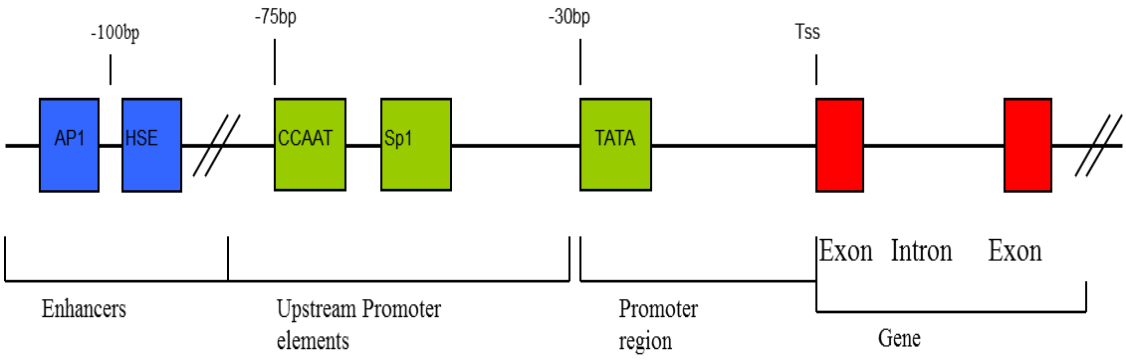

Figure 1.4:.

The classic TATA promoter initiation site, which initiates transcription and drives Gene expression. Enhancers and other upstream promoter elements will influence activity levels of the basal promoter. This is followed by the Transcription start stie (TSS) and the gene with exons containing the coding regions and introns containing noncoding regions. (Adapted from Latchman D, Eukaryotic Transcription Factors (Latchman 1998))

1.4.2.1 Constitutive/Basal Promoter

Many genes including *mAcyap1r1* do not have a TATA box. Interestingly the promoter regions for genes encoding the GpII G-protein coupled receptors lack a TATA box. These include the Calcitonin (Zolnierowicz et al. 1994), Corticotropin releasing hormone type 2 receptor (CRHR2) (Catalano et al. 2003). In place of a TATA box, there is a highly GC rich region flanking exon 1 known as a CpG island, which are alternative promoter regions to TATA boxes (Antequera 2003). In *mAcyap1r1* promoter this CpG island has about 80% GC content (own observations).

The basal expression of the gene is usually called constitutive expression and is controlled by 'housekeeping' Transcription Factors. The zinc finger protein SP family of transcription factors would be a very good example. Two members, the widely expressed SP1 and SP3 are expressed in a wide range of cells and react with multiple transcription factors (Latchman 1998; Wierstra 2008), Sp1 in particular is considered a constitutive TF (Latchman 1998). Sp1 -/- mouse embryos consistently died round day E9.5-10 while Sp1 +/- survived but were smaller than wild type (Marin et al. 1997). SP TF bind to GC boxes (GC rich regions of DNA) and also GT boxes though Sp1 has higher affinity for GC boxes and vice versa for Sp3(Wierstra 2008). The Sp1/Sp3 ratio seems to play an important role in gene regulation as demonstrated by their regulation of the Secretin gene, where it was observed that Sp3 suppressed Sp1 dependant promoter activity in a dose dependant manner (Lee et al. 2004). This effect was noticed on genes that have 2 or more Sp1 binding sites (Wierstra 2008).

Though Sp1 binding sites are considered part of the basal promoter in regulating genes lacking a TATA box (like *Adcyap1r1*), Sp1 also interacts with many other TF groups and it is clear now that SP1 can be induced (Wierstra 2008). The MAPK/ERK pathway through phosphorylation of Sp1on Thr266 regulates Sp1 activity (Zheng et al. 2001; Samson and Wong 2002). Sp1 can also be induced by other signalling cascades such as PKC (Zheng et al. 2001; Samson and Wong 2002). Sp1 also has a role in protecting CpG islands from methylation (Macleod et al. 1994). CpG island methylation is implicated in suppressing transcription and

silencing gene expression in many species of plants, fungi and vertebrae (Colot and Rossignol 1999; Bird and Wolffe 1999; Lee et al. 2004) in many genes such as the silenced X chromosome in females (Bird and Wolffe 1999). There is however, great variation in effects of CpG island methylation. TF that bind to GC rich regions cant bind to methylated CpG islands, some TF factors however are unaffected like Sp1(Bird and Wolffe 1999). Though not a TF, CpG methylation affects the GC rich domains that many TF bind to through inhibiting their binding (Bird and Wolffe 1999). It seems it may be an evolutionary tool in adding an extra layer of complexity resulting in multiple transcription pathways. In some cases, CpG methylation appears as a constitutive control factor and in others appearing to be induced or even cell specific (Colot and Rossignol 1999; Bird and Wolffe 1999). CpG methylation is a very complicated factor with a variable and wide range of actions. It cannot be explained or studied in one study, therefore the focus of this study will be on other transcription control mechanisms.

1.4.2.2 Tissue Specific Regulation

Tissue specific promoters include the pituitary specific Pit-1 and Myoblast specific MyoDI, which are selective for a tissue type or several related tissues. Inducible TF respond to various conditions/substances like the heat responsive HSE (Heat shock element) and Glucocorticoid response element (GRE) (Latchman 1998; Brown 1999). Developmental TF activate a gene at a specific time in the organisms development, like Fushi tarazu (Ftz) and bicoid (Latchman 1998; Brown 1999). Finally Sp1 and nuclear factor 1 (NF1) are examples of constitutive TF required for general expression of ‘housekeeping’ genes (Latchman 1998; Brown 1999; Wierstra 2008). They are however not exclusively restricted to housekeeping only and may be induced for example.

The PAC1 receptor is expressed mainly in neuronal and neuroendocrine tissue as well as in immune cells like macrophages (Martinez et al. 2002) and some peripheral organs like the heart, lung and testis (Vaudry et al. 2009; Dickson and Finlayson 2009). Several cell types express PAC1 receptor for example, pituitary derived αT3-1 gonadotrophs (Rawlings et al. 1995), but not somatotroph-like GH4C1 which contains VPAC2 (Rawlings et al. 1995). It also expressed in SH-SY5Y, Kelly, SK-N-Be neuroblastoma cells (Basille et al. 2000) Other cells where PAC1r is not present include CHO (Chinese hamster ovary) (Ushiyama et al. 2007) and COS7 cells (MacKenzie et al. 2001). There are also differences in expression levels of PAC1 between similar cell lines such as the SK-N-Be, SH-SY5Y and Kelly neuroblastoma cell lines (Lutz et al. 2006) where the expression levels, measured by quantitative PCR were 300, 87 and 7.1 (number of copies per 100 copies of β-actin) respectively. This differential tissue expression is strongly indicative of tissue specific transcription factors essential in controlling receptor expression.

Examples of tissue specific TF are the Pit-1 pituitary specific TF (Latchman 1998; Brown 1999) which might be involved in PAC1 receptor expression in the pituitary (Rawlings et al. 1995; Vaudry et al. 2009). Such as in, the pituitary gonadotroph cell line αT3-1 which express PAC1 receptor (Rawlings et al. 1995). Another tissue specific TF is GATA-3 part of the GATA family of TF. GATA-3 is expressed in lymphatic tissue playing an essential role in the development, differentiation and activation of T cells (Joulin et al. 1991; Yamashita et al. 2004). PAC1 receptor is expressed in T cells in the lymphatic system such as in the thymus (Tokuda et al. 2004; Tokuda et al. 2006). This may suggest that GATA-3 TF may be involved in the regulation of PAC1 receptor expression.

1.4.2.3 Developmental Expression

As mentioned earlier PACAP shows differential expression and distribution in different stages of development (Watanabe et al. 2007; Dickson and Finlayson 2009). It is also apparent that the PAC1 also shows different expression in development. In an *in vitro* model mimicking neuronal cell development (discussed previously in section, 1.3.3), Hirose et al induced the growth of undifferentiated EB5 Embryonic stem cells through 5 stages mimicking different development phases. Glial cell differentiation was induced in stage 5 (Hirose et al. 2005). PAC1 showed modest expression in the first stage gradually rising through stages 2-4, it was further upregulated in the final stage as the cells terminally differentiated into neurons (Hirose et al. 2005). PAC1 expression was detected as early as rat embryonic day 14 (E14) with the highest levels in the medullary neuroepithelium. After birth receptor expression disappeared in some areas such as the diencephalic neuroepithelium and decreased markedly in all germinative areas (Basille et al. 2000). In mouse it was detected as early as E9.5 in the germinative areas of the CNS (Sheward et al. 1998). In another study different temporal distribution was observed in rat embryonic brains with PAC1 mRNA detected in different tissues at different embryonic development days. At E11 for example, it was detected in the neuroepithelium of the mesencephalon and it was detected in the olfactory bulb neuroepithelium after E16 (Zhou et al. 1999).

This developmental pattern of expression would involve TF involved in development such as the CCAAT/ Enhancer binding proteins (C/EBPs) which bind to the CCAAT box and is important in cellular differentiation (Ramji and Foka 2002) which is present upstream of the PAC1 receptor TSS (Aino et al. 1995; Rodríguez-Henche et al. 2002). Another examples of developmental TF is OCT4 which controls cellular differentiation (Rodda et al. 2005). OCT4 knockout resulted in cellular differentiation of human embryonic stem (hES) cells (Zaehres et al. 2005). OCT4 gene was also expressed alongside PAC1 receptor in the early stages of murine ES cell differentiation models, stage1 undifferentiated stem cells and stage 2 EB (Hirose et al. 2005). Therefore OCT4 may have some effect on the regulation of PAC1 receptor. Some developmental transcription factors can also be induced like C/EBP

which is induced in inflammation, where IL-1,and IL-6 induce C/EBPβ-dependant transcription (Ramji and Foka 2002).

1.4.2.4 Inducible Expression

There is a growing body of evidence that there is an inducible component to the expression of PAC1 receptor. PACAP-38 is involved in inflammatory, immune and apoptosis processes (Delgado and Ganea 1999; Allais et al. 2007; Monaghan et al. 2008b). During transient focal cerebral ischemia it was observed that PAC1 mRNA expression was increased in the post ischemic tissue (Gillardon et al. 1998; Ciani et al. 1999) which is consistent with PACAP's role in neuroprotection where an upregulation of PAC1 receptors would increase PACAP's protective effects. It was also observed that PAC1 can be induced by TF involved in apoptosis, covered in the next paragraph (Ciani et al. 1999). PAC1 mRNA is upregulated by progesterone in rat ovarian granulosa cells and rat hypothalamus (Ha et al. 2000). PACAP not only affects sex hormone levels (Vaudry et al. 2009) there also seems to be a progesterone induced feedback mechanism controlling PAC1 expression(Ha et al. 2000). It was also observed that luteinizing hormone induced PAC1 expression, this induction however, was dependant on progesterone receptor activation (Ko and Park-Sarge 2000). This induced expression of PAC1 mRNA would be controlled by inducible TFs. One would therefore expect progesterone hormone TF binding domains (Latchman 1998) or other hormone response elements to influence PAC1 expression. However hormones may also act through downstream signal transduction pathways to induce PAC1r gene expression. We therefore may find steroid hormone TF binding domains in the PAC1 promoter.

Zac1, also known as Lot1, is a gene encoding a zinc finger protein TF which along with P53 regulate apoptosis and cell cycle arrest. mRNA levels of Zac1 were increased in the same areas as PAC1 mRNA increased, as a result of ischemia (Gillardon et al. 1998). In other studies it was observed that Zac1 and P53 upregulated PAC1 expression in cerebral ischemia (Gillardon et al. 1998; Ciani et al. 1999; Rodríguez-Henche et al. 2002). Hoffman et al also tested PAC1 induction by

P53 and Zac1 in different cell lines like LLC-PK1 epithelial kidney cells, PC12 pheochomocytoma and CV-1 kidney fibroblast. Zac1 and P53 induced PAC1 mRNA expression in most cell lines with slightly varying degrees. There was slight Zac1 induced expression of PAC1 in C6 glioma cells and no induction of PAC1 by both Zac1 and P53 in CV-1 cells (Hoffmann et al. 1998). The increased PAC1 receptor expression induced by Zac1, appears to be induced by a direct Zac1 transcriptional mechanism on PAC1 receptor gene (Hoffmann et al. 1998; Fila et al. 2009). These observations would partially explain the PAC1r mediated cell protective response which would be activated via P53 and Zac1 which are upregulated in ischemia (Li et al. 1997; Gillardon et al. 1998).

Growth factors such as nerve growth factor (NGF) and insulin like growth factor-1 (IGF-1) also have an effect on PAC1 expression. This was observed in rat PC12 cells and was due to a MAPK dependant mechanism (Jamen et al. 2004). Therefore, TF downstream of MAPK, like c-Fos may be involved in PAC1r gene expression. Strengthening this assumption would be the fact that c-Fos dimerises with c-jun to form the AP-1 TF (Hess et al. 2004), AP-1 TF binding domain is present in the PAC1 gene promoter region (Rodríguez-Henche et al. 2002). Downstream in the signalling cascade in the cAMP/PKA pathway, is cAMP regulatory element binder protein(CREB) (Trumper et al. 2002). CREB can also be activated by MAPK specifically p38 MAPK (Hönscheid et al. 2011). We therefore might expect the TF CREB binding domain to be involved in PAC1r expression though this is speculation at this point. This proposed CREB dependant effect may be as a result of neutrophins like IGF or other substances that activate MAPK, or through other receptors which increase cAMP levels, maybe even PAC1 itself.

In some cases, induced expression of PAC1r was not consistent in all cell types. This may suggest how the presence or absence of tissue specific TF factors that may affect the activity of inducible TF on PAC1 expression. This is highlighted with progesterone, where it upregulated different PAC1 splice variants in basal hypothalmus but in the preoptic area it wasn't effective in upregulating $PAC1_{-hop1}$ receptor splice variant (Ha et al. 2000). The mounting body of evidence of induced

expression of PAC1, discussed in this section strongly suggests an inducible component to the expression of PAC1r gene. Though only a handful of TFs have been confirmed to both induce PAC1r and also bind to TF binding domains in the PAC1 receptor promoter.

1.4.3 *mAdcyap1r1* promoter region in previous studies

Aino et al characterised the PAC1 gene, promoter region (*Figure 1.5*), up stream of the TSS in a highly GC rich region, were 2 Sp-1 binding sites a CCAAT box and an activator protein-2 (AP-2) binding domain all within -81bp upstream of the TSS (Aino et al. 1995). Further upstream at -311bp is a binding domain for NF-1 (Aino et al. 1995) which is a constitutive TF capable of stimulating genes containing CCAAT boxes(Latchman 1998). This would mean there may be 2 NF-1 binding domains (NF-1 and CCAAT) in the putative promoter region. The CCAAT box present can also bind to C/EBP which has developmental expression profiles but can also respond to stimuli and give inducible expression (Ramji and Foka 2002; Zaehres et al. 2005). The SP-1 TF regulates both constitutive and inducible expression as discussed in the previous paragraph (Section 1.4.2.1) and AP-2 is expressed early in development in neural cell lines (Mitchell et al. 1991; Hilger-Eversheim et al. 2000) and also has a role in apoptosis (Hilger-Eversheim et al. 2000). This highlighted how several potential transcription factors domains like inducible, developmental and tissue specific can influence transcription and have multiple TF binding to them like the CCAAT box.

In another study Rodiguez-Henche et al made several Luciferase reporter gene plasmid constructs, containing various fragments of the upstream region of *mAdcyap1r1*, obtained by restriction digests. The plasmid constructs were then transfected into various cell lines and Luciferase expression measured (Rodríguez-Henche et al. 2002). A construct containing the region -180bp upstream of the *mAdcyap1r1* TSS, was suggested to be the minimum promoter region and showed the highest levels of expression in αT3-1 gonadotrophs and SaOs-2 osteosarcoma

cells. The region -25bp:0bp showed lower levels of expression but they were still high in αT3-1 cells but very low in SaOs-2 indicating a neuronal tissue specific promoter in the region between -180: -25bp upstream of TSS. Luciferase reporter gene expression was still produced, though much lower, when a construct from -2665bp to -180bp was used. This shows that there are further upstream promoters before the -180bp fragment and that there may be repressor elements acting upstream of -180bp region influencing promoter activity (Rodríguez-Henche et al. 2002). It was also found that the region from -390 to -180bp had an inhibitory effect on expression which may have a role in cell specific expression (Rodríguez-Henche et al. 2002).

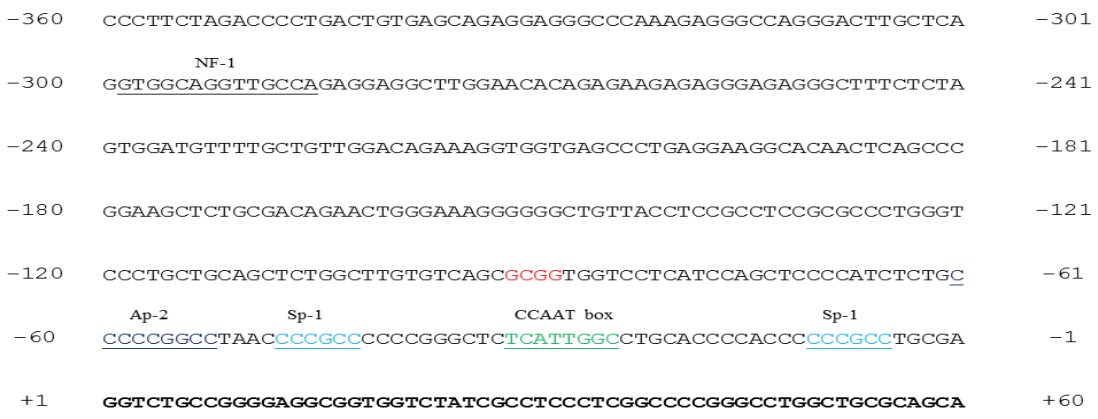

Figure 1.5

The promoter region of PAC1 receptor from Aino et al 1995, +1 is the TSS. The diagram shows NF-1 binding site, 2 Sp1 sites a CCAAT box and an AP-2 site.

Though the Rodriguez-Henche et al paper demonstrated the minimum promoter region, there was no explanation of the promoter regions chosen for testing where it seemed to be at random. The study did mention the various TF binding sites observed upstream of exon 1, the proximal promoter region showed a CCAAT box, GC boxes, and AP-2 sites. TF mentioned were the constitutive TF NF-1, Sp-1, CCAAT, the developmental TF AP-1 and C/EBP. Other TF mentioned were the inducible TF CREB, P53 and the tissue specific GATA TF factors and anterior pituitary Pit-1. There was no mention however of the exact location of these TF except the ones reported previously by Aino et al in proximal promoter region (Aino et al. 1995; Rodríguez-Henche et al. 2002). More importantly none of them were tested to see if they actually bind to the promoter region except Zac1. Zac1 was shown to bind to a region -390 bp ustream of TSS using electrophoretic mobility shift assay (EMSA)(Rodríguez-Henche et al. 2002).

1.5. Aims and objectives

The aim of this study is to investigate the expression of *mAdcyap1r1* and determine what factors control the expression of the PAC1 receptor - and hence its physiological roles.

Objectives:

1. Identify potential transcription factor binding sites in the PAC1r gene using bioinformatic analysis
2. Determine which binding sites are functional in a reporter gene assay
3. Investigate tissue specific regulation
4. Investigate inducible regulation in response to external factors.

The work will be carried out using a combination of bionformatic analysis and cell based assays using model cell lines, which were used to investigate potential promoter regions. In addition, the ability of transcription factors to bind to fragments of DNA will also be investigated.

Chapter 2

Materials and methods

2. Materials and Methods

2.1 Materials

2.1.1 Cell lines

Cell lines were obtained originally from the American Type Culture Collection (ATCC).

α-T3 are mouse anterior pituitary gonadotroph derived cells (Windle et al. 1990).

Cos 7 cells are monkey kidney CV-1 cells transformed with SV40 virus (Gluzman 1981).

Neuro-2a. is a mouse neuroblastoma cell line from the C1300 tumour from albino mice (Olmsted et al. 1970; Pons et al. 1982).

2.1.2 Bacterial cells

JM109 cells were obtained from Stratagene, Agilent technologies, Cheshire, UK.

2.1.3 Plasmids and BACs

The RP23-154D15 BAC in pBACe3.6 was obtained from BacPac resources, Oakland, CA, USA

pBluescript SK- vector was obtained from Stratagene, Agilent technologies, Cheshire, UK.

The pRL-TK vector was obtained from Promega

TOPO-XL and TOPO-Blunt were obtained from Invitrogen, Paisley, UK

2.1.3. Chemicals and Reagents

All chemicals and reagents were obtained from Fisher scientific, Loughborough, UK or Sigma chemical company Poole, UK, unless otherwise stated

2.1.4 Tissue culture media and antibiotics

Tissue culture media, newborn calf serum (NCS), SYBR green, pUC19, Sigma-Aldrich, Poole, UK; foetal calf serum (FCS) from Hyclone laboratories, Fisher scientific, Loughborough, UK; L-glutamine was obtained from Biowhittaker, Berkshire, UK. Primocin was obtained from InvivoGen, SanDiego, CA, USA.

2.1.5 Transfection Reagents

Lipofectamine and Optimem were obtained from Invitrogen, Paisley. Fugene transfection reagent was obtained from Roche products Ltd, Hertfordshire, UK. GeneJuice was obtained from Novagen, Merck chemicals Ltd, Nottingham, UK.

2.1.6 Luciferase Assay

Dual-Glo Luciferase and Renilla Luciferase assay system was obtained from Promega UK Ltd, Hampshire, UK.

2.1.7 Molecular Biology and cloning reagents

Restriction enzymes and buffers and antarctic phosphatase were obtained from New England Biolabs (UK) Ltd, Hertfordshire, UK. TOPO XL PCR cloning kit, Zero Blunt TOPO PCR cloning kit for sequencing and TOPO XL Gel Purification Kit were obtained from Invitrogen, Paisley, UK. 1kb DNA ladder, Blue/Orange loading dye, PureYield Plasmid miniprep system, Pfu DNA polymerase, Terminal Deoxynucleotidyl Transferase (TDT) were obtained from Promega UK Ltd, Hampshire, UK. GelRed fluorescent nucleic acid dye was obtained from Biotium, Cambridge, UK. Expand Long Range dNTPPack was obtained from Roche products Ltd, Hertfordshire, UK. PCR oligonucleotide primers were obtained from Eurofins MWG Operon, Ebersberg, Germany.

2.1.8 EMSA Assay Reagents

Digoxigenin-11-dUTP (Dig-dUTP) was obtained from Enzo Life Sciences (UK) LTD, Exeter,UK. Anti-Digoxigenin AP, nitro blue tetrazolium chloride /5-bromo-4-chloro-3-indolyl-phosphate, toluidine-salt (NBT/BCIP) and Blocking solution were obtained from Roche products Ltd, Hertfordshire, UK;

2.2 Methods

2.2.1 Bioinformatic analysis

DNA sequences of human, chimpanzee, mouse and rat were obtained from Ensembl database and were then compared using RankVISTA (rVISTA) software (http://genome.lbl.gov/vista/index.shtml), and the GEMS Launcher tool in Genomatrix analysis software (http://www.genomatix.de/products/GEMSLauncher/index.html).

The DNA sequences were aligned and cross species conserved regions were marked and TF binging sites within them were annotated. Separate analysis of TF binding sites for each sequence alone and each pairwise comparison of sequences was performed using CLC Genomics Workbench 6 from CLC Bio (http://www.clcbio.com/)

2.2.2 Plasmid and DNA preparation

2.2.2.1 Bacterial culture

Luria-bertani broth (LB) was prepared by mixing peptone 10% (w/v), 10% NaCl and 5% yeast extract with ultra high purity (UHP) water then autoclaved. Agar plates were prepared by adding agar to LB broth to make 1.5% (w/v) then autoclaved. The agar was then microwaved and allowed to cool until it could be held by hand before selective antibiotic was added before pouring into petri dishes and allowed to set.

DH10 E.coli cells containing RP23-154D15 mouse genomic DNA clone in pBACe3.6 were grown in media containing 12.5 μg/ml chlorampenicol.

pBluscript SK-, pGL-3 Basic and pGL-3 Promoter plasmids were grown in media containing 75μg/ml ampicillin. Bacteria containing TOPO-XL and TOPO-Blunt

were grown in media with 75μg/ml ampicillin. Glycerol stocks of bacteria containing plasmids were frozen down in 15% glycerol, and stored at -80°C.

2.2.2.2 BAC and Plasmid DNA Extraction

For the purification of RP23-154D15 mouse genomic DNA clone and pBluscript SK- DNA, bacteria were streaked on 1.5% agar+appropriate antibiotic and incubated at 37°C overnight. One colony was then picked with a sterile loop and inoculated into 50ml LB broth + appropriate antibiotic, which was then incubated overnight.
The 50ml bacterial culture was placed on ice before DNA was purified. The DNA was purified using the PhasePrep BAC DNA kit (Sigma-Aldrich, Poole,UK) according to the manufacturer's instructions. The concentration of purified DNA was then measured using an Eppendorf tube photoluminometer.

Purification of plasmid DNA was done in a similar fashion but on a smaller in 6-10ml inoculates of LB + Antibiotic. The DNA was then extracted using the Pureyield plasmid mini prep system (Promega), according to manufacturer's instructions.

2.2.3 Restriction digests and gel DNA extraction

2.2.4.1 Endonuclease Digestion

Digests were performed for 2 h at 37°C using appropriate buffer and compatible buffers in dual digests. Digests containing KpnI were performed overnight at room temperature, while digests containing SmaI were perfomed at 25°C. The digests were adjusted for volume to make sure restriction enzyme volume did not exceed 10% of total reaction volume by diluting it by UHP water.

2.2.3.3 End treatment

Vectors with compatible ends were treated with Antarctic Phosphatase directly after digests to prevent self ligation during ligation reactions. Digests of vectors or inserts with compatible ended DNA were treated with Antarctic phosphatase and incubated in water bath for 15 minutes at 37°C directly after digestion. Antartic phosphatase was heat inactivated at 70°C for 5 mins before DNA gel extractions.

PCR fragments with blunt ends obtained using Pfu DNA polymerase and were ligated to pGL-3 vectors were treated with T4 polynucleotide kinase for 10 mins at 37°C before gel DNA extraction to add a phosphate to DNA to allow for ligation.

2.2.3.4 Gel DNA extraction

Preparative gel electrophoresis was performed on the digests and PCR products in 0.8% agarose/Tris-acetate-EDTA(TAE) gel containing 1xSYBR Green dsDNA stain alongside a 1kb or 100bp DNA ladder for reference. The gel was then visualised in UV light and the gel containing appropriate sized DNA fragments, was excised using a sterile scalpel and placed in sterile eppendorf tubes. The DNA fragments were then extracted from the gel using the QIAEX II Gel Extraction Kit (UK Qiagen Ltd, Crawley, UK) according to manufacturer's instructions.

2.2.3.5 Ligations

After the fragments and vectors were extracted from agarose gel with QIAEX II kit, the fragments were ligated using an insert:vector ratio of 3:1 or 5:1. For most cloning, this was done by adding Quick-Stick Ligase and incubating the DNA for 5-15 minutes at room temperature. The total reaction volume was 20µl for each ligation. The resultant DNA ligations were then transformed into JM109 cells as described above

Ligations into TOPO-XL and TOPO-Blunt vectors did not use Quick-Stick. Instead the PCR fragments were incubated with 1µl TOPO vector and 1µl TOPO kit salt solution (1.2M NaCl and 0.06M $MgCl_2$) and the reaction volume brought up to 6 µl

with sterile water. TOPO ligation reactions were then incubated for 5 mins at room temperature before transformation.

Ligation reactions were then directly transformed into appropriate competent cells

2.2.4 Bacterial transformation

2.2.4.1 Preparing Competent Bacterial Cells

JM109 cells were streaked onto 1.5% L-agar plate and incubated overnight. 1ml culture of LB broth was then inoculated with one colony using a sterile loop and incubated at 37°C in shaker overnight. The 1ml culture was poured into 50ml of LB broth and incubated in shaker at 37°C until optical density at 600nm(OD_{600}) reached 0.4. The culture was placed on ice for 15 minutes, transferred to ice cold sterile tubes and spun for 10 minutes at 3500rpm. The supernatant was discarded and the bacterial pellets were resuspended with 5ml 75mM $CaCl_2$ and incubated on ice for 20 minutes. The bacterial suspension was centrifuged and pelleted in ice cold tubes, the supernatant discarded. The pellet was resuspended with 2ml TFB2 solution (10mM 3-(N-morpholino)propanesulfonic acid (MOPS)) pH7.0, 75mM $CaCl_2$, 10mM RbCl, 15% glycerol). The cell suspension was aliquoted into ice cold eppendorf tubes (200ul/tube) and snap frozen in liquid nitrogen then stored in -80°C.

2.2.4.2 Transformation Protocol

pBluscript SK-, pGL-3 Basic and pGL-3 constructs were transformed into JM109 E.coli cells. Clones that used the TOPO-XL and TOPO-Blunt were transformed into One Shot TOP10 E.coli (Invitrogen).

Before the cells were transformed with DNA constructs the transformation efficiency of competent cells was checked by using puc19 standard vector which allows for blue/white screening. 10µl of puc19 DNA was placed in 100µl ice cold TMC(10mM Tris.Cl pH8.0, 10mM $MgCl_2$, 10mM $CaCl_2$) in a sterile Eppendorf tube and placed on ice. 200µl of competent cells was added and mixed by gentle tapping, then placed on ice for 30 minutes. The mixture was then placed in 42°C water bath for 2 minutes, 1ml LB broth was added and then the mixture was incubated in a shaker at 37°C for

one hour. The mixture was then centrifuged for 2 minutes at full speed; supernatant was poured of and resuspended in residual supernatant. The cell suspension was then spread onto 1.5% agar LB, ampicillin, X-gal plates (section 2.2.2.1) and incubated at 37°C overnight. Clone with pBluscript SK- were transformed using this protocol.
Once competence efficiency was determined to be sufficient, construct DNA was transformed using the same procedures.

Clones that used the TOPO-XL and TOPO-Blunt vectors were transformed into One Shot TOP10 E.coli cells (Invitrogen), briefly 2µl ligations reaction were placed in One Shot competent cell vial and incubated for 30 mins on ice, before placing in 42°C water bath for 30 sec and then immediately placing them on ice. After 2 mins 250µl of 4°C sterile LB was added, then cells were incubated in shaker at 37 for 1 hour at 200 rpm.

Clones with pGL-3 Basic and pGL-3 Promoter vectors were transformed into JM109 E.coli cells from Promega, the cells were thawed on ice for 5 mins then10µl of Quick stick ligase ligation reactions were added to 50µl JM109 cells and placed on ice for 10 mins. The cells were then placed in a 42°C water bath for 55 secs and immediately placed on ice for 2 mins. 900 µl of 4°C LB was then added to transformation reaction and the cells incubated in a shaker for 1 hour at 37 and 200 rpm.

After incubation for 1 hour the transformation reaction was centrifuged for 30 secs and most of the supernatant removed leaving 200 µl. The pellet was then gently resuspended in remaining supernatant and spread on 1.5% agar LB agar plates containing appropriate antibiotic and incubated at 37°C overnight.

2.2.4.3 Bluewhite screening

For pBluescript plasmids, transformed cells were spread onto 1.5% L-agar plates which contained 100μg/ml ampicillin, 0.5mM IPTG (Isopropyl β-D-1-thiogalactopyranoside), 40μg/ml X-gal (bromo-chloro-indolyl-galactopyranoside) and appropriate antibiotic. The plates where then incubated overnight at 37°C. Cells untransformed with pBluscript SK- did not grow while transformed cells gave either Blue or white colonies.

White colonies were picked and used to inoculate LB broth and glycerol stocks frozen down and DNA purified following methods mentioned above. The size of insert DNA in constructs was checked using restriction digests then agarose gel electrophoresis.

2.2.5 PCR

2.2.5.1 Primers

PCR oligonucleotide primers were designed by using Primer-3 software (http://frodo.wi.mit.edu/primer3/)
Table 2.1 b) shows which primers were used to make each constructs.
The primers had SalI and BamHI restriction sites designed in them, except AdD1 For, AdD1 Rev, AdD2 For and AdD2 Rev primers which had NheI and XhoI restriction sites designed in them (*Table2.1 a*) (*Table 2.1 b*). to allow ligation into pGL-3 Basic vector(*Figure 2.*1).

Primers		**Orientation**	**Restiction site**
Web1	GTCGACCTGCAGCTCTGGCTTGTGTCA	5’	Sal I
Web2	GGATCCAGCGCTGAAGGGAAGGAAAGAC	3’	BamHI
Web3	GGATCCAGGGGCTGAAGGTGCAGG	3’	BamHI
Web4	GTCGACGGAAGCTCTGCGACAGAA	5’	Sal I
Web5	GGATCCGCGGTGTGTGCGTACTG	3’	BamHI
Web6	GTCGACTCGGGGAGGTAGCTGAGCA	5’	Sal I
AdD1For	GGCGCTAGCGCAGGTAAGGCTGGAGGAG	5’	NheI
AdD1Rev	GGCCCTCGAGGACAGACAGACAGACCCTTGG	3’	XhoI
AdD2For	GGCGCTAGCTGGGCTTGTACGTCTGAATG	5’	NheI
AdD2Rev	GGCCCTCGAGTTGCTGCCTACTTCCCTCTC	3’	XhoI

a)

PCR Construct	**5’ primer**	**3’primer**	**Size**
PcrAd1	web1	web3	469bp
PcrAd2	web4	web5	386bp
PcrAd3	web1	web2	8.2kb
PcrAd4	Web6	web	6.1kb
PcrAdD1	AdD1 For	AdD1 Rev	306bp
PcrAdD2	AdD2 For	AdD2 Rev	241bp

b)

Table.2.1:

Primers were used to make the PCR constructs with built in Restriction sites underlined **a).** Panel **b)** shows which primers were used to make the PCR constructs and their sizes.

2.2.5.2 PCR Reactions

Hyclone Hypure cell culture grade water was used to make 10pmol/µl stocks of the primers. For PCRAD1 and PCRAD2 each had 3 PCR reactions performed a blank with no DNA template, 150ng DNA template and 250ng RP23-154D15 DNA template. Each reaction involved mixing 5 µl Pfu DNA polymerase buffer, 200 µM dNTPs, 2.5 µl of 100% DMSO, 10pmol 5', 10pmol 3' primer, DNA template (Blank, 150ng, 250ng). Hyclone Hypure cell culture grade water was used to bring up reaction volume to 50 µl. 1 µl Pfu Polymerase was added to each reaction mixture right before placing reaction tubes into PCR machine. The PCR cycle involved initial denaturation at 95°C for 1min; 25 cycles of Denaturation 95°C 30 sec, annealing 65°C for 30 sec, extension 72°C for 2min. This was followed by Final extension step at 72°C for 5min.

For the large ~8.2kb PcrAD3 and ~6.1kb PcrAd4, 3 PCR reactions were performed a blank with no DNA template, 150ng DNA template and 250ng RP23-154D15 DNA template, the reagents used for this reaction were from the Expand long range dNTP pack kit(Roche products Ltd, Hertfordshire, UK). Each reaction involved mixing 10 µl Expand long range buffer with 12.5mM $MgCl_2$, 500 µM dNTPs, 5 µl of 100% DMSO, 10pmol 5'primer, 10pmol 3' primer, DNA template (Blank, 150ng, 250ng). Hyclone Hypure cell culture grade water was used to bring up reaction volume to 50 µl. 3.5 µl Expand long range enzyme mix (Mix of DNA polymerases) was added to each reaction mixture right before placing reaction tubes into PCR machine. The PCR cycle involved initial denaturation at 92°C for 2min; 25 cycles of Denaturation 92°C 30 sec, annealing 60°C for 50 sec, extension 68°C for 6min. This was followed by Final extension step at 68°C for 15min.

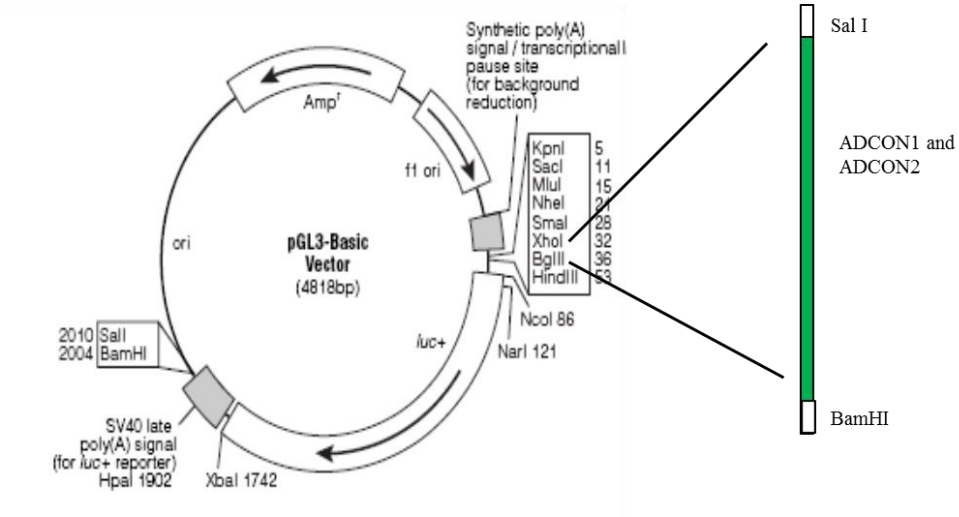

Figure 2.1:

The primers had SalI and BamHI restriction sites which were compatible with XhoI and BglII respectively. This was to allow them to be subcloned into pGL-3 vector for future Reporter gene analysis.

2.2.5.3 Cloning of PCR Fragments

The PcrAD3 and PcrAd4 PCR reactions were visualised by gel electrophoresis in 0.8% TAE agarose gel containing 1xSYBR Green dsDNA stain alongside a 1kb DNA ladder for reference. The gel was then visualised in UV light and the gel containing appropriate sized DNA fragments, was excised using a sterile scalpel and placed in sterile eppendorf tubes. The DNA was extracted using the Qiaex II gel extraction kit following the manufacturer's instructions as described above. The extracted DNA was then cloned into pCR-XL-TOPO vector (*Figure* 2.2) and then transformed into TOP10 chemically competent cells using the TOPO XL PCR cloning kit (Invitrogen, Paisley, UK) following the manufacturer's instructions.

The PcrAD1 and PcrAD2 PCR reactions were visualised by gel electrophoresis using 0.8% TAE agarose gel conatining 1xSYBR Green dsDNA stain alongside a 100bp DNA ladder for reference. The PcrAD1 and PcrAD2 PCR reactions were then cloned directly into pCR-Blunt II-Topo (*Figure 2.3*) vector then transformed into TOP10 chemically competent cells using the Zero Blunt TOPO PCR cloning kit following the manufacturer's instructions. PcrAd1 and PcrAd2 were also directly cloned into SmaI digested pGL-3 Basic vector after they were treated with T4 polynucleotide kinase (see section 2.2.3.3 above).

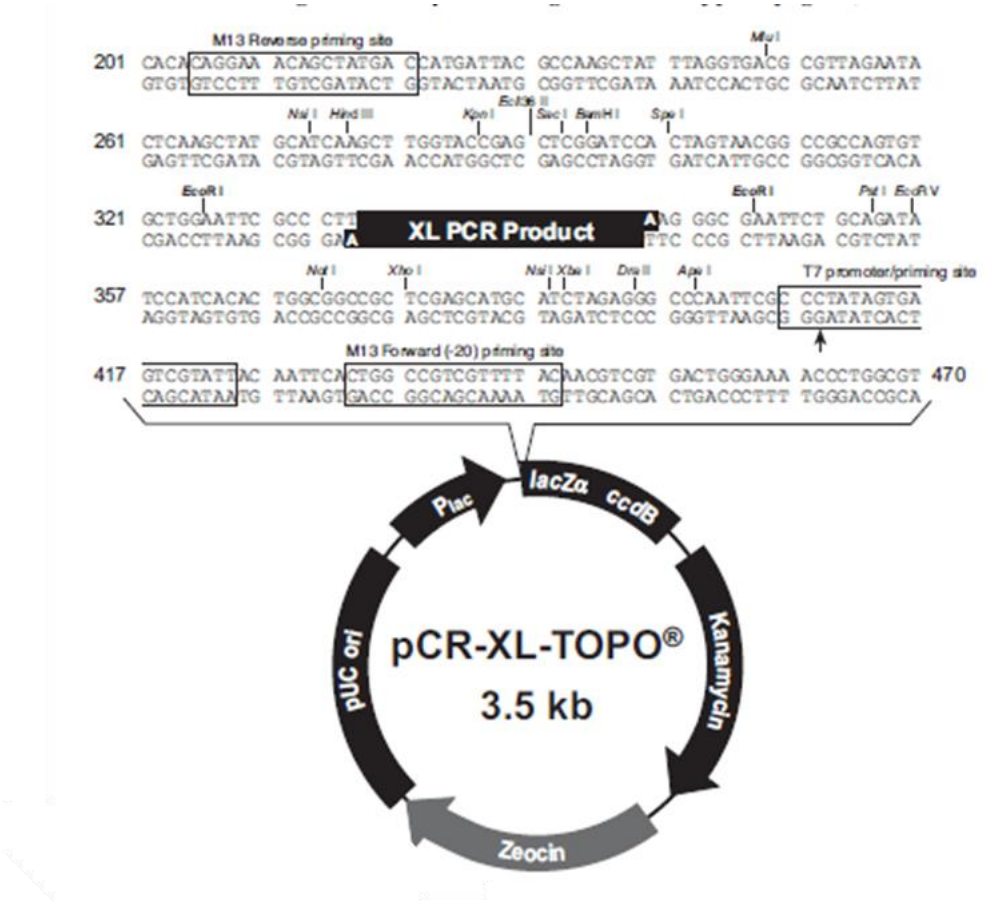

Figure 2.2: The PcrAd3 PCR fragment was cloned into the 3.5 kb pCR-XL-TOPO selective vector. This was to allow its growth and manipulation in future experiments.The vector allows for Antibiotic resistance selection and blue/white screening of clones with insert.

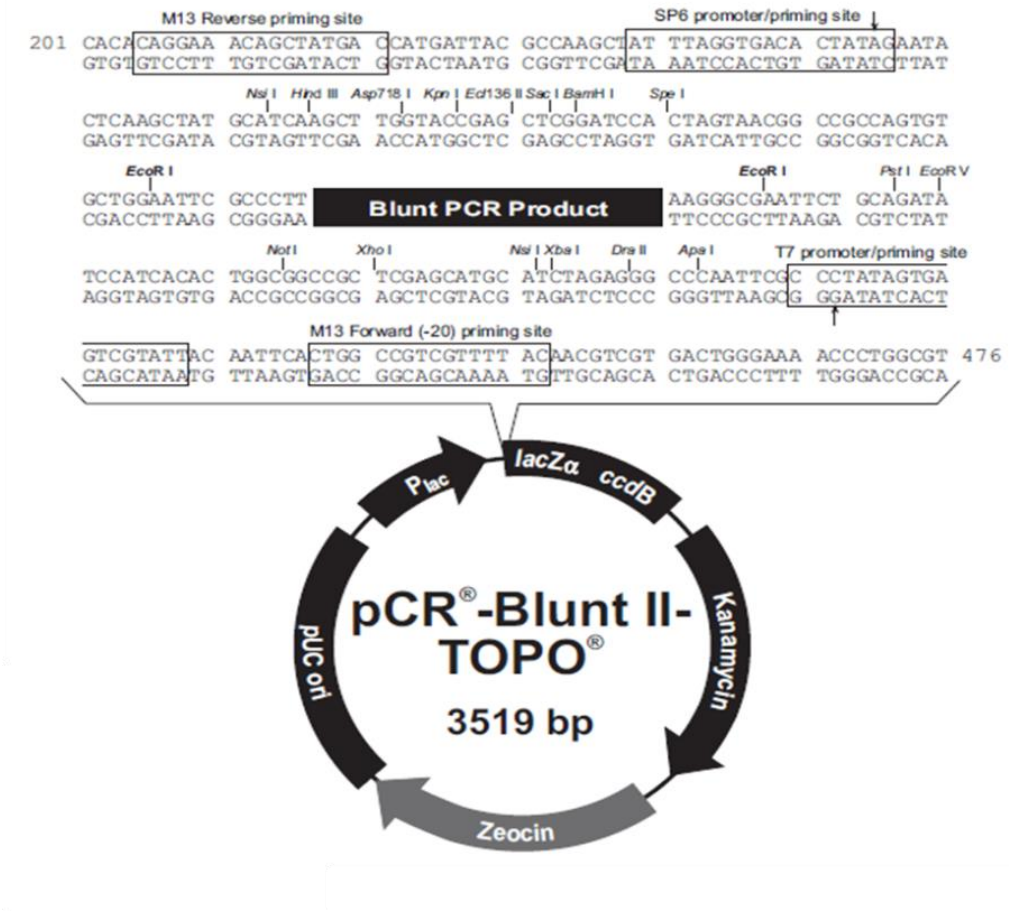

Figure 2.3: The PcrAd1 and PcrAd2 PCR fragments were cloned into the ~3.5kb pCR-Blunt II-TOPO selective vector. The vector allows for Antibiotic resistance selection and blue/white screening of clones with insert.

2.2.5.4 Sequencing

The cloned PCR fragments were sequenced in-house by Dr R. Tate using Applied Biosystems BigDye Terminator v3.1 sequencing chemistry (Warrington, UK) with the appropriate vector primers. The samples were analysed on an Applied Biosystems 3100-Avant Genetic Analyser (Warrington, UK) with Data Collection v2.0 Software using an 80-cm capillary array with POP-4 polymer (Applied Biosystems, Warrington, UK).

2.2.6 Mammalian Cell culture

α-T3 gonadotrophs were maintained in Dulbecos modified eagle medium (DMEM) with 10%(v/v) FCS supplemented with 1% Na pyruvate and 5µg/ml Primocin. Neuro 2A neuroblasts were maintained in 1:1 mixture of minimum essential medium eagle (MEM) supplemented with 1% Non-Essential Amino Acids (NEAA), 1% Na pyruvate, 1% L-glutamate and Ham's F12 supplemented with 1% L-glutamate. The MEM and Ham's F12 1:1 mix was then supplemented with 5% FCS, and 5µg/ml Primocin. The Cos 7 cells were maintained in Dulbecco's modified eagle medium (DMEM) supplemented with 10% NCS and 5µg/ml Primocin.

Cells were passaged when they reached 80-90% confluence, briefly, the cells were washed with hanks balanced salt solution (HBSS) then trypsinised. The cells were then resuspended in 5ml media, 1ml cell suspension transferred to 75cm cell culture flask, the remaining cell suspension would be discarded. 15ml media was then added to the cells in flask and then placed in an incubator. All cells were maintained at 37°C, 5% CO_2 and the media replaced every 3 days.

2.2.7 Cell transfection

α-T3, Neuro 2A and Cos 7 cells were washed with HPSS then trypsinised and resuspended in media and plated in 12 well plates at $100x10^4$/well for Neuro2a , Cos-7 and α-T3 cells 24 h prior to transfection.

For the transfection reagent optimisation experiment α-T3 and Neuro 2a were transfected using three different transfection reagents Lipofectamine, Genejuice and Fugene. Cos 7 cells however, were transfected using only Genejuice as they were sensitive and die from the other transfection reagents (supervisor's observation). The cells were transfected with pRL-TK (0.3μg/well) containing the renilla luciferase reporter gene. The gene was driven by the herpes simplex virus thymidine kinase promoter (HSV-TK) which provides constitutive low level expression. The transfection was done as follows: for Fugene and Gene juice, 0.9μl/well of the transfection reagent was added to Optimem and incubated for 5minutes at room temperature, 0.3μg/well of pRL-TK was then added and incubated for 15 min at room temperature, then 50ul/well of this mixture was added to cells. For transfection with Lipofectamine 0.3μl/well pRL-TK was added to 50 μl/well Optimem and 0.9μl/well of Lipofectamine was added to 50 μl/well Optimem, the 2 mixtures were incubated at room temperature for 5 mins. The 2 mixtures were then mixed together and incubated at room temperature for 15 mins, 100μl/well of this mixture was then added to the cells. The transfections were done in 6 wells for each transfection reagent. 6 wells of untransfected cells were used as negative controls for each transfection reagent 12 well plate.

Luminescence was measured 24 hours after transfection as described below. After determining which transfection protocol gave highest luminescence for Neuro 2A and α-T3 cells. the time-course expression of renilla luciferase was assessed by transfecting the cells with that transfection reagent and measuring the luminescence at 24 h, 48 h and 72 h after transfection. Cos-7 cells were transfected using Genejuice. The transfections were done in 6 wells for each cell line for each time point in separate plates. 6 wells of untransfected cells per cell line were used as controls.

After determining time post transfection and transfection reagent to use, the pGL-3 Basic and pGL-3 Promoter reporter gene constructs were co-transfected with pRL-TK Renilla luciferase at a ratio of 3:1. The cells were transfected with 0.9µg/well of pGL-3 and 0.3µg/well of pRL-TK the DNA using 2.7µl/well of transfection reagent. The luminescence was measured 48hrs post-transfection as described below .

Hydrogen Peroxide Treatment

Cells were co-transfected with pRL-TK and pGL-3 reporter constructs then treated with 30µM H_2O_2 the following day and luminescence measured after 24hrs exposure to H_2O_2.

2.2.8 Luciferase Assays

Luminescence was measured using the Promega Dual-Glo luciferase assay system following manufacturer's instructions. Briefly, media was removed form cells in 12 well plates and washed with HBSS, then 100µl of 1x lysis buffer was added to each well. The plates were then placed on shaker for 15 min at room temperature. 10µl of cell lysate was then transferred to white 96 well plate and 75µl Renilla Luciferase reagent was added (1:100 substrate:buffer) to each well. The luminescence was measured immediately after using a Spectramax M5 luminometer (Molecular Devices).

2.2.9 Hydrogen Peroxide Viability Assays

A stock solution of 200mM H_2O_2 dissolved in DMSO was prepared, the H_2O_2 stock solution was added to appropriate media to form 200 µM media H_2O_2 stock with DMSO not exceeding 0.1%. The media H_2O_2 stock was serially diluted to form several concentrations of H_2O_2, 100µl/well of media H_2O_2 stocks was added to 96 well plates of Neuro-2a α-T3 and Cos-7 cells $1x10^4$ cells/well in triplicate. 24hrs post H_2O_2 treatment media was removed and 1.2mg/ml MTT (3-(4,5-dimethylthiazol-2-yl)-2,5-diphenyltetrazolium bromide, a yellow tetrazole) solution diluted in media at 100µl/well was added to wells and left for 2 hrs in incubator at 37°C, 5% CO_2. MTT

media was removed and cells lysed with 100µl/well DMSO and placed on a shaker for 1 hour at room temperature. Absorbance was then measured at 570 nm in plate in Lambda 12 spectrometer (Perkin Elmer).

2.2.10 Preparation of Nuclear extracts

Two flasks for each cell line were until they reach ~90% confluence in 75cm flasks, and 1 flask for each cell line was treated with H_2O_2 24hrs before cell lysis. The media was removed and cells were washed 2x with ice cold PBS, the cells were scraped to the bottom of the flask. 200µl of Buffer A was added to each flask, and the cells suspended. The cellular suspension was transferred to sterile 1.5 ml Eppendorf tubes vortexed for 15 secs then placed on ice for 10 mins. The tubes were centrifuged at 5000rpm for 2 mins at 4°C, supernatant was then removed and the cell pellet was resuspended in 500µl Buffer B. The cells were then centrifuged at 5000rpm for 2 mins at 4°C, supernatant was discarded and pellet resuspended with 100µl Buffer C the cells were then placed on ice for 30 mins and agitated by flicking every 3 mins. The Eppendorf tubes were then spun at full speed for 15 mins at 4°C, the supernatant containing the whole nuclear extract was transferred to a sterile Eppendorf tubes and stored at -80°C.

Protease inhibitors and 7mM 2-mercaptoethanol were added to buffers A, B and C directly before use.

Buffer A:

50mM NaCl, 10mM HEPES pH8.0, 500mM sucrose, 1mM EDTA pH8.0, 0.15mM spermine, 0.2% TX-100.

Buffer B:

50mM NaCl, 10mM HEPES pH8.0, 1mM EDTA pH8.0, 25% glycerol, 0.15mM spermine, 0.5mM spermidine.

Buffer C:

350mM NaCl, 10mM HEPES pH8.0, 1mM EDTA pH8.0, 25% glycerol, 0.15mM spermine, 0.5mM spermidine.

Protease inhibitor mix:

1mM Phenylmethanesulfonyl fluoride (PMSF), 2mM benzamidine, 1µg/µl leupeptin, 1µg/ml pepstatin, 0.2 IU/ml aprotinin.

2.2.11 Electrophoretic Mobility Shift Assays

The DNA fragments of the putative promoter regions PcrAd1, PcrAd2, , PcrAdD1 and PcrAdD2 were prepared by PCR while AdU1 AdU2 AdU3 were excised by restriction digest out of their pGL-3 constructs. The DNA was then labelled by digoxigenin on the 3' terminal using DIG-dUTP; 1µg of promoter region DNA was mixed in a sterile Eppendorf tubes with 1x TDT buffer, 20 units of TDT and 1µl of 25nmol DIG-DUTP stock. The mixture was brought up to a total volume of 20µl with sterile UHP water and incubuated in 37°C water bath at for 30 mins. The Eppendorf tube was the then cooled on ice for 2 mins then 1µl of 200mM EDTA pH8.0 was added to stop reactions. DIG labelled DNA was stored in -20°C until binding reaction with nuclear extracts.

Binding Assay

50ng of DIG-dUTP labelled DNA was mixed with 2µg poly(dI-dC)-poly(dI-dC), 10µl of whole nuclear extract, 4µl Binding buffer (0.1M Tris/Hcl pH 7.5, 0.5M NaCl, 10mM EDTA pH 8.0, 25mM $MgCl_2$) the reaction volume was bought up to 20µl with sterile UHP water and incubated for 15 mins at room temperature. poly(dI-dC)-poly(dI-dC) was used to stop non-specific binding between DNA and nuclear extracts.

Electrophoresis and Blotting

4% (30:1, Acryl:Bis), 0.3 x Tris/Borate/EDTA (TBE) buffer acrylamide gel was pre run for 1.5 hours in 4°C 0.5 x TBE at 200V in 4°C. DNA bound to nuclear extract was loaded into acrylamide gel and run for 2 hours at 200V at 4°C. The DNA/Nuclear extract were then transferred onto cationic nylon membrane presoaked in 0.5 x TBE for 5 mins by running in 0.5 x TBE for 1 hr at 400mA. The nylon membrane was dried on blotting paper then DNA cross-linked to it by exposure to UV light for 50 secs.

Membrane development

Nylon with DNA fixed to it using UV light was washed in maleic acid buffer (100mM Maleic acid, 150mM NaCl, pH 7.5) for 1min then treated with Blocking solution (Roche Blocking reagent 10% in Maleic acid buffer) overnight on shaker at room temperature. The membrane was then treated with Antibody solution (Roche Anti-Digoxigenin-AP final concentration 150mU/ml in Maleic acid buffer) for 1 hour on shaker at room temperature. The Membrane was then washed 2x for 15 mins with washing Buffer (100ml maleic acid buffer, 300µl Tween 20), equilibrated in detections buffer (100mM Tris-HCl, 100mM NaCl adjusted to pH 9.5) for 5 mins. The membrane was placed in 10ml detection buffer with DNA facing up and 10-15 drops of NBT/BCIP were used to cover membrane, left in the dark for 10min then 10ml of detection buffer was added to completely immerse membrane which was left to develop in the dark for at least 6 hours without shaking. The membrane was removed and washed in sterile UHP water to stop reaction and then photographed using a Las-3000 darkbox camera (Fujifilm).

2.2.12 Statistical analysis

Two-way ANOVA with Dunnett's or Sidak's multiple comparison tests were used to assess the difference in expression of promoter constructs compared to positive controls; as well as differences between H_2O_2 induced and uninduced expression . One-way ANOVA was used to analyse differences in expression of a single clone between each cell line with Bonferroni's multiple comparison test. Values were expressed as means±SEM , $p<0.05$ was considered statistically significant. GraphPad Prism 6 software was used to perform the statistical analysis.

Chapter 3

Bioinformatic Analysis of the mouse Adcyap1r1 promoter

3. Bioinformatic Analysis of the Adcyap1r1 promoter

3.1 Previous promoter analysis

Previous studies have found that the translational start site of PAC1 gene is located in exon 2, 7.8kb upstream of TSS in exon 1. Aino et al 1995 and Rodruigez-Henche et al 2002 determined that that there are several TSS located at the start of the exon1, where there were several TF binding sites located upstream of TSS in what appears to be a canonical promoter. Namely no TATA box was found and TF binding sites CCAAT, GC boxes, AP-2, SP-1 and NF-1 were located upstream of TSS. Other TF binding sites were reported further upstream of canonical promoter, but their locations were not shown such as CAAT, C/EBP, GATA factors, P53 and PIT-1 (Aino et al. 1995; Rodríguez-Henche et al. 2002).

Rodriguez-Henche used primer extension experiments to identify two major TSS and several other minor TSS which appear to depend in the tissue or cell line. The presence of longer expressed sequence tags from databases also supports the presence of several TSS depending on tissue examined. The two main TSS were within 3 bp of each other, and lay 141 to 143 bp upstream of a SacII (+206) site. The minor TSS are 50-60 bp upstream of the major TSS and are also indicated (205 bp from the SacII site).

In this study we used the TSS +1 provided by Ensembl database, which appears to be the minor TSS 50-60 bp upstream of major TSS used in Rodriguez Henche study. For ease of reference, positions of conserved suspected promoter regions will be indicated relative to the Ensembl database TSS (http://www.ensembl.org/index.html). The minimum promoter reported by Rodriguez-Henche et al starts -113 from the TSS used in his study and ends at SacII site located +206 in exon 1. Relative to Ensembl, Rodriguez-Henche TSS starts at +68 the minimum promoter starts -113 to SacII site at +206 relative to Ensembl. Aino et al used a TSS start site at +10 relative to the ensemble TSS. Figure 3.1 summarises the various TSS used and location of minimum promoter form previous study.

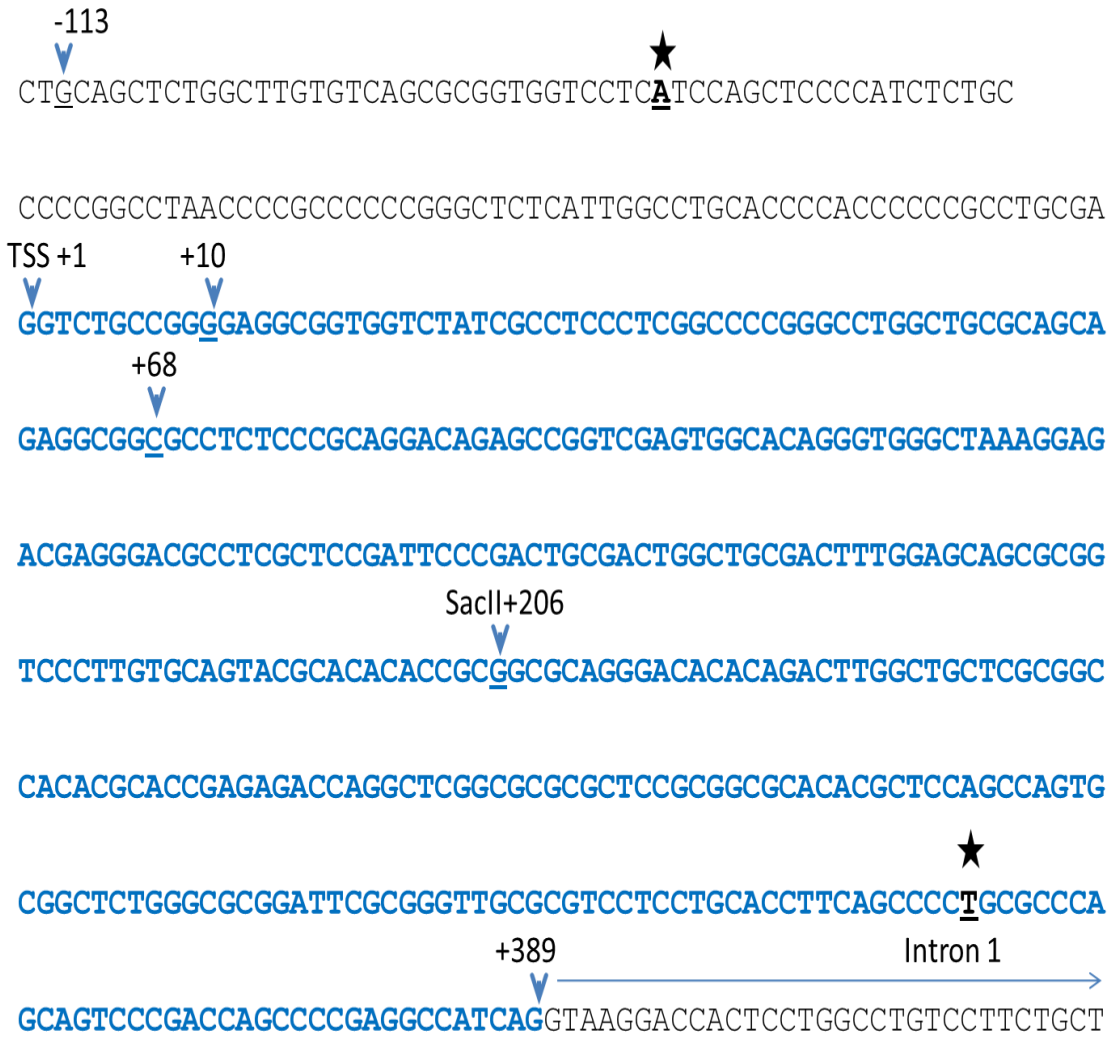

Figure 3.1:

The location of the TSS of various studies in relations to Ensembl TSS used in this study shown as TSS +1. The Aino et all study used +10 as a TSS, while Rodriguez-Henche et al used +68 as TSS. The minimum promoter region previously reported by Rodriguez-Henche et al is from -113 to the SacII site at +206. New minimum promoter region based on bioinformatic analysis from -80 to +353 marked with stars. Exon1 according to Ensemble database finishes at +389, intron 1 continues for about 7.8kb until start of exon 2. Underlined nucleotides marked with stars indicate new proposed basal promoter region Ad1 (see section 3.2.1.1 below).

3.2 Results of bioinformatic analysis

3.2.1 Species comparison of Adcyap1r1 promoter regions

Given the relative conservation of the Adcyap1r1 gene in function and expression across species, the sequences involved in regulating its expression should conserved across different species. To determine which regions of the Adcyap1r1 promoter are conserved across different species, human, chimpanzee, mouse and rat receptor gene sequences were compared.

The Adcyap1r1 gene is located on the forward strand of mouse chromosome 6 at positions 55451978-55501451 (Ensembl numbering). The nucleotide sequence and was downloaded from Ensembl (http://www.ensembl.org/index.html), including the region -6000 nucleotides upstream of the TSS, and 8179 nucleotides downstream of TSS to the start of Exon 2 was used for analysis.

Initially rVISTA software was used for pairwise comparison of the sequences and conserved regions are highlighted in *Figure 3.2a*. Subsequently, TF binding sites across each aligned pair of sequences were obtained. A very similar pattern of conserved regions was observed between each pairwise comparison. There were however, some differences between the different pairs of sequences being compared. To circumvent this problem the Genomatrix GEMS launcher tool was used, as it allowed the simultaneous comparison of all 4 sequences, and enabled finding possible TF-binding sites in conserved regions across all 4 species (*Figure.3.2b*). The rVISTA and Genomatrix comparisons showed a high degree of similarity in the location of conserved regions, and these are shown in *Figure 3.3*.

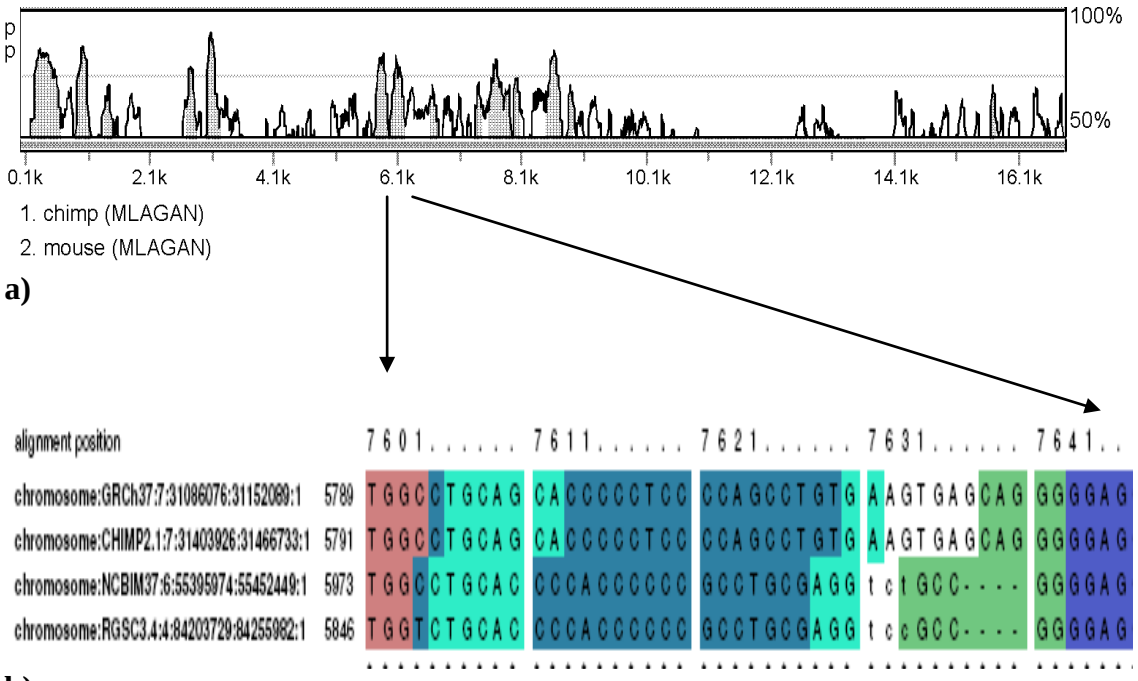

Figure 3.2

Bioinformatic analysis output showing a sample of the *Adcyap1r1* gene sequence comparison, in this case mouse and chimpanzee sequences using rVISTA **(a)** the peaks represent the % of conservation with the horizontal line representing a 75% threshold of conservation. The numbering at the bottom represent the full sequence -6000bp to exon 2, the 6k peak in panel **a** corresponds to TSS and exon 1 conserved region. Panel **(b)** shows a sample of Genomatrix output comparing, from top to bottom, human, chimpanzee, mouse and rat sequences of exon1 conserved region Ad1. This region shown corresponds to part of the rVISTA peak flanking and covering exon1 as shown by the arrows. The different coloured areas represent different TF binding sites in regions conserved across all 4 sequences.

3.2.1.1 Identification of Conserved regions

The bioinformatics analysis showed several cross species conserved regions (*Figure 3.3*). 3 of these are upstream of the +1 TSS, which were named AdU1 (-4540 to -4260), AdU2 (-3845 to -3710) and AdU3 (-2829 to -2627). 2 conserved regions were located downstream of exon 1, and these were named AdD1 (+1739 to +1965) and AdD2 (+2710 to +2860). A conserved region was found directly before the +1 TSS at the start of exon 1, and this was named Ad1, starting from -80 to +353 within exon 1 (exon 1 ends at +389) (Figure 3.1).

A previous study had reported that the basal promoter lies within the -113 bp upstream of the TSS (Rodríguez-Henche et al. 2002). The conserved region data presented here suggests that the basal promoter could be smaller and starts at -80.

A second observation noticed with the exon 1 conserved region, was that it stopped at +353 rather than the full length of the mouse exon 1 at +389. Carrying out a BLAST search using the mouse exon 1 sequence shows that there is a 91% identity with the rat exon 1 sequence and 72% identity with human and chimpanzee exon 1 sequences. These differences in the exon 1 sequences may account for why when aligned, the conserved Ad1 region in exon 1 does not cover the whole mouse sequence for exon 1.

3.2.2 Identification of Putative Transcription Factor Binding Sites

MatInspector tool in the Genomatrix software was used to analyse the various conserved regions for the presence of putative TF binding sites. The regions examined were AdU1, AdU2 and AdU3 (upstream regions); AdD1 and AdD2 (downstream regions); and Ad1 (exon 1) (*Figure 3.2*) and assess the sequence similarity to matrix (TF binding site). A matrix has a core sequence being essential, while other bases can have some variability (Cartharius et al. 2005). This would cause several TF to bind to similar matrices. The software compared the DNA sequence and calculated the matrix similarity as well as the optimised matrix

threshold which minimises the number of false positive matches. This analysis produced a large amount of matrix matches in the sequence; therefore a high threshold of similarity was used where matches with <0.85 optimised matrix threshold where rejected.

Putative TF binding sites were found in high concentrations in the conserved regions, where they often overlapped, and in some cases 20 to 30 different, overlapping, TF binding sites were clustered in a single conserved region. An example of this is the AdD1 +1739 to +1935 region which contained many different putative TF binding sites for C/EBP. Other examples of TF-binding sequences found in the conserved regions are AP-1, P-53, SP-1, CREB, NF-1 GATA-1, 2&3 and Pit-1. There were some TF binding sites identified in regions that were not conserved across species, but the majority of the TF binding sites, were found within the conserved regions. This would support the hypothesis that the major TF binding sites controlling gene expression would be conserved across several species.

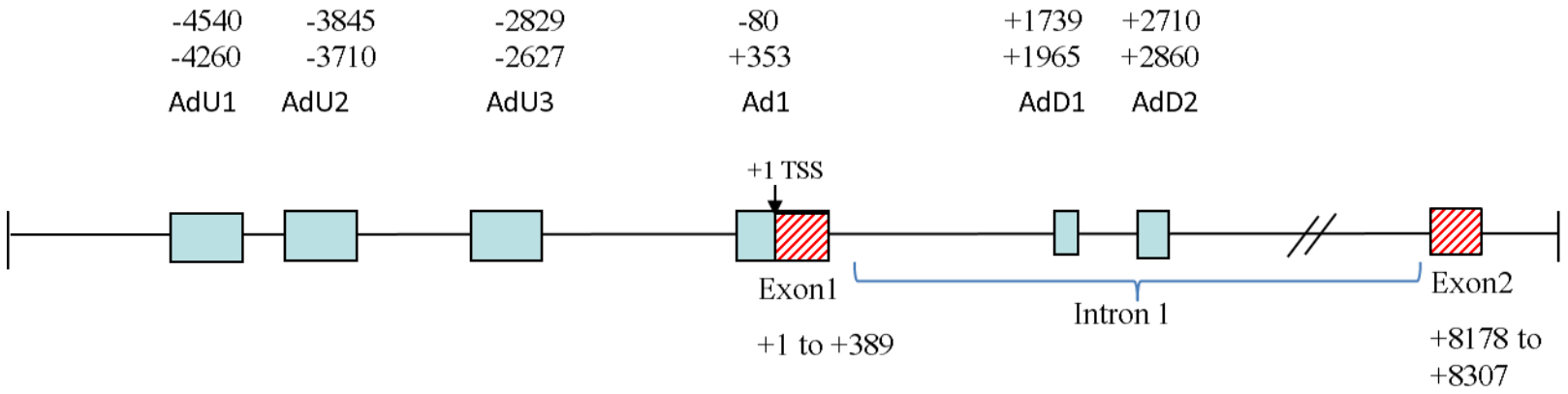

Figure 3.3:

A map of the mouse *Adcyap1r1* gene sequence starting -6000bp upstream of exon1 up to and including exon2 (line shaded boxes). The map shows a summary of the bioinformatic analysis, where the shaded boxes represent regions that are conserved across all 4 mamalian species compared. There are 3 upstream regions AdU1, AdU2 and AdU3; 2 downstream AdD1 and AdD2; the Ad1 conserved region started -80 to +353 which is almost at end of exon 1 which ends at +389 .The location of these regions is indicated in relation to start of TSS (+1) by the numbers above. Intron 1 is also indicated on the diagram starting at +390 and extending till +8177.

3.2.2.1 Ad1 TF binding sites

The 433 bp Ad1 conserved region (-80 to +353) showed a major cluster of matrices from -60 to +1 in the forward orientation (Figure 3.4). A list of TF binding sites in forward orientation are shown in Table.3.1. No sites for the binding of basal transcription factors or transcription initiation sites were identified in this region in the forward orientation.

TF-binding sites identified included several zinc finger TF such as ZBP89 and ZNF219, that are involved in cell proliferation, differentiation and apoptosis (Sakai et al. 2003; Zhang et al. 2010; Takigawa et al. 2010; Zhang et al. 2012). GLIS3 is a transcription factor involved in β-cell apoptosis and a susceptibility gene for type I and II diabetes (Nogueira et al. 2013). Also found in the -60 to +1bp cluster is a site for the early growth response 1 (EGR1) that is important in mitogenesis and cell differentiation, as well as apoptosis (Ravni et al. 2008; Jeon et al. 2013; Kang et al. 2013).

Across the rest of the Ad1, from +1 onwards within exon 1 several binding sites were identified for E2F, E2F2, E2F3 . These factors are involved in cell cycle and cancer (Dong et al. 2002; Tsantoulis and Gorgoulis 2005; Xanthoulis and Tiniakos 2013; Zhou et al. 2013). A BACH2 site was also identified and this is involved in B cell and T cell proliferation (Le Gallou et al. 2012; Tsukumo et al. 2013). A cell cycle-dependent element (CDE) binding site was present 5 times (Müller and Engeland 2010).

Most of these TF binding sites identified are involved in cell differentiation, apoptosis and cancer which would not be surprising given PAC1 receptors role in anti-apoptotic and in neuronal cell differentiation.

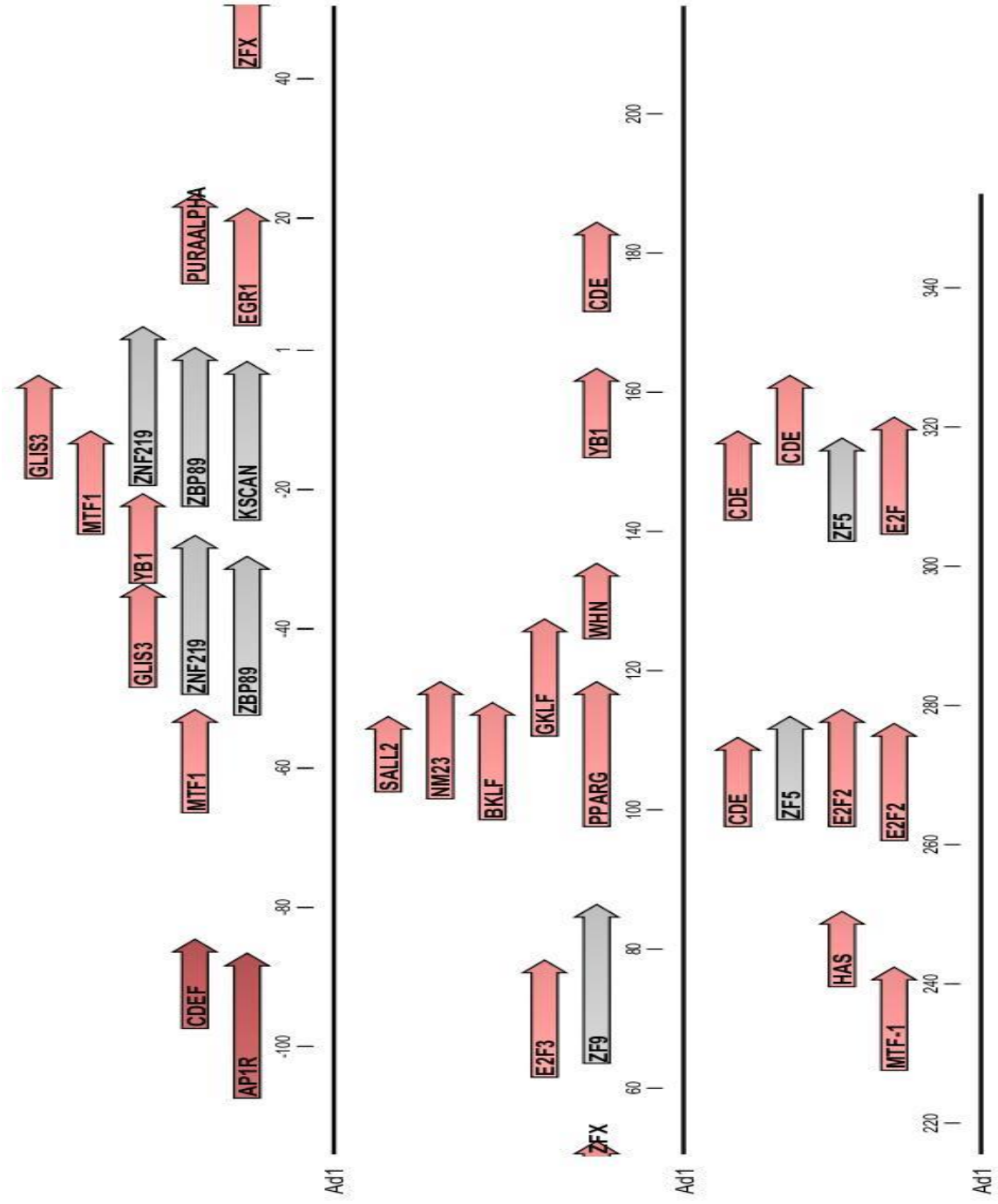

Figure 3.4 Ad1 Forward

Forward oriented TF binding sites for conserved region Ad1. Start of exon1 is marked as +1. TF matrices shown have >0.85 optimised matrix threshold.

Matrix	Matrix family	Description
BACH2	AP1R	Bach2 bound TRE
CDE	CDEF	Cell cycle-dependent element, CDF-1 binding site (CDE/CHR tandem elements regulate cell cycle dependent repression)
MTF-1	MTF1	Metal transcription factor 1, MRE
ZBP89	ZF02	Zinc finger transcription factor ZBP-89
ZNF219	ZF02	Kruppel-like zinc finger protein 219
GLIS3	GLIF	GLIS family zinc finger 3, Gli-similar 3
YB1	YBXF	Y box binding protein 1, has a preference for binding ssDNA
ZKSCAN3	ZF02	Zinc finger with KRAB and SCAN domains 3
EGR1	EGRF	EGR1, early growth response 1
PURALPHA	PURA	Purine-rich element binding protein A
ZFX	ZFXY	X-linked zinc finger protein
E2F3	E2FF	E2F transcription factor 3 (secondary DNA binding preference)
ZF9	ZF02	Core promoter-binding protein (CPBP) with 3 Krueppel-type zinc fingers, KLF6
BKLF	KLFS	Basic krueppel-like factor (KLF3)
NM23	NDPK	NME/NM23 nucleoside diphosphate kinase1 and 2
PPARG	PERO	Peroxisome proliferator-activated receptor gamma
SALL2	SAL2	Zinc finger protein Spalt-2, sal-like 2, p150(sal2)
GKLF	KLFS	Gut-enriched Krueppel-like factor, KLF4
WHN	WHNF	Winged helix protein, involved in hair keratinization and thymus epithelium differentiation
HAS	HASF	HIF-1 ancillary sequence
E2F2	E2FF	E2F transcription factor 2
ZF5	ZF5F	Zinc finger / POZ domain transcription factor
E2F	E2FF	E2F, involved in cell cycle regulation, interacts with Rb p107 protein

Table 3.1:
Full list of TF binding sites found in the forward orientation in conserved region Ad1. The table shows the name of the TF, matrix family it belongs to and the Genomatrix output description of the TF.

Similar to the forward orientation, A large cluster of TF binding sites was also found in the reverse orientation of Ad1, between -60 to +1bp (Figure 3.5). A list of TF binding sites in reverse are shown in Table.3.2. This cluster included 15 binding sites like the constitutive TF SP1 as well as a GC box site which also binds to SP1(Latchman 1998; Wierstra 2008). The cluster also included sites for members of the KLF family KKLF(KLF15) BKLF(KLF3) which are involved in proliferation, differentiation and apoptosis (Asada et al. 2010; Pearson et al. 2011; Mallipattu et al. 2012); and for AP2 which is involved in neuronal development and apoptosis (Mitchell et al.; 1991; Hilger-Eversheim et al. 2000), and the tumour suppressor CDP(CUX1) (Boultwood 2013).

Within Ad1 in exon 1, an important cluster at +120 to +160 can be seen that contains a CCAAT box involved in development, cell differentiation and also inducible transcription (Ramji and Foka 2002), as well as the transcription initiator (Thomas and Chiang 2006; Cianfrocco et al. 2013). Other transcription initiation elements are 3 Human Motif Ten Element (HMTE) sites (Thomas and Chiang 2006; Juven-Gershon and Kadonaga 2010; Cianfrocco et al. 2013). Within the +120 to +160 cluster was a site for the calcium response factor (CARF), an inducible, neurotrophic TF with roles in neuronal plasticity and survival (Xia and Storm 2002; Tao et al. 2002; West 2011). This cluster at +120 to +160 is downstream of a TF2B binding site present at +310bp, which may be part of an alternative transcription initiation complex (Thomas and Chiang 2006; Juven-Gershon and Kadonaga 2010). In positions +260 to +300 are 2 E2F2 binding sites and 3 sites for ZF5 which is may have some tumour suppressor effects (Numoto et al. 1995; Maia et al. 2012).

Overall, the general pattern in the Ad1 conserved region is 3 clusters of overlapping TF binding sites at -60 to +1, +100 to +160 and +260 to +300 both forward and reverse orientations. There appears to be a large number of sites for TF involved in cell-cycle, apoptosis, cell growth and development, such as ZBP89 ZNF219, E2F, CDE and KLF family. There were sites for several inducible and tissue specific TF such as CARF and BACH2. The main point of interest were the binding sites for TF involved in transcriptional initiation, including the HMTE CCAAT sites at +120 to +160bp and the TF2B site at +310, found in the reverse orientation supporting the presence of alternative transcription start sites.

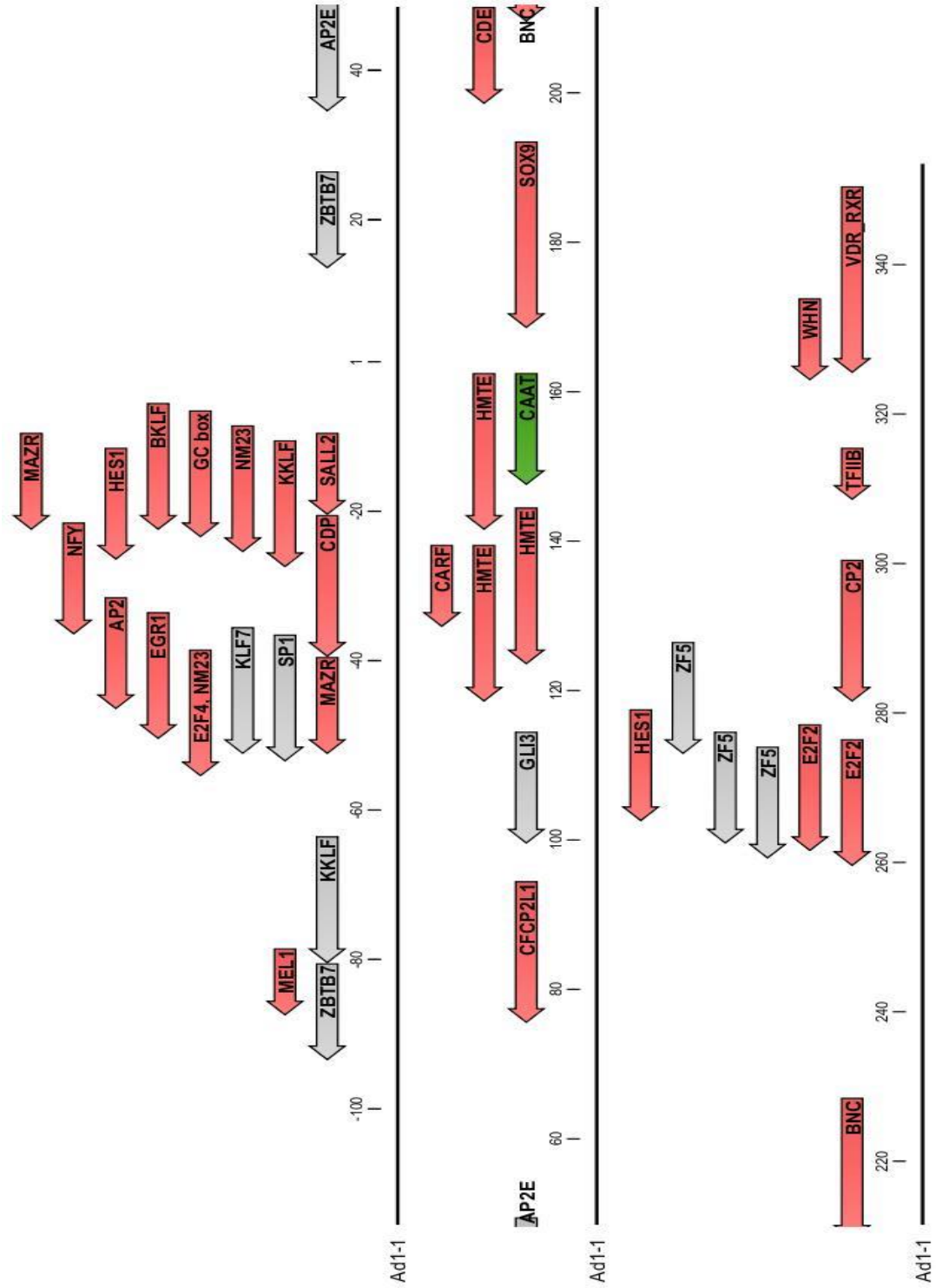

Figure.3.5 Ad1 Reverse

Reverse oriented TF binding sites for conserved region Ad1, start of exon1 is marked as +1. TF matrices shown have >0.85 optimised matrix threshold.

Matrix	Matrix family	Description
ZBTB7	ZF06	Zinc finger and BTB domain containing 7, Proto-oncogene FBI-1, Pokemon (secondary DNA binding preference)
MEL1	EVI1	MEL1 (MDS1/EVI1-like gene 1) DNA-binding domain 2
KKLF	KLFS	Kidney-enriched kruppel-like factor, KLF15
E2F4	E2FF	E2F transcription factor 4, p107/p130-binding protein
NM23	NDPK	NME/NM23 nucleoside diphosphate kinase1 and 2
SP1	SP1F	Stimulating protein 1, ubiquitous zinc finger transcription factor
KLF7	KLFS	Kruppel-like factor 7 (ubiquitous, UKLF)
MAZR	MAZF	MYC-associated zinc finger protein related transcription factor
EGR1	EGRF	EGR1, early growth response 1
AP2	AP2F	Activator protein 2 alpha
CDP	CLOX	Transcriptional repressor CDP (CCAAT displacement protein)
NFY	CAAT	Nuclear factor Y (Y-box binding factor)
HES1	HESF	Drosophila hairy and enhancer of split homologue 1 (HES-1)
GC	SP1F	GC box elements
BKLF	KLFS	Basic krueppel-like factor (KLF3)
SALL2	SAL2	Zinc finger protein Spalt-2, sal-like 2, p150(sal2)
SPZ1	SPZ1	Spermatogenic Zip 1 transcription factor
TCFAP 2E	AP2F	Transcription factor AP-2, epsilon
TCFCP 2L1	CP2F	Transcription factor CP2-like 1 (LBP-9)
GLI3	GLIF	GLI-Kruppel family member GLI3
HMTE	MTEN	Human motif ten element
CARF	CARE	Calcium-reponse factor
CAAT	CAAT	Cellular and viral CCAAT box
SOX9	SORY	SRY (sex-determining region Y) box 9
CDE	CDEF	Cell cycle-dependent element, CDF-1 binding site (CDE/CHR tandem elements regulate cell cycle dependent repression)
BNC	BNCF	Basonuclin, cooperates with UBF1 in rDNA PolI transcription
E2F2	E2FF	E2F transcription factor 2
ZF5	ZF5F	Zinc finger / POZ domain transcription factor
CP2	CP2F	CP2
BRE	TF2B	Transcription factor II B (TF2B) recognition element
WHN	WHNF	Winged helix protein, involved in hair keratinization and thymus epithelium differentiation
VDR_RXR	RXRF	VDR/RXR Vitamin D receptor RXR heterodimer, DR3 sites

Table 3.2:
Full list of TF binding sites found in the reverse orientation in conserved region Ad1. The table shows the name of the TF, matrix family it belongs to and the Genomatrix output description of the TF.

3.2.2.2 Ad2 TF binding sites

The minimum promoter reported by Rodriguez-Henche 2002 et al starts -113bp from the TSS to SacII site at +206bp in exon 1. Other clones tested included a -323 to +206 clone and had comparable expression to the minimum promoter reported(Rodríguez-Henche et al. 2002). The 386 bp Ad2 conserved region starts at -180 to +206 and therefore overlaps with the Ad1 region (-80 to +353) as shown above. Ad2 was chosen to mimic Rodriguez-Henche minimum promoter but include the 65 bp -180 to -115 region, which is not present in Ad1 is shown below (*Figure 3.6*). This region has a very interesting cluster of TF binding sites located at around -140. In the forward orientation there are 2 binding sites, namely for TF2B, involved in transcriptional initiation (Thomas and Chiang 2006) and for oncogene pleomorphic adenoma gene 1 (PLAG1) (Bahrami et al. 2012; Akhtar et al. 2012). A list of the TF binding sites found in Ad2 are shown in Table 3.3.

In the same region of Ad2 in the reverse orientation a site for E2F binding was identified. This TF is involved in the cell cycle and cancer (Dong et al. 2002; Tsantoulis and Gorgoulis 2005; Xanthoulis and Tiniakos 2013; Zhou et al. 2013). This was in addition to a site for EGR1 binding, a TF important in mitogenesis, cell differentiation and apoptosis (Ravni et al. 2008; Jeon et al. 2013; Kang et al. 2013). Binding sites also found in the -140 cluster of Ad2 were for: RFX1, an inducible TF modulating the immune system and appears to be critical in mouse survival (Feng et al. 2009; Zhao et al. 2010b; Zhao et al. 2010a); ZBTB7, (also known as Pokémon) involved in cancer and cell lineage development (Aggarwal et al. 2010; Lee and Maeda 2012); PURα, an evolutionarily conserved TF important in postnatal neuronal development, cancer and cell cycle regulation (Gallia et al. 2000; White et al. 2009).

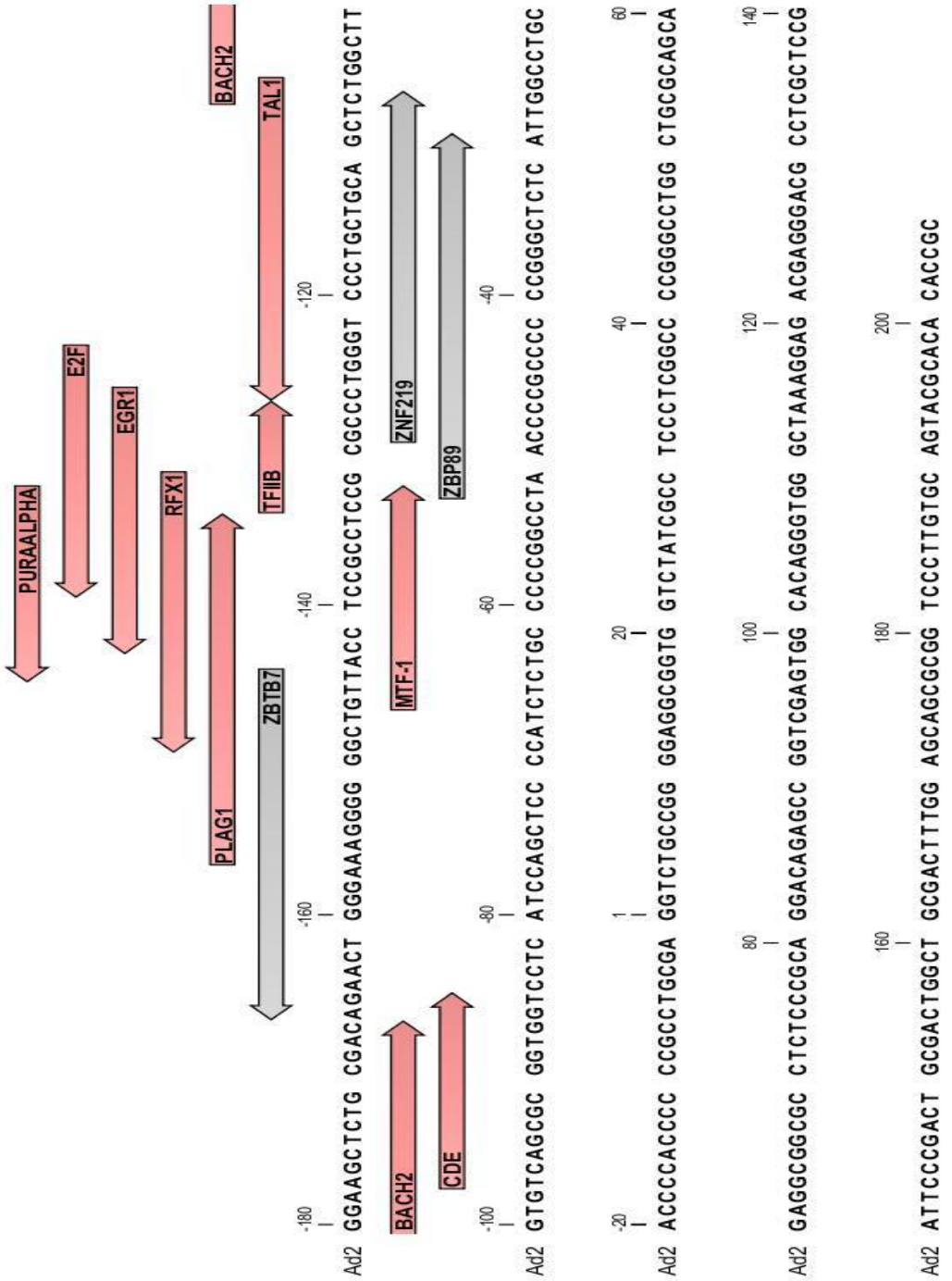

Figure 3.6

Forward and reverse oriented TF binding sites for conserved region Ad2, start of exon1 is marked as +1. TF binding sites shown are between -180bp and -80bp, downstream TF binding sites located -80bp to end of exon 1 to are same as Ad1 (shown above Figure.12). TF matrices shown have >0.85 optimised matrix threshold.

Matrix	Matrix family	Description	Orientation
PLAG1	PLAG	Pleomorphic adenoma gene 1	(+)
BRE	TF2B	Transcription factor II B (TF2B) recognition element	(+)
ZBTB7	ZF02	Zinc finger and BTB domain containing 7, Proto-oncogene FBI-1, Pokemon	(-)
RFX1	XBBF	X-box binding protein RFX1	(-)
PURALPHA	PURA	Purine-rich element binding protein A	(-)
EGR1	EGRF	EGR1, early growth response 1	(-)
E2F	E2FF	E2F, involved in cell cycle regulation, interacts with Rb p107 protein	(-)
TAL1_E2A	HAND	T-cell acute lymphocytic leukemia 1, SCL	(-)

Table 3.3:
Full list of TF binding sites found in conserved region Ad2. Orientation is marked by (+) for forward and (–) for reverse. The table shows the name of the TF, matrix family it belongs to and the Genomatrix output description of the TF.

3.2.2.3 AdU1 TF binding sites

AdU1 conserved region is located furthest upstream of exon 1 at position -4540 to -4260. Multiple TF binding sites are present in the forward orientation, most of which are concentrated in a massive overlapping cluster (*Figure.3.7* and *Table 3.4*).
This cluster includes binding sites for several TF involved in neural development such as LMX1B involved in differentiation and proliferation of dopaminergic and serotonergic neurons (Lin et al. 2009; Song et al. 2011; Yan et al. 2013); and DLX1 which plays a role in the hippocampal GABAergic neuron development (Long et al. 2009; Jones et al. 2011). Binding sites for the POU family of TF are also present, with BRN3 (Pou4F1), ganglia and Oct-1 (POU2F1) which play a role in neuronal cell development and differentiation of retinal and dorsal root ganglia (Latchman 1999; Liu et al. 2000; Wang et al. 2002; Kiyota et al. 2008). Oct-1 also plays a role in cell stress response as well as cancer and cellular metabolism (Park et al. 2009; Wang et al. 2013). Outside this central cluster are several other developmental TF binding sites, such as for Myelin transcription factor 1 (MYT1) and TCF7L1 T cell specific homeobox, both of which are involved in neural cell differentiation and cell lineage development respectively (Vana et al. 2007; Mao and Byers 2011; Sorrell et al. 2013). The binding site for STAT, involved in immune response and apoptosis (Wang et al. 2012), and MEIS1 which plays a role in the embryonic development of the brain (Barber et al. 2013) were also found outside the initial cluster.

In the reverse orientation (Figure 3.8, Table 3.5) there is a TF binding site cluster at a similar position to the forward orientation. The 120 to -150 cluster contained several binding sites for TF involved in neuronal development such as PAX6, Oct-1 and DLX2 HOXC13 (Yun et al. 2001; Bel-Vialar et al. 2007; Kiyota et al. 2008; Long et al. 2009; Carney et al. 2009; van de Ven et al. 2011) as well as other TF motifs such as one for the product of the Y chromosome SRY male sex determining gene responsible for testes development (Clement et al. 2011). Other TF motifs include tissue specific GATA-6 involved in embryogenesis and steroidogenic cell differentiation (Kiiveri et al. 2002; Rong et al. 2012). Downstream of the TF cluster at 120 there are several other developmental TF motifs that bind factors involved in

neuronal development such as the HOXC13 and GSH2 homeoboxes (Yun et al. 2001; van de Ven et al. 2011). There are also binding sites for the
tissue specific GATA-1 factor involved in erythropoiesis; CKROX which has a role in T cell lineage commitment (Joulin et al. 1991; Fujiwara et al. 1996; Sun et al. 2005); and STAT3 which is phosphorylated by cytokines such as IL-6 and IFN playing a role in inflammation and apoptosis (Icardi et al. 2012; Wang et al. 2012; Kurosaka and Machida 2013).

Unlike the situation in Ad1 and Ad2, there are no transcription initiation motifs in AdU1, which is as expected, given its distance from the TSS. There was however a very high concentration of sites for homeodomain TFs. These included HOXC13, PAX6, GSH1 & 2, MIES1, DLX1 and the POU family such as OCT-1 and BRN3. Most of these TFs are involved in the differentiation and development of the nervous system and many were clustered at ~120 to 150 in both the forward and reverse orientations; the rest were spread out throughout the AdU1 clone. Some of the Homeobox TFs show inducible functions such as Oct-1, which also plays a role in immune-modulation. TF binding sites for TFs other than homeoboxes were also present, such as for SRY involved in testicular development, and for STAT3, which plays an important role in inflammation and apoptosis.

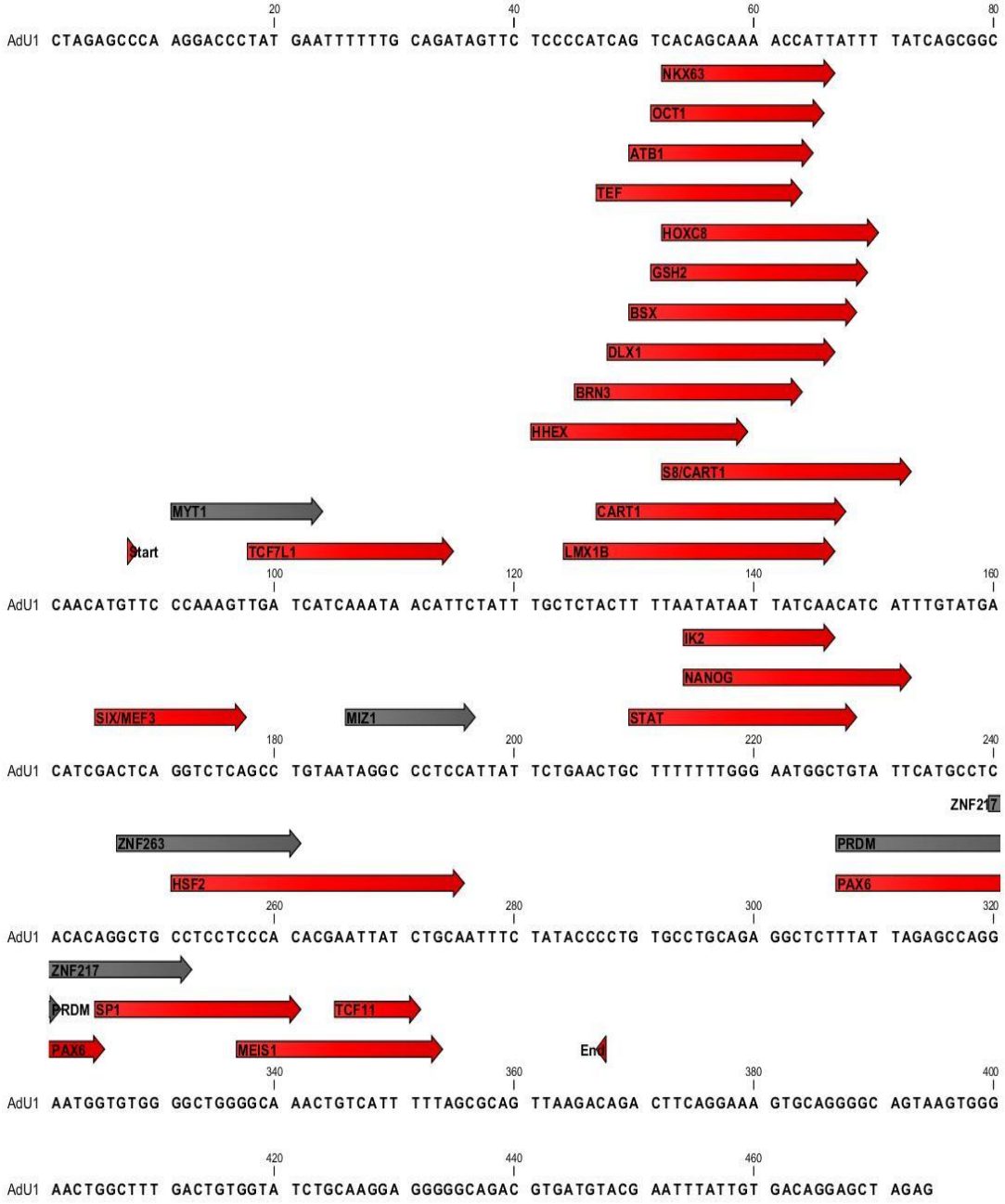

Figure 3.7

Forward and oriented TF binding sites for conserved region AdU1, start and end of conserved region are indicated by arrows. TF matrices shown have >0.85 optimised matrix threshold.

Matrix	Matrix family	Description
MYT1	MYT1	MyT1 zinc finger transcription factor involved in primary neurogenesis
TCF7L1	LEFF	HMG box transcription factor Tcf7l1 (TCF3)
HHEX	HOMF	Hematopoietically expressed homeobox, proline-rich homeodomain protein
LMX1B	LHXF	LIM-homeodomain transcription factor
BRN3	BRNF	Brn-3, POU-IV protein class
CART1	CART	Cart-1 (cartilage homeoprotein 1)
TEF	PARF	Thyrotrophic embryonic factor
DLX1	DLXF	DLX-1, -2, and -5 binding sites
BSX	HOMF	Brain specific homeobox
SATB1	SATB	Special AT-rich sequence-binding protein 1, predominantly expressed in thymocytes, binds to matrix attachment regions (MARs)
GSH2	HBOX	Homeodomain transcription factor Gsh-2
Oct-01	Oct-01	Octamer-binding transcription factor-1, POU class 2 homeobox 1 (POU2F1)
S8	CART	Binding site for S8 type homeodomains
NKX63	NKX6	NK6 homeobox 3
HOXC8	HOXF	Homeobox C8 / Hox-3alpha
SIX	MEF3	Binding sites for Six1, Six4 and Six5
MIZ1	MIZ1	Myc-interacting Zn finger protein 1, zinc finger and BTB domain containing 17 (ZBTB17)
STAT	STAT	Signal transducers and activators of transcription
IK2	IKRS	Ikaros 2, potential regulator of lymphocyte differentiation
NANOG	HOXF	Homeobox transcription factor Nanog
ZNF263	ZF07	Zinc finger protein 263, ZKSCAN12 (zinc finger protein with KRAB and SCAN domains 12)
HSF2	HEAT	Heat shock factor 2
PAX6	PAX6	PAX6 paired domain and homeodomain are required for binding to this site
PRDM14	ZF10	PR domain zinc finger protein 14
ZNF217	ZF03	Zinc finger protein 217
SP1	SP1F	Stimulating protein 1, ubiquitous zinc finger transcription factor
MEIS1	TALE	Binding site for monomeric Meis1 homeodomain protein
TCF11	TCFF	TCF11/LCR-F1/Nrf1 homodimers

Table 3.4

Full list of TF binding sites found in forward orientation in conserved region AdU1. The table shows the name of the TF, matrix family it belongs to and the Genomatrix output description of the TF.

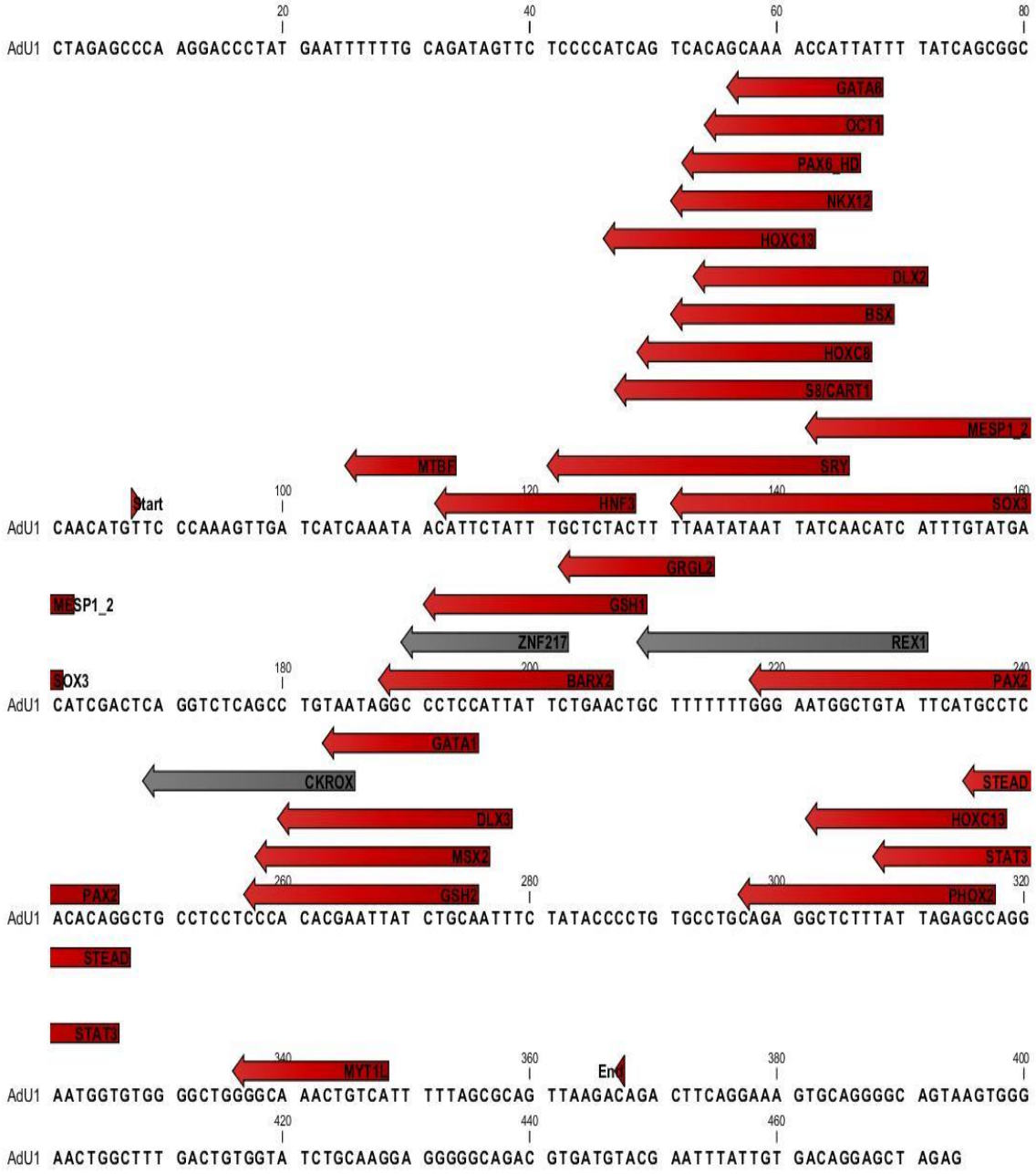

Figure 3.8

Reverse oriented TF binding sites for conserved region AdU1, start and end of conserved region are indicated by arrows. TF matrices shown have >0.85 optimised matrix threshold.

Matrix	Matrix family	Description
MTBF	HMTB	Muscle-specific Mt binding site
HNF3	FKHD	Hepatocyte nuclear factor 3 (alpha, beta) (FOXA1, FOXA2)
SRY	SORY	Sex determining region Y
HOXC13	ABDB	Homeodomain transcription factor HOXC13
S8	CART	Binding site for S8 type homeodomains
HOXC8	HOXF	Homeobox C8 / Hox-3alpha
BSX	HOMF	Brain specific homeobox
NKX12	NKX1	NK1 homeobox 2, Sax1-like
PAX6_HD	PAXH	Paired box 6, homeodomain binding site
DLX2	DLXF	Distal-less homeobox 2
Oct-1	Oct--1	Octamer-binding transcription factor-1, POU class 2 homeobox 1 (POU2F1)
GATA6	GATA	GATA-binding protein 6
SOX3	SORY	SRY-box containing gene 3
MESP1_2	HAND	Mesoderm posterior 1 and 2
BARX2	HOMF	Barx2, homeobox transcription factor that preferentially binds to paired TAAT motifs
ZNF217	ZF03	Zinc finger protein 217
GSH1	HBOX	Homeobox transcription factor Gsh-1
GRHL2	GRHL	Grainyhead-like 2 (BOM, TFCP2L3)
REX1	YY1F	REX1 transcription factor; zinc finger protein 42
PAX2	PAX5	Paired box protein 2
CKROX	EGRF	Collagen krox protein (zinc finger protein 67 - zfp67)
GSH2	HBOX	Homeodomain transcription factor Gsh-2
MSX2	HOMF	Muscle-segment homeobox 2, msh homeobox 2
DLX3	DLXF	Distal-less homeobox 3
GATA1	GATA	GATA-binding factor 1
PHOX2	CART	Phox2a (ARIX) and Phox2b
HOXC13	ABDB	Homeodomain transcription factor HOXC13
STAT3	STAT	Signal transducer and activator of transcription 3
TEAD	TEAF	TEA domain-containing factors, transcriptional enhancer factors 1,3,4,5
MYT1L	MYT1	Myelin transcription factor 1-like, neuronal C2HC zinc finger factor 1

Table 3.5

Full list of TF binding sites found in reverse orientation in conserved region AdU1.The table shows the name of the TF, matrix family it belongs to and the Genomatrix output description of the TF.

3.2.2.4 AdU2 TF binding sites

The second upstream region AdU2 is located -3845 to -3710 upstream of the TSS and is 135 bp long. Unlike the other conserved regions the TF binding sites in this region were spread throughout AdU2, with no clear overlapping clusters of TF binding sites (Figure 3.9 and Table 3.7). In the forward orientation there are several developmental TF binding sites such as for the neuronal BRN2 TF involved in embryonic neuronal development (Dominguez et al. 2012); for NANOG expressed in ESCs and implicated in pluripotency (Rodda et al. 2005; Darr et al. 2006). Other developmental TF motifs include those for TCFAP2A (activator protein 2α) which plays an important role in early embryonic neural development, cell cycle and apoptosis (Hilger-Eversheim et al. 2000), as well as for SPL1(PU1) involved in hematopoietic T cell development (Franco et al. 2006). Several binding sites for inducible TF are also present, including those involved in immune system modulation such as AP-1 which is regulated by cytokines and stress stimuli controlling cell differentiation and apoptosis (Hess et al. 2004; Wagner 2010). Other motifs present for inducible/immune TF include Interferon response factor 7 (IRF7) which is activated as a response to viral infections (Ersing et al. 2013) and STAT5 which mediates cytokine activation and cell apoptosis (Le Gallou et al. 2012; Jung et al. 2013).

In the reverse orientation of the AdU2 conserved region there are repeats of motifs for the inducible/immune modulating AP-1 and STAT5. Also present, are 2 motifs for the cell cycle regulator HBP1 which shuts down proliferation of cells and acts as a transcriptional repressor (Sampson et al. 2001; Xiu et al. 2003). TF binding sites for the B cell lymphoma 6 protein BCL6 were located overlapping the STAT5 site, BCL6 acts as a regulator of T cell and B cell differentiation in lymphoid germinal centres (Basso and Dalla-Favera 2012; Okada et al. 2012). A binding site for the Homeobox protein TGIF1 was identified, which in addition to its role in brain development has an role in the immune system regulating necrosis via TNF-α (Demange et al. 2009; Taniguchi et al. 2012).

In summary, the AdU2 conserved region has far fewer binding sites for TF associated with brain development such as BRN2 and TGIF1 compared to AdU1. Mostly however, there are binding sites for TFs involved in immune cell activation and proliferation such as BCL-6, STAT5, SPL1 and AP-1. Several of the TF also play roles in apoptosis and control of the cell cycle like transcriptional repressor HBP1 and AP-1 and AP-2α.

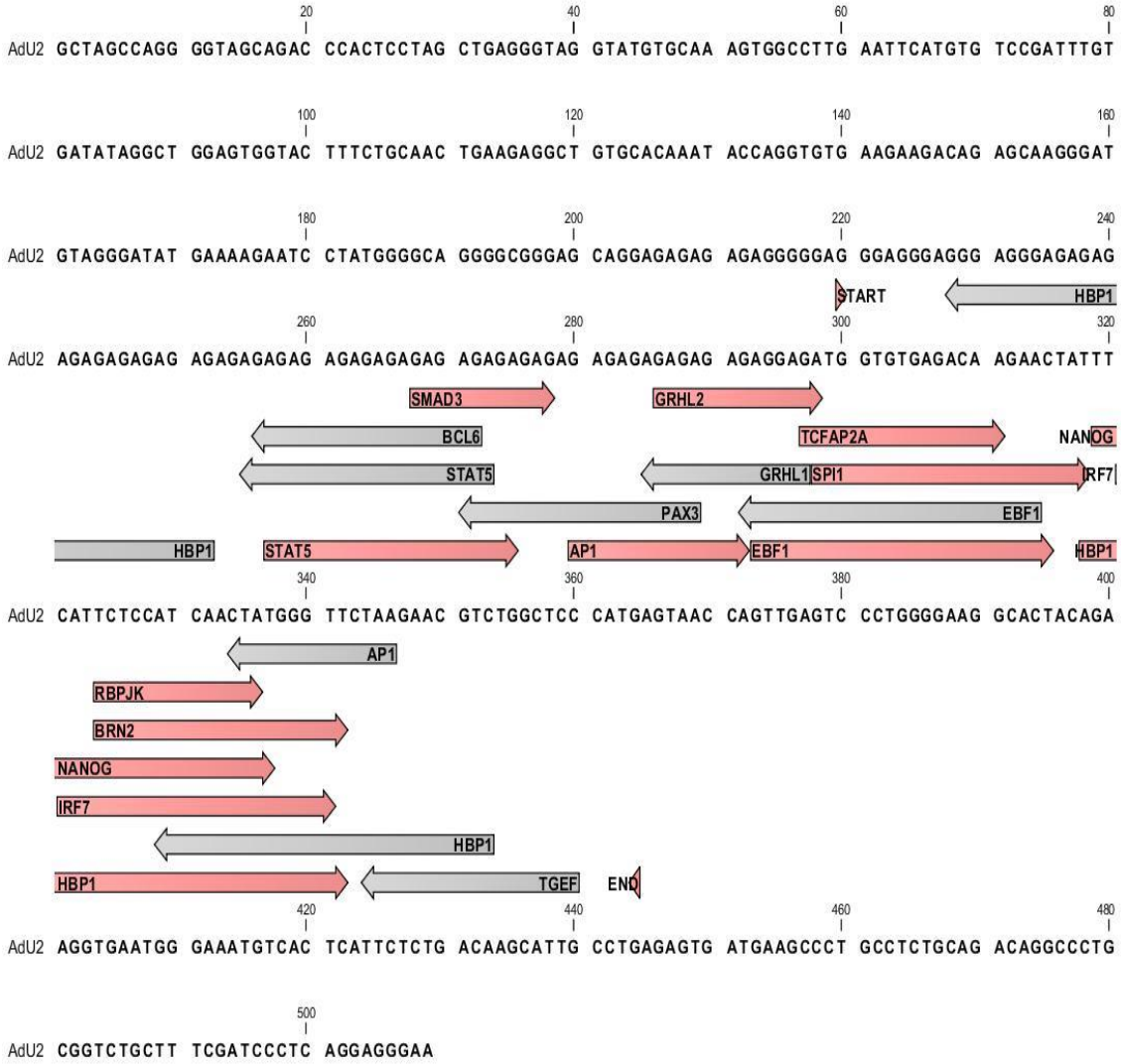

Figure 3.9

Forward and reverse oriented TF binding sites for conserved region AdU2, , start and end of conserved region are indicated by arrows. TF matrices shown have >0.85 optimised matrix threshold.

Matrix	Matrix family	Description	Orientation
STAT5	STAT	STAT5: signal transducer and activator of transcription 5	(+)
SMAD3	SMAD	Smad3 transcription factor involved in TGF-beta signaling	(+)
AP1	AP1F	Activator protein 1	(+)
GRHL2	GRHL	Grainyhead-like 2 (BOM, TFCP2L3)	(+)
EBF1	NOLF	Early B-cell factor 1	(+)
TCFAP2A	AP2F	Transcription factor AP-2, alpha	(+)
SPI1	ETSF	SPI-1 proto-oncogene; hematopoietic transcription factor PU.1	(+)
HBP1	SORY	HMG box-containing protein 1	(+)
NANOG	HOXF	Homeobox transcription factor Nanog	(+)
IRF7	IRFF	Interferon regulatory factor 7 (IRF-7)	(+)
RBPJK	RBPF	Mammalian transcriptional repressor RBP-Jkappa/CBF1	(+)
BRN2	BRNF	Brn-2, POU-III protein class	(+)
HBP1	SORY	HMG box-containing protein 1	(-)
STAT5	STAT	STAT5: signal transducer and activator of transcription 5	(-)
BCL6.04	BCL6	B-cell CLL/lymphoma 6, member B (BCL6B)	(-)
PAX3	PAX3	Pax-3 paired domain protein	(-)
GRHL1	GRHL	Grainyhead-like 1 (LBP32, MGR, TFCP2L2)	(-)
EBF1	NOLF	Early B-cell factor 1	(-)
HBP1	SORY	HMG box-containing protein 1	(-)
AP1	AP1F	Activator protein 1	(-)
TGIF	TALE	TG-interacting factor belonging to TALE class of homeodomain factors	(-)

Table 3.6

Full list of TF binding sites found in in conserved region AdU2. Orientation is marked by (+)for forward (–) for reverse.The table shows the name of the TF, matrix family it belongs to and the Genomatrix output description of the TF.

3.2.2.5 AdU3 TF binding sites

The AdU3 conserved region is 202 bp long, located -2829 to -2627 upstream of exon 1, and is the closest of the upstream conserved regions to exon 1. Most of the forward oriented TF binding sites in this region are present in an overlapping cluster located ~220bp to ~250bp (Figure. 3.10 and Table 3.7). Several of them are associated with brain development such as BRN4 (POU3F4) and Oct-1 (POU2F1) which play a role in neuronal cell development and differentiation (Latchman 1999; Liu et al. 2000; Wang et al. 2002; Kiyota et al. 2008) and ISL2 (LIM homeobox) involved in differentiation and maturation of motor neurons and pattern formation of embryonic neural tube (Tsuchida et al. 1994). MSX (homeobox, msh-like 1 and 2) TF binding site for MSX-1 and MSX-2 is another example of neural developmental TF, where it's important for craniofacial development and survival of neural crest cells (Cillo et al. 2001). There were also 2 DLX2 sites which are involved in GABAergic neuron development (Long et al. 2009). Several other developmental TF sites not involved in brain/CNS developments were found in the ~220bp cluster. Examples of this are like HOXA3 which promotes hematopoietic differentiation (Mahdipour et al. 2011) and HOXD1 which regulates angiogenesis (Park et al. 2011). A nuclear factor Y (NFY) binding site which binds to CCAAT box (Dolfini et al. 2012) is present in the ~220 cluster. NFY shows tissue specific and developmental activation of genes and is part of the constitutive transcription machinery of several genes (Maity and de Crombrugghe 1998; Zhu et al. 2012).

Downstream of the cluster of TF binding sites at 220 to 250 are binding sites for KKLF(KLF15) which induces podocyte differentiation in kidneys (Asada et al. 2010; Pearson et al. 2011; Mallipattu et al. 2012). There is also a binding site for ZFX, x-linked zinc finger protein, which modulates the proliferation and apoptosis of glioma cells and the renewal of ECs and hematopoietic Stem cells (HCS). There is also a NF-1 binding site at 343bp position near the end of the conserved region. NF-1 is a constitutive TF which can stimulate genes with CCAAT boxes, as well as having developmental functions in synapse and dendrite formation from cerebellar granule cells (Latchman 1998; Kilpatrick et al. 2012).

In the reverse orientation a TF binding site cluster is located at~220 to ~250 similar to the forward orientation (Figure 3.11 and Table 3.8). It contains binding sites for several TF involved in neural development such as Oct-1 (POU2F1) which plays a role in neuronal cell development and differentiation of retinal and dorsal root ganglia (Latchman 1999; Liu et al. 2000; Wang et al. 2002; Kiyota et al. 2008) and also plays a role in cell stress response as well as cancer and cellular metabolism (Park et al. 2009; Wang et al. 2013), BRN4 (POU3F4) and GSH2 homeoboxes. There is also a site for DLX1 binding which plays a role in the hippocampal GABAergic neuron development (Long et al. 2009; Jones et al. 2011). There is also a site for tissue specific GATA-1 involved in erythropoiesis (Fujiwara et al. 1996; Pope and Bresnick 2010) and for GATA-4 which induces cardiomyocyte-like cells from fibroblast as well as having an important regulatory role in cardiac development (Kiiveri et al. 2002; Ola et al. 2010).

The AdU3 conserved regions like the other upstream regions, AdU1 and AdU2, has several neuronal developmental TF and such as OCT-1, BRN4 and DLX1&2. There are several TF binding sites associated with cardiac development such as GATA-4 and hematopoietic modulation such as GATA-1 and HOXA3. Interestingly TF NFY and NF-1 both are associated with CCAAT boxes which play a role in the transcriptional initiation mechanism.

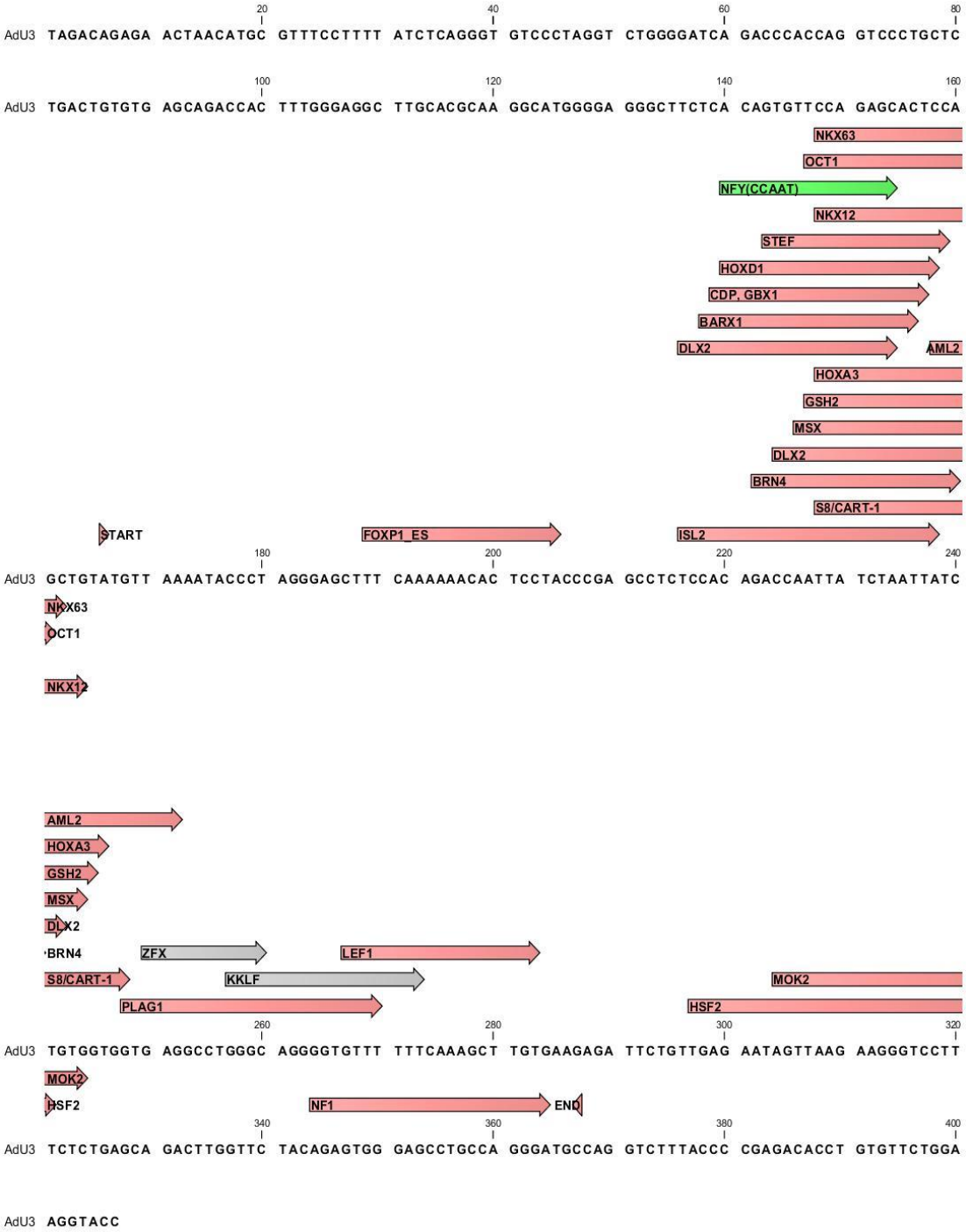

Figure 3.10

Forward oriented TF binding sites for conserved region AdU3, start and end of conserved region are indicated by arrows. TF matrices shown have >0.85 optimised matrix threshold.

Matrix	Matrix family	Description
FOXP1_ES	FKHD	Alternative splicing variant of FOXP1, activated in ESCs
DLX2	DLXF	Distal-less homeobox 2
ISL2	LHXF	ISL LIM homeobox 2
BARX1	HOMF	BARX homeobox 1
CDP	CLOX	Transcriptional repressor CDP
GBX1	HBOX	Gastrulation brain homeobox 1
NFY.04	CAAT	Nuclear factor Y (Y-box binding factor)
HOXD1	HOXF	Homeobox D1 / Hox-4gamma
BRN4	BRNF	POU domain transcription factor brain 4
TEF	PARF	Thyrotrophic embryonic factor
DLX2	DLXF	Distal-less homeobox 2
MSX	HOMF	Homeodomain proteins MSX-1 and MSX-2
GSH2	HBOX	Homeodomain transcription factor Gsh-2
Oct-01	Oct-01	Octamer-binding transcription factor-1, POU class 2 homeobox 1 (POU2F1)
S8	CART	Binding site for S8 type homeodomains
NKX12	NKX1	NK1 homeobox 2, Sax1-like
HOXA3	HOXF	Homeobox A3
NKX63	NKX6	NK6 homeobox 3
AML2	HAML	RUNX3 (Runt-related transcription factor 3), AML2 (Acute myeloid leukemia 2)
PLAG1	PLAG	Pleomorphic adenoma gene (PLAG) 1, a developmentally regulated C2H2 zinc finger protein
ZFX	ZFXY	X-linked zinc finger protein
KKLF	KLFS	Kidney-enriched kruppel-like factor, KLF15
LEF1	LEFF	TCF/LEF-1, involved in the Wnt signal transduction pathway
HSF2	HEAT	Heat shock factor 2
MOK2	MOKF	Ribonucleoprotein associated zinc finger protein MOK-2 (human)
NF1	NF1F	Non-palindromic nuclear factor I binding sites

Table 3.7

Full list of TF binding sites found in forward orientation in conserved region AdU3.The table shows the name of the TF, matrix family it belongs to and the Genomatrix output description of the TF.

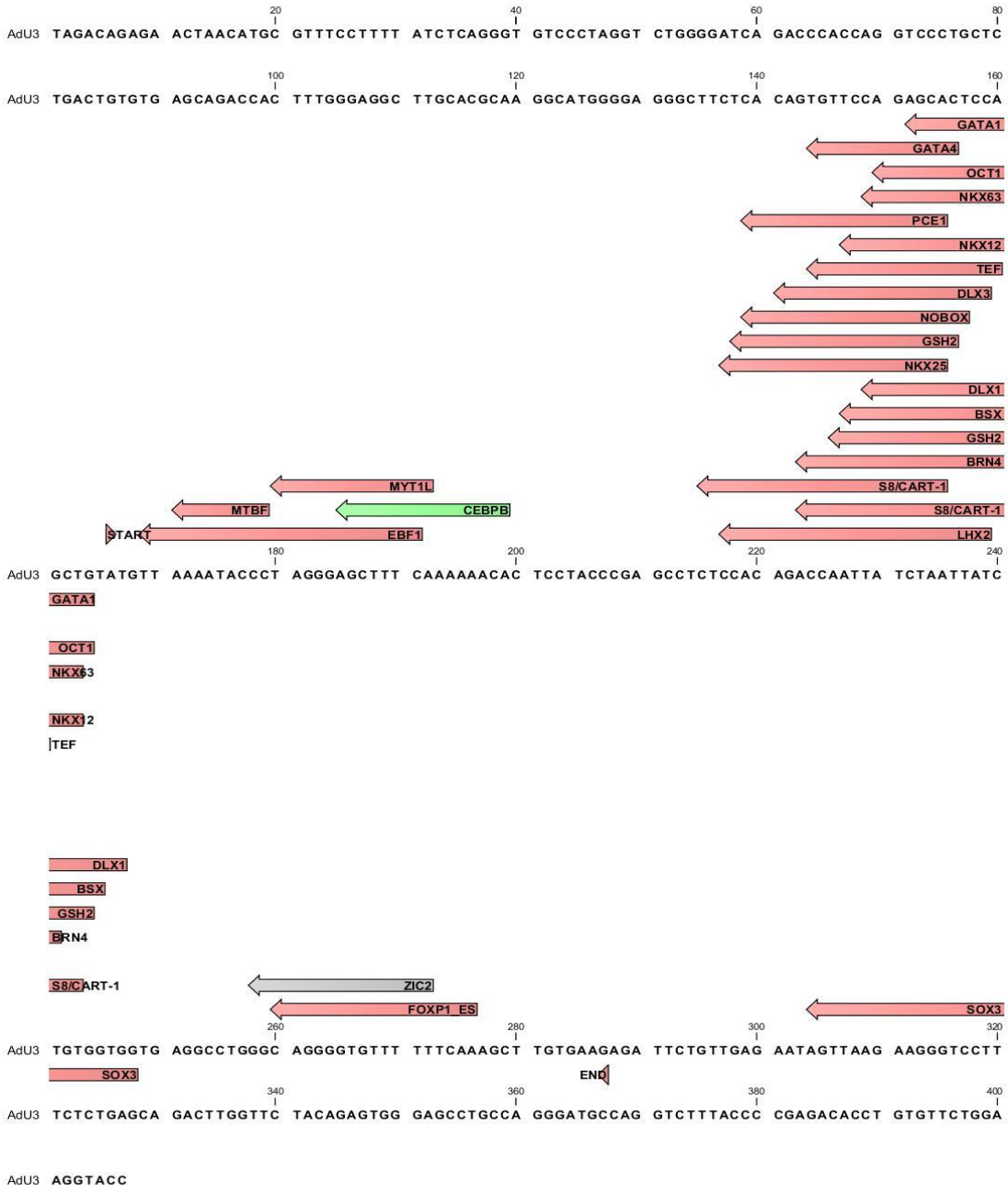

Figure 3.11

Reverse oriented TF binding sites for conserved region AdU3, , start and end of conserved region are indicated by arrows. TF matrices shown have >0.85 optimised matrix threshold.

Matrix	Matrix family	Description
EBF1	NOLF	Early B-cell factor 1
MTBF	HMTB	Muscle-specific Mt binding site
MYT1L	MYT1	Myelin transcription factor 1-like, neuronal C2HC zinc finger factor 1
CEBPB	CEBP	CCAAT/enhancer binding protein beta
S8	CART	Binding site for S8 type homeodomains
NKX25	NKXH	Homeo domain factor Nkx-2.5/Csx, tinman homolog low affinity sites
LHX2	LHXF	LIM homeobox 2
GSH2	HBOX	Homeodomain transcription factor Gsh-2
NOBOX	HOMF	Homeobox containing germ cell-specific transcription factor NOBOX
PCE1	BCDF	Photoreceptor conserved element 1
DLX3	DLXF	Distal-less 3 homeodomain transcription factor
S8	CART	Binding site for S8 type homeodomains
BRN4	BRNF	POU domain transcription factor brain 4
GATA4	GATA	GATA binding protein 4
TEF	PARF	Thyrotrophic embryonic factor
GSH2	HBOX	Homeodomain transcription factor Gsh-2
BSX	HOMF	Brain specific homeobox
NKX12	NKX1	NK1 homeobox 2, Sax1-like
DLX1	DLXF	DLX-1, -2, and -5 binding sites
NKX63	NKX6	NK6 homeobox 3
Oct-01	Oct-01	Octamer-binding transcription factor-1, POU class 2 homeobox 1 (POU2F1)
GATA1	GATA	GATA-binding factor 1
ZIC2	GLIF	Zinc finger transcription factor, Zic family member 2 (odd-paired homolog, Drosophila)
FOXP1_ ES	FKHD	Alternative splicing variant of FOXP1, activated in ESCs
SOX3	SORY	SRY-box containing gene 3

Table 3.8
Full list of TF binding sites found in reverse orientation in conserved region AdU3. The table shows the name of the TF, matrix family it belongs to and the Genomatrix output description of the TF.

3.2.2.6 AdD1 TF binding sites

The AdD1 downstream conserved regions is located +1739 to +1965 downstream of the TSS and is 226bp long. There appears to be a clear difference compared to other conserved regions where most of the TF binding sites are located in the reverse orientation (Figure 3.12; Table 3.9). In the forward orientation there are 2 NF1 binding sites and 3 SMAD3 binding sites spread out over AdD1. The Constitutive TF NF-1 which, stimulates genes with CCAAT boxes, and has developmental functions in synapse and dendrite formation form cerebellar granule cells (Latchman 1998; Kilpatrick et al. 2012). SMAD3 TF supresses macrophage activation by affecting the production of IL-6 and TNF-α (Sugiyama et al. 2012), it also modulates cell migration during wound healing in normal circumstances but also in cancer metastasis (Boudreau et al. 2012).

In the reverse orientation there was a large overlapping cluster of TF binding sites, at 40bp most of which were for steroidal factors such as Estrogen related factor alpha (ESRRA), Progesterone receptor binding site (PRE), Steroidogenic factor 1(SF1) Vitamin D receptor/Retinoid X receptor heterodimer (VDR/RXR) and Nerve growth factor IB response element (NBRE). ESRRA plays a role in bone development and by regulating osteoblast differentiation and also regulates T-cell differentiation (Auld et al. 2012; Felizola et al. 2013) Progesterone and its receptor have been shown to upregulate levels of PAC1 receptor in previous studies (Ha et al. 2000; Ko and Park-Sarge 2000),SF-1 is a regulator of gonadal and adrenal development and steroidogenesis (Ferraz-de-Souza et al. 2011). TheVDR/RXR binding site is a binding site for a VDR and RXR dimer, vitamin D receptor has the well-established role in bone homeostasis (Haussler, M RHaussler et al. 1997), the retinoid X receptor dimerises with several nuclear receptors and acts as a co-regulator it plays a role in the growth and differentiation of several tissues like the CNS and hematopoeitc tissue during embryonic development (Orlov et al. 2012; Thomas et al. 2012). These steroidal TF binding sites were also present outside the cluster at 40bp. Other TF binding sites found in in the reverse orientation included the constitutive NF1 and PAX5 involved in B cell lymphopoiesis (Revilla-I-Domingo et al. 2012).

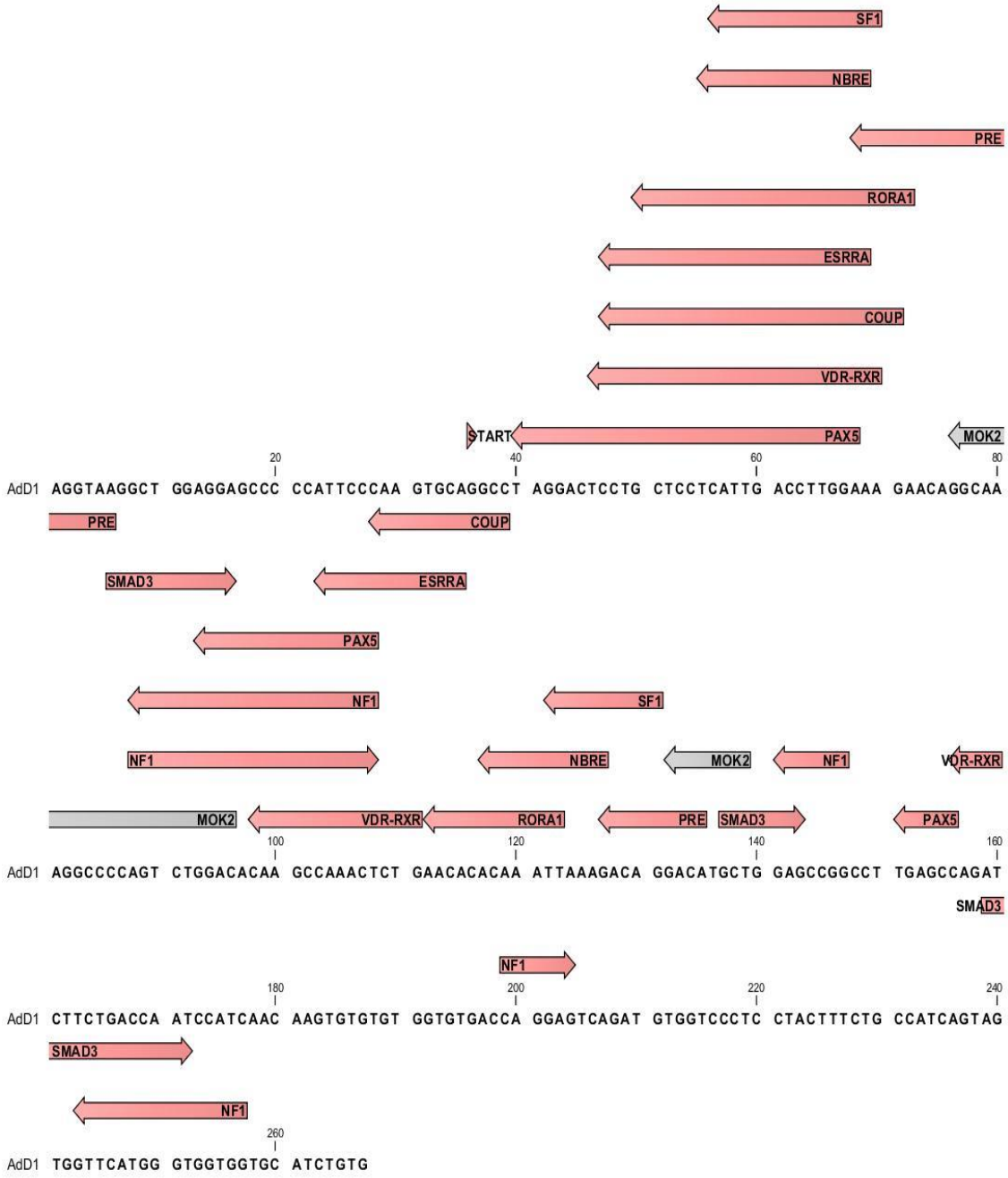

Figure 3.12

Forward and reverse oriented TF binding sites for conserved region AdD1, start of conserved region is marked by arrow and ends at 261. TF matrices shown have >0.85 optimised matrix threshold.

Matrix	Matrix family	Description	Orientation
SMAD 3	SMAD	Smad3 transcription factor involved in TGF-beta signaling	(+)
NF1	NF1F	Nuclear factor 1 (CTF1)	(+)
PAX5	PAX5	B-cell-specific activator protein	(-)
VDR_RXR	RXRF	VDR/RXR Vitamin D receptor RXR heterodimer, DR3 sites	(-)
ESRRA	EREF	Estrogen-related receptor alpha	(-)
COUP	NR2F	Chicken ovalbumin upstream promoter (COUP-TF), DR0 sites	
RORA1	RORA	RAR-related orphan receptor alpha1	(-)
NBRE	NBRE	Monomers of the nur subfamily of nuclear receptors (nur77, nurr1, nor-1)	(-)
SF1	SF1F	SF1 steroidogenic factor 1	(-)
PRE	GREF	Progesterone receptor binding site, IR3 sites	(-)
MOK2	MOKF	Ribonucleoprotein associated zinc finger protein MOK-2 (human)	(-)
NF1	NF1F	Nuclear factor 1	(-)

Table 3.9

Full list of TF binding sites found in in conserved region AdD1. Orientation is marked by (+) for forward (–) for reverse. The table shows the name of the TF, matrix family it belongs to and the Genomatrix output description of the TF.

3.2.2.7 AdD2 TF binding sites

The AdD2 conserved region is located at +2710 to +2860 downstream from the TSS and is 150bp long. In the forward orientation several TF binding sites are present scattered all over AdD2 (*Figure 3.13* and *Table 3.10*), These include sites for ZBP89, BKLF (KLF3), involved in cell proliferation differentiation and apoptosis (Petrovic et al. 2009; Zhang et al. 2010; Pearson et al. 2011; Zhang et al. 2012); E2F3, which modulates cell cycle and cancer (Dong et al. 2002; Tsantoulis and Gorgoulis 2005; Xanthoulis and Tiniakos 2013; Zhou et al. 2013); EGR1, important in mitogenesis and cell differentiation and apoptosis (Ravni et al. 2008; Jeon et al. 2013; Kang et al. 2013). There are also 2 TF binding sites for c-AMP response element binding protein (CREB) and Ras-responsive element binding protein (RREB). The TF CREB controls gene expression across many species in response to PKA pathway activation or MAPK specifically p38 MAPK (Trumper et al. 2002; Hönscheid et al. 2011). As well as basic transcription machinery CREB has been associated with modulating synaptic plasticity and playing a role in memory and diseases like Alzheimer's (Silva et al. 1998; Li et al. 2012). RREB is the response element of RAS protein which is involved in the MAPK/ERK pathway and controls cell growth and differentiation and cell cycle control, its malfunction is often associated with cancer and is classified as a proto oncogene (Thiagalingam et al. 1996; Chappell et al. 2011; Steinbrunn et al. 2012).

In In the reverse orientation there are several binding sites for TF associated with cell growth proliferation and development such as BACH2 involved in B cell and T cell proliferation and EGR1 (Le Gallou et al. 2012; Tsukumo et al. 2013) as well as TGIF1 which has a role in brain development and in regulating necrosis via TNF-α (Demange et al. 2009; Taniguchi et al. 2012). There is also a TF binding site for activating transcription factor 2 (ATF2). This binds to other co-factors such as Jun and Fos (Jun, Fos ATF and CREB protein families form heterodimers that are known as AP-1) (Hess et al. 2004; Lau and Ronai 2012). ATF2 is activated via the MAPK/ERK pathways in response to cellular stress stimuli and ATF2 also plays a role in development (Lau and Ronai 2012). There is also an association of AP-1 ATF-2 interactions in the control of cell cycle and the development of cancer

(Lopez-Bergami et al. 2010). There is also a Forkhead box N1 (FOXN1 or WHN) binding site which is associated with normal hair development (gene knockouts give ‘nude’ mice) but also crucially the development of immune system. Knockout mice show athymia and severe T-cell immunodeficiency (Romano et al. 2013).

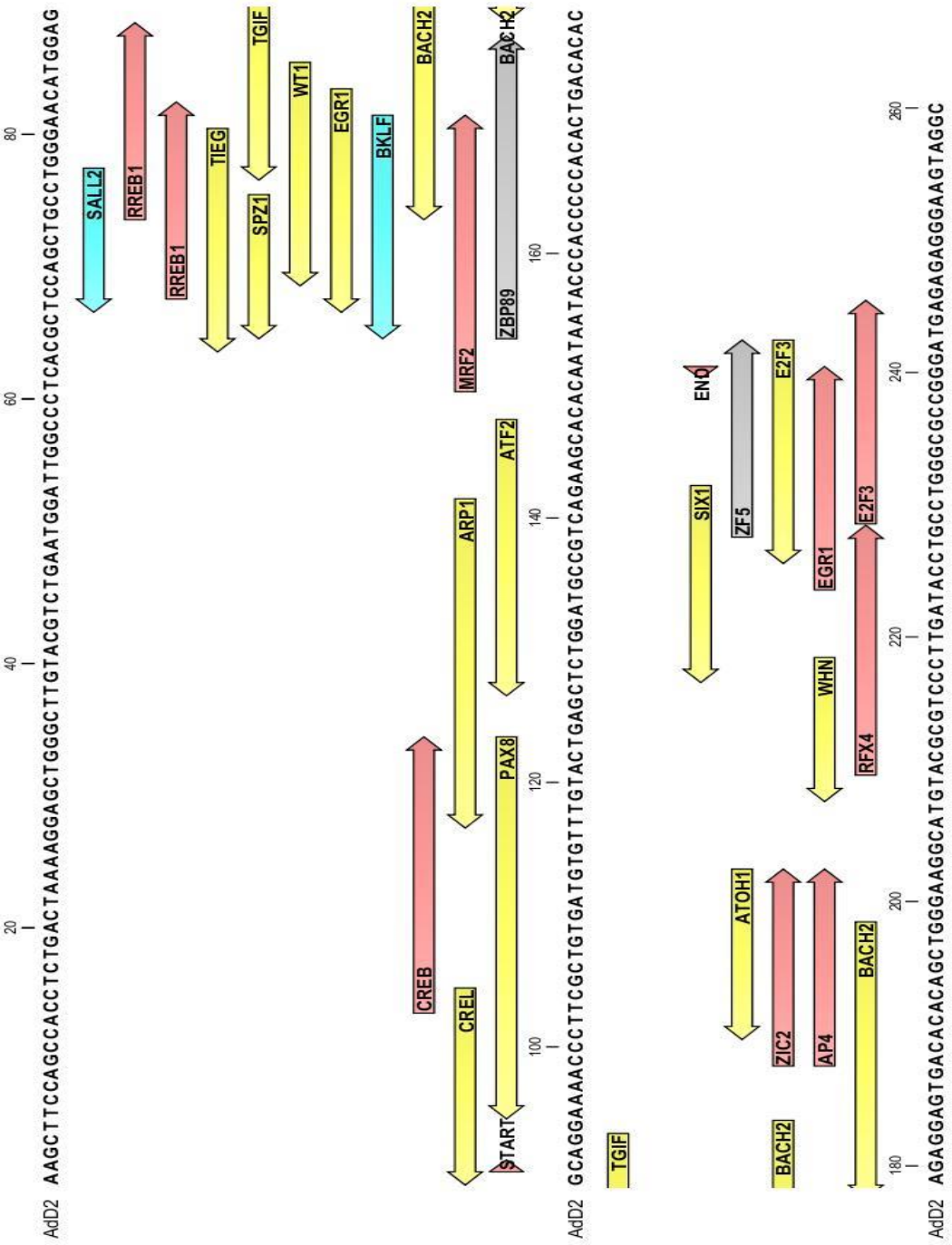

Figure 3.13

Forward and reverse oriented TF binding sites for conserved region AdD2, start and end of conserved regions is marked by arrows. TF matrices shown have >0.85 optimised matrix threshold.

Matrix	Matrix family	Description	Orientation
CREB	CREB	cAMP-response element-binding protein	(+)
MRF2	ARID	Modulator recognition factor 2 (MRF2, ARID5B)	(+)
ZBP89	ZF02	Zinc finger transcription factor ZBP-89	(+)
RREB1	RREB	Ras-responsive element binding protein 1	(+)
RREB1	RREB	Ras-responsive element binding protein 1	(+)
AP4	AP4R	Activator protein 4	(+)
ZIC2	ZICF	Zic family member 2 (odd-paired Drosophila homolog) (secondary DNA binding preference)	(+)
RFX4	XBBF	Regulatory factor X, 4 (secondary DNA binding preference)	(+)
EGR1	EGRF	Egr-1/Krox-24/NGFI-A immediate-early gene product	(+)
ZF5	ZF5F	Zinc finger / POZ domain transcription factor	(+)
E2F3	E2FF	E2F transcription factor 3 (secondary DNA binding preference)	(+)
CREL	NFKB	c-Rel	(-)
PAX8	PAX5	PAX 2/5/8 binding site	(-)
ARP1	NR2F	Apolipoprotein AI regulatory protein 1, NR2F2, DR1 sites	(-)
ATF2	CREB	Activating transcription factor 2	(-)
TIEG	SP1F	TGFbeta-inducible early gene (TIEG) / Early growth response gene alpha (EGRalpha)	(-)
SPZ1	SPZ1	Spermatogenic Zip 1 transcription factor	(-)
BKLF	KLFS	Basic krueppel-like factor (KLF3)	(-)
SALL2	SAL2	Zinc finger protein Spalt-2, sal-like 2, p150(sal2)	(-)
EGR1	EGRF	EGR1, early growth response 1	(-)
WT1	EGRF	Wilms Tumor Suppressor	(-)
BACH2	AP1R	Bach2 bound TRE	(-)
TGIF	TALE	TG-interacting factor belonging to TALE class of homeodomain factors	(-)
BACH2	AP1R	Bach2 bound TRE	(-)
ATOH1	NEUR	Atonal homolog 1, HATH1, MATH-1	(-)
WHN	WHNF	Winged helix protein, involved in hair keratinization and thymus epithelium differentiation	(-)
SIX1	SIXF	Sine oculis homeobox homolog 1	(-)
E2F3	E2FF	E2F transcription factor 3 (secondary DNA binding preference)	(-)

Table 3.10

Full list of TF binding sites found in in conserved region AdD2. Orientation is marked by (+) for forward (–) for reverse. The table shows the name of the TF, matrix family it belongs to and the Genomatrix output description of the TF.

3.3. Summary and Discussion

Analysis of the aligned mouse, rat, human and chimpanzee sequences showed 6 conserved regions or promoter regions conserved across the 4 species. 3 putative promoter regions were found upstream and 2 downstream of TSS and a conserved region proximal to TSS and including most of exon 1 (-80 to +353) known as Ad1. The Ad1 conserved region is suspected to be the basal promoter region and is different than previously reported basal reporter region (-113 to +206). Based on TF binding site analysis TF involved in transcription start are located at -130 and +310 It was therefore decided that when constructing clones for cell transfections, 2 exon1 spanning clones would be made the -80 to +353 Ad1 and the -180 to +206 Ad2. Ad1 corresponds to the new proposed minimum promoter region, while Ad2 would mimic minimum promoter from previous study by excluding TF binding sites after +206 but including sites upstream of -113 (TF2B at -130), similar to a -323 to +206 construct, which had similar expression to minimum promoter, used in the same study(Rodríguez-Henche et al. 2002).

The upstream and downstream conserved regions have not been previously reported or investigated. They showed TF binding sites for TF involved in many physiological functions but mainly, neuronal development, cell cycle control and cell stress protection. The upstream conserved regions mainly appear to be involved neuronal developmental, while the downstream promoter regions appear to modulate stress induced protective response.

The following Chapter will deal with the isolation and cloning of conserved regions into reporter gene constructs.

Chapter 4

Preparation of Promoter Constructs

4. Preparation of Promoter Constructs

4.1 Introduction

The entire PAC1 gene was located on a 175kb BAC clone RP23-154D15, in order to isolate the region of interest (-6000 to +8179) several approaches were used. The regions upstream and downstream of exon 1, would be isolated and ligated into Blue white screening vectors. Then the conserved regions AdU1 AdU2 etc would be sub-cloned into our reporter gene plasmids Such as pGL-3 Basc. Restrictions digests and agarose gel electrophoresis were largely used to isolate the conserved regions. In some cases PCR was used to amplify a desired region, before ligation into a selective vector, the Subcloning into pGL-3 Basic would follow.

Initially in order to avoid any mutations in the gene, it was decided to isolate the -6000 to +8179 region using restriction digests from RP23-154D15. When this approach proved to be not viable PCR amplification was used followed by restriction digest isolation and Subcloning into pGL-3 plasmids.

4.2 Restriction digest cloning from RP23-154D15

4.2.1 Isolating of Adcyap1r1 conserved regions using restriction digests

The insert in the BAC RP23-154D15 which contains the entire *mAdcyap1r1* gene is ~175Kb in length. In an attempt to isolate the region of interest from the *mAdcyap1r1* gene, restriction endonuclease digestion and gel electrophoresis was used. As it would be difficult to isolate the individual conserved regions which are only 200-400bp in length from 175kb, the whole region from -6000 upstream up until the start of exon 3 was planned to be isolated in 2 separate restriction digests. This approach would give 2 overlapping DNA segments of 7868bp (EcoRI digest) and 9385bp (SacII+BamHI) (*Figure 4.1*), which could be separated by gel electrophoresis.

The two restriction digests were therefore performed on RP23-154D15 DNA. Gel electrophoresis of the digests revealed multiple bands (*Figure 4.2*). A preparative gel

was used to separate the different sized bands and the 2 fragments of interest were excised from the gel. The pBluscript SK- cloning vector was also digested with EcoRI and with SacII+BamHI. The digested DNA was treated with Antarctic phosphatase to prevent religation before separating the 3kb linear DNA on an agarose gel (*Figure 4.2*)

The DNA fragments of required size from RP23-154D15 and the digested pBluscript SK- were excised from the gel and the DNA was extracted and purified using Qiex beads as described in Materials and Methods. The EcoRI RP23-154D15 fragment was ligated to EcoRI digested pBluscript SK- and the SacII+BamHI RP23-154D15 fragment was ligated to SacII+BamHI digested pBluscript SK- using Quick-Stick ligase to give constructs that should be able to be identified by blue/white screening (*Figure 4.3*). The pBluscript SK- vector encodes β-galactosidase which forms a blue dye in the presence of IPTG and X-gal. Vectors with DNA inserts in the multiple cloning site (MCS) have β -galactosidase formation disrupted giving white bacterial colonies. Bluescript vector without a DNA insert in MCS (original state) should give blue colonies.

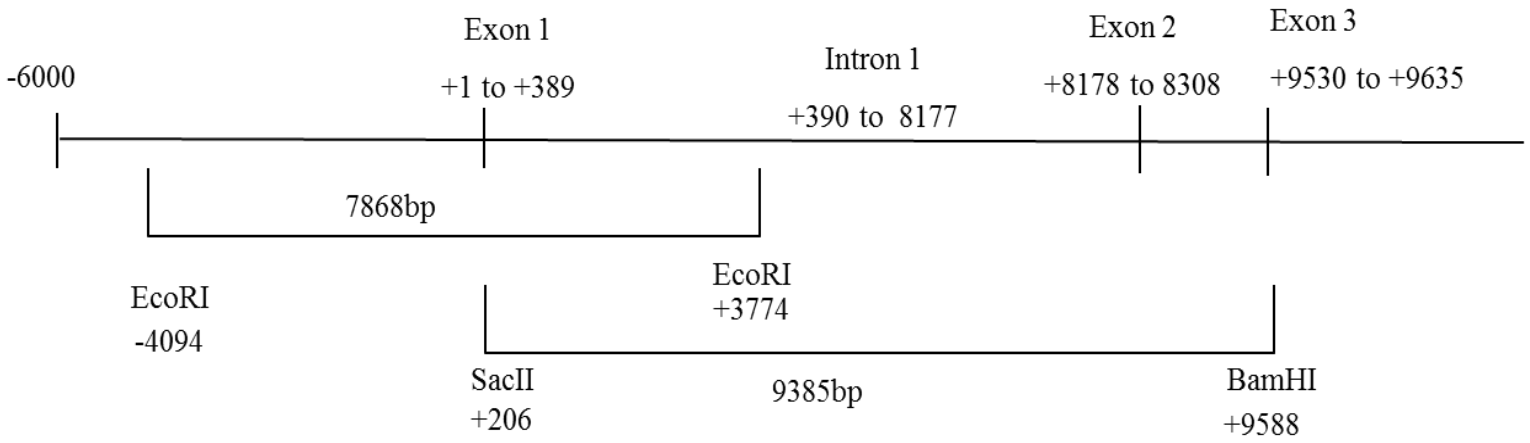

Figure 4.1:
The restriction map of *mAdcyap1r1* showing the 2 separate restriction digests EcoRI and SacII+BamHI used to extract 2 overlapping DNA fragments that span the entire region of interest. The location of the restriction sites is indicated in relation to the start of exon 1. Exons 1 2 and 3 are represented by a vertical line.

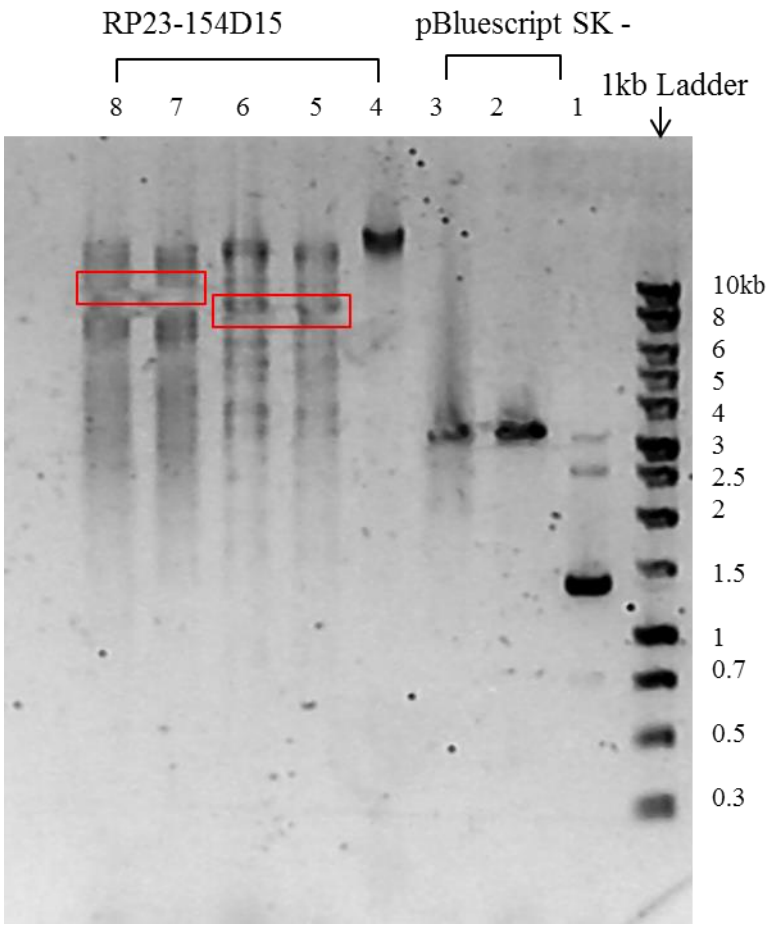

Figure 4.2:
The restriction digests of RP23-154D15 and pBluscript SK- were run on 0.8% agarose gel alongside a 1kb ladder to separate the different sized bands for excision and DNA extraction. pBluscript SK- was digested using EcoRI **(lane 2)** and SacII+BamHI **(lane 3)** both giving bands 3kb in size, RP23-154D15, EcoRI **(lane 5, 6)** and SacII+BamHI **(lane 7, 8)** digests gave multiple fragments. The bands of interest 7.8kb for EcoRI and 9.3 SacII+BamHI digests are highlighted by boxes. Unrestricted pBluscript SK- **(lane 1)** and RP23-154D15 **(lane 4)** were used as controls for digestion.

A)

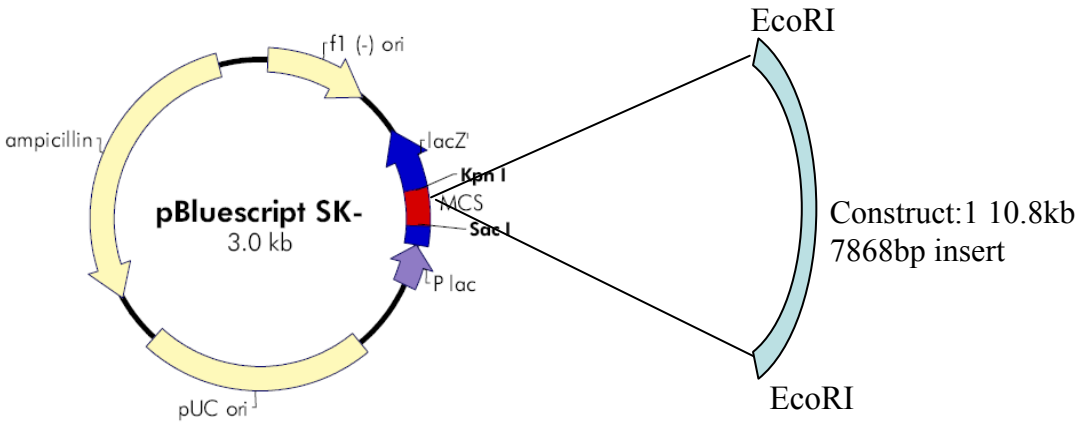

B)

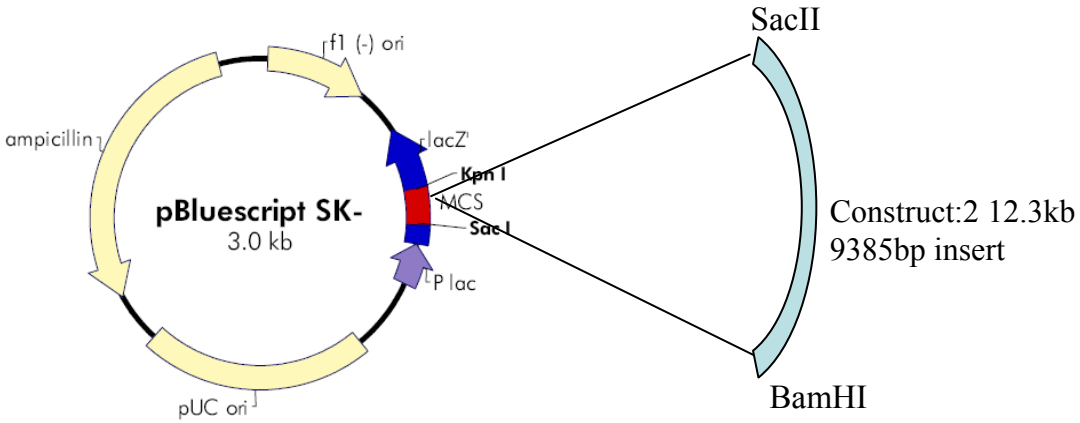

Figure 4.3:

The cloning strategy used showing DNA extracted form gel electrophoresis ligated into pBluescript SK- plasmid digested with appropriate restriction enzymes to form 2 constructs. **(A)** Construct:1 will have the EcoRI 7.8kb digest fragment. **(B)** Constuct:2 will have the SacII+BamHI 9.3kb digest fragment.

The constructs termed Construct 1 (EcoRI) (*Figure 4.3 a*) and Construct 2 (SacII+BamHI) (*Figure 4.3 b*) were transformed into competent JM109 E. coli cells and screened on IPTG, X-gal plates. After incubation on X-gal plates, 4 white colonies were identified on the plates containing Construct 1. The plates with Construct 2 gave very few colonies and none of these were white.

The white colonies for Construct:1 were colony-purified, grown in LB broth and the DNA from the plasmid constructs was extracted.

4.2.2 Checking Identity of construct:1

The DNA isolated from 4 white colonies may contain Construct:1 To check the size of the DNA extracted and that it is indeed Construct:1, restriction digests and gel electrophoresis was performed on the DNA. Two digests were performed: an EcoRI digest that should give 2 fragments, being the 3kb Bluscript vector and the 7.8kb insert; and an EcoRI+SacII dual digest that should give the 3kb Bluescript vector and 2 insert fragments 4297bp and 3571bp in length. Undigested DNA was also separated on the agarose gel to visualise the size of the construct before and after digestion. Figure 4.6 shows the digest analysis of DNA from 2 white colonies from a total of 4 isolated that should contain construct:1. The agarose gel electrophoresis showed that the approximate size of the suspected Construct:1 plasmid DNA is 8.5kb as opposed to the expected 10.8kb (*Figure 4.4 lanes 1&2*). Digestion with EcoRI gave the 3kb fragment of Bluescript vector and an insert fragment 5.5kb long (*Figure 4.4 lanes 3&4*). The dual digest with EcoRI+SacII gave the Bluescript 3kb fragment and cutting the 5.5kb insert fragment into a ~750bp fragment and a ~4.5kb fragment. Further restriction digests on the other 2 constructs isolated gave the same results (data not shown). This taken together indicates that the isolated constructs do not correspond to Construct:1 due to differences in insert size.

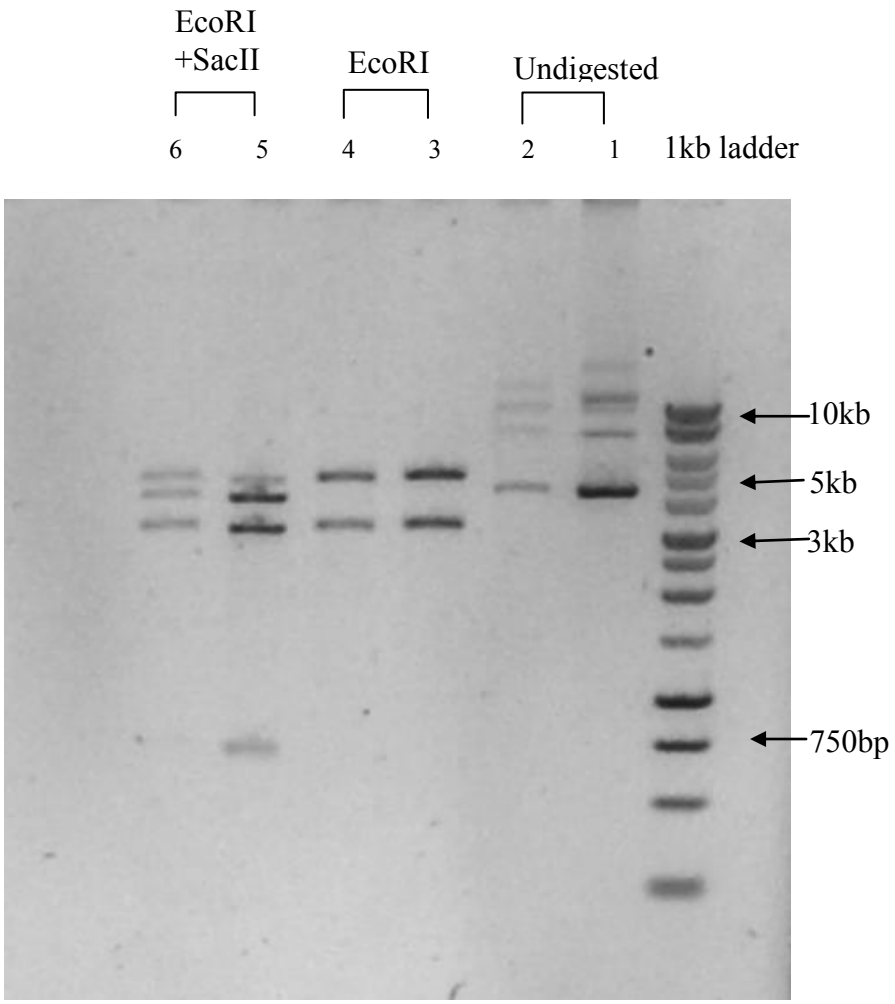

Figure 4.4:
Gel electrophoresis of Construct:1 DNA was used to check its size alongside a 1kb ladder for reference. EcoRI digest of Construct :1 **(lanes 3, 4)** gave a Undigested Construct:1 DNA gave bands at 3kb and 5.5kb. EcoRI+SacII digests gave bands at 3kb, 4.5kb and 750bp as well as a bands at 5.5kb due to incomplete digestion**(Lanes 5, 6)**.

4.3 Cloning of conserved regions by PCR

4.3.1 Amplification of Conserved Regions by PCR.

As the isolation of the conserved potential promoter regions of mADCYAP1r1 (*Figure 3.3*) using restriction digests of the ~175kb RP23-154D15 sequence had proved unsuccessful it was decided to amplify the conserved regions using Polymerase Chain Reaction. Four amplicons were designed (*Figure 4.5*): the 469 bp PcrAd1, which is from -115 upstream of the TSS to +354 at end of exon 1, corresponding to the minimum promoter region from bioinformatics analysis (Chapter 3); the 386bp PcrAd2 clone, from -180 to +206 corresponding to a minimum promoter similar to Rodriguez-Henche (Rodríguez-Henche et al. 2002); the 8.2kb PcrAd3 -115 to +8181, that covers the area from the potential minimum promoter region to the start of exon 2. This region covers the 2 downstream conserved regions. For the upstream conserved regions primers were designed to amplify PcrAd4 which is 6.1 kb in size and covers the region -5749 to +354 (*Figure 4.5*). A list of primers and reaction conditions are listed in Chapter 2 (Materials and Methods).

PCR reactions were performed using RP23-154D15 BAC DNA as template over a range of concentrations as described in Materials and Methods. The products were separated on an 0.8% TAE agarose gel to verify that the amplification had been successful.

For PcrAd1 (*Figure 4.5* the negative control reaction did not produce a band, as was expected. One of the PCR reactions (250 ng template) gave a 500bp band, as expected for successful amplification. For PcrAd2, one of the PCR reactions (150ng template) gave a 400bp band, close to what was expected. For PcrAd1 only one of the PCR reactions yielded a product (*Figure 4.6*).

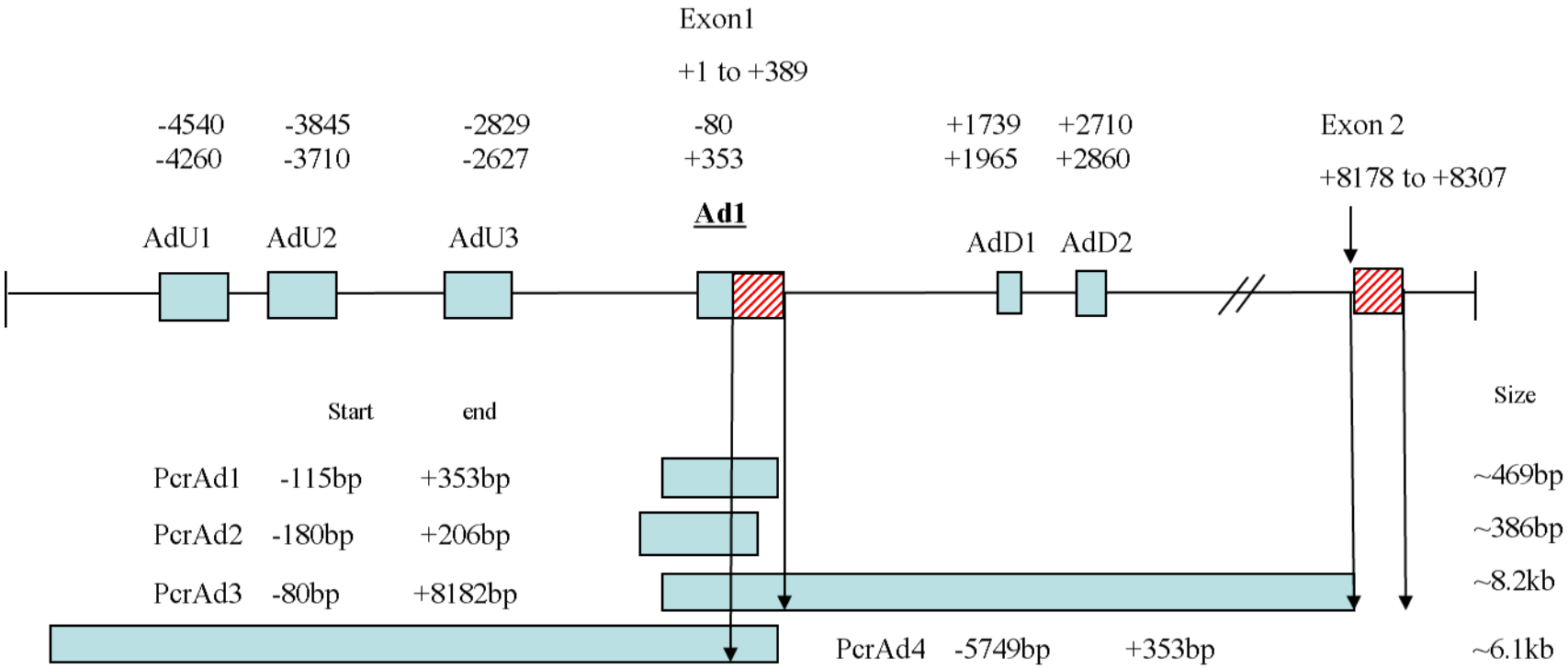

Figure 4.5 Design of PCR Primers for Amplification of Conserved regions

The 3 PCR primers shown above are aligned with the conserved regions in relation to Exon 1 and exon 2. Both PcrAd1 and PcrAd2 end in exon 1. PcrAd3 ends in exon 2 just before the ATG translational start site. PcrAd4 covers the upstream region from -5749 to +353 in exon1

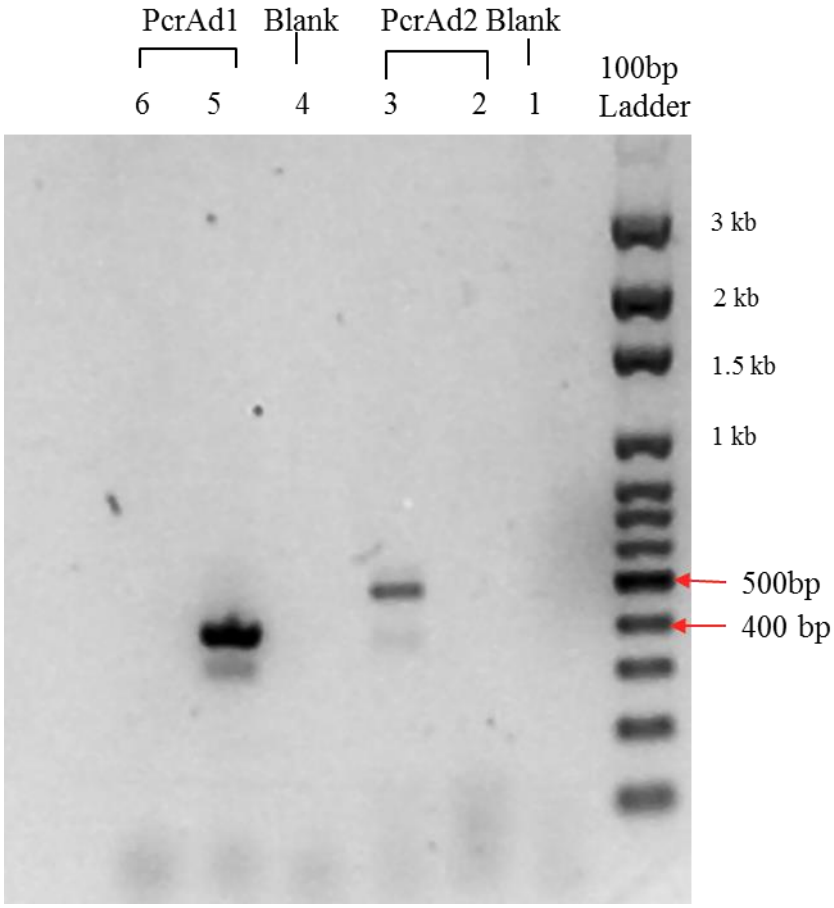

Figure 4.6:

Gel electrophoresis of PCR products PcrAd1 and PcrAd2 PCR shows the ~400bp band of PcrAd2 lane 5 and the ~500bp band of PcrAd1. Lanes 1 and 4 labelled Blank indicate –ve control PCR reactions without DNA template.

Gel electrophoresis of PcrAd3 PCR reactions gave several bands (*Figure 4. 7*), a very dark and thick 8-9kb band and fainter bands at 2kb, 0.8kb and 0.5kb. The blank sample gave no bands. The expected product from the PcrAd3 PCR reaction was 8.2kb the large dark bands at 8-9kb corresponds to that however the reaction was not very selective and gave other bands compared to PcrAd1 and PcrAd2. For PcrAd4 PCR reactions all reactions gave a dark band about 6-7kb which corresponds to the expected 6.1kb fragment size (*Figure 4.8*). The gel containing the large 8-9kb for PcrAd3 and the 6-7kb PcrAd4 band was excised and the DNA extracted, the extracted DNA was then used in the cloning reactions. The PcrAd1 and PcrAd2 PCR samples were directly used in the cloning reactions.

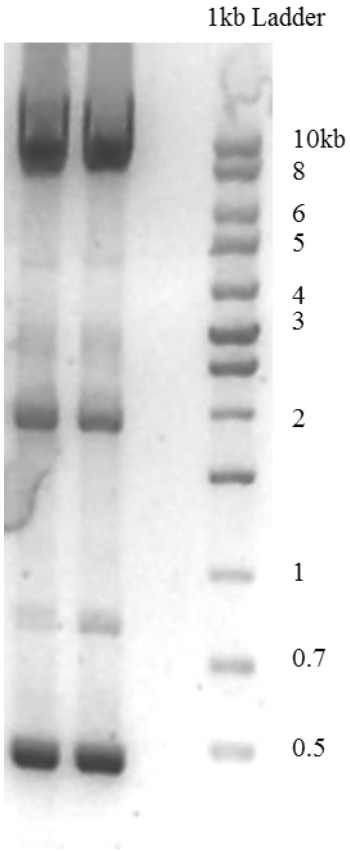

Figure 4.7:
PcrAd3 PCR gave several bands including 2 wide bands around 8-9kb which is close to the 8.2kb size of PcrAd3.

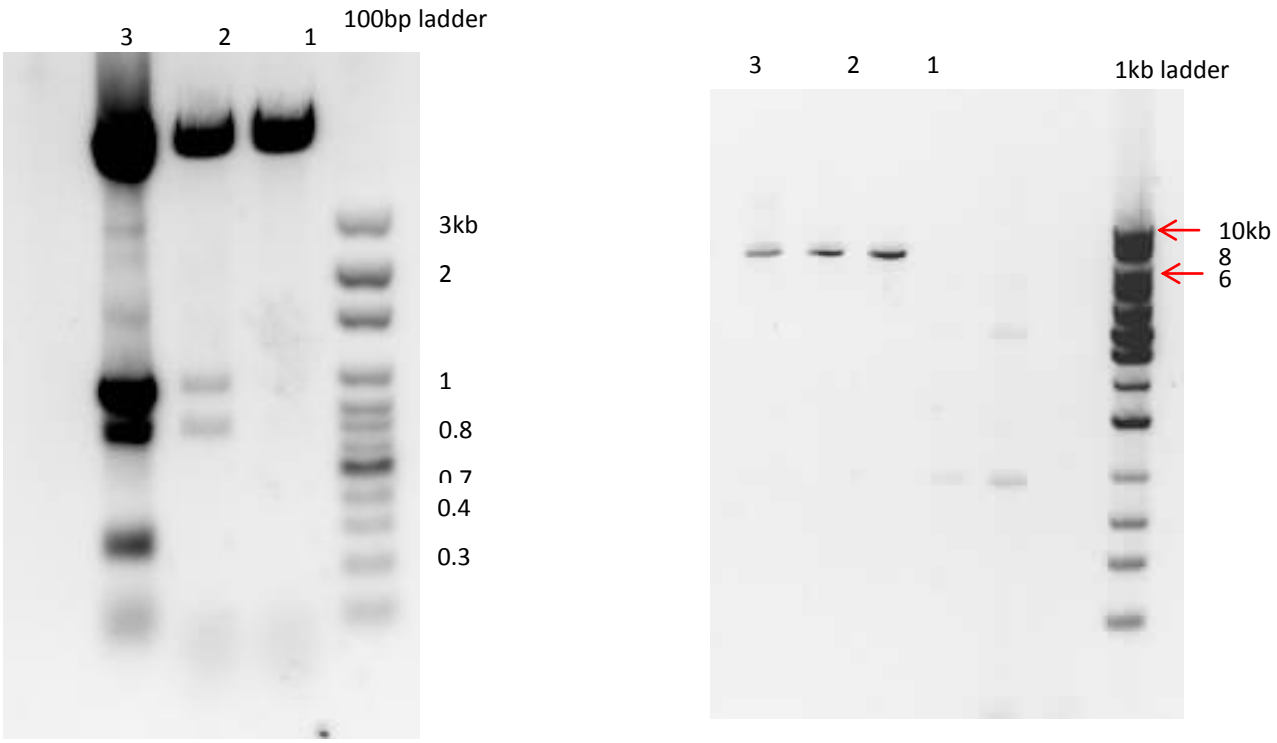

A) **B)**

Figure 4.8:

(A) PcrAd4 PCR gave several bands in lane 2 and 3 including 2 wide bands around 1, 0.7kb. However all 3 lanes gave a large band above 3kb which may correspond to the 6.1kb size of PcrAd4. **(B)** The PCR products were run again with a 1kb ladder where the DNA bands where ~7kb close to the 6.1kb PCR products size.

.

4.3.2 Cloning of PCR products into Cloning Vectors

The Pfu DNA polymerase used in the amplification of PcrAd1 and PcrAd2 gives blunt ends. This allowed the fragments to be cloned into the pCR-Blunt II-Topo vector (*Figure.8*). PcrAd3 and PcrAd4 were cloned into pCR-XL-TOPO vector (*Figure.7*), because the Expand long range DNA polymerase used made sticky ended PCR products with a protruding adenine at the end. The resulting plasmid constructs with PcrAd1, PcrAd2, PcrAd3 and PcrAd4 inserts were named pTopAd1, pTopAd2, pTopAd3 and pTopAd4 respectively.

After the ligation of inserts into their respective vectors, the plasmid constructs were transformed into bacterial cells and the plasmid DNA from several bacterial colonies was purified. Restriction digests were used to check that the recombinant plasmids have an insert and to check the insert size before being sent for sequencing.

4.3.2.1 pTopAd1

The 469bp PcrAd1 fragment was ligated into the 3.5kb pCR-Blunt II-Topo vector giving pTopAd1. An EcoRI digest was performed on 6 recombinant plasmid constructs. The EcoRI sites flanked the site where the PcrAd1 PCR fragment should be inserted (section 4.3.2.5; *Figure 4.11*). Therefore a 550bp insert was expected, along with the 3.4kb pCR-Blunt II-Topo vector fragment. Agarose gel electrophoresis of the digests of the six samples gave 3.4kb bands in all the samples. One of the samples gave both the 3.4 kb vector band and a 550 bp insert band (*Figure.4.9 a*) and this was named as pTopAd1.

4.3.2.2 pTopAd2

A similar approach was used to produce the recombinant plasmid construct pTopAd2 containing PcrAd2. The expected fragments after EcoRI digestion were 386 bp and 3.4kb corresponding to insert and vector respectively. Gel electrophoresis of the

digests of 6 TopAd2 recombinant plasmid preparations gave the required 2 bands for all 6 samples (*Figure 4.9 b*). One of these plasmids was selected and named as pTopAd2.

4.3.2.3 pTopAd3

The 8.2kb PcrAd3 fragment was ligated to the 3.5kb pCR-XL-TOPO vector to give the pTopAd3 construct. If successful the recombinant plasmid would be 11.7 kb and an EcoRI digest of pTopAd3 clone would give 5 fragments of 3.9 kb, 3.8 kb, 3.5 kb, 0.3 kb and 0.2 kb. Gel electrophoresis of 6 recombinant plasmid digests was carried out (*Figure 4.10a*), despite poor resolution, 4 constructs gave bands as expected with strong bands in the 3.5 to 3.9 kb range, and 2 smaller bands at 0.3kb and 0.4kb. One of these plasmids was selected and named as pTopAd3.

4.3.2.4 pTopAd4

The putative ~9.6kb pTopAd4 constructs containing the PcrAd4 insert were digested separately with BamHI and EcoRI. If correct the BamHI digest should give two bands at 3.7kb and 5.8kb, while EcoRI digests three bands at 1.6kb, 3.5kb and 4.4kb. The digests were visualised on an agarose gel and all 3 of the tested plasmids gave the expected bands after BamHI and EcoRI digests (*Figure 4.10b*).

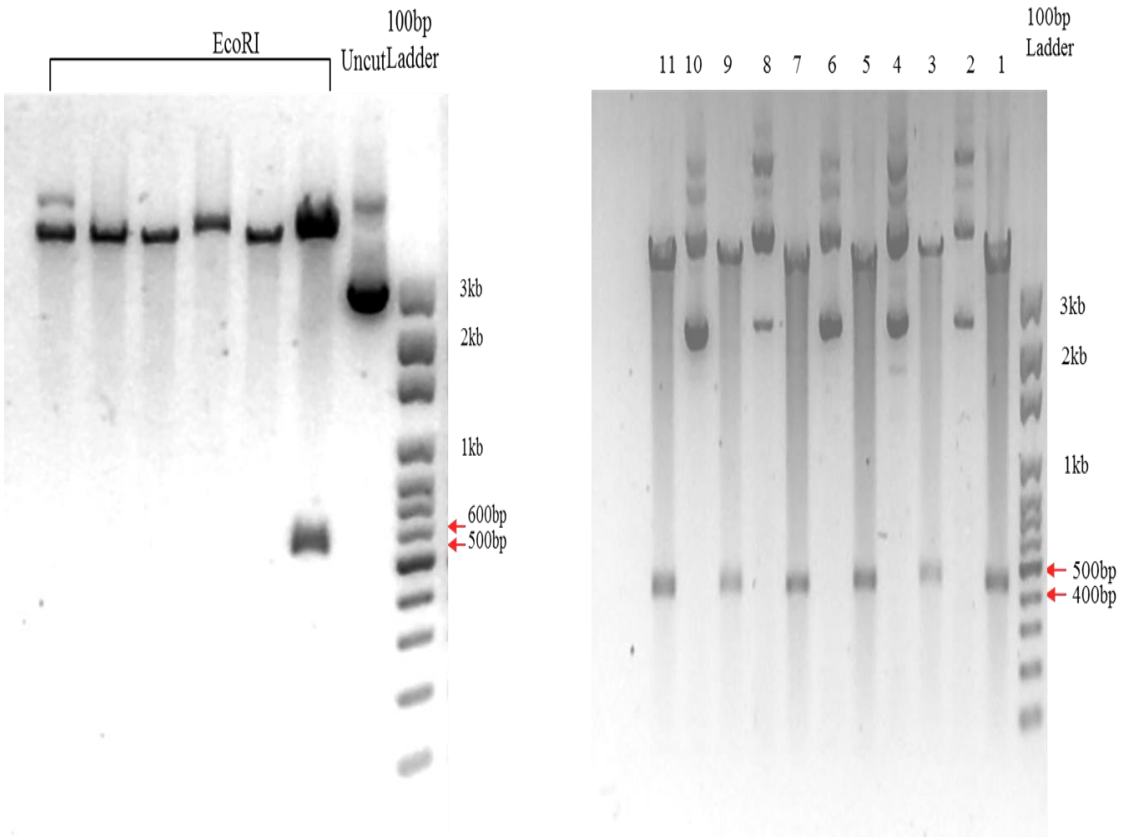

a) b)

Figure 4.9:

A) 0.8% agarose gel electrophoresis of EcoRI digests of pTopAd1, gave a ~550bp insert band and a 3.5kb band of the TOPO blunt vector in only 1 sample tested. The other 5 samples proved to have no PcrAd11 insert**. (B)** EcoRI digests of pTopAd2 constructs, odd numbered lanes, gave a 450bp band and the 3.5kb band of the TOPO blunt vector, showing that they may have PcrAd1 insert. The corresponding undigested samples are shown in even numbered lanes.

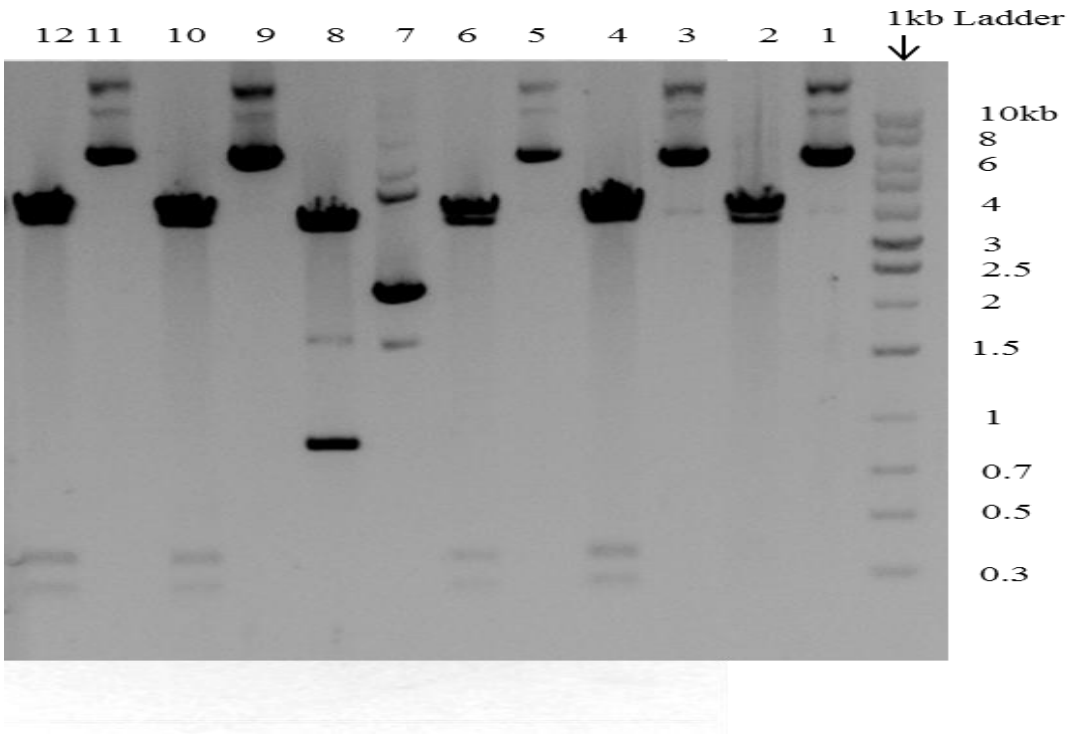

A)

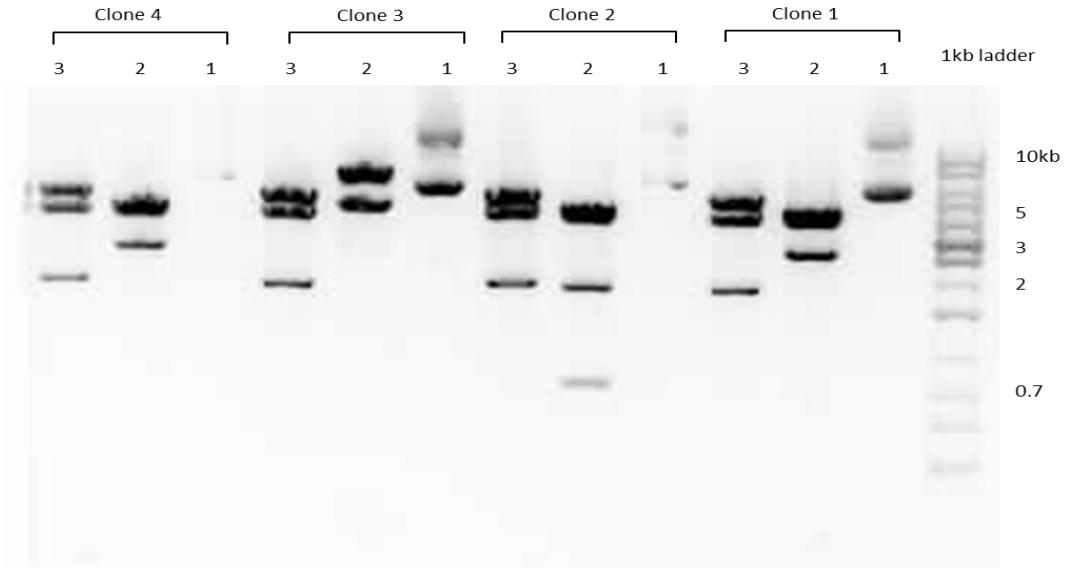

B)

Figure 4.10:

A) EcoRI digests of pTopAd3 constructs that may contain PcrAd3 insert were visualised by gel electrophoresis. The corresponding undigested samples are shown in odd numbered lanes. 4 samples (lanes 4, 6, 10, 12) gave 2 small fragments ~0.3bp and ~0.4bp, as well as a cluster of 2-3 bands at 3.5-4kb range as predicted. **B)** Undigested (lanes 1), BamHI (lanes 2) and EcoRI (lanes 3) digests of pTopAd4 constructs that may contain PcrAd4 insert were visualised by gel electrophoresis. All

samples gave 2 bands ~3.7kb and ~5.8kb after BamHI digest and 3 bands after EcoRI digest ~1.6kb. ~3.5kb and ~4.4kb. Clone 2 gave an unexpected 700bp band after BamHI digest.

4.3.2.5 Sequencing of TOPO plasmid constructs

To make sure that the proper insert had been ligated into the TOPO vectors, selected plasmids (4 from pTopAd3, 1 pTopAd1 and 6 TopAd2) were sequenced. This was especially important for PcrAd3 fragment since the resolution of the gel electrophoresis was poor. The sequence data was analysed by Blastn (http://blast.ncbi.nlm.nih.gov/Blast.cgi) pairwise sequence comparison to ascertain their identity and orientation. All the sequenced samples contained the required PCR fragments PcrAd1, PcrAd2 and PcrAd3. The orientation and sequence of the constructs are shown in the figures below, pTopAd1 (*Figure 4.11*) containing PcrAd1 fragment. pTopAd2 (*Figure 4.12*) containing the PcrAd2 fragment and pTopAd3 clone (*Figure 4.13*) containing PcrAd3 fragment. Sequencing for pTopAd4 and the pGL-3 basic and pGL-3 promoter clones was deemed not necessary given their clear identity by restriction digests.

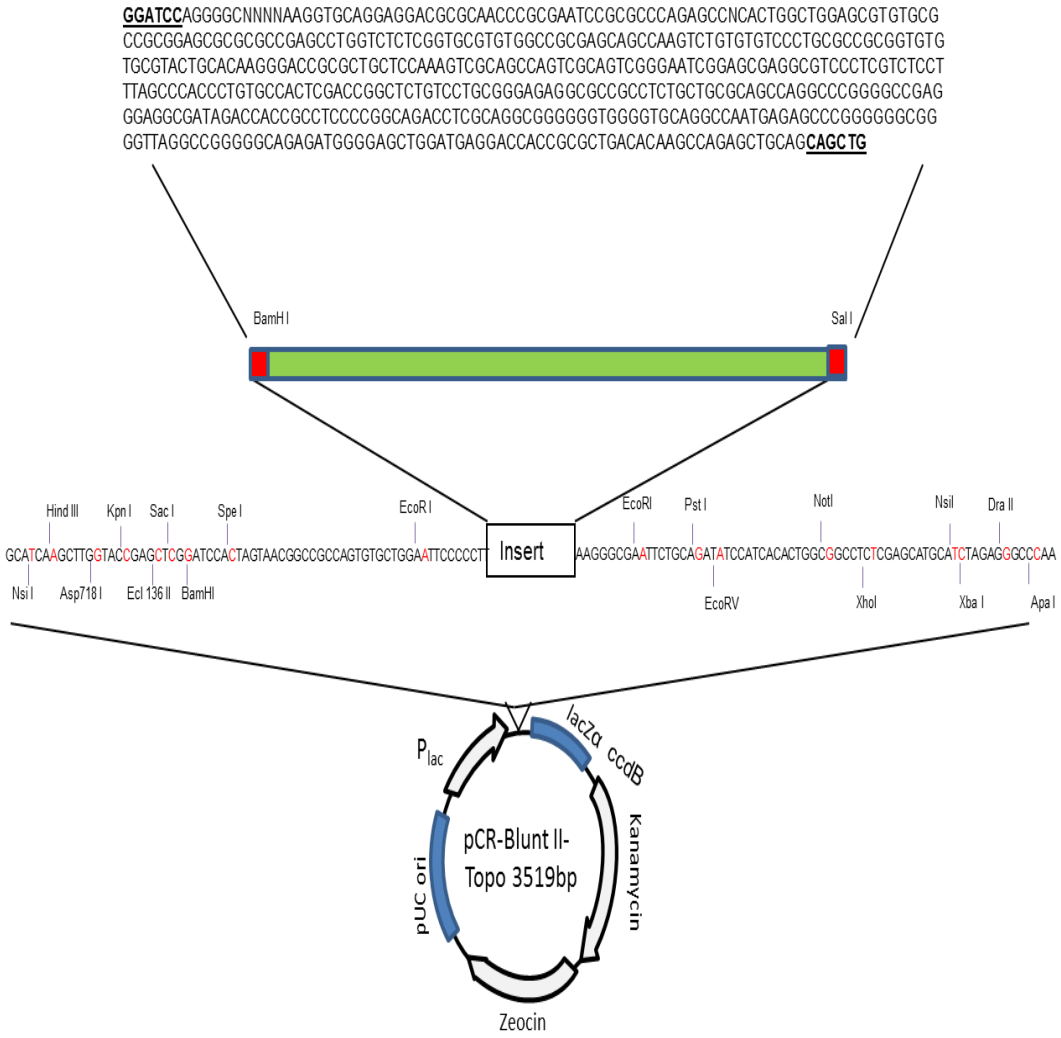

Figure 4.11: pTopAD1 containing the PcrAd1 fragment ligated to pCR-Blunt II-TOPO vector. The DNA sequence shown is the reverse strand of PcrAd1. The underlined Sequences are the Restriction sites BamHI and SalI.

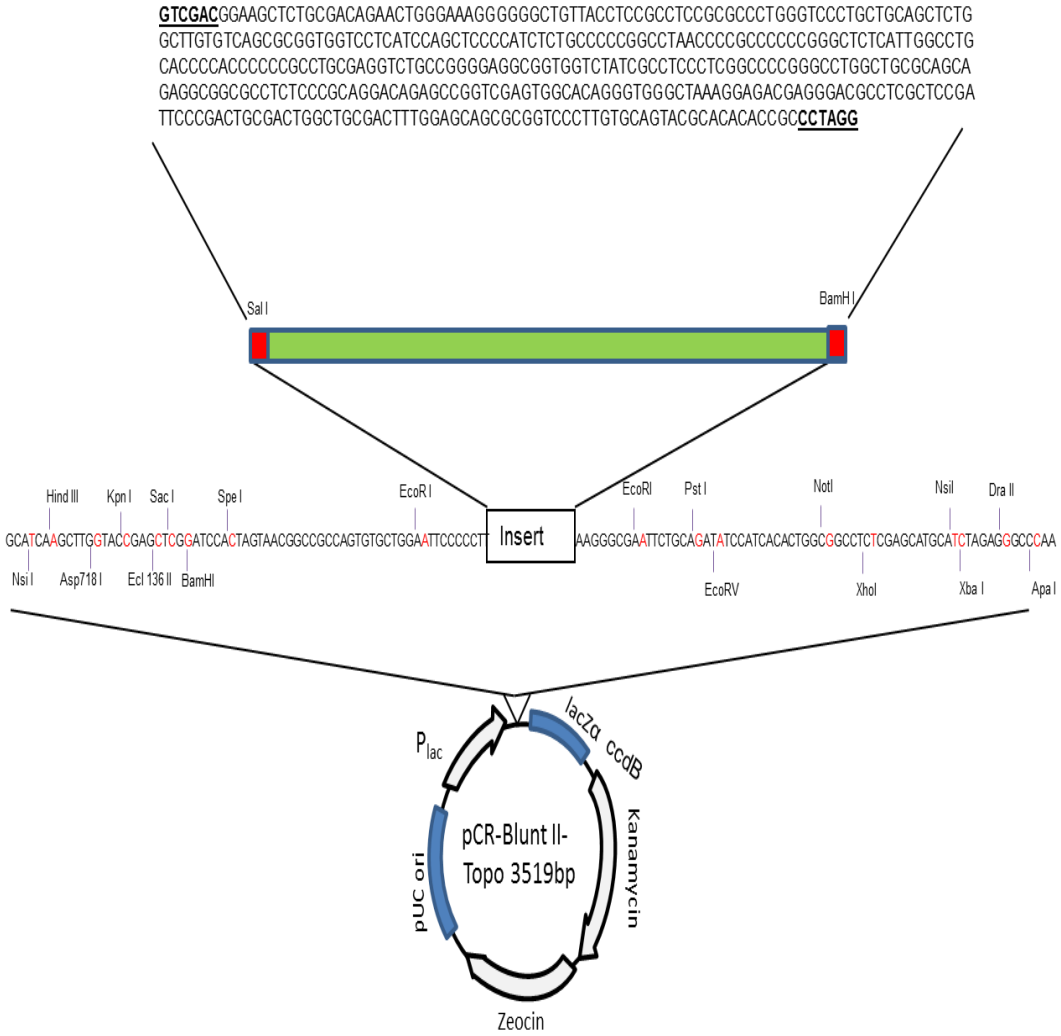

Figure 4.12:

pTopAd2 plasmid containing the PcrAd2 fragment ligated to pCR-Blunt II-TOPO vector. The underlined Sequences are the Restriction sites BamHI and SalI.

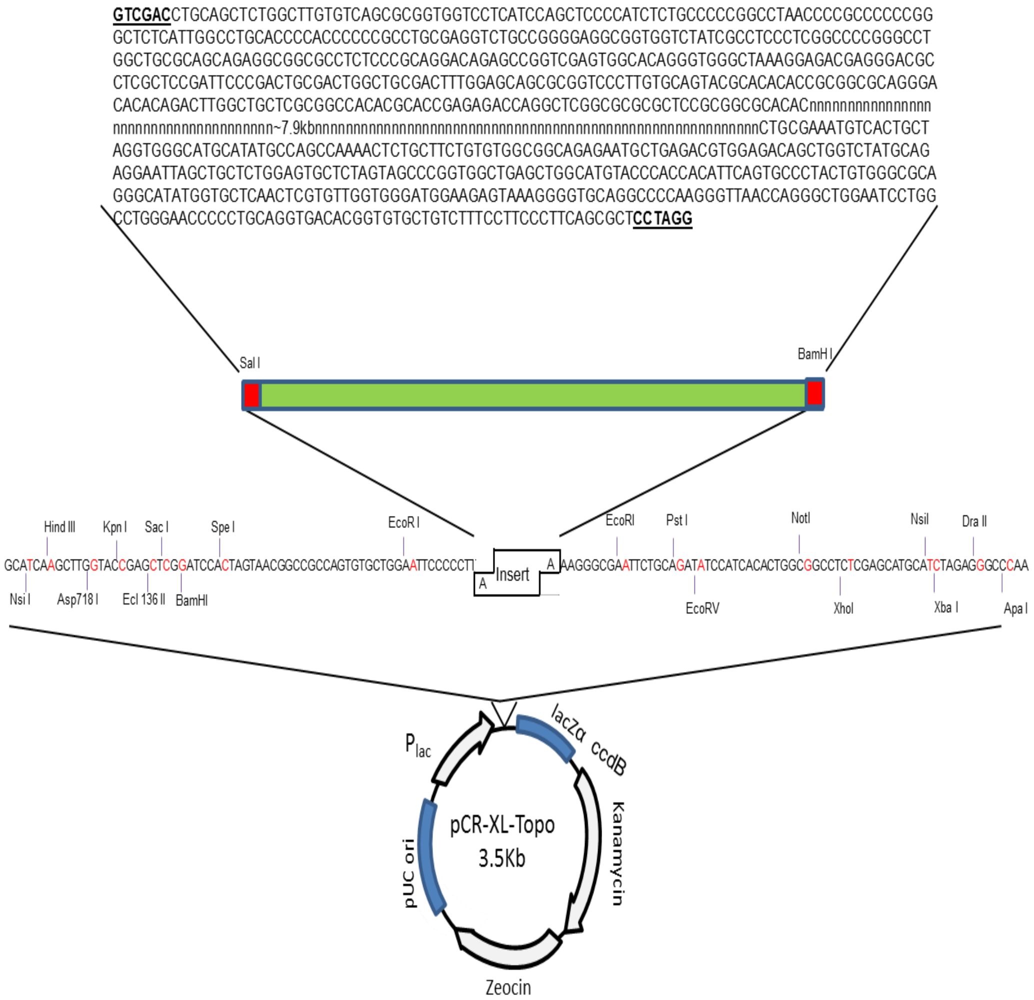

Figure 4.13:

pTopAd3 plasmid containing the PcrAd3 fragment ligated to pCR-XL-TOPO vector. The underlined Sequences are the Restriction sites BamHI and SalI.

4.3.3 Subcloning of Ad1 and Ad2 into pGL-3 Basic

After verification by restriction digestion and sequencing that all the conserved region fragments were successfully cloned into TOPO vectors, the next step was subcloning the fragments into the promoter fusion vector pGL-3Basic.

4.3.3.1 Construction of pGAd1F, pGAd1R, pGAd2F and pGAd2R

The original cloning strategy for Ad1 and Ad2 was to cut out the inserts, using the SalI and BamHI sites that had been designed into the PCR primers (*Figure.4.11-13*), then ligation into a XhoI-BglII double digest of pGL-3Basic vector. However, the BglII and XhoI restriction sites on the pGL-3 vector overlapped, and therefore a double digest of pGL-3Basic using these enzymes was not possible.

It was therefore decided to blunt-end ligate the original PCR products PcrAd1 (469 bp) and PcrAd2 (386 bp) into pGL-3 basic digested following its digestion with SmaI which gives blunt ends. The resulting constructs would be formed in both the forward and reverse orientation.

To prevent self-ligation of the pGL-3Basic vector, it was treated with Antarctic phosphatase after digestion to remove the terminal phosphate groups from each of the ends. The PCR products were treated with T4 polynucleotide kinase so that a phosphate group was added to enable ligation, before resolution and extraction of DNA from agarose gel. After ligation the DNA was transformed into JM109 cells, and plasmid DNA isolated.

Restriction digests were used to check for the presence and orientation of the insert in the new constructs. SmaI digests would linearize the vector and release an 80bp fragment.

For the construct with the PcrAd1 insert, the SmaI digests linearized the constructs giving large bands 5kb bands and an 80bp which was very faint and barely visible (*Figure 4.14a*). Since the SmaI digests were not a good indicator of identity due to the faintness of the 80bp band, a SalI digest was carried out.

For the constructs with the PcrAd1 insert, a SalI digest would give bands at 2837bp and 2461bp for the forward oriented insert, and 3311bp and 1987bp bands for reverse oriented insert. Gel electrophoresis of the SalI digests for the PcrAd1 constructs showed 2 of the plasmids with inserts in the forward orientation (constructs 1 and 2) with bands at 3 and 2kb following SalI digestion. One of these was selected as pGAdB1F while constructs 3 and 4 gave bands indicating a reverse orientation of PcrAd1 insert at 3 and 2.8kb (pGAd1 R).

The PcrAd2 constructs were only digested using SalI. A SalI digest would give 2837bp and 2379bp bands in forward orientation and 3229bp and 1987bp bands for reverse orientation. The agarose gel resolved fragments showed that constructs 2 and 4 gave the bands expected of a forward orientation at 3 and 2 kb (named as pGAd2 F) while constructs 3 and 5 gave closer spaced bands at 2.8 and 2.5kb indicating a reverse oriented insert (pGAd2R). Clone 1 gave bands similar to reverse orientation but had a third band at 0.4kb which would not be expected if the desired PcrAd2 insert was present (*Figure 4.14b*).

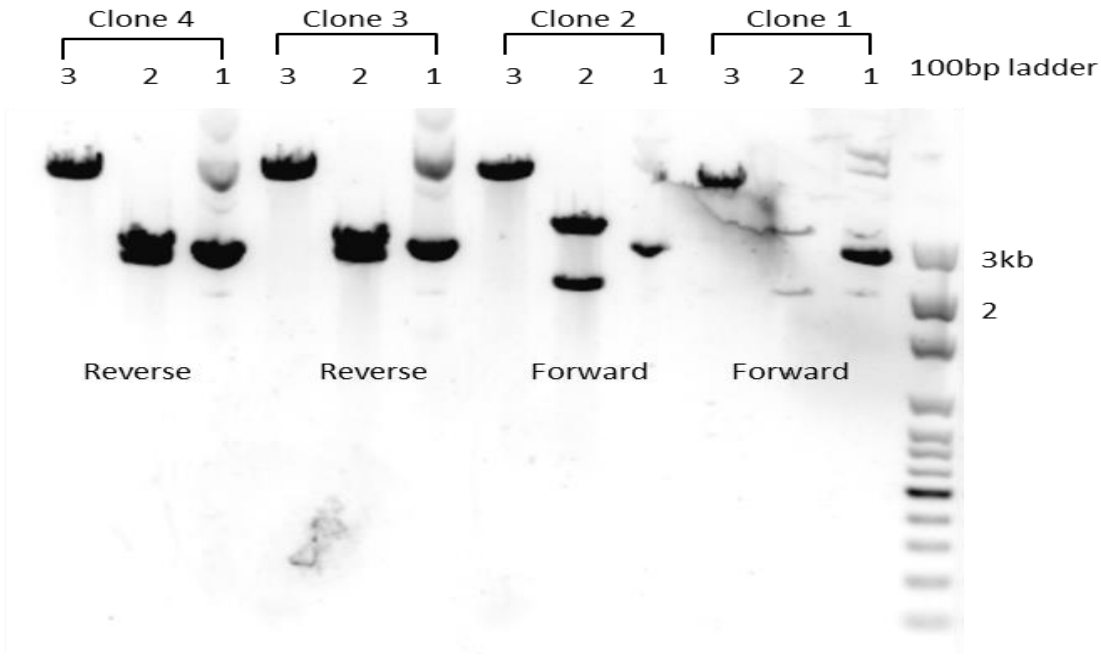

a)

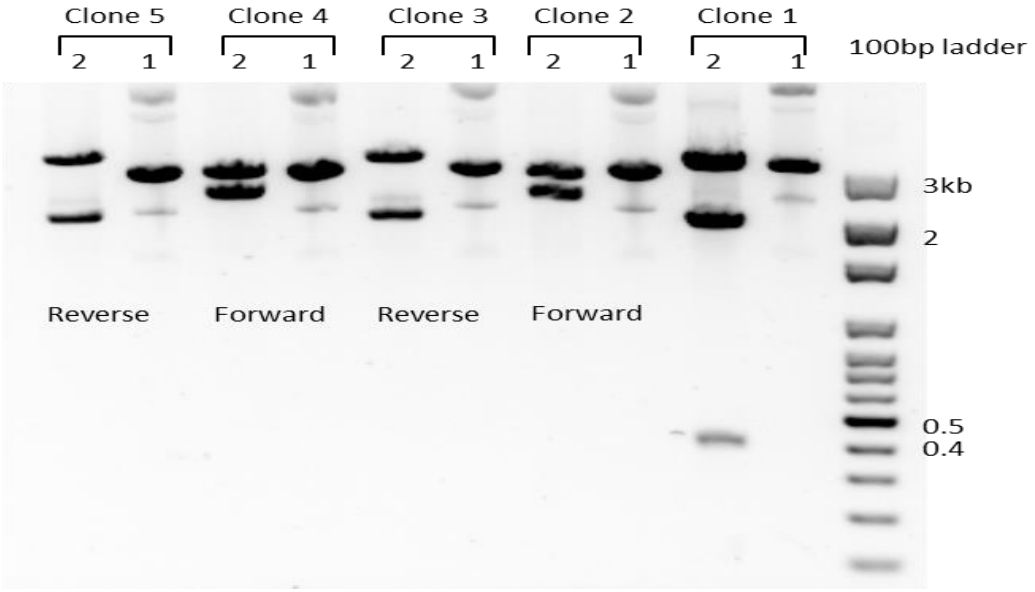

b)

Figure 4.14:

A) pGAd1clone digests, undigested (lanes 1), SalI (lanes 2) and SmaI (lanes 3). Constructs 1 and 2 SalI digests gave bands at ~3.3 and ~2kb corresponding to the PcrAd1 insert in the forward orientation. Constructs 3 and 4 SalI digests gave 2 bands at ~2.8 and ~2.4kb indicating the reverse orientation. SmaI digests for all constructs show a large band of the linearized plasmid at around 5kb the 80bp band was very faint and was only visible using high exposure times. **B)** pGAd2 clone, undigested (lanes 1) and SalI (lanes 2). SalI Digests of clones 2 and 4 gave bands at ~3 and ~2.3kb corresponding to the PcrAd2 insert in the forward orientation. Clones 3 and 5 SalI digests gave 2 bands at ~2.8 and ~2.5kb indicating the reverse orientation. Clone 1 SmaI digests gave 3 bands at ~3 and ~2kb and a small band at ~0.4kb.

4.3.4 Subcloning of AdD1, AdD2 AdU1, AdU2 and AdU3 into pGL-3 Basic

Restriction digests were used to excise the conserved regions AdD1 and AdD2 downstream of exon 1, from the pTopAd3 plasmid, and AdU1, AdU2 and AdU3 upstream of exon 1 from pTopAd4 plasmid (*Figure 4.15*). The DNA was resolved, excised and extracted from agarose gels, then ligated into digested pGL-3 Basic plasmid with compatible ends.

4.3.4.1 Construction of pGAdD1F&R and pGAdD2F&R

HindIII restriction sites flanked the AdD1 and AdD2 conserved regions in the pTopAd3 plasmid. The digest would result in 6 bands ~4kb, 2778bp, 2244bp, 1717bp 1019bp and 457bp. The second band at 2778bp containing the AdD2 conserved region and the fourth band at 1717bp containing the AdD1 conserved region were excised form agarose gel (*Figure 4.16*) and ligated into HindIII digested pGL-3 Basic. The ligations were transformed in bacteria, plated and the DNA from several constructs extracted and identified using restriction digests.

Plasmids containing AdD1 were digested with BglII and resolved on agarose gel, with forward oriented inserts giving bands at 5779bp, 654bp, 307bp, and reverse oriented inserts giving 5125bp, 740bp and 654bp bands (*Figure 4.17a*). Plasmids 1, 3, 5 and 6 showed the band pattern of forward-oriented inserts while constructs 2 and 4 showed the pattern of a reverse oriented insert. pGL-3Basic constructs containing the conserved AdD1 region were called pGAdD1F and pGAdD1R respectively.

Plasmids containing AdD2 inserts were digested using NheI and resolved on agarose gel to identify them. A forward oriented insert gave 2 bands at 6818bp and 712bp (plasmids 3 and 6), while a reverse oriented insert gave bands at 5500bp and 2000bp like constructs 1, 2, 4 and 5 (*Figure 4.17b*). pGL-3Basic constructs containing the conserved AdD2 region were called pGAdD2F and pGAdD2R respectively.

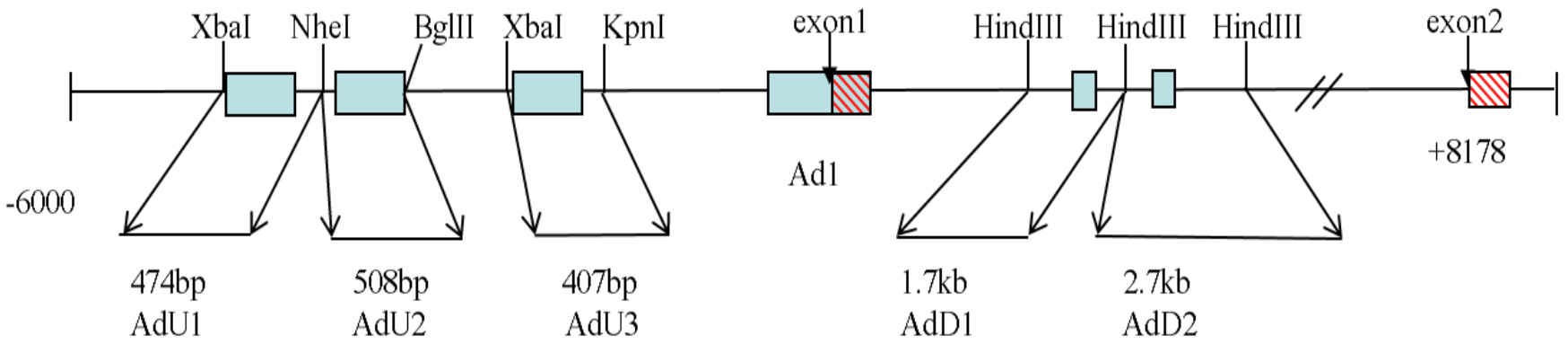

Figure 4.15:

Diagram of the strategy of isolating the conserved putative promoter regions upstream and downstream of exon 1, for Subcloning into pGL-3 Basic vector. Exon1 and 2 are shown as line shaded boxes, conserved regions are shown as shaded boxes. Restriction enzymes used to cut conserved regions are indicated on the tope with restriction fragment sizes indicated at the bottom.

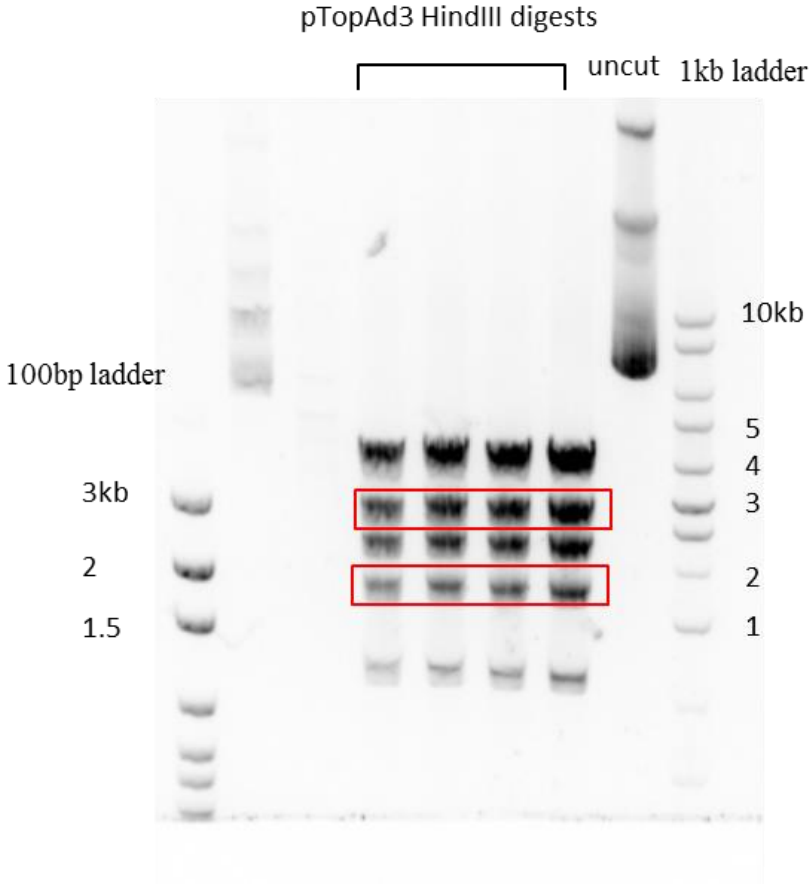

Figure 4.16:
HindIII digest of pTopAd3 resolved on agarose gel. The 2 boxed areas show the bands that were excised containing the 1.7kb AdD1 and the 2.7kb AdD2 conserved regions.

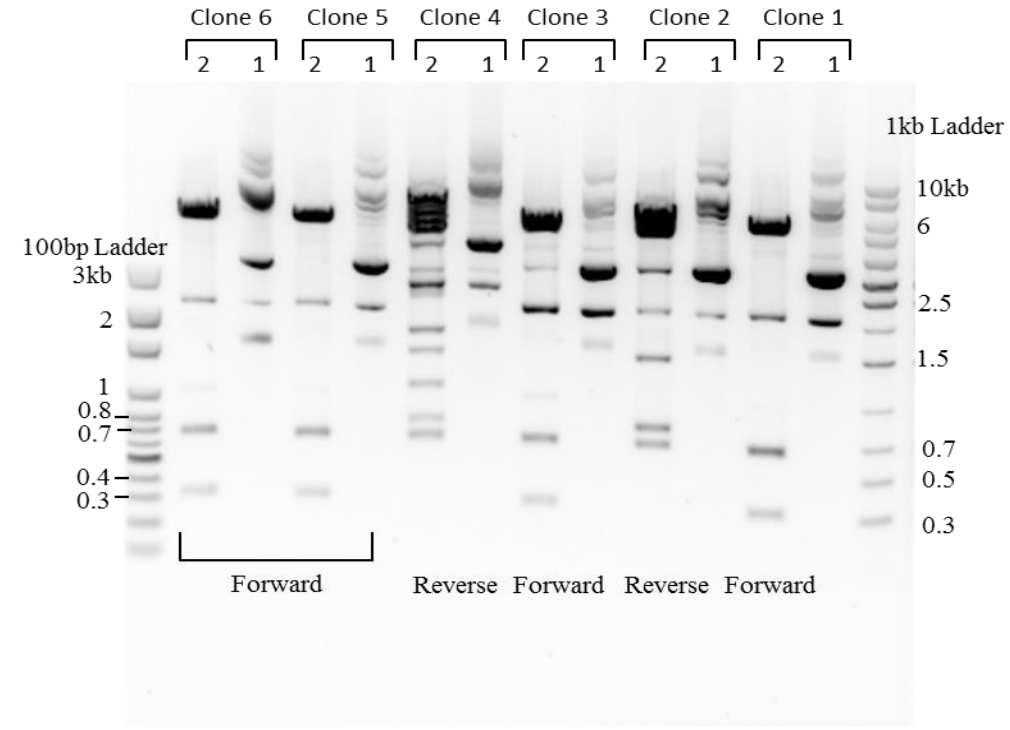

a)

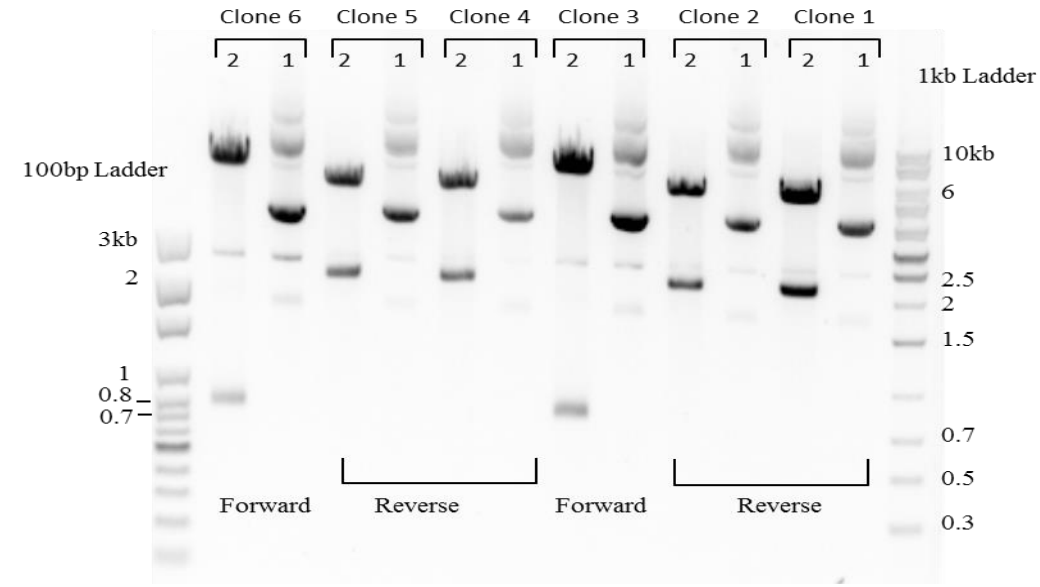

b)

Figure 4.17:

A) pGAdD1 constructs were digested with BglII (lanes 1) and resolved on agarose gel with undigested plasmid (lanes 2) to ascertain identity. Constructs with forward oriented inserts, Clones 1, 3, 5 and 6, gave bands at ~6000, ~700 and 300bp. Clones 2 and 4, however gave fragmentation bands at ~5000, and 2 bands at ~700 similar to a reverse oriented insert. Clones 2 and 4 also showed multiple unexpected bands (especially clone 4). **B)** pGAdD2 NheI digests were expected to give bands at 6818bp and 712bp for forward oriented inserts while reverse oriented inserts would 5497bp and 2099bp. Clones 3 and 6 gave band at ~6kb and 750bp indicating forward oriented insert. While clones 1, 2, 4 and 5 gave a pattern similar to a reverse oriented insert with 2 large bands at ~6 and 2kb. Lanes numbered 1 are undigested clones while lanes numbered 2 are the NheI digested clones.

Some of the pGAdD1 clones showed incomplete digests and potential nonspecific cutting giving extra unexpected bands. To check for the correct insert an additional HindIII digest was carried out. HindIII sites flank the insert and digestion with this enzyme would give the insert and vector bands. pGAdD1R&F digests gave the 1.7kb insert and the 4.8kb vector bands (*Figure 4.18 a)*, while pGAdD2R&F gave 2.7kb insert and 4.8kb pGL-3 basic vector band (*Figure 4.18 b*).

4.3.4.2 Construction of pGAdU1F&R and pGAdU2F and pGAdU3R

The 3 upstream conserved regions were subcloned from pTopAd4 were also cloned into pGL-3Basic using restriction digests. The conserved region AdU1 was cut out by a NheI + XbaI double digest; AdU2 was removed using a BglII+NheI dual digest and AdU3 using a KpnI+XbaI double digest (*Figure 4.15*). pTopAd4 digested with NheI+XbaI gives multiple bands, and the 6th band at 474bp would contain AdU1 conserved region which would then be ligated into NheI digested pGL-3 basic (see summary below). BglII+NheI digests of pTopAd4 gives 3 bands at 8247, 878 and 508bp: the 508bp fragment contains the AdU2 conserved region while KpnI+XbaI digest of pTopAd4 gives 8 bands, the 8th at 407bp containing AdU3.

The digests of pTopAd4 were resolved on agarose gel and the 474bp, 508bp and 407bp bands containing AdU1, AdU2 AdU3 respectively (Figure 4.19), were excised and the DNA extracted.

A problem with this approach was the inability to generate a construct with the AdU3 conserved region in a forward orientation, only in reverse. Other restriction digests produced inserts with AdU3 that were too large, and given the limited time remaining only the reverse oriented construct was made.

pTopAd4 Digests

AdU1 NheI+XbaI → pGL-3 NheI

AdU2 BglII+NheI→ pGL-3 BglII+NheI

AdU3 KpnI+XbaI→ pGL-3 KpnI+NheI

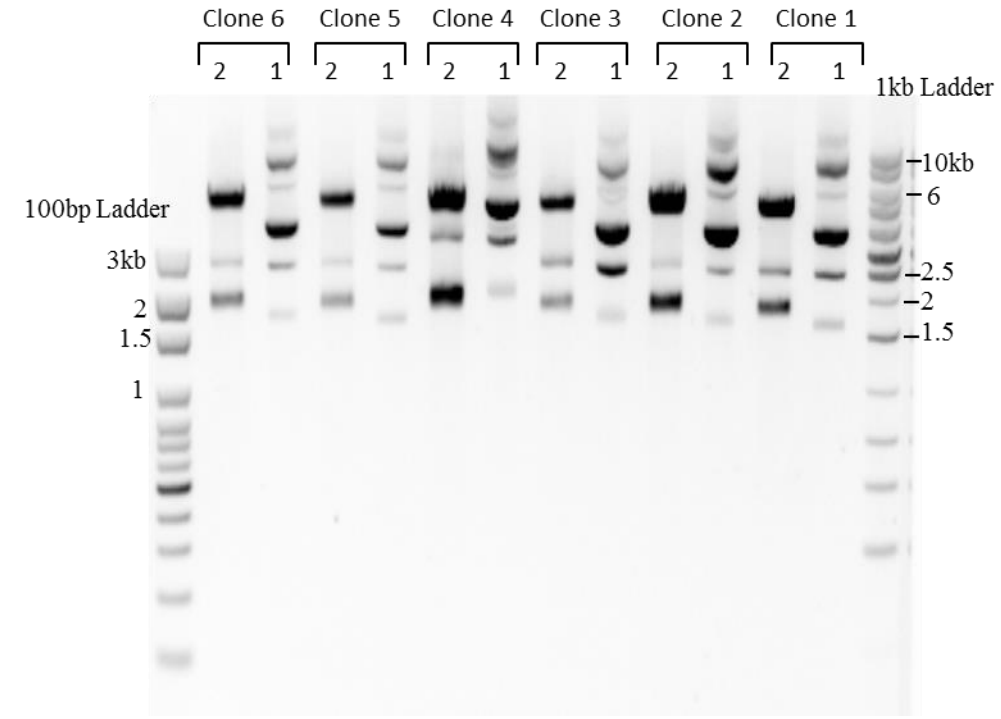

a)

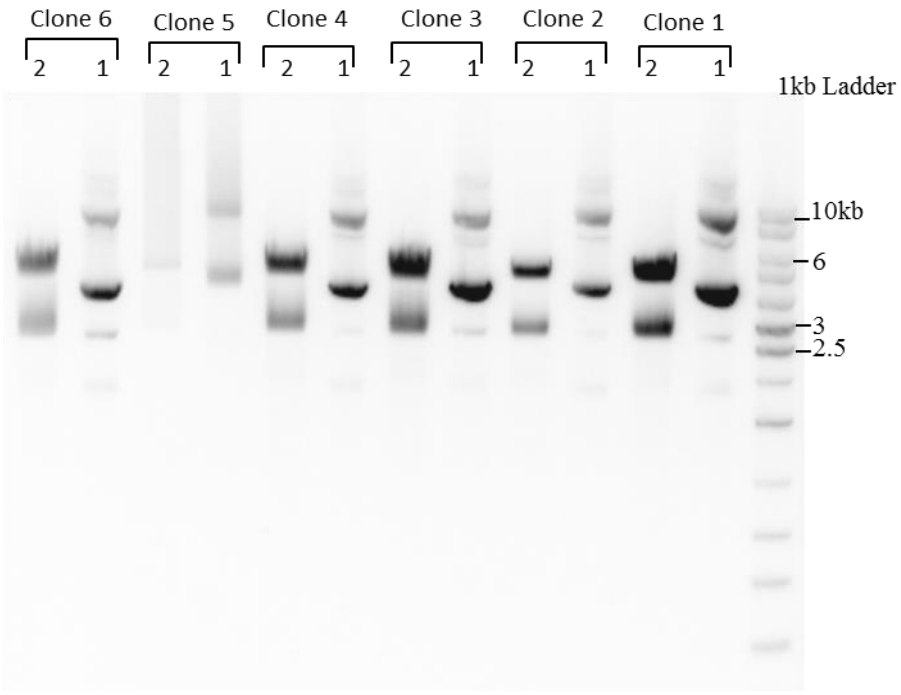

b)

Figure 4.18: pGAdD1 and pGAdD2 were digested with HindIII to cut out the insert, 1.7 and 2.7kb respectively, and resolved on agarose gel. **(A)** pGAdD1 digests gave a band at ~1.7kb and a vector band at ~5kb as expected . **(B)** pGAdD2 digests gave a band at ~2.7kb corresponding to the insert and ~5kb band corresponding to the vector. Undigested plasmids are in lanes 1 and HindIII digests in lanes 2 for each.

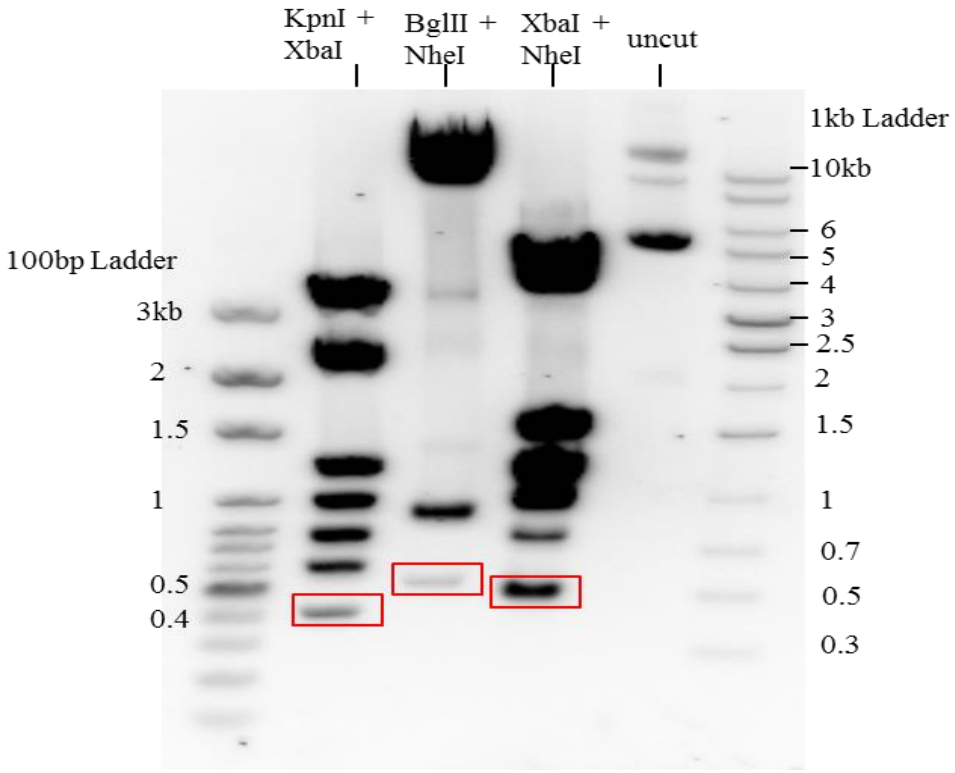

Figure4.19:

Digests of pTopAd4 were visualised alongside a 1kb ladder on 0.8% agarose gel. pTopAd4 digested with XbaI+NheI gave 6 bands as expected where the smallest band at ~450bp containing AdU1 was excised. BglII+NheI digests gave 3 bands at ~10kb, ~900bp and a ~500bp band containing AdU2. KpnI+XbaI digests gave 7 bands with the smallest band which contains AdD3 at ~400bp. The excised bands containing the conserved regions are marked by a box.

The extracted DNA was then ligated into pGL-3 Basic with compatible ends. AdU1 was cloned into NheI digested pGL-3 Basic giving pGAdU1F&R clone, AdU2 into BglII+NheI digested pGL-3 Basic giving pGAdU2F&R clone. The AdU3 conserved region would be ligated into KpnI+NheI digested pGL-3 Basic giving pGAdU3R clone. The plasmids were transformed, plated and colonies were inoculated into LB then the DNA was extracted. Restriction digests were used to check identity of the constructs.

pGAdU1 plasmids were digested with NheI+HindIII giving bands at 32bp 5260 for forward oriented insert and 506bp 4786bp for reverse (*Figure 4.20*). The plasmids were also digested using KpnI+NheI with forward oriented inserts giving bands at 490bp and 4802bp, while reverse oriented inserts give bands at 16bp and 5276bp. Clones 3-6 showed clear bands at ~500bp when digested with NheI+HindIII (lanes 2) indicating a clone with a reverse oriented insert. The corresponding KpnI+NheI digests (lanes 3) of clones 3-6 gave no bands at ~500bp further confirming a reverse oriented insert. Clones 1 and 2 gave no band at ~500bp when digested with NheI+HindIII, however the KpnI+NheI digests gave a band at ~500bp only for Clone 1 this may indicate a forward oriented insert in clone 1(*Figure 4.20 a*). The KpnI+NheI digests showed many unexpected bands which may indicate altered restriction enzyme specificity known as star activity or an incorrect clone for clone 1 and possibly 2 (*Figure.4.20 a*). Therefore further analysis of all plasmids was required.

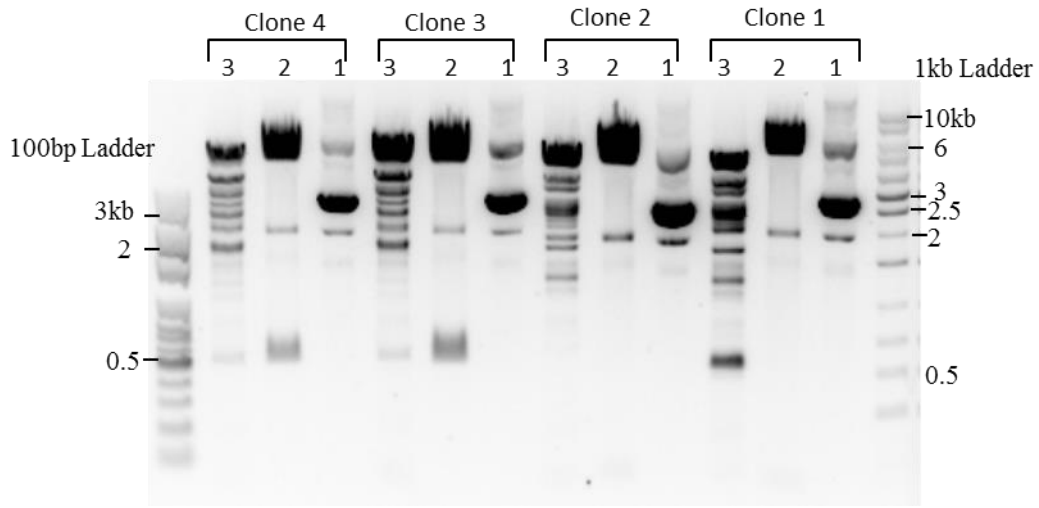

a)

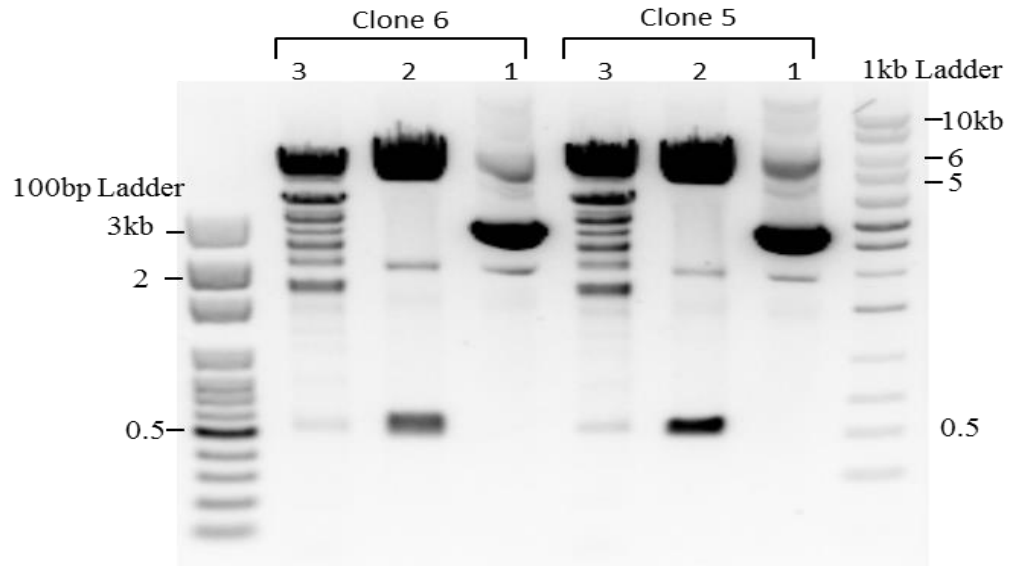

b)

Figure 4.20:

Potential pGAdU1 constructs were digested with NheI+HindIII (lanes 2) and KpnI+NheI (lanes3) and resolved on agarose gel alongside 10kb and 100bp ladder. **(A)** NheI+HindIII digests of clones1 and 2 did gave a linear ~5.5kb band and did not give bands at ~500bp. KpnI+NheI digests gave a clear ~500bp band only for clone 1 but gave unexpected multiple bands for both clones 1 and 2. This may indicate a forward oriented insert in clone 1 and incorrect inert in clone 2. **(A)&(B)** clone 3-6 NheI+HindIII digests gave 2 bands at ~6kb and 500bp, kpnI+NheI digests of clones 3-6 gave multiple unexpected bands but did not show clear bands at ~500bp like clone 1. This may indicate reverse oriented insert for 3-6.

Due to the multiple cutting of KpnI+NheI digests of pGAdU1 (lanes 3) there was a problem in identifying correct constructs mainly ones with suspected forward oriented inserts. To make sure there is an insert, a PstI digest was performed, as it cuts once in the middle of the insert, giving a linear band. The digests resolved on agarose showed that clone 2 does not contain the AdU1 insert as no cutting occurred, while clone 1 showed a clear difference in the PstI digested and undigested bands (*Figure 4.21 a*). This coupled with digest pattern in *Figure 4.20* indicate that clone 1 has a forward oriented AdU1 insert (pGAdU1F), while clone 2 doesn't have AdU1 insert.

pGAdU2 constructs, which can only be have a forward oriented AdU2 insert, were digested with NheI+BglII and resolved on agarose gel. This would cut out the insert and separate it from the pGL-3 basic vector giving a ~5kb vector band and a 508bp band of the insert. All the plasmids tested showed a clear ~500bp band and a ~5kb band when digested showing the correct construct was isolated (*Figure 4.21 b*).

To determine the identity of pGAdU3 constructs, which can only have a reverse oriented insert, they were digested with HindIII giving 2 bands at 309bp and 4892bp. The digests were resolved on agarose gel and all the plasmids gave a clear band at about ~350bp and a large ~5kb band as expected (*Figure 4.21 c*). This shows the correct construct containing AdU3 was isolated.

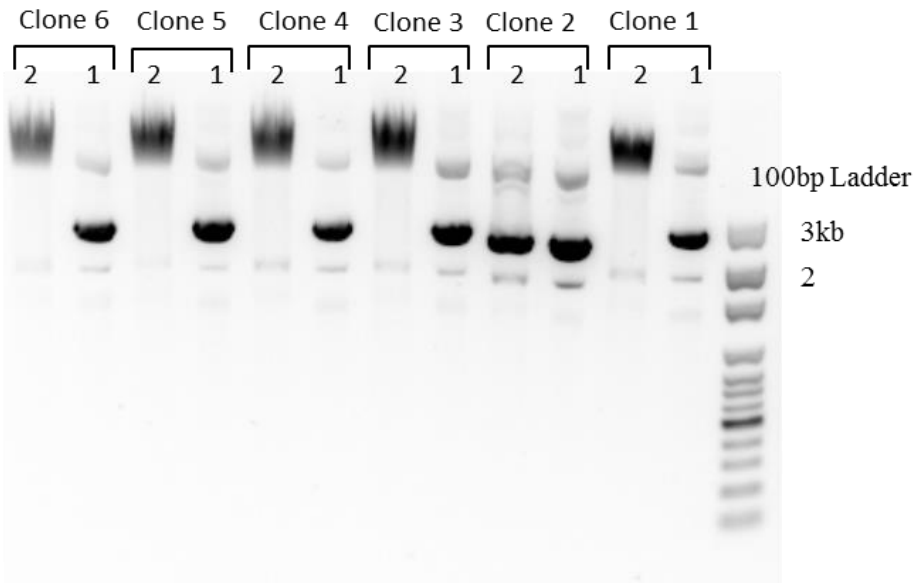

a)

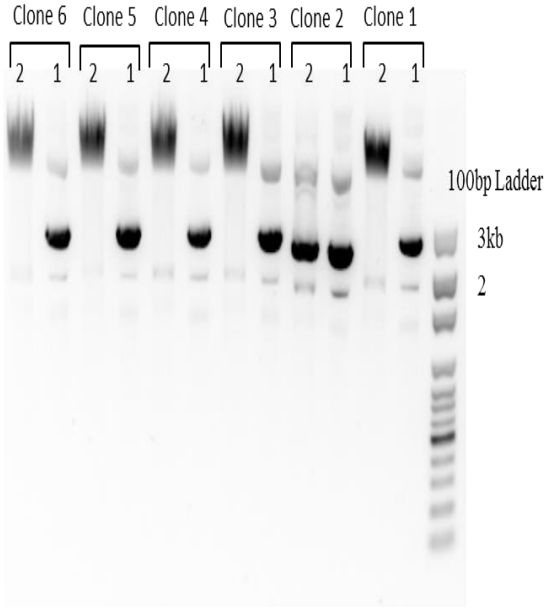

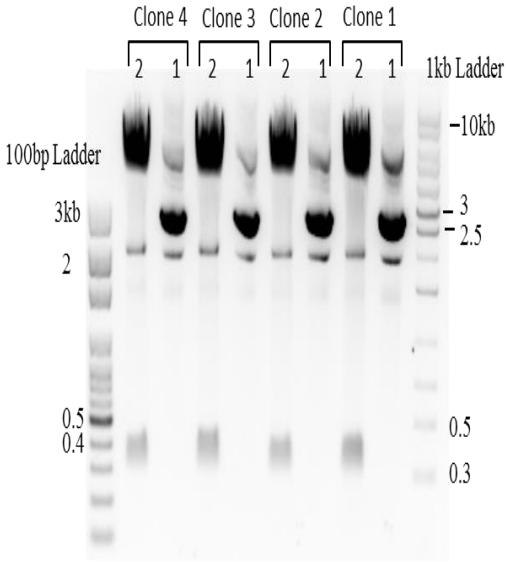

b) **c)**

Figure 4.21:
A) 6 potential pGAdU1 constructs were digested with PstI and resolved on agarose gel alongside 100bp ladder. All plasmids except clone 2 gave a large linear fragment when digested with PstI (lanes 2) and showed a clear difference compared to uncut DNA (Lane1). Clone 2 digested and undigested DNA showed do difference. **B)** pGAdU2 NheI+BglII (lane 2) digests resolved alongside 1kb and 100bp ladder on agarose gel. All constructs gave a band at ~500bp and ~5kb after digestion which indicates all constructs have AdU2 insert. **C)** pGAdU3 HindIII (lane 2) digested and undigested (lanes1) DNA resolved against 1kb and 100bp ladder. All constructs gave bands at ~5kb and ~400bp when digested with HindIII.

4.3.5 Subcloning of inserts into pGL-3 Promoter

The conserved regions AdD1, AdD2, AdU1, AdU2 and AdU3 are not likely to contain a basal promoter region, so in order to determine whether these regions contain active regulatory elements, it was necessary to sub-clone these conserved regions into pGL-3 Promoter, which contains a basal SV40 promoter. The conserved regions AdD1 and AdD2 lying in exon1 were not cloned into pGL-3 Promoter as these were likely to contain a basal promoter.

4.3.5.1 Construction of pGPAdU1, pGPAdU2 and pGPAdU3

The 3 upstream conserved regions were subcloned into pGL-3 Promoter vector.
The concentration of DNA insert after purification from the large pTopAd4 clone was very low and proved insufficient for ligations. In order to save time digestion and DNA purification from pGAdU1-3 constructs was used. The disadvantage of this approach is the inability of forming constructs with a forward oriented AdU1, only reverse. Constructs with AdU2 will be in forward orientation and constructs with AdU3 only in reverse, as previously with pGL-3 Basic constructs.

pGLAdU digests

pGLAdU1	AdU1 NheI+XbaI →	pGL-3 Promoter, NheI
pGLAdU2	AdU2 BglII+NheI→	pGL-3 promoter, BglII+NheI
pGLAdU3	AdU3 KpnI+XbaI→	pGL-3 Promoter, KpnI+NheI

The digests were resolved on agarose and DNA excised, purified and ligated into appropriately digested pGL-3 Promoter vector. The new pGL-3 Promoter constructs with AdU1, AdU2 and AdU3 were named pGPAdU1, pGPAdU2 and pGPAdU3 respectively.

The identity of potential pGL-3 Promoter constructs was checked using restriction digests, pGPAdU1 reverse and pGPAdU2 forward were double-digested with NheI+BglII. This would cut out the insert ~489bp for pGPAdU1 and ~508bp for pGPAdU2. The resolved digests showed that pGPAdU1 clone 2 and pGPAdU2

clones 1 and 3 of gave ~500bp insert band and ~5kb vector band, confirming successful sub-cloning (*Figure 4.22a*).

To confirm successful cloning of pGPAdU3, constructs were digested with HindIII and KpnI+BglII. HindIII digests would give bands at 4892bp and 501bp, while KpnI+BglII give bands at 414bp and 4979bp. Clones 2, 3 and showed the expected fragmentation pattern with the HindIII giving a ~500bp band and KpnI+BglII giving a ~400bp band, with both also giving a large ~5kb band (*Figure 4.22 b*).

4.3.5.2 Construction of pGPAdD1, pGPAdD2

pGL-3 Promoter does not contain a HindIII site in the multiple cloning site, making cloning AdD1 and AdD2 using HindIII digests of pTopAd3 not possible (see *Figure 4.13* above). As a consequence PCR primers flanking AdD1 and AdD2 were designed (Chapter 2, *Table.2.1*) to isolate the conserved regions for cloning into pGL-3 Promoter. PCR product PcrAdD1 containing AdD1 would be 306bp, while PcrAdD2 containing AdD2 would be 241bp. Portions of the PCR reactions (5µl) were resolved on agarose gel where PcrAdD1 gave a ~300bp band and PcrAdD2 gave a ~250bp band as expected (*Figure 4.23 a*).

The primers were designed with restriction sites on the flanks NheI in the 5' and XhoI in the 3' primers. A second aliquot of PCR reaction DNA was double digested with NheI+XhoI and the DNA resolved on agarose gel, excised and the DNA extracted. The extracted Dual digested PCR fragments were then ligated to NheI+XhoI dual digested pGL-3 Promoter, which was also agarose gel purified. The resulting ligates would result in constructs with forward oriented inserts pGPAdD1 containing PcrAdD1 and pGPAdD2 containing PcrAdD2. After transformation and plating of ligates, DNA from several colonies was identified using restriction digests. Both putative constructs pGPAdD1 and pGPAdD2 were dual digested with NheI+XhoI which would separate the inserts and the vectors. pGPAdD1 constructs 1-3 digests gave bands at ~300bp and pGPAdD2 constructs 2 and 3 gave bands at ~250bp as expected (*Figure 4.23 b*). This confirmed that constructs with correct inserts were isolated.

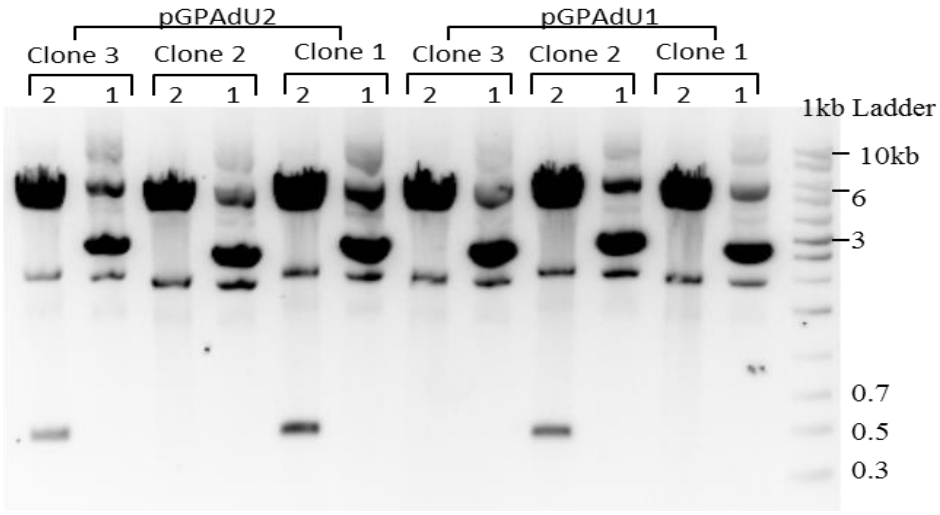

a)

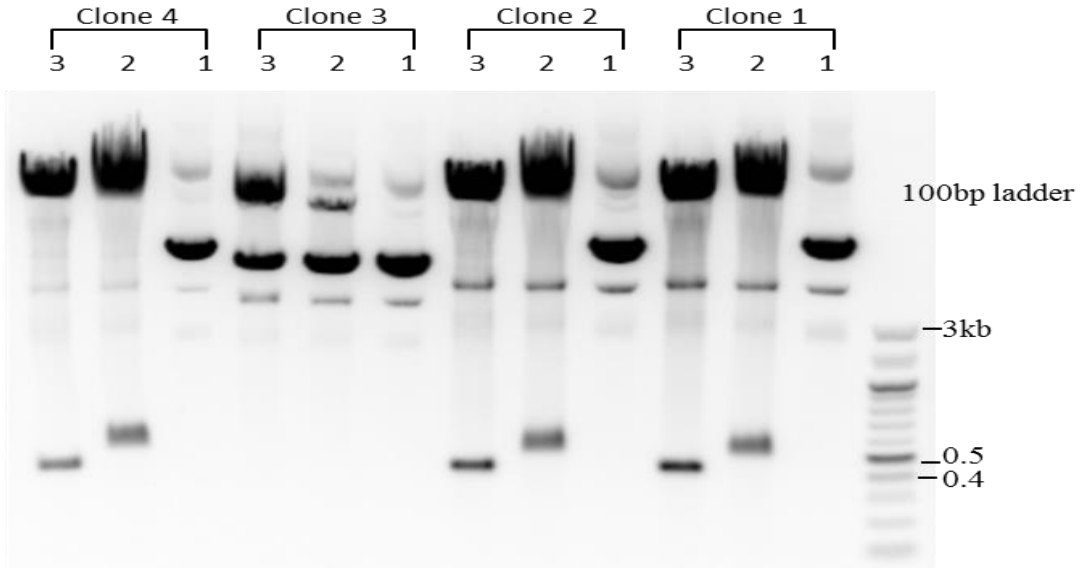

b)

Figure 4.22:

A) pGPAdU1 and pGPAdU2 undigested (lanes 1) and NheI+BglII (lanes 2) dual digested DNA resolved on agarose gel again 1kb and 100bp ladders. pGPAdU1 constructs 1 and 3 digests gave a large ~5kb band of linearized vector, Clone 2 gave ~5kb vector band and ~500bp insert band. pGPAdU2 clone 2 digests gave ~5kb vector band and no band at ~500bp corresponding to insert. Constructs 1 and 3digests of pGPAdU2 gave bands at ~5kb and ~500bp. **B)** pGPAdU3 was undigested DNA (lanes 1) was run alongside HindIII (lanes 2) and KpnI+BglII (lanes 3) digests, with 100bp ladder as reference. Constructs 1,2 and 4 HindIII digests gave ~500bp and ~5kb bands, KpnI+BglII digests gave ~400bp and ~5kb bands. Clone 3 digests showed partial digestion with a large ~5kb band appearing compared to undigested band. Clone 3 digests also showed no small bands at ~400-500bp.

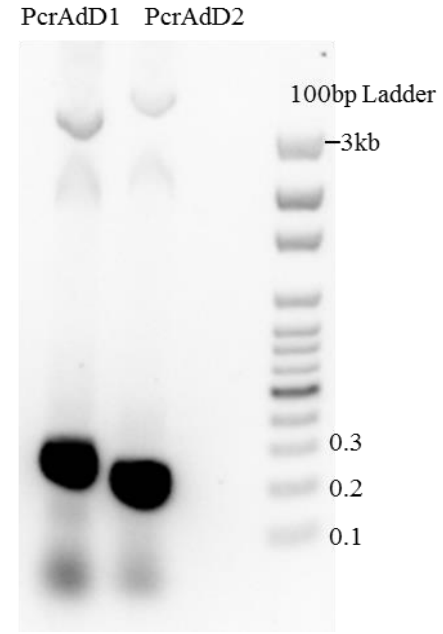

a)

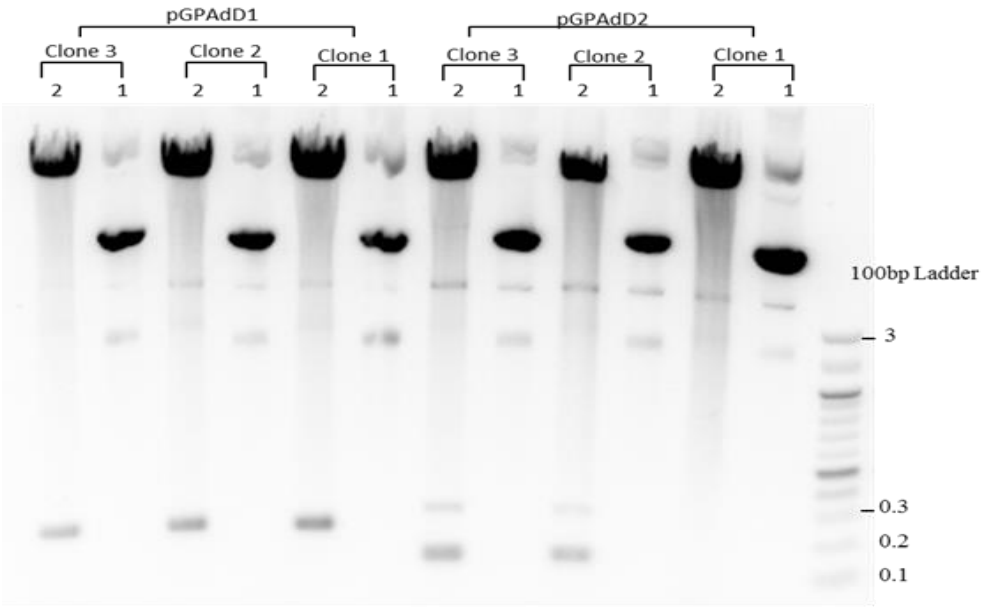

b)

Figure 4.23:
A) PCR reactions for PcrAdD1 and PcrAdD2 resolved on agarose gel with 100bp ladder. PcrAdD1gave a band at ~300bp while PcrAdD2 gave a band at ~200bp. **B)** Constructs of pGPAdD1 and pGPAdD2 undigested DNA (lanes 1) with NheI+XhoI (lanes 2) digests were resolved on agarose gel with 100bp ladder. pGPAdD1 clone 1-3 NheI+XhoI digests gave bands at ~300bp and a large vector band ~5kb. pGPAdD2 clone 2 and 3 gave bands at ~200bp and ~5kb when digested with NheI+XhoI while clone 1 only gave a linear band at ~5kb indicating no insert in clone 1.

4.3.5.3 Final Constructs

The various pGL-3 constructs formed were made by different methods. Some like TopAd1 and TopAd2 were PCR products directly ligated into SmaI digested pGL-3 basic vector. Other constructs were double-digested plasmid and inserts. *Figure 4.24* below shows the pGL-3 basic clones with the orientation and identity of the insert and the restriction enzymes used. pGL-3 promoter clones are shown in *Figure 4.25*.

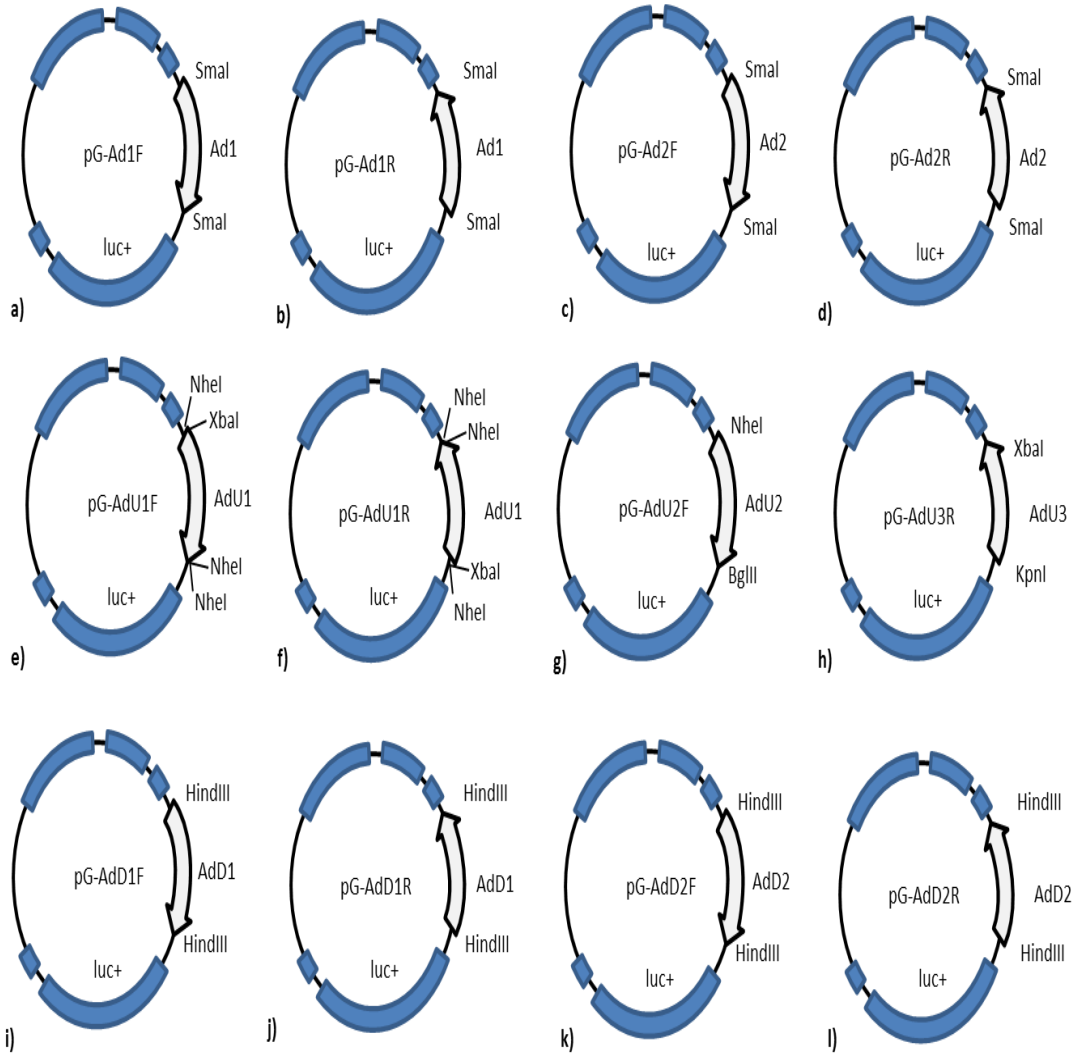

Figure 4.24

pGL-3 Basic clones isolated, clockwise insert arrows indicate a forward oriented insert, while reverse oriented inserts are indicated by anticlockwise arrows, luc+ indicates the luciferase gene. The name of each clone is shown in the middle of each clone. The restriction enzymes used are indicated flanking the insert, in panels **e)** and **f)** the innermost restriction enzymes, XbaI and NheI were used to isolate the insert. Insert names shown represent the conserved putative promoter region in insert (Figure 4.15).

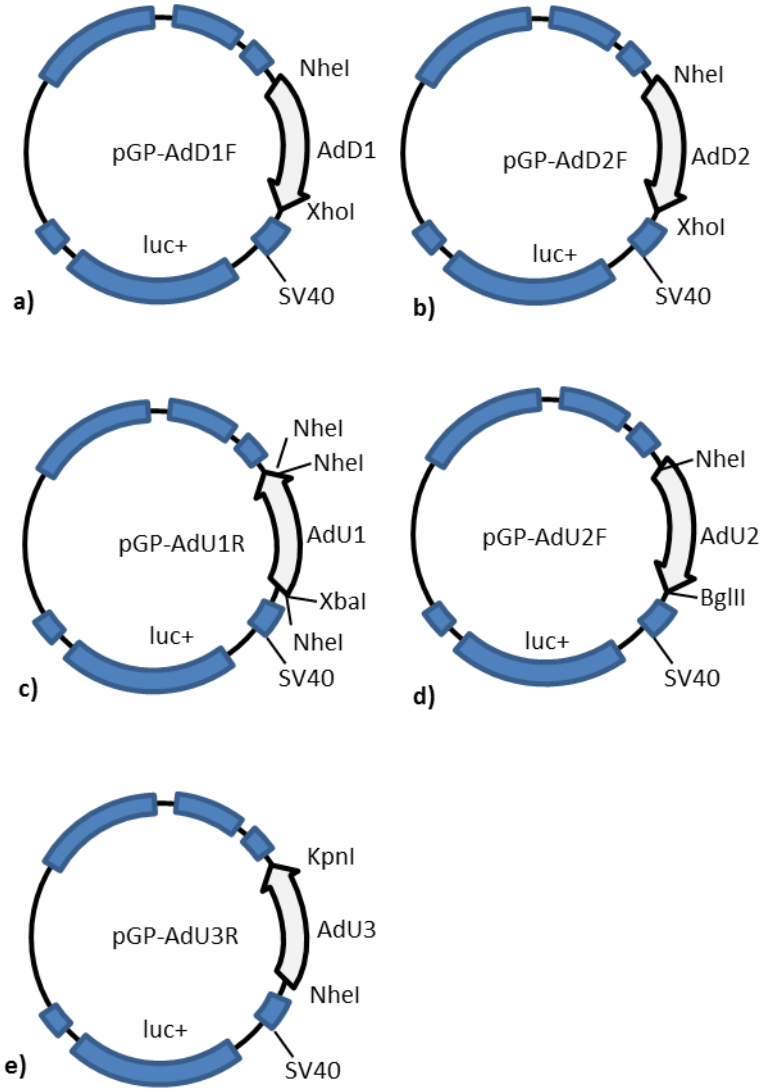

Figure 4.25:

The pGL-3 Promoter that were isolated are shown, with the clone name shown in the middle of each plasmid. Clockwise insert arrows indicate forward oriented inserts while anticlockwise indicates reverse orientation. The restriction enzymes used are indicated flanking the insert, in panels **c)** the innermost restriction enzymes, XbaI and NheI were used to isolate the insert. Insert names shown represent the conserved putative promoter region in insert (Figure 4.15).

4.4 Summary

In this Chapter, constructs were made in two different vectors, pGL3-Basic and pGL3-Promoter using the conserved regions identified in Chapter 3.

The following Table 4.1 summarises the constructs made, showing the vectors used and the insert ligated into the multiple cloning site, as well as the orientation of constructs.

The expression of the pGL-3 reporter gene constructs using cell transfection will be assessed in the next Chapter.

Insert	Vector	Orientation	Name
PcrAd1	Topo-Blunt	N/A	pTopAd1
PcrAd2	Topo-Blunt	N/A	pTopAd2
PcrAd3	Topo-XL	N/A	pTopAd3
PcrAd4	Topo-XL	N/A	pTopAd4
PcrAd1	pGL-3 Basic	Forward	pGAdB1F
PcrAd1	pGL-3 Basic	Reverse	pGAdB1R
PcrAd2	pGL-3 Basic	Forward	pGAdB2F
PcrAd2	pGL-3 Basic	Reverse	pGAdB2R
AdD1	pGL-3 Basic	Forward	pGAdD1F
AdD1	pGL-3 Basic	Reverse	pGAdD1R
AdD2	pGL-3 Basic	Forward	pGAdD2F
AdD2	pGL-3 Basic	Reverse	pGAdD2R
AdU1	pGL-3 Basic	Forward	pGAdU1F
AdU1	pGL-3 Basic	Reverse	pGAdU1R
AdU2	pGL-3 Basic	Forward	pGAdU2F
AdU3	pGL-3 Basic	Forward	pGAdU3R
PcrAdD1	pGL-3 Promoter	Forward	pGPAdD1
PcrAdD2	pGL-3 Promoter	Forward	pGPAdD2
AdU1	pGL-3 Promoter	Reverse	pGPAdU1R
AdU2	pGL-3 Promoter	Forward	pGPAdU2F
AdU3	pGL-3 Promoter	Reverse	pGPAdU3R

Table 4.1:
A summary of all 21 constructs formed, the orientation of the first 4 constructs pTopAd1-4 was unimportant. They were used for only subcloning into pGL-3 Basic and promoter vectors and were not transfected. The F and R at the end of clone names indicates the orientation of insert forward and reverse respectively.

Chapter 5

Assessment of Adcyap1r1 promoter elements by Reporter Gene assays

5. Assessment of Adcyap1r1promoter elements by Reporter Gene assays

5.1 Introduction

In the preceding Chapter, a series of promoter constructs were made containing regions of the mouse Adcyap1r1 gene. In order to evaluate their function in regulating gene expression, the constructs needed to be transfected into suitable cell lines, and the expression of the luciferase enzyme assayed. As a control, the cells were also transfected with another plasmid expressing Renilla luciferase. By comparing the expression of the two different luciferases, the relative strength of promoters and the effect of regulatory regions can be evaluated.

Three cell lines were chosen in this study for the testing of Adcyap1r1 reporter constructs. Cos 7 cells were chosen as a negative control as they do not normally express the PAC1 receptor (McCulloch et al. 2000; Lutz et al. 2006). Neuro-2a neuroblastoma cells and α-T3 gonadotrophs however, both express PAC1 receptor (Rodríguez-Henche et al. 2002; Miura et al. 2013). Neuro 2a cells are a neuronal precursor model and would be a useful model in investigating developmental expression. α-T3 gonadotrophs will be used as a neuroendocrine model to investigate tissue specific expression.

The aims of this Chapter were therefore to:

- establish an efficient transfection procedure for the three cell lines
- establish a protocol for measuring luciferase activity
- evaluate expression from each of the promoter constructs
- determine which regions are responsible for conferring tissue-specific expression and also inducibility by hydrogen peroxide

5.2 Method Development

5.2.1 Establishing Efficient Transfection procedures

There are various transfection reagents available for transfection, and before any transfections were made, a comparison was made to determine the most efficient transfection reagent for each cell line.

The Cos 7 cells were transfected using GeneJuice, as it is known from previous studies to be an efficient transfection reagent for this cell line. The Cos 7 cells were therefore used as a positive control for transfection. The Neuro 2a and α-T3 cells were transfected using Lipofectamine, GeneJuice and Fugene transfection reagents. All three cell lines were transfected with 0.3μg/well pRL-TK which encodes renilla luciferase. The luminescence arising from expression of the enzyme was measured 24hrs after transfection , using Spectramax M5 microplate reader, where expression level was an indication of transfection efficiency. Untransfected cells from all 3 cell lines were used as negative controls.

In both the α-T3 and Neuro 2a cells (*Figure 5.1*) Fugene gave very low levels of luminescence, while transfection with GeneJuice gave moderate levels of luminescence equivalent to Cos 7 controls (*Figure 5.1*). Transfection using Lipofectamine gave the highest levels of luminescence in both α-T3 and Neuro 2a cells being almost double that of luminescence produced when GeneJuice was used.

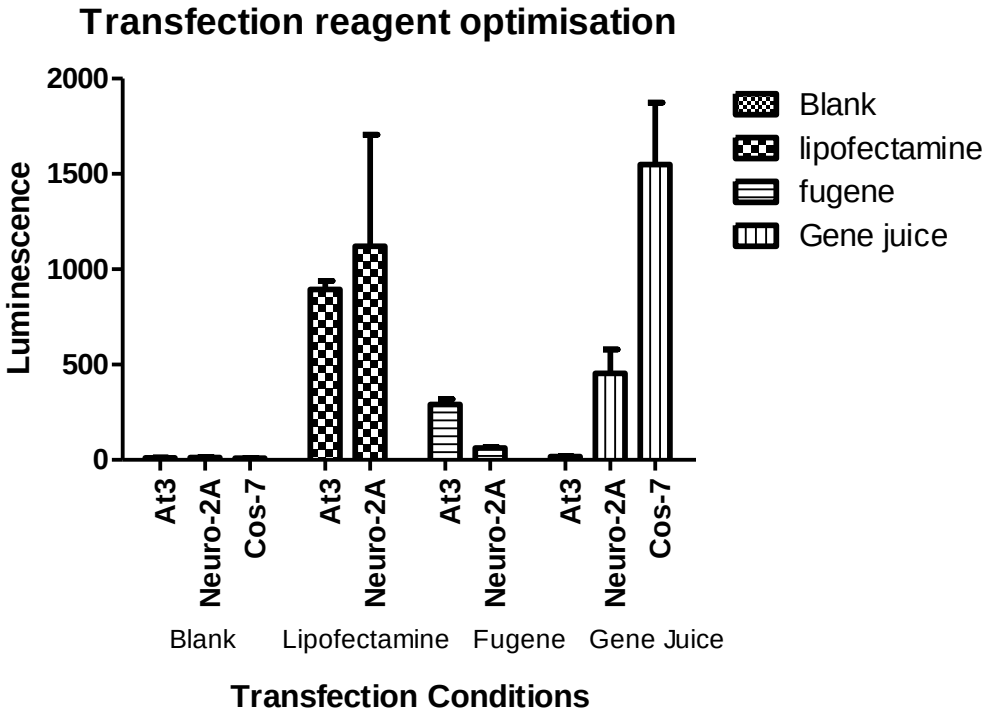

Figure 5.1

Optimisation of Transfection of α-T3 and Neuro-2A cells using Lipofectamine, GeneJuice and Fugene transfection reagents. Cos 7 cells transfected using GeneJuice were used as positive controls, blank untransfected cells were used as negative controls for all 3 cell lines. Renilla luciferase acitivity was determined as described in Materials and Methods and is based on the the level of luminescence observed. Results represent the mean ± SE from 6 measurements (n=6) for each condition, 24 hrs post transfection.

5.2.2 Optimizing luciferase assay

After establishing Lipofectamine as the most efficient transfection reagent for both α-T3 and Neuro 2a cells and Gene Juice for Cos-7, it was important to determine the time window for measuring luciferase expression. The expression of Renilla luciferase was measured over a period of 72 hrs after transfection. This was done to make sure that when luciferase activity was measured it would be done at the time giving highest expression, allowing for accurate comparison of promoter activity. Measurements were taken at 24 hrs, 48 hrs and 72 hrs in α-T3, Neuro 2a and Cos 7 cells transfected with the Renilla luciferase plasmid pRL-TK. α-T3 and Neuro 2a cells were transfected using Lipofectamine while Genejuice was used for Cos 7 cells. Untransfected cells were used as negative controls for all 3 cell lines. The α-T3 cells showed a similar expression pattern as Cos7, with a peak at 48hrs, where there was moderate increase in luciferase activity at 24hrs followed by a 2- and 4-fold increase for α-T3 and Cos 7 cells respectively at 48hrs. At 72 hrs there was a decrease in luciferase activity to the same levels as 24hrs for α-T3 cells (*Figure 5.2a*) while Cos 7 cells decreased slightly (*Figure 5.2c*). Neuro 2a cells however showed a moderate plateau of luminescence at 24hrs and 48hrs then a peak in luminescence at 72 hrs (*Figure 5.2b*). These results indicate that the time to detect the highest levels of expression in Cos7 and α-T3 cells would be 48 hrs after transfection, while for Neuro 2a cells it would be at 72 hrs, although it is important to mention that the Neuro 2a levels of expression are much lower than that of α-T3 cells and lower still than Cos 7 cells. It was decided that the best time to measure expression would be 48 hrs post-transfection for all 3 cell lines as a compromise between expression levels and convenience in large scale multi well transfections.

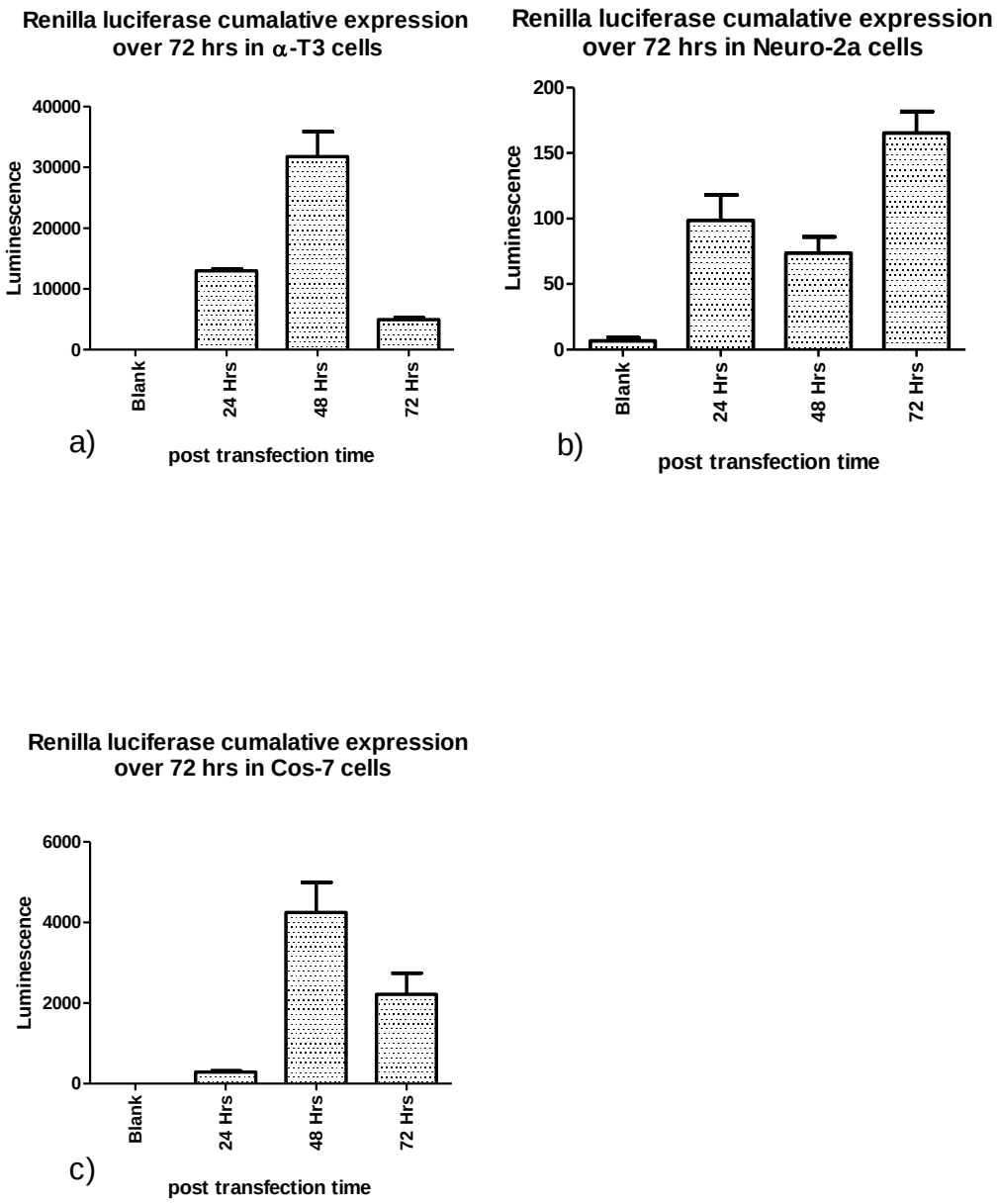

Figure 5.2

The cumulative expression of Renilla Luciferase was measured by transecting α-T3 **(a**) and Neuro 2A **(b**) cells with pRL-TK using Lipofectamine transfection reagent. Cos 7 cells **(c)** were transfected using GeneJuice, untransfected cells for all 3 cell lines were used as negative controls. Results represent the mean ± SE from 6 measurements (n=6) for each condition, 24, 48 and 72 hrs post transfection.

5.2.3 Selecting a suitable concentration of H_2O_2

For the planned experiments to test for induced expression of luciferase after cell stress, the cell were treated with H_20_2 24hrs post transfection. The intent was to stress the cells with sub-lethal concentrations and induce the anti-apoptotic protective role of PAC1. Several concentrations of H_20_2 had been used previously for the different cell lines, so in order to find a suitable concentration, an MTT assay was performed on the cells following exposure to various concentrations of H_2O_2, to determine which concentration of H_20_2 should be used to achieve sub-lethal cell.

Neuro-2A, Cos-7 and α-T3 cells were treated with H_2O_2 at 0, 5, 10, 20, 50, 100, 200μM concentrations and MTT assay performed the following day (*Figure 5.3*). There was a detectable loss of viability at concentrations greater than 20μM and more than half of cells were non-viable at 100μM. A concentration of 30μM appears to be sufficient to start stressing the cells without killing too many, so that there are sufficient cells to measure luciferase activity post-transfection.

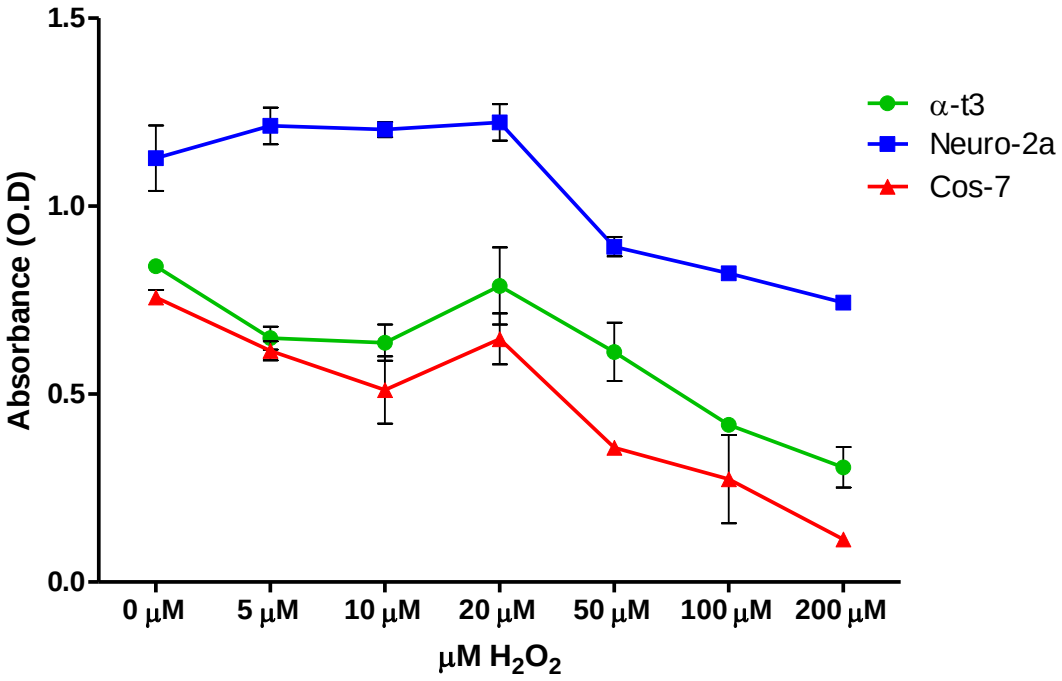

Figure 5.3:

A Standard concentration curve of different concentrations of H_2O_2 in Neuro-2a Cos-7 and α-T3 cells. The absorbance was measured 24hrs after treatment with H_2O_2. Results represent the mean ± SE from 3 measurements (n=3) for each concentration.

5.3 Results

5.3.1 Analysis of Basal Promoter Elements Using pGL3-Basic Constructs

Neuro-2a, Cos-7 and α-T3 were co-transfected with the pGL-3 Basic plasmid constructs made in the previous Chapter, and the pRL-TK plasmid containing Renilla luciferase as an internal positive control as described in Chapter 2. The dual luciferase activity was measured 48 hrs post-transfection and normalised against control untransfected cells. Expression results were analysed for difference between constructs compared to control pGL-3 Basic to measure expression level for each clone.

5.3.1.1 Ad1 and Ad2 basal promoter regions

The Ad1 and Ad2 inserts spanning the transcription start site as expected appear to contain the basal promoter regions involved in constitutive expression of mouse *Adcyap1r1*. The results in Figure 5.4 show clearly that the Ad1 and Ad2 inserts that directly flank the transcription start site (both forward and reverse orientations) give a significantly higher level of expression in all cell lines than expression from pGL-3 Basic. The exception being Ad2R which showed no difference in expression compared to pGL-3 Basic control in Neuro2a and α-T3 cells but showed significantly higher expression than pGL-3 Basic in Cos-7 cells (*Figure 5.4*). The highest level of expression observed in all the clones was observed in Neuro-2a cells (*Figure 5.4 a*). The expression observed using the proposed new Ad1 minimum promoter region (-80 to +353) is higher compared to the Ad2 reported minimum promoter region (-180 to +206) in all 3 cell lines but only in forward orientation (*Figure 5.4*).

The forward oriented Ad1 fragment gave slightly higher expression than the reverse Ad1 fragment in Neuro-2a cells; however, there was minimal difference due to orientation in the other 2 cell lines.

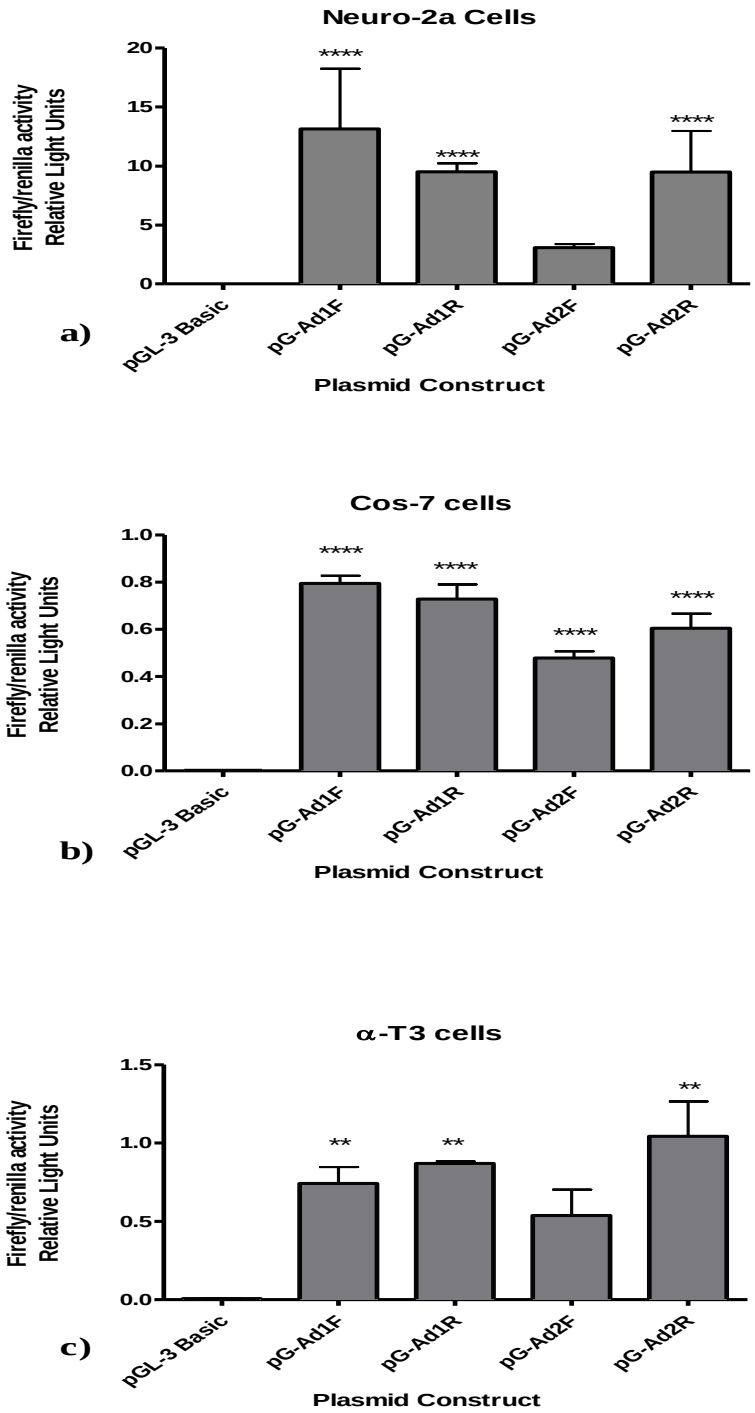

Figure 5.4 Luciferase expression from basal promoter regions

Basal promoter regions Ad1 and Ad2 in pGL-3 Basic vectors were transfected into Neuro-2a **a)** Cos-7 **b)** and α-T3 cells **c).** Dual luciferase activity was measured and the relative light units calculated as described in materials and methods. Results represent the mean ± SE from 3 measurements (n=3) for each condition, 48 hrs post transfection. Significant increase in expression compared to pGL-3 Basic is indicated. **** $p<0.001$; ** $p<0.01$; * $p<0.05$.

Ad2F and Ad2R show a very clear difference in expression in Neuro-2a cells, with the forward orientated fragment giving significantly lower expression ($p<0.001$). This indicates that the orientation of the Ad2 fragment has an influence on the degree of expression from this region. Taken together the results indicate that there is an element in the region between -80 and -180 that reduces the expression from the basal promoter but only in the forward orientation. Also, the region downstream of SacII site at +206 to +353 may induce expression of basal promoter but only in forward orientation.

5.3.1.2 AdU1, AdU2, AdU3 Upstream regions

The upstream regions AdU1, AdU2 and AdU3 were not known previously to contain a basal promoter, but it was important to determine whether there was any low level expression due to this region. The results in Figure 5.5 shows that expression from these upstream regions is significantly lower in all cell lines than expression from the basal promoter regions Ad1 and Ad2 ($p<0.001$)(*Figure 5.4*). Of the upstream regions, the AdU1F insert gave the highest expression of all the upstream promoter regions in Neuro-2a cells but this was still 20-fold less than the Ad1 region in the forward orientation and 4.5-fold lower than Ad2 in the forward orientation. There is also some expression from the AdU2 insert and also from the AdU3 insert in the reverse orientation, for all cell lines in AdU3 and Cos-7 and α-T3 cells for AdU2. It is therefore possible that there are alternative transcription start sites in the upstream regions but transcription from this region is very low.

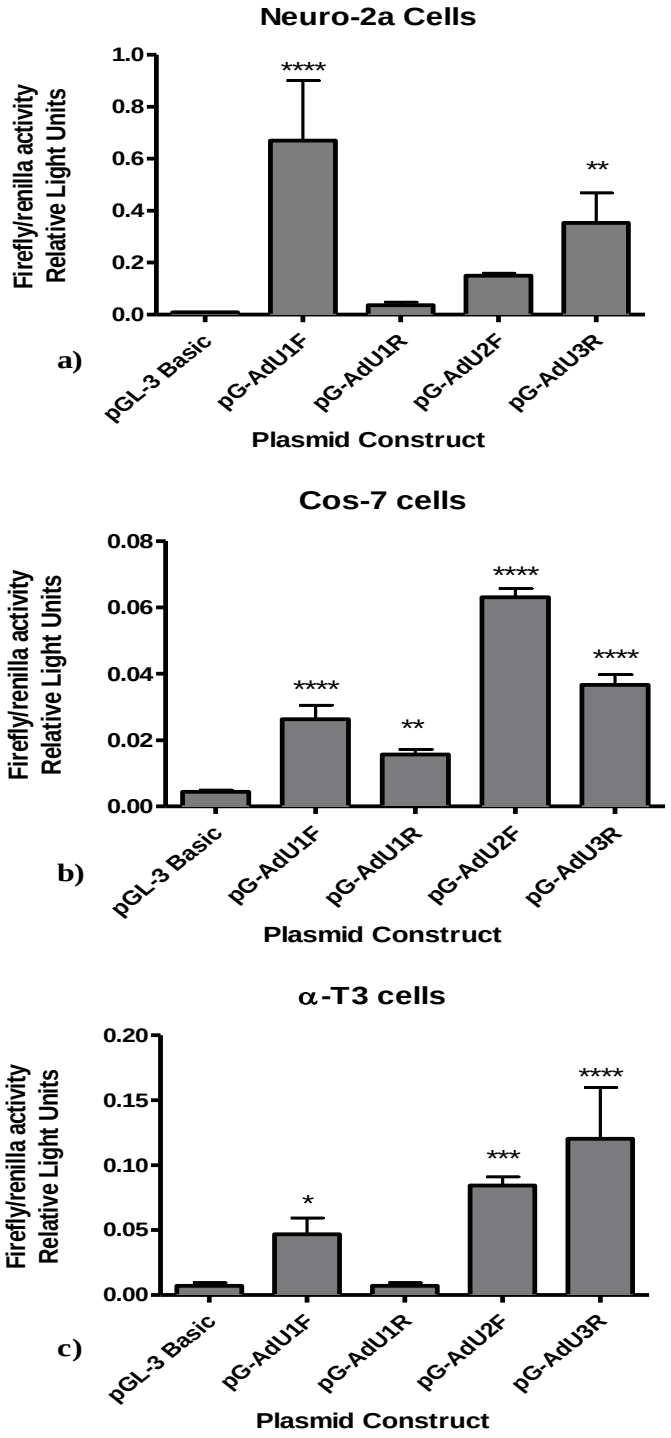

Figure 5.5 Luciferase expression from upstream regions

Upstream promoter regions AdU1 and AdU2 and AdU3 in pGL-3 Basic vectors were transfected into Neuro-2a **a)** Cos-7 **b)** and α-T3 cells **c).** Dual luciferase activity was measured and the relative light units calculated as described in materials and methods. Results represent the mean ± SE from 3 measurements (n=3) for each condition, 48 hrs post transfection. Significant increase in expression compared to pGL-3 Basic is indicated. **** $p<0.001$; ** $p<0.01$; * $p<0.05$.

5.3.1.3 AdD1 and AdD2 Downstream regions

There was also very low expression from the downstream regions in all of the cell lines (Figure 5.6) Like upstream regions expression was significantly lower than basal promoters Ad1 and Ad2 ($p<0.001$). The only insert that gave any significant level of activity was AdD2 in the reverse orientation, and this was the case in all three cell lines. It’s possible that there is a basal promoter sequence within this region, but it doesn't appear to be functional in the forward orientation so it is unlikely that this is biologically relevant.

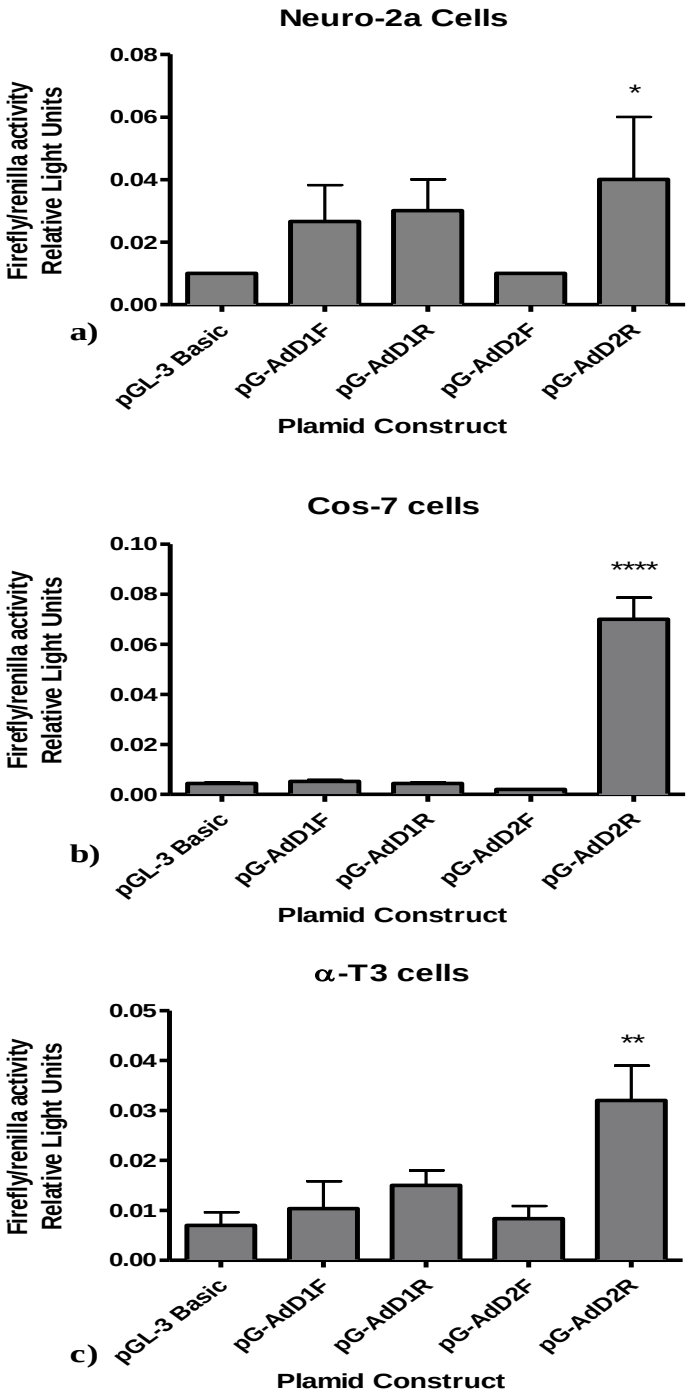

Figure 5.6 Luciferase expression from downstream regions

Downstream promoter regions AdD1 and AdD2 in pGL-3 Basic vectors were transfected into Neuro-2a **a)** Cos-7 **b)** and α-T3 cells **c)**. Dual luciferase activity was measured and the relative light units calculated as described in materials and methods. Results represent the mean ± SE from 3 measurements (n=3) for each condition, 48 hrs post transfection. Significant increase in expression compared to pGL-3 Basic is indicated. **** $p<0.001$; ** $p<0.01$; * $p<0.05$.

5.3.1.4 Differences in expression between cell lines

Using one way ANOVA and Bonferroni's post-test comparison of expression for each construct individually across the 3 cell lines, showed clearly higher expression in Neuro-2a for most constructs (Figure 5.7). The basal promoter constructs in particular show very high expression levels in Neuro2a cells, indicating selective expression in this neuronal precursor model (*Figure 5.7 a*). This would indicate that there is an element of developmental or tissue specific selectivity in the basal promoter regions.

There was some evidence of differences between the cell lines for the upstream regions which may contain alternative transcription start sites when expression in Neuro-2a was compared to expression in Cos-7 and α-T3 ($P<0.05$). The expression of AdU1F was significantly higher than reverse AdU1R in Neuro-2a which may indicate a developmental or tissue specific inducer in forward orientation or and inhibitor in reverse (*Figure 5.7 b*).

AdD1F also showed a significantly higher level of expression in Neuro-2a than in α-T3 cells ($p<0.05$), there was no significant difference between Neuro-2a and Cos-7 or α-T3 and Cos-7 cells. Reverse oriented AdD1R however, showed significantly higher level of expression in Neuro-2a than the other 2 cell lines but no significant difference between Cos-7 and α-T3. The expression of forward oriented AdD1F when compared, to reverse oriented AdD1R putative promoter region indicate developmental specific regulatory TF binding sites located in the reverse orientation or an inhibitor located in the forward orientation (*Figure 5.7 c*).

There was no significant difference in expression of AdD2F between any of the cell lines. However, when AdD2 is in reverse orientation in AdD2R expression levels in Cos-7 were higher than in α-T3 cells ($P<0.05$). This might suggest a neuroendocrine specific transcriptional inhibitor, located in AdD2F in the forward orientation or due to the increase in α-T3 expression of AdD2R compared to AdD2F, a neuroendocrine specific inducer locater in reverse orientation (*Figure 5.7 c*).

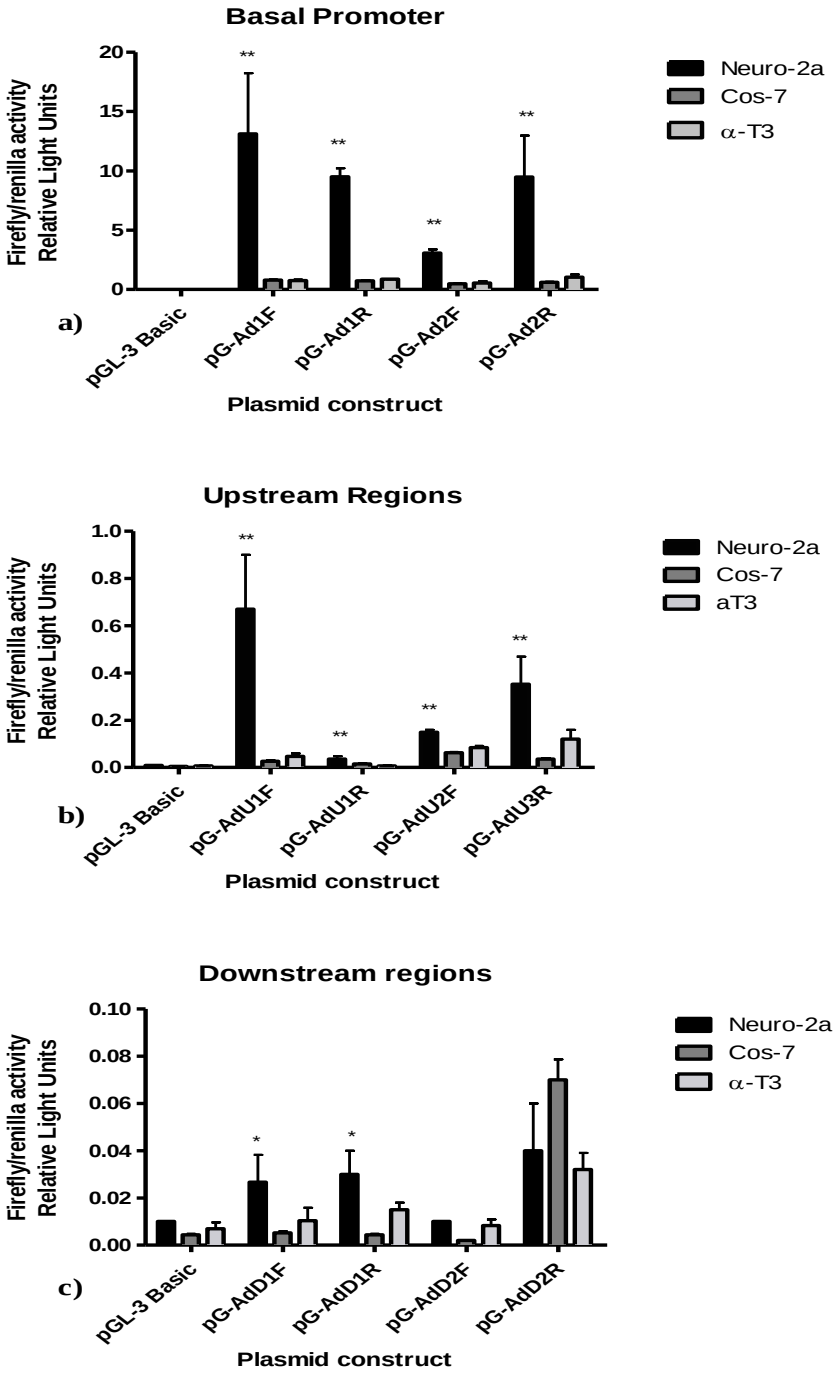

Figure 5.7 Comparison of Luciferase expression from promoter regions in all 3 cell lines

Data from different cell lines are compared. Most clones showed significantly higher expression in Neuro-2a cells compared to the other 2 cell lines. Basal promoters are shown in **a)** upstream in **b)** and downstream in **c)** Results represent the mean ± SE from 3 measurements (n=3) for each condition, 48 hrs post transfection. Significant differences between the cell lines are indicated. ** $p<0.01$; * $p<0.05$.

5.3.1.5 Effect of oxidant stress on Expression of pGL-3 Basic constructs.

To test for stress induced expression from the basal promoter and the putative alternate basal promoters in the upstream and downstream regions, Neuro-2a, Cos-7 and α-T3 were co-transfected with pGL-3 basic constructs and pRL-TK as an internal positive control as described in *Chapter 2*. Cells were treated with or without 30 μM H_2O_2 24hrs post-transfection and luciferase activity was measured 48 hrs post-transfection and normalised against control untransfected cells. The luciferase activity for the untreated cells was used as a reference and compared to H_2O_2 treated cells and the change in expression calculated.

When comparing the inducibility between each construct what is immediately evident from the results in Figure 5.8 is that Ad1 and Ad2 show low levels of induction after H_2O_2 treatment in all cells, despite showing the highest levels of expression overall. The Ad1F insert was the only one that showed a significant increase in expression in all three cell lines following H_2O_2 treatment but this was only 1.5-fold in Neuro-2a, and 2-fold in α-T3 cells.

One of the upstream regions AdU1F showed a significant 2-fold increase in expression following Hydrogen peroxide treatment. This was evident in Neuro-2a cells as well as in α-T3 cells, but there was no increase in Cos-7 cells (*Figure 5.9*). AdU2F and AdU3R showed a significant increase in expression after Hydrogen peroxide treatment, but only in Cos-7 cells, 1.3 and 1.5 fold respectively.

Also, one of the constructs containing the downstream promoter region AdD2R showed a significant level of inducibility, with a 2.3-fold increase in expression Neuro-2a cells ($p<0.01$). This was significantly higher than for any of the other constructs (*Figure 5.10*). AdD2R showed a significant decrease in expression after Hydrogen peroxide treatment in α-T3 cells but it is not significantly different than the other constructs.

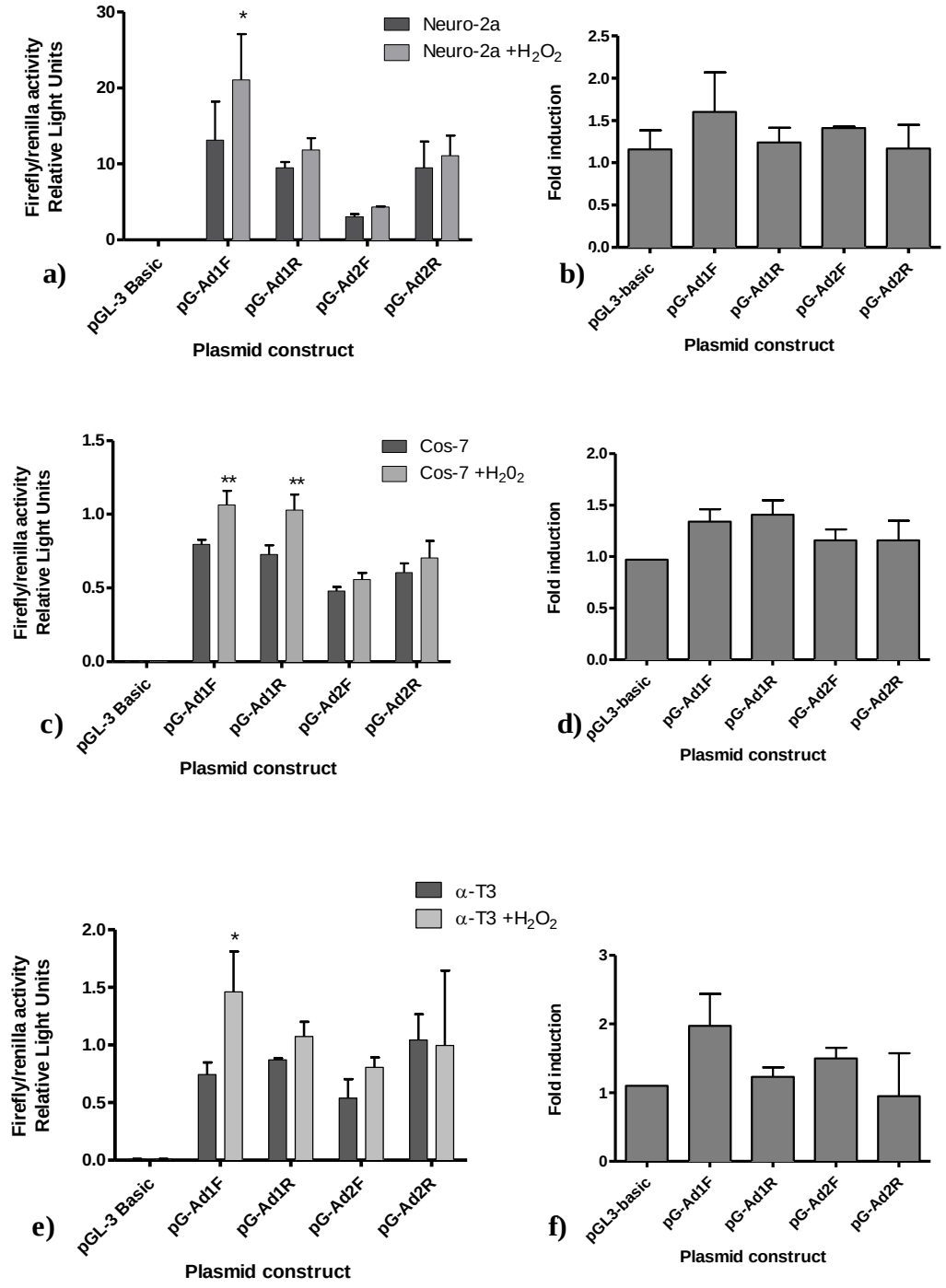

Figure 5.8. H_2O_2 induction of expression from basal promoter regions

Basal promoter regions in pGL-3 Basic were transfected into Neuro-2a **a)** Cos-7 **c)** and α-T3 cells **e)** and treated with 30μM H_2O_2 24 hours after transfection. Firefly and Renilla luciferase activity was measured 48 hours after transfection. The panels on the right show the fold induction of expression for Neuro-2a **b)** Cos-7 **d)** and α-T3 cells **f)**. The fold induction indicates the ratio of activity of treated v untreated cells. Results represent the mean ± SE from 3 measurements (n=3) for each condition. Expression levels of H_2O_2 treated and untreated cells that are significantly different are indicated. **** $p<0.001$; ** $p<0.01$; * $p<0.05$.

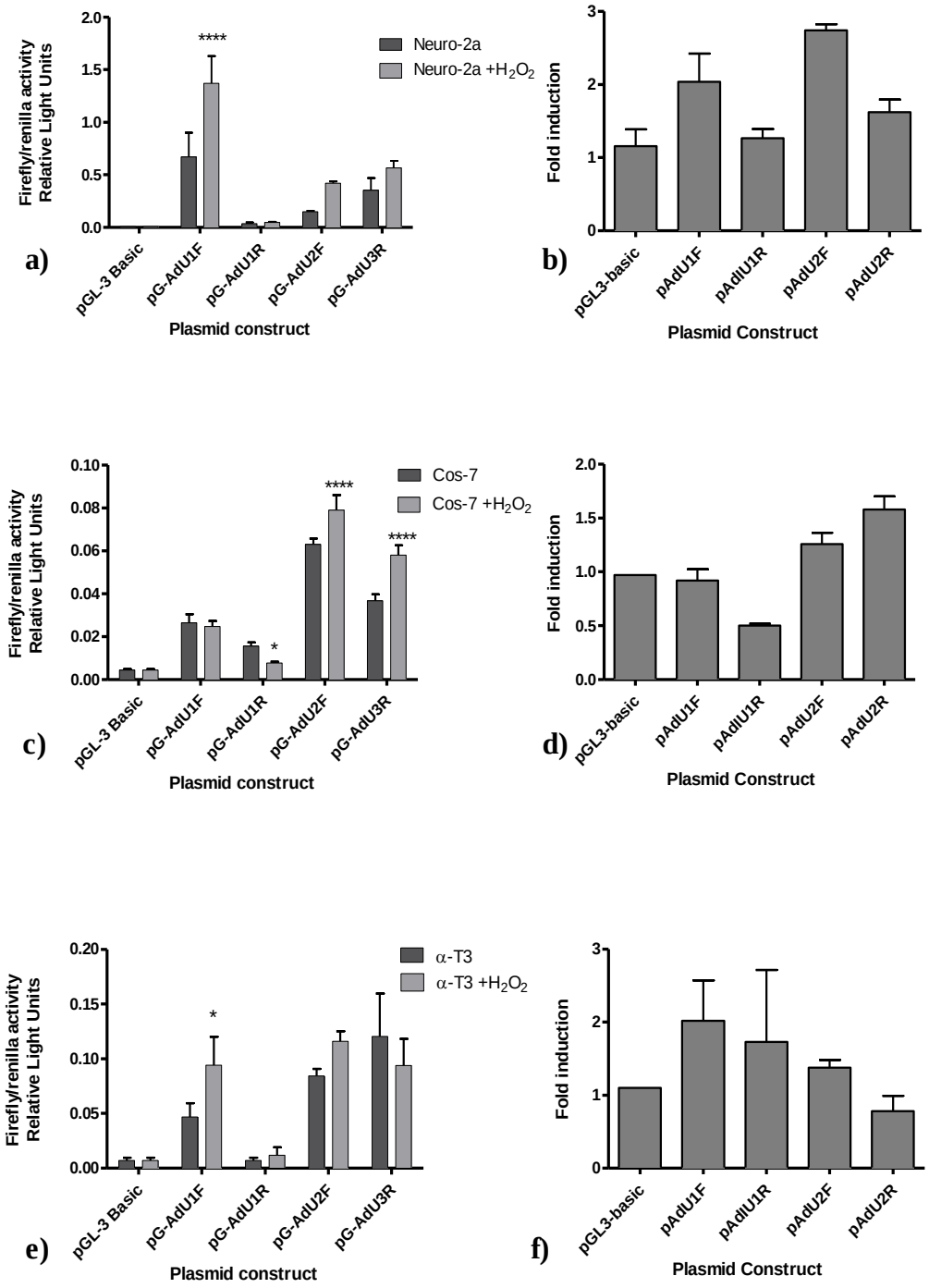

Figure 5.9. H_2O_2 induction of expression from upstream regions

Upstream promoter regions in pGL-3 Basic were transfected into Neuro-2a **a)** Cos-7 **c)** and α-T3 cells **e)** and treated with 30μM H_2O_2 24 hours after transfection. Firefly and Renilla luciferase activity was measured 48 hours after transfection. The panels on the right show the fold induction of expression for Neuro-2a **b)** Cos-7 **d)** and α-T3 cells **f)**. The fold induction indicates the ratio of activity of treated v untreated cells. Results represent the mean ± SE from 3 measurements (n=3) for each condition. Expression levels of H_2O_2 treated and untreated cells that are significantly different are indicated. **** $p<0.001$; ** $p<0.01$; * $p<0.05$.

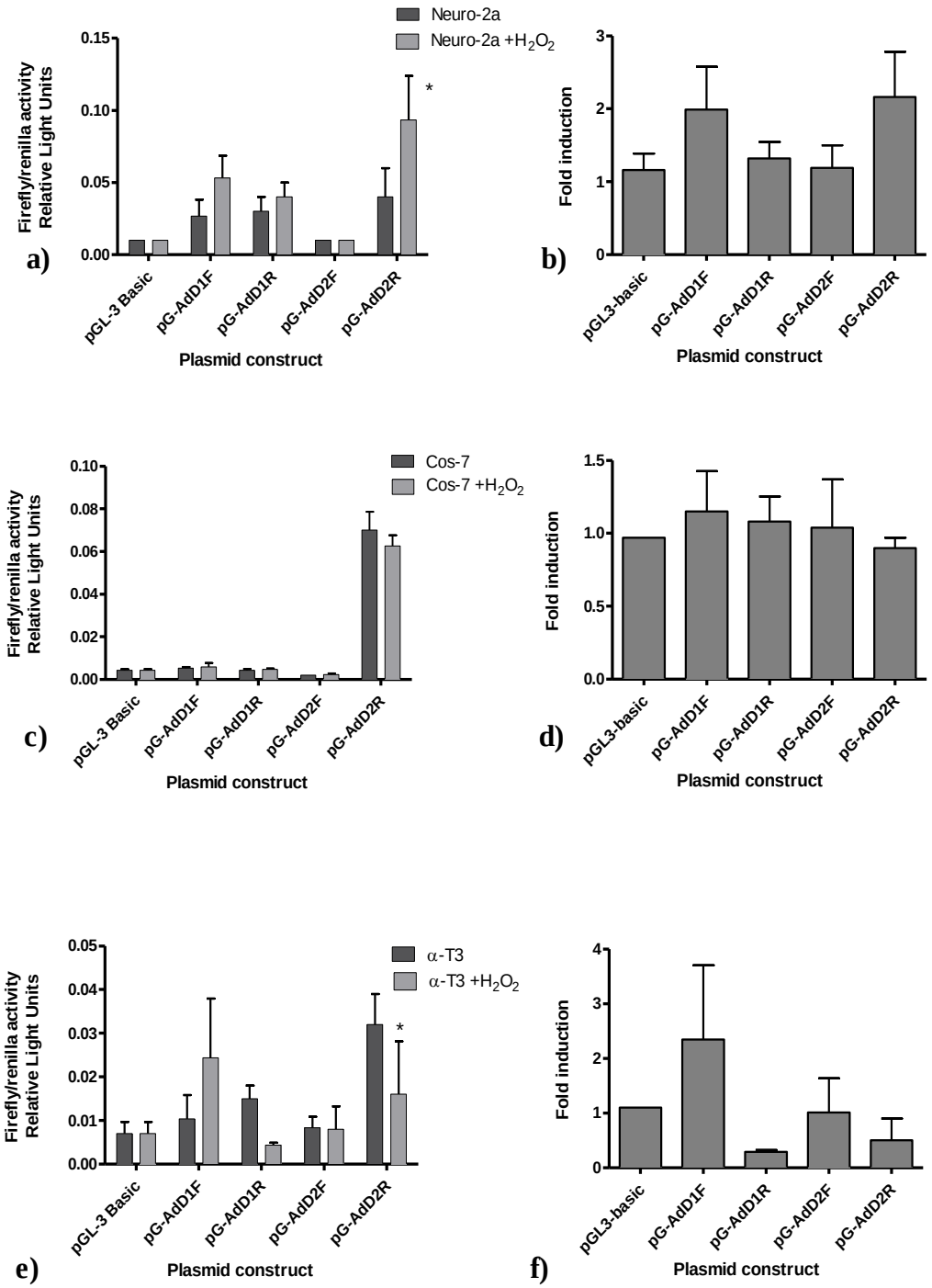

Figure 5.10. H_2O_2 induction of expression from downstream regions

Downstream promoter regions in pGL-3 Basic were transfected into Neuro-2a **a)** Cos-7 **c)** and α-T3 cells **e)** and treated with 30μM H_2O_2 24 hours after transfection. Firefly and Renilla luciferase activity was measured 48 hours after transfection. The panels on the right show the fold induction of expression for Neuro-2a **b)** Cos-7 **d)** and α-T3 cells **f)**. The fold induction indicates the ratio of activity of treated v untreated cells. Results represent the mean ± SE from 3 measurements (n=3) for each condition. Expression levels of H_2O_2 treated and untreated cells that are significantly different are indicated. **** $p<0.001$; ** $p<0.01$; * $p<0.05$.

5.3.2 Analysis of Enhancer Elements using pGL-3 Promoter Constructs

To investigate the functionality of upstream and downstream regions in controlling expression from a basal promoter, the fragments were subcloned into pGL3 Promoter, which contains an SV40 basal promoter. This is a strong promoter so may give higher levels of expression than the Adcyap1r1 basal promoter. A description of the constructs is outlined in *Chapter 4*. The plasmid constructs were transfected into Neuro-2a, Cos-7 and α-T3 cells and luciferase activity was measured. The activity was normalised against untransfected cells as negative controls and compared to pGL-3 Promoter as a positive control. Cells were co-transfected with pRL-TK as a transfection control.

5.3.2.1 pGL-3 Promoter Expression

Expression from the control pGL-3 Promoter was significantly higher than for the pGL-3 Basic control in all cell lines (*Figure 5.11*). pGL-3 Promoter expression was highest in Cos-7 cells, relatively low in Neuro-2a cells and very low in α-T3 cells. The high level of expression in Cos-7 is due to the strong SV40 promoter which is known to give good expression in Cos-7 cells.

Expression from the control pGL-3 Promoter was also significantly higher in Cos-7 cells and in α-T3 α-T3 cells than from the basal Adcyap1r1 contained within Ad1 in the pGL-3 Basic construct pG-Ad1F (*Figure 5.11*). However this was not the case in Neuro-2a cells, mainly due to the very high level of expression from Ad1F in these cells. This indicates that the strength of the Adcyap1r1 basal promoter shows some cell-specific dependency that is dependent on elements contained the Ad1 region, leading to the significantly higher expression in Neuro-2a cells. This also indicates that the Adcyap1r1 basal promoter is stronger than SV40 promoter, dependent on these factors.

5.3.2.2 Effect of Upstream and Downstream regions on Expression from SV40 promoter

In Neuro-2a cells the downstream AdD1F region gave the highest expression of all the inserts. This insert significantly increased expression from the basal SV40 promoter by 60-fold, indicating that there are elements within this region that can enhance transcription from a basal promoter in this cell line. However this region did not appear functional in the Cos-7 or α-T3 cells, indicating some cell specificity for Neuro-2a. All of the upstream inserts (AdU1, AdU2, AdU3) gave significantly higher expression in Neuro-2a cells compared to expression from the control pGL-3 Promoter vector (*Fig 5.11 a*), with between 20 and 60 RLU, for all constructs.

In Cos-7 cells, the increase in expression due to inserts was not as great in this cell line because of the already high level of expression from the SV40 promoter as seen with pGL-3 Promoter control. However, the highest expression was from the AdU3R insert and the AdD2F insert, although all of the inserts gave significantly higher expression compared to expression from the control pGL-3 Promoter vector (*Fig 5.11 b*), with between 20 and 60 RLU, for all constructs. The exception was the low level of expression from the AdD1F insert, which was in clear contrast to the situation observed in Neuro-2a cells. This indicates that there is a cell-specific element in the AdD1F insert that functions in Neuro-2a cells to enhance expression but does not function in Cos-7 cells.

Expression was very low in α-T3 cells for all the constructs and there was no significant difference in expression over the control pGL-3 Promoter vector (*Fig 5.11 c*).

A comparison of expression levels in all three lines is shown in Figure 5.12

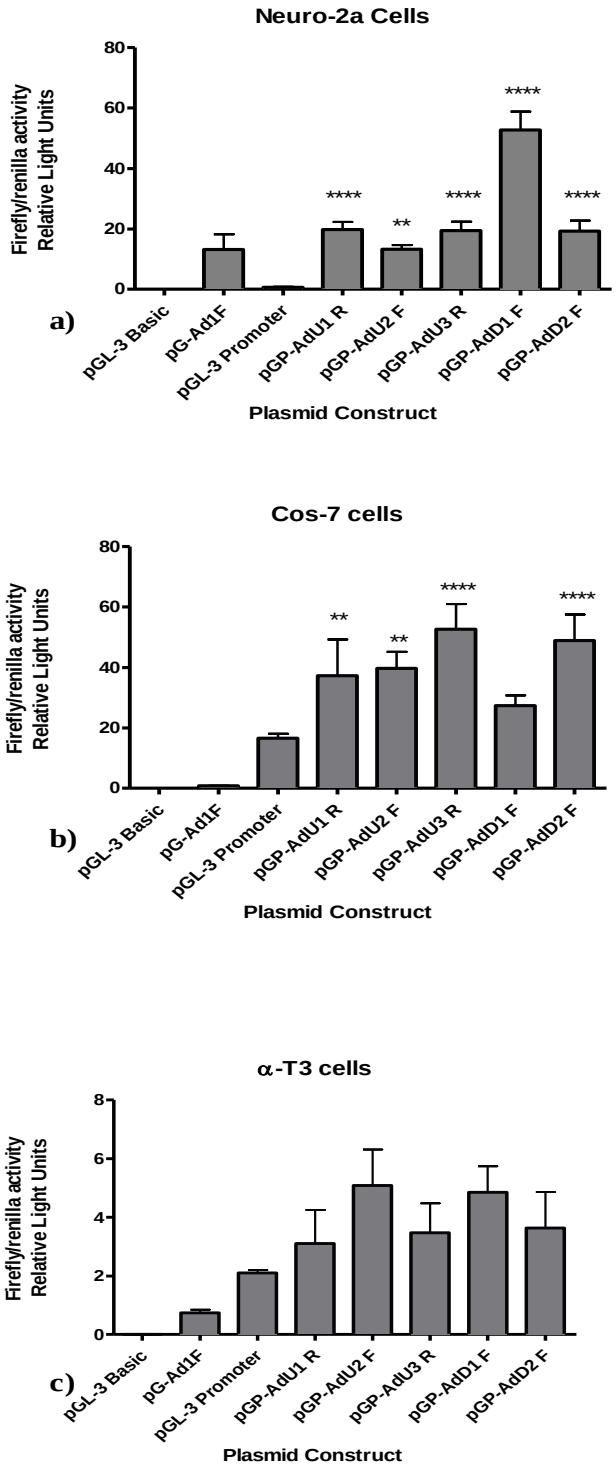

Figure 5.11: Luciferase Expression from pGL-3 Promoter constructs.

Neuro-2a **a)** Cos-7 **b)** and α-T3 cells **c)** were transfected with the various pGL-3 Promoter reporter constructs and Firefly and Renilla luciferase was measured 48 hours after transfection. Results represent the mean ± SE from 3 measurements (n=3) for each condition. Expression levels that are significantly different from the control pGL-3 Promoter control vector are indicated. **** $p<0.001$; ** $p<0.01$; * $p<0.05$.

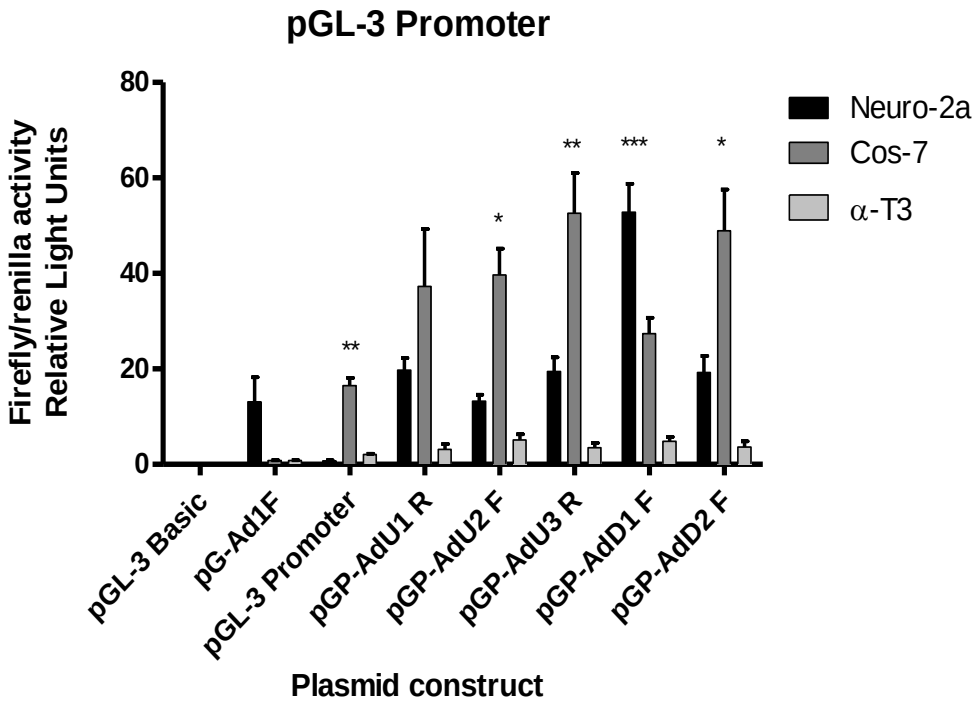

Figure 5.12: Comparison of expression levels for each construct in different cell lines

Cells were transfected with the various pGL-3 Promoter reporter constructs and Firefly and Renilla luciferase was measured 48 hours after transfection. pGL-3 Promoter, pGP-AdU3 R and pGP-AdD2 F showed significantly higher in Cos-7 cells compared to the other cells. pGP-AdU2 F showed significantly higher expression in Cos-7 than in αT-3. pGP-AdD1F showed significantly higher expression in Neuro-2a compared to the other 2 cell lines. Results represent the mean ± SE from 3 measurements (n=3) for each condition. Significant differences are indicated. *** $p<0.001$; ** $p<0.01$; * $p<0.0$.

5.3.2.3 Effect of oxidant stress on expression from pGL-3 Promoter constructs

To test for stress-induced expression from potential enhancers in the upstream and downstream regions, Neuro-2a, Cos-7 and α-T3 were co-transfected with pGL-3 Promoter constructs and pRL-TK containing Renilla luciferase, as an internal positive control as described in *Chapter 2*. Cells were treated with or without 30 μM H_2O_2 24hrs post-transfection and luciferase activity was measured 48 hrs post-transfection and normalised against untransfected cells. The luciferase activity in the untreated cells was used as a reference and compared to H_2O_2 treated cells, and the fold change calculated

The inducible expression results are shown in Figure 5.13.

In Neuro-2a cells, there is a significant 2.7-fold increase in expression due to peroxide treatment with the AdU1R insert, but no other insert gave an inducible increased expression in this cell line (*Figure 5.13 a, b*). This is in contrast to the results using the endogenous weak promoter in the pGL-3 Basic constructs where the AdD2R insert gave inducible expression.

In Cos-7 cells, none of the inserts conferred inducible expression on the SV40 promoter (Figure 5.13 c, d). In α-T3 cells, only the AdU3R insert conferred inducible expression, which was significantly increased by 2.8-fold by peroxide treatment (*Figure 5.13 e, f*).

In addition, there appears to be some inhibition of expression in some of the constructs in some cell lines in response to H_20_2, in particular AdD1F which led to a significant decrease in expression in Neuro-2a cells (*Figure 5.13 a, b*). Again this is in contrast to the results obtained with the basal promoter constructs, where AdD1F conferred inducibility in this cell line.

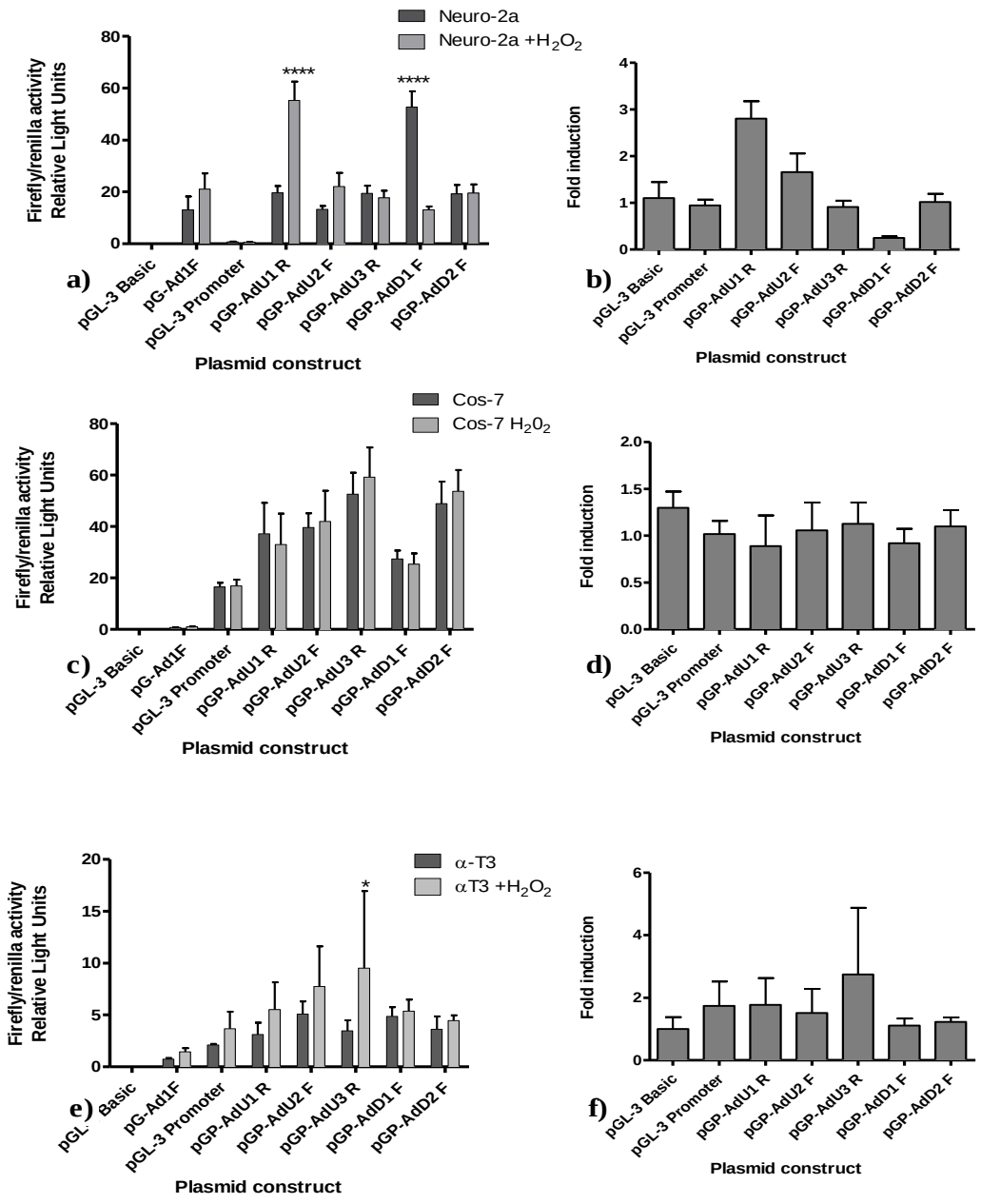

Figure 5.13: Change in expression after H_2O_2 insult of pGL-3 Promoter constructs.

pGL-3 Promoter constructs were transfected into Neuro-2a **a)** Cos-7 **c)** and α-T3 cells **e)** and treated with 30μM H_2O_2 24 hours after transfection. Firefly and Renilla luciferase activity was measured 48 hours after transfection. The panels on the right show the fold induction of expression for Neuro-2a **b)** Cos-7 **d)** and α-T3 cells **f)**. The fold induction indicates the ratio of activity of treated v untreated cells. Results represent the mean ± SE from 3 measurements (n=3) for each condition Expression levels of H_2O_2 treated and untreated cells that are significantly different are indicated. **** $p<0.001$; ** $p<0.01$; * $p<0.05$.

5.4 Discussion

5.4.1 Definition of the Basal Promoter

The results in this chapter have helped to define the minimal promoter region required for expression in the three cell lines investigated. The data shows that the basal promoter region is contained within the shorter Ad1 region and that this functions in either orientation, acting as the main site for assembly of the basal transcription complex, presumably via TF2B binding. The Ad2 region is also a functional promoter and similarly can function in forward and reverse orientation. However Ad1 gave much higher levels of expression than Ad2 indicating that there are sequences within the -80 to -180 region in Ad2 that negatively affect the binding of basal transcription factors to the promoter region. Removal of -180 to-80 regions in Ad1 appears to enhance transcription and addition. Also the +206 to +353 region present only in Ad1 may be responsible for the higher expression of Ad1 compared to Ad2. The specific sequences that may be involved will be discussed in *Chapter 7*.

The upstream and downstream regions all gave much lower levels of expression in all cell lines compared to Ad1 and Ad2 ($p<0.001$). The most significant expression was seen with AdD1F, which indicates the possibility of a weak promoter in this region, which may initiate transcription from an alternate transcription initiation site. This possibility is supported by evidence which revealed the presence of shorter transcripts when analysed by primer walking (Rodríguez-Henche et al. 2002).

5.4.2 Tissue Specific Expression

The strength of the main *Adcyap1r1* basal promoter appears to vary depending on cell type. Neuro-2a cells display significantly higher expression driven from the Ad1 and Ad2 regions, compared to expression observed from the same construct in Cos-7 or α-T3. Neuro-2a is a model for neuronal development, and the increased expression is likely because there are tissue-specific transcription factors that bind to sites close to the basal promoter to increase basal expression. The specific sequences that may be involved will be discussed in *Chapter 7*.

5.4.3 Regions responsible for stress induction in pGL-3 Basic constructs

Although the basal expression was very low, the downstream AdD2R region did give a low level of expression, indicating a very weak basal promoter was present in this region. The experiments with H_2O_2 treatment revealed that expression from this weak promoter could be induced significantly in Neuro-2a cells. This indicates a Neuro-2a specific inducible transcription factor binding site may be present adjacent to this weak promoter that allows the gene to be expressed in response to cell stress in this cell line.

Ad1F also showed increased expression after Hydrogen peroxide treatment across all 3 cell lines indicating some inducibility present in basal promoter regions. Other regions showed some inducibility some in a tissue specific manner like AdU1F which showed significant increased expression after H_2O_2 treatment in Neuro-2a and αT-3 cells but not Cos-7cells. AdU2F and AdU3R also a significant increase in expression following H_2O_2 treatment but only in Cos-7 cells.

5.4.4 Tissue Specific Enhancer Regions in pGL-3 Promoter constructs

Using the pGL-3 Promoter vectors, it was possible to investigate the ability of the various promoter regions to enhance expression from the basal SV40 promoter. In this regard, the downstream region AdD1 in the forward orientation showed the highest level of expression in Neuro-2a cells of any of the constructs and expression was significantly higher than for other regions. This indicates the presence of a neuronal-specific transcription factor binding site in this region, but this doesn't appear to function in either Cos-7 or α-T3 cells. Other regions also gave significantly enhanced expression in Neuro-2a cells and Cos-7 cells compared to the pGL-3 Promoter alone, indicating the presence of a range of elements that can enhance expression in these upstream and downstream regions. These specific sequences will be discussed in *Chapter 7*.

5.4.5 Regions responsible for inducibility in pGL-3 Promoter constructs.

Using the pGL-3 Promoter constructs, the ability of each insert to confer inducibility on the SV40 promoter was investigated. The only significant inducible expression appears to be due to the AdU1 insert in Neuro-2a cells, and the AdU3 insert in α-T3 cells. The previously observed inducibility conferred by the AdD2 region on expression Neuro-2a cells was not apparent with the SV40 promoter. It is possible that context and spacing is important for the inducibility observed earlier, and that the position of the AdD2 insert relative to the SV40 basal promoter was not optimal. There is also a possible interaction with SV40 and pro-apoptotic signalling via SV40 interaction with P53 (Bocchetta et al. 2008) P53 is upregulated in stress response situations and induces apoptosis (Gurley and Kemp 1996; Goh and Lane 2012). This interaction may have prevented induction of promoter regions as seen previously in pGL-3 Basic constructs (see above section 5.3.1.5)

5.4.6 Conclusions

The results in this chapter have revealed the functionality of the various regions of the promoter in a reporter gene assay in three cell lines. Although it would be tempting to extrapolate these results to the situation in cells and tissues in the mouse, further experiments need to be carried out to test whether the promoter regions affect expression in *in vitro* cell model and *in vivo* mouse models. Ideally, reporter constructs would be inserted or knocked down in transgenic mice so that the tissue specific and inducible responses could be measured *in vivo.*

The ability of transcription factors to bind to the proposed elements will be investigated in the next Chapter.

Chapter 6

Binding of proteins to promoter regions:

Electrophoretic Mobility shift Assays

6. Binding of proteins to promoter regions: Electrophoretic Mobility Shift Assays

6.1 Introduction

The presence of a TF binding sites in the promoter regions doesn't guarantee promoter regions are functional. One way to investigate its functionality is to investigate the binding of the TF to the TF binding site and support transfections data. This may also help elucidate functionality, of promoter regions, that was missed in the transfection experiments. For example, some TF binding sites may be active in different conditions than the ones used in Chapter 5 and would not show activity in transfection experiments. TF binding may help show that binding to TF occurs in promoter construct and there is a function that was missed in transfection experiments.

It was decided to use EMSA to investigate TF binding to promoter constructs, it works in a principle similar to gel electrophoresis where small DNA fragments migrate faster in gel. Whole nuclear extracts which contain the TF active in the cell line were isolated from the cell lines. If the DNA promoter region fragments bind to transcription factors that are present in nuclear extracts, a complex will form that will cause an increase in size. A band shift will occur when compared to unbound labelled DNA fragments. This should provide further evidence of the functionality of promoter regions, supporting the transfection data in the previous chapter.

6.2 Results

The conserved regions were labelled with digoxigenin and incubated with nuclear extracts from H_2O_2-treated and control cells for all three cell lines as described in *Chapter 2*. Digoxigenin-labelled promoter regions without nuclear extracts were used as a negative control.

Each conserved region was run on a gel separately, in 7 lanes as described in the legend to *Figure 6.1*. The negative control DIG-labelled DNA gave strong bands for all the promoter regions, indicating good labelling of the DNA.

For the AdU1 fragment, incubation of the labelled DNA with nuclear extracts led to a loss of the band corresponding to unbound DNA (*Figure 6.1 a, b*). This loss of unbound band suggests binding of the DNA to multiple factors in nuclear extracts. However, in most cases a smear was observed rather than clear band shifts. Since the bands were faint 2 camera exposure times are shown below with the longer exposure time (*Figure.6.1 a*) clearly showing the unbound DNA band but the nuclear extracts treated lanes are partially obscured by the pigment stain applied to develop the colour. Panel b) shows the nuclear extract treated lanes fainter but not obscured by development stains.

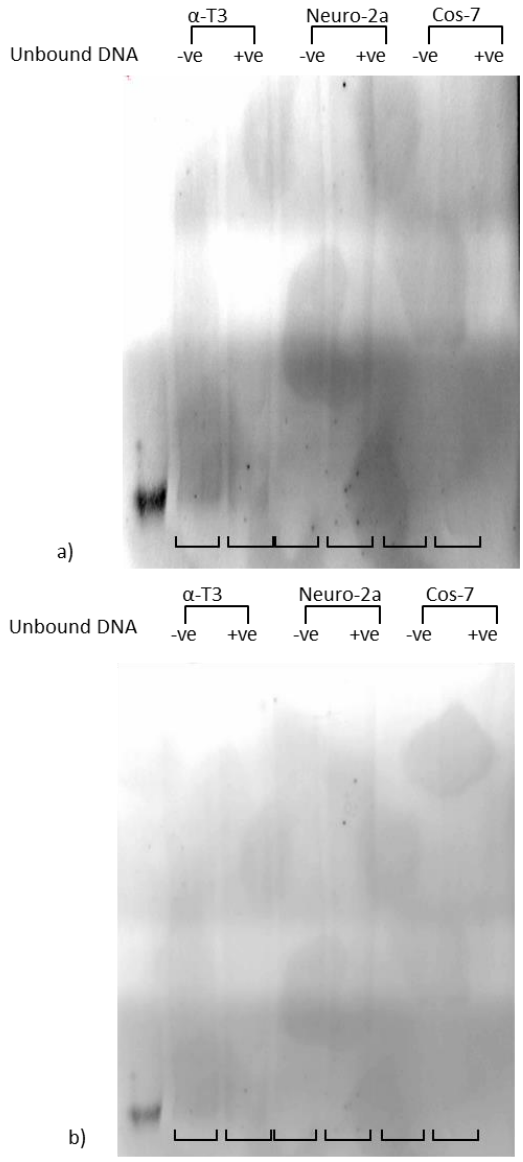

Figure 6.1:

EMSA assay of AdU1 promoter region. The lane on the left represents DNA fragment alone with no nuclear extract used as a control. A loss of the band equivalent to unbound DNA is observed in all cell conditions with multiple shifts causing a smearing effect. Whole nuclear extracts of cells untreated (-ve) and treated (+ve) with H_2O_2 were incubated with DNA for 15 mins. Panel **a)** is a ¼ second camera exposure while panel **b)** is a 1/100 second.

The AdU2 promoter region showed a clear band for the control DNA and the same smears as the AdU1 fragment in the nuclear extract bound DNA. This again may indicate binding of DNA with multiple TF causing a smear as the band corresponding to control DNA is lost (*Figure 6.2*).

The AdU3 putative promoter region gave a smear with the nuclear extract bound DNA and a loss of band corresponding to negative control. A decrease or abrogation of band corresponding to negative control DNA in the band shift cell lines and the presence of a smear supports that multiple binding occurs and causes multiple bands if similar size. However, a band shift is clearly observed in DNA incubated with nuclear extracts from Neuro-2a cells (both H_2O_2 treated and untreated) and in untreated Cos-7 cells (marked by red arrow). This may indicate a strong single TF binding site causing this band shift (*Figure.6.3*).

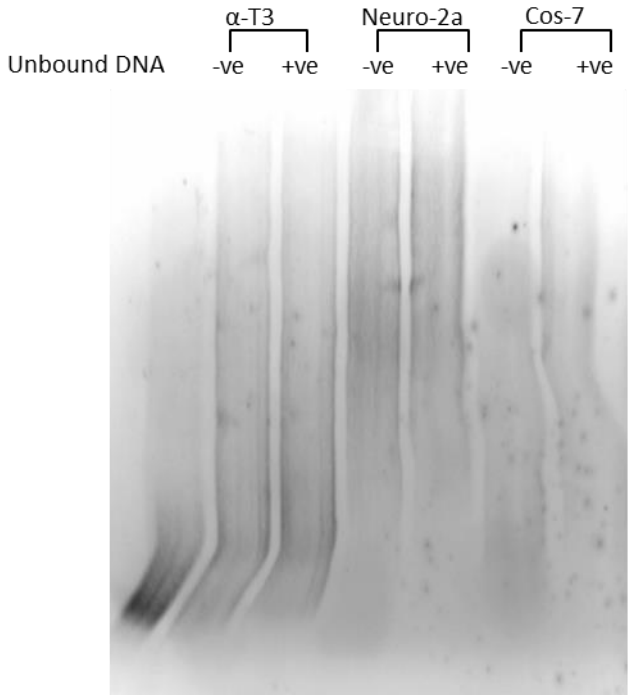

Figure 6.2:

EMSA assay of AdU2 promoter region. The lane on the left represents DNA fragment with no nuclear extract used as a control. A loss of the band equivalent to unbound DNA is observed in all cell conditions with multiple shifts causing a smearing effect. Whole nuclear extracts of cells untreated (-ve) and treated (+ve) with H_2O_2 were incubated with DNA for 15 mins.

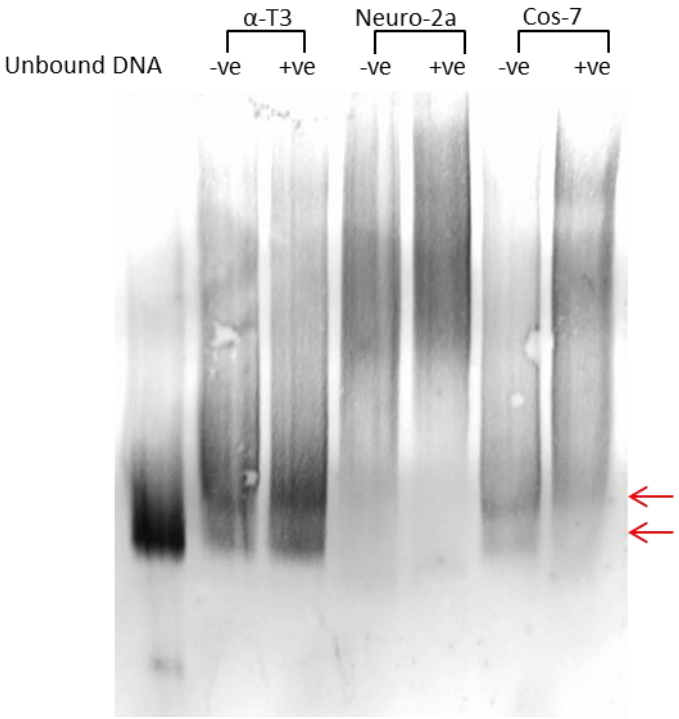

Figure 6.3

EMSA assay of AdU3 promoter region. The lane on the left represents DNA fragment with no nuclear extract used as a control. A loss of the band equivalent to unbound DNA is observed in all cell conditions with multiple shifts causing a smearing effect. However a clear band shift is observed in α-T3 and Cos-7 nuclear extracts –ve and +ve H_2O_2 . Whole nuclear extracts of cells untreated (-ve) and treated (+ve) with H_2O_2 were incubated with DNA for 15 mins.

The Ad1 basal promoter region gave a clear control DNA band there was no band shift observed in a clear band, only a loss of the control DNA band, and a smear (*Figure 6.4*). Given the very high level of expression with pG-Ad1 F and R described in the previous Chapter, it is likely that multiple binding is occurring as previously observed with AdU1, 2 & 3.

The Ad2 basal promoter regions gave similar results as Ad1, with a loss of band corresponding to unbound negative control in the nuclear extract treated cells and a smearing of the lanes. The lanes were faint so 2 camera exposure times were used with Panel a) having shorter exposure than b) (*Figure.6.5 a, b*).

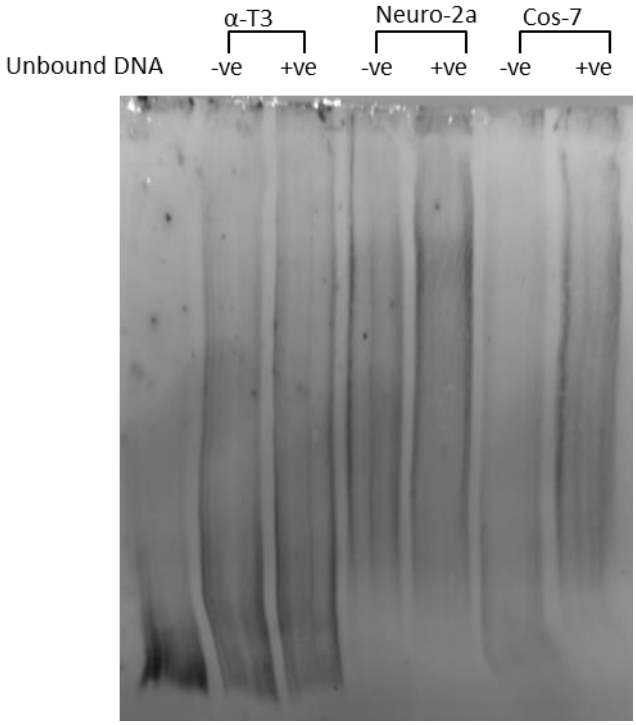

Figure 6.4:

EMSA assay of Ad1 promoter region. The lane on the left represents DNA fragment with no nuclear extract used as a control. A loss of the band equivalent to unbound DNA is observed in all cell conditions with multiple shifts causing a smearing effect. Whole nuclear extracts of cells untreated (-ve) and treated (+ve) with H_2O_2were incubated with DNA for 15 mins.

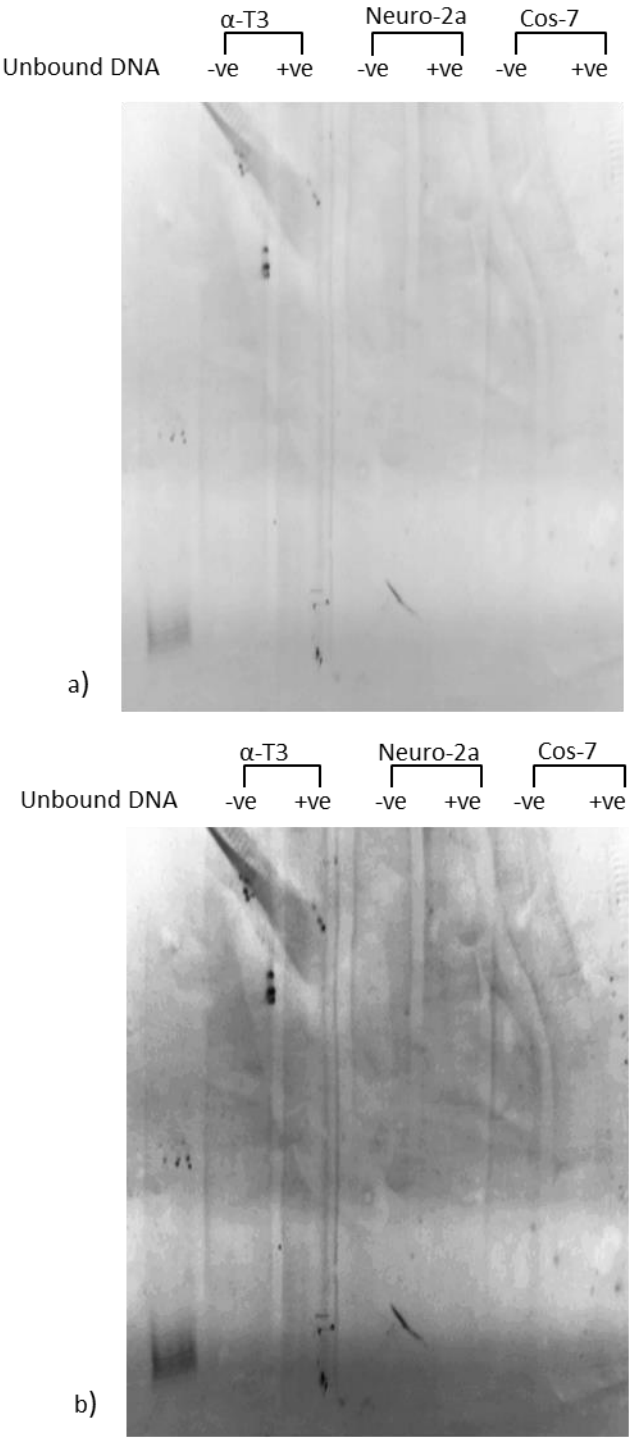

Figure 6.5

EMSA assay of Ad2 promoter region. The lane on the left represents DNA fragment with no nuclear extract used as a control. A loss of the band equivalent to unbound DNA is observed in all cell conditions with multiple shifts causing a smearing effect. Whole nuclear extracts of cells untreated (-ve) and treated (+ve) with H_2O_2were incubated with DNA for 15 mins. . Panel **a)** is a 1/100 second camera exposure while panel **b)** is a 1/4 second esposure.

The AdD1 promoter region showed 3 bands for the unbound DNA control, this may be due to the coiling of the DNA. What is clear however is the loss of the band corresponding to negative control DNA in in all 3 cell lines -ve and +ve H_2O_2. This loss of the control band and the resulting smear like pattern indicates binding between TF and their binding sites in the promoter region (*Figure 6.6*).

The Last downstream promoter region AdD2 showed a faint band shift in the α-T3 – ve and +ve H_2O_2 but no loss of band corresponding to control unbound DNA. AdD2 incubated with whole nuclear extract from Cos-7 cells +ve H_2O_2 gave a clear band shift and a partial loss of control equivalent band. The Neuro-2a cell nuclear extracts caused a loss of the control equivalent band and the multiple shift smear seen before also indicating multiple binding. This was expected given the strong expression seen in Neuro-2a cells when transfected with pG-AdD2 clone. The clear band shift caused by Cos-7 nuclear extracts binding to the DNA was surprising, given that there was no significant difference or inductions in expression in Cos-7 cells (*Figure 6.7*).

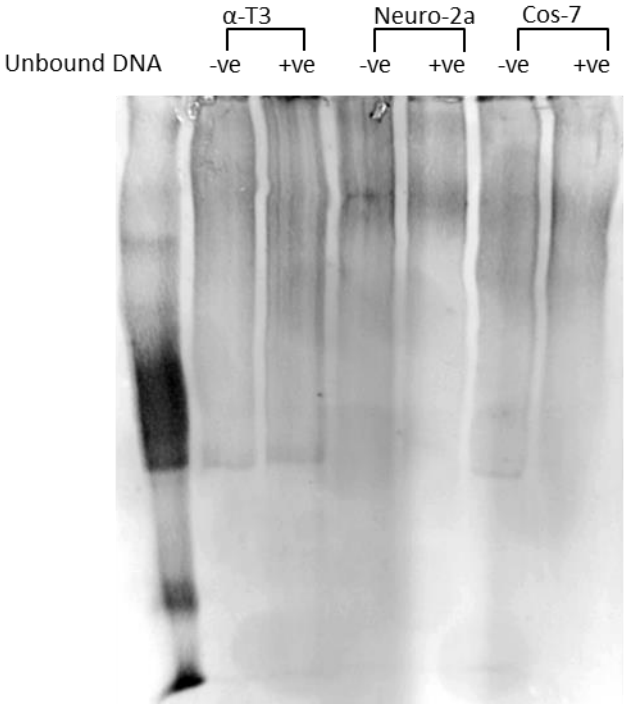

Figure 6.6

EMSA assay of AdD1 promoter region. The lane on the left represents DNA fragment with no nuclear extract used as a control showing 3 bands. A loss of the band equivalent to the largest unbound DNA band is observed in all cell conditions with multiple shifts causing a smearing effect. Whole nuclear extracts of cells untreated (-ve) and treated (+ve) with H_2O_2 were incubated with DNA for 15 mins.

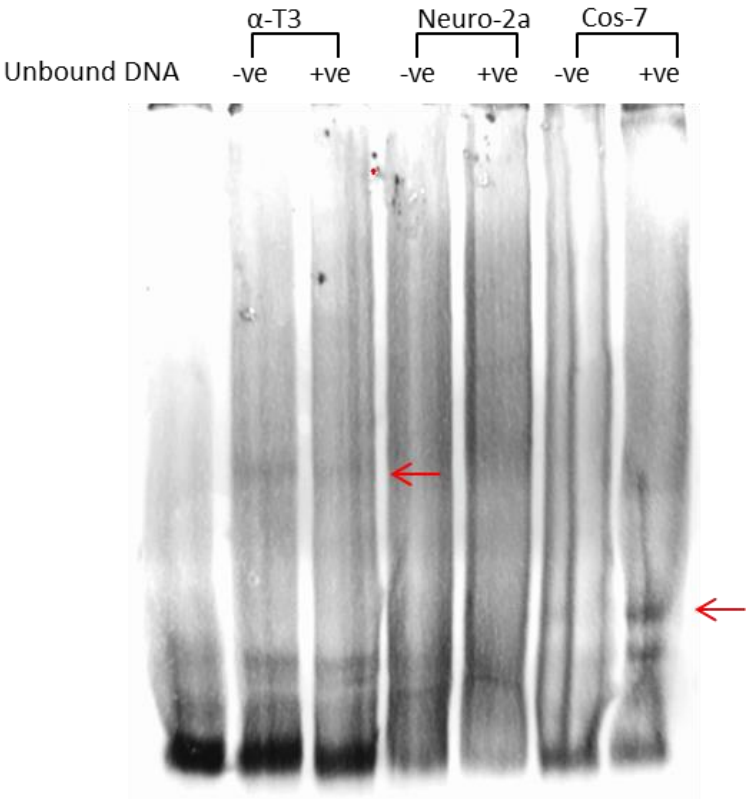

Figure 6.7

EMSA assay of AdD2 promoter region. The lane on the left represents DNA fragment with no nuclear extract used as a control. A loss of the band equivalent to unbound DNA is observed in all cell conditions with multiple shifts causing a smearing effect. Specific band shifts were observed in Cos-7 +ve H_2O_2 and faint bands in α-T3 -ve and +ve H_2O_2 marked with red arrows. Whole nuclear extracts of cells untreated (-ve) and treated (+ve) with H_2O_2 were incubated with DNA for 15 mins.

6.3 Summary and Conclusions

Based on the band shifts observed it appears that in most cases the EMSA assays supported the results of the transfection experiments. Where, most promoter regions showed a loss of the control unbound band and multiple binding resulting in a smear in all cell lines negative or positive H_2O_2 insult. However, AdU3 and AdD2 also showed specific band shifts Figure 6.3 and Figure 6.7 respectively. AdU3 gave band shift in both Cos-7 and α-T3 cells negative and positive hydrogen peroxide, AdD2 was the same but only extracts from Hydrogen peroxide treated Cos-7 cells gave a band shift. Also, AdD2 in Cos-7 cells 2 band shifts are observed in the Hydrogen peroxide positive cells may show binding to at mainly 2 regions in AdD2 involved in oxidative stress response. This can be used to narrow down TF binding sites in theory and their specific identity can be investigated in future studies.

The EMSA assays also in some cases showed results different than transfection experiments. The AdD2 Neuro2a extracts negative Hydrogen peroxide showed a loss of control band and a smear due to multiple binding the same as Hydrogen peroxide positive Neuro-2a. The stands in contrast to the transfection results where AdD2 showed no significant difference in expression compared to pGL-3 Basic control in Neuro-2a untreated with Hydrogen peroxide. A significant difference in expression in Neuro-2a was only observed after hydrogen peroxide treatment. This binding observed in Neuro-2a cell without insult lends to the future investigation of AdD2 expression in Neuro-2a cells.

In summary all the conserved regions show binding mostly non-specific multiple binding, some show specific band shift in some tissues/conditions. This in some cases has supported findings of transfection experiments. The binding experiments also showed interesting possible roles that were missed in the transfection experiments. However the definitive function and identity for the TF cause these bands need to be elucidated by mutating TF binding sites or using siRNA, for example, to investigate specific TFs.

Chapter 7

Discussion

7. Discussion

7.1 Overview

Previous work had cloned and characterized the mouse PAC1 gene *mAdcyap1r1* (Aino et al. 1995; Li et al. 1997; Rodríguez-Henche et al. 2002; Lutz et al. 2006). Its 5' flanking region is GC rich and lacks a TATA box(Aino et al. 1995; Rodríguez-Henche et al. 2002). Its expression patterns are rather complex and show elements of tissue, induced and developmental expression. Previous studies have indicated multiple Transcription Start Sites (TSS) over a ~70bp region with Aino et al reporting TSS at +10 and Rodriguez-Henche et al reporting TSS at +67. Examples of TF binding sites reported included, CAAT, GC boxes, Sp1, GATA, CREB and C/EBP (Aino et al. 1995; Rodríguez-Henche et al. 2002) Rodriguez-Henche et al 2002 study using reporter gene assays narrowed down the minimum promoter region to be -113 to +67 and also investigated the binding of Zac1 by mutating the Zac1 binding site located -329 (Rodríguez-Henche et al. 2002).

The primary focus of previous studies was to investigate the effect of specific TF on expression of PAC1 receptor gene through measuring PAC1 receptor mRNA levels or through reporter gene assays. There were several unanswered questions in the previous studies. There was no previous investigation of TF binding sites in intron 1 and only minimal investigation of upstream regions and no investigation upstream of -2598. Another issue encountered in previous studies was that *mAdcyap1r1* was analysed for TF binding sites in one species at a time or isolating PAC1 receptor sequence from mRNA via RT-PCR from different species variants or tissue to find the TSS (Aino et al. 1995; Rodríguez-Henche et al. 2002). This approach has a weakness where expression of various reporter gene constructs is specific to a single cell line or species. The different splice variants of PAC1 receptor and mutations between species, is also an issue. For example the Zac1 binding site at -329 is not present in the conserved promoter regions and might be specific to mice, rather than a conserved cross species TF binding site.

The work described in this thesis attempts to circumvent previous problems by specifically investigating the various TF binding domains and regions controlling *mAdcyap1r1* expression. In Chapter 3, to avoid species and tissue specific variation, the genomic DNA of 4 mammal species, mouse, rat, chimpanzee and human were aligned and the conserved species mapped out. The logic being since PAC1 conserved across mammalian species and has similar functions and expression (Harmar 2001; Hirose et al. 2005; Vaudry et al. 2009), then the main TF binding sites that regulate it should be conserved as well. We also analysed the DNA sequences from -6000 to +8307 which included all exon 1, intron1 and exon 2. The TF binding sites across the DNA sequences being tested were marked out across the individual sequences and also in aligned sequences. Ideally sequences from several rodent species should have been compared; this was not possible however. This is because of unsequenced or missing fragments in the *Adcyap1r1* gene sequences of rodent species in the ensemble database. The only complete rodent *Adcyap1r1* gene sequences were the mouse and rat sequences.

Cross species comparison of DNA revealed that there are 6 conserved regions, 3 upstream of exon 1, a conserved region directly before and including exon 1 and 2 downstream of exon 1. Although TF binding sites are found all over the sequences, most are clustered in very high density mainly in the conserved regions, often with several (10-15) TF binding sites overlapping each other. Furthermore, the downstream and upstream conserved regions had not been previously observed or the TF binding site in them analysed. These were exciting findings as there was clear clustering of TF binding sites in conserved regions and the TF sites downstream of exon1 and this far upstream have not been reported before. The presence of many TF binding sites in very high density in these conserved regions and the fact they were previously not investigated using reporter gene constructs made a compelling case for their investigation.

In order to investigate the promoter activity of the conserved regions they were inserted into firefly luciferase plasmids to form reporter gene constructs and transfected into mouse Neuro-2a, α-T3 cells and green monkey kidney Cos-7 cells.

The expression levels of constructs were measured and inducible expression measured after H_2O_2 insult to simulate cellular stress. EMSA studies were also performed to assess nuclear extract binding. This experimental data is supplemented by copious bioinformatics analysis of each conserved region.

7.2 Basal Promoter regions Ad1 and Ad2

7.2.1 Ad1 promoter region

This study showed that the Ad1 conserved region from -115bp to +353 gave the highest level of expression of all the promoter regions. This effect was more obvious in Neuro-2a neuroblastoma cells, than in Cos-7 and α-T3 cells. The high level of expression is expected as this conserved region is the proposed basal promoter region, the main 'On Switch'. The bioinformatics analysis supported this assumption since the basic transcriptional machinery TF sites such as HMTE and TF2B (Lim et al. 2004; Juven-Gershon and Kadonaga 2010; Cianfrocco et al. 2013) and CCAAT binding site are usually found ~70bp from transcription initiation (Song and Young 1998; Yang and Elnitski 2008). The TF2B site is plays a role in transcription start site selection and recruitment of other cofactors (Thomas and Chiang 2006). The transcriptional machinery is located in the reverse orientation mainly +120 to +160 with TF2B site at +310, there is also a main cluster at -60 to -10 which contains other constitutive TF binding sites; GC box, SP1 and CDP (CCAAT displacement protein)(Latchman 1998; Wierstra 2008; Stern et al. 2008). It is important to note that the construct containing a forward oriented Ad1 showed no significant difference in expression than reverse.

The Neuro-2a specific expression isn't surprising given the early expression PAC1 receptor in neuronal tissue and high number of TF binding sites observed involved in control of cell cycle, growth differentiation and apoptosis such as EGR1 E2F, E2F2 E2F3, ZBP89, ZNF219 KKLF and BKLF (Dong et al. 2002; Tsantoulis and Gorgoulis 2005; Ravni et al. 2008; Jeon et al. 2013; Kang et al. 2013; Xanthoulis and

Tiniakos 2013; Zhou et al. 2013). This effect appears to be developmentally specific rather than neuronal cell line specific given that the TF binding sites not specific to neuronal cell development like the POU domain family such as OCT-1 andPIT-1 (Latchman 1999; Kiyota et al. 2008) . E2F family for example are important general cell cycle control in a broad range of tissue cell lines for example $E2F2^{-/-}$ mice had impaired angiogenesis (Zhou et al. 2013). MYC induced Synthesis phase of cell cycle was impaired in E2F2 and $E2F3^{-/-}$ mice in mouse embryonic fibroblasts (Leone et al. 2001), E2F1 sensitises tumours to apoptosis after treatment with topoisomerase II inhibitors Adriamycin and Etoposide (Dong et al. 2002). One possible exception to being developmentally specific is EGR1 which is involved in in PACAP induced neurite growth in PC12 cells (Ravni et al. 2008) the presence of a binding site perhaps may act as a negative feedback mechanism.

Some inducible expression was also expected since AP-1 site which can be play a role in cell damage response and apoptosis (Raivich and Behrens 2006; Ola et al. 2010) and EGR1 which is upregulated by 2'-Benzoyloxycinnamaldehyde which causes damage through reactive oxygen species (Kang et al. 2013) and EGR1 is also induced by reactive oxygen species like H_2O_2 (Jeon et al. 2013). This data shows that after H_2O_2 insult Ad1 showed significant 1.5 fold increased expression in all 3 cell lines, in forward orientation. Reverse oriented Ad1R however, showed a significant increase in expression only in Cos-7, after insult H_2O_2. The induction it seems is affected by a tissue specific TF that is affected by the orientation. The EMSA assays using this region did show multiple band shifts in all the cell lines indicated binding of the TF in nuclear extracts to the Ad1 conserved region in both H_2O_2 treated and untreated cells..

7.2.2 Ad2 promoter region

The Ad2 conserved regions is almost identical to Ad1 but it is shifted 65bp to the 5' side starting from -180 to +206. This means Ad2 includes a second TF2B binding site at -123 but excludes the TF2B site at +310 and binding sites for several cell cycle TF like ZF5 and E2F2 at +260. The difference in TF binding sites although

small is contrasted by a substantial difference in expression between them. Only reverse Ad2R expression showed the same Neuro2a specific expression, seen with Ad1, which was significantly higher than the other cell lines. However, forward oriented Ad2 expression in Neuro-2a was 4 fold lower than Ad1 forward and did not show a significant higher expression level than pGL-3 Basic positive control. This clear difference between Ad1 and Ad2 indicate that the TF2B site at +310 is essential for high levels of expression.

There is also a strong possibility that an inhibitory effect is present in Ad2 in forward orientation or a transcription inducing effect when in reverse. This is due to the clear 2.5 fold lower expression of Ad2 forward compared to Ad2 reverse, seen in Neuro-2a cells. The difference in orientation did not show any difference in expression in Cos-7 or α-T3 cells. In fact Ad2 reverse showed levels of expression comparable to forward oriented Ad1 with no difference between them in any cell line.

Ad2 induced expression after H_2O_2 insult was a stark contrast to Ad1, where there was no significant difference in expression between post-insult and before in all cell lines in both orientation. It would seem that the difference in H_2O_2 induced expression between Ad1 and Ad2 is narrowed down to the TF binding sites that are different between them in locations -180 to -80 and +206 to +353. Though which ones specifically needs to determined experimentally. EMSA assay of Ad2 was near identical to Ad1 showing the distinct multiple band shift, with nuclear extracts from all cell lines positive or negative H_2O_2, seen in Ad1 with no clear bands showing and a loss of control band corresponding to unbound DNA.

7.3 Upstream regions

7.3.1 AdU1 promoter region

The 280bp AdU1 conserved region is the furthest upstream from TSS located at -4540 to -4260. Our bioinformatics analysis shows a clear difference is observed in types of TF binding sites found in AdU1 compared to the basal promoters Ad1 and Ad2. AdU1 in both forward and reverse shows a high amount of neuronal

developmental homeo domain TF. Neuronal homeobox TF included MYT1, MEIS1, PAX6, DLX2, HOXC13 and GSH2. The POU family of TF like BRN3 (Pou4F1) ganglia and Oct-1 (POU2F1) (Latchman 1999; Liu et al. 2000; Wang et al. 2002; Kiyota et al. 2008). Oct-1 knockdown with Morpholino oligonucleotides for example, demonstrated it's essential for radial glia formation in embryonic *Xenopus* hindbrain (Kiyota et al. 2008). MYT1 was upregulated in mouse spinal cord demyelinated with murine hepatitis virus strain A59 (Vana et al. 2007). The neuronal specificity of the ADU1 was demonstrated in its expression in Neuro-2a which was higher than Cos-7 and α-T3 expression in forward and reverse orientation. AdU1 also had the highest levels of expression in Neuro-2a cells of all the upstream regions. However there is a large difference between forward oriented pG-AdU1 F which was almost 15 fold higher than Neuro-2a expression of reverse oriented pG-AdU1 R. However, this difference was not statistically significant in a multi clone ANOVA comparing all clones against each other in Neuro-2a. The reverse oriented AdU1R however was also not statistically different than control pGL-3 basic expression in Neuro-2a cells. It would still be worth investigating a possible tissue specific inhibitory effect in this region possibly in a reverse orientation as AdU1R showed similar lower expression in α-T3 cells. In Cos-7 cells however, both AdU1F and reverse showed significantly higher levels of expression compared to positive control reinforcing a tissue specific inhibitory role in expression in this region.

AdU1 transfection experiments showed a 2 fold induction of expression after H_2O_2 insult in Neuro-2a and α-T3 cells, but only in forward oriented AdU1F. The reverse AdU1R showed a 0.5 fold reduction in expression in Cos-7 cells. The induction of expression appears to be cell specific and also affected by orientation. The AdU1R in pGL-3 Promoter plasmid showed different expression induction than pG-AdU1R. In pG-AdU1R there was no difference in expression after H_2O_2, while in pGP-AdU1R there was a 3 fold increase in expression. The 0.5 fold reduction in expression was also lost on pGP-AdU3 in Cos-7 cells. This change in expression may be due to some inducible TF sites like Oct-1 or STAT3 which is activated by IFNα2 in response to viral infections (Icardi et al. 2012). Oct-1 for example, binds and upregulates human inducible nitric oxide synthetase (hiNOS) gene, in response to

mix of 100 U/ml IL-1β, 1000 U/ml TNF-α and 250 U/ml IFNγ in human HepG2 hepatoblastoma cells (Park et al. 2009). EMSA assays supported the binding of TF from cell nuclear extracts, all cell conditions and cell lines showed the loss of unbound DNA band and multiple shift smear observed in most EMSA assays.

7.3.2 AdU2 promoter region

The AdU2 conserved region is 135bp in size and is located at -3845 to -3710; it shows different characteristics to AdU1. Neuro-2a specificity in expression observed in other conserved regions is not present. It only shows significantly higher levels of expression in Cos-7 and α-T3 compared to positive control. This is not surprising given that there is a low presence of neuronal developmental TF binding sites, examples included BRN2 and AP-2α. Mice with AP-2α -/- knocked out for example, show failure of neural tube closure by day E9.5(Schorle et al. 1996). Higher apoptotic cell death in migrating neural cells was also observed, similar to increased apoptosis in cell migrating to IGL in PACAP -/- and PAC1r knockout mice (Allais et al. 2007; Falluel-Morel et al. 2008).

The main difference seen in AdU2 promoter region compared to AdU1, was far fewer neuronal development associated TF binding sites which is also supported by the expression data. More importantly another difference was a large number of TF binding sites for inducible/immune response such as AP-1, AP-2, IRF7 and STAT5 (Schorle et al. 1996; Wagner 2010; Le Gallou et al. 2012; Ersing et al. 2013; Jung et al. 2013) and TF binding sites for immune cell development like BCL-6 and SPL1 (PU.1) (Franco et al. 2006; Basso and Dalla-Favera 2012; Okada et al. 2012). These immune/stress response TF binding sites appear to be relevant in cell specific manner, since AdU2 Showed a clear significant 1.4 fold increase in expression after H_2O_2 treatment only in Cos-7 cells. This induction effect was lost in pGL-3 Promoter clone pGP-AdU2F. The EMSA assays didn't show a specific band shift, only the multiple shift and control band loss seen before, indicating multiple binding of several TF.

7.3.3 AdU3 conserved region

The closest upstream promoter region to TSS is the 202bp AdU3, located at -2829 to -2627. Most of the TF sites present are involved in early neuronal development as seen in most conserved regions like BRN4, Oct-1, ISL2, DLX1,2 and they are found in both orientations (Ruiz i Altaba 1996; Kiyota et al. 2008; Long et al. 2009; Tan et al. 2010; Jones et al. 2011). These neuronal development TF sites appear to be functional as transfection experiments of AdU3 show Neuro-2a cell specificity which had higher levels of expression than in the other cell lines.

Some non-neuronal tissue specific TF were also found such as GATA-1, HOXA3 which modulate haematopoiesis (Fujiwara et al. 1996; Pope and Bresnick 2010; Mahdipour et al. 2011), GATA-4 and HOXD1 involved in cardiac development and angiogenesis (Ola et al. 2010; Park et al. 2011). There were also TF sites involved in cell cycle control like the KLF family.

Almost all the TF sites found, in both orientations, were located in one major cluster in AdU3 conserved regions (+50 in relation to AdU3 start). These TF sites overlap each other and cant bind at the same time, this singular location binding is clearly seen in the EMSA assays. The nuclear extracts from Cos-7 and α-T3 cells, both H_2O_2 negative and positive, show a decrease in band equivalent to control unbound DNA but more importantly, a single band shift. This may indicate that at least 1 major TF is binding to AdU3 and it appears to be not neuronal development specific. This is supported by the contrasting shifts of Neuro-2a, where very interestingly the Neuro-2a band shifts show loss of control band and multiple binding. This may be an indication that binding in Neuro-2a cells is due to multiple TF factors in competition for 1 major site, while binding and non-neuronal cell lines is mainly due to 1 or a small number of TF.

Some TF sites present may be induced due to cellular stress such as Oct-1 and C/EBP (Ramji and Foka 2002). They do appear to have some role in stress response in AdU3 as H_2O_2 induction showed significant 1.5 fold increase in expression in Cos-7 cells.

Two interesting factors stands out in AdU3, the massing of TF binding sites in mainly 1 cluster and rather interestingly the presence of several TF sites involved in transcription initiation. These included NFY and NF1 sites which are mostly considered constitutive TF ((Maity and de Crombrugghe 1998; Dolfini et al. 2012; Zhu et al. 2012) which may be an indicator of a strong transcriptional regulation role of AdU3 promoter region, though probably not as an initiation complex but as a upstream enhancer. Even perhaps as a enhancer for the neuronal developmental TF site cluster in AdU3, similar to the synergy seen in hiNOS gene expression, when induced with both Oct-1 and cytokine (Park et al. 2009).

7.4 Downstream promoter regions

7.4.1 AdD1 promoter region

The 226bp AdD1 downstream promoter region is the closest of 2 promoter to exon 1 it is located at +1739 to +1965 in intron 1. Most conserved regions so far had large numbers of neuronal developmental TF sites, AdD1 stands out from the rest on 2 accounts. Most of its TF binding sites are located in reverse orientation (22 TF binding sites), while only 5 are forward oriented. The second difference is the large number of steroid related TF binding sites such as ESSRA, PRE, VDR/RXR, SF1 and NBRE. Although there are no TF binding sites specific for neuronal development some Neuro-2a specific activity is present in AdD1. This is not shown in the pGL-3 Basic AdD1 constructs as there was no significant difference in expression with pGL-3 Basic positive control in any cell line. There appears higher expression in Neuro-2a cells but it did not achieve statistical significance. However, the AdD1 pGL-3 Promoter construct pGP-AdD1F however showed significantly higher expression than pGL-3 Promoter positive control ($p<0.0001$, almost 81 fold higher) only in Neuro-2a cells. pGP-AdD1R was also the only constructs in the upstream and downstream pGL-3 Promoter constructs that had significantly higher expression in Neuro-2a cells than the other 2 cell lines. This Neuro-2a specific activity is supported by the EMSA assays which showed the loss of control band with nuclear extracts of all cell lines with or without H_2O_2 insult. The Neuro-2a

specificity observed is probably to the multiple functions of RXR which plays a role in CNS development (Rowe et al. 1991; Kastner et al. 1997; Toresson et al. 1999) or perhaps NBRE. NBRE, as the name implies (Nerve growth factor IB response element) plays a role in neuronal development. NBRE acts as a binding site for Nurr1 which is important in development and migration of dopaminergic neurons (Kim et al. 2013; Tan et al. 2013).

We did not expect a significant change in expression after H_2O_2 insult, due lack of TF binding sites that play a role in stress protection. As we expected the expression levels of AdD1 showed no significant difference in any of the cell lines after H_2O_2 insult in both forward and reverse orientated constructs. However in contrast to pGL-3 Basic construct transfection, AdD1 when ligated into pGL-3 Promoter appears to have a significant decrease in expression of SV40 after H_2O_2 treatment in Neuro-2a cells. Further investigation into AdD1 neuronal function and induction would be quite important to clarify its function, preferably with mutation of TF binding sites or siRNA inhibition of TF.

7.4.2 AdD2 promoter region

The 150bp AdD2 promoter region, at +2710 to +2860 based on our experimental data, appears to be the major stress response promoter region in the regulation of the PAC1 receptor gene, at least from H_2O_2 insult. This is shown clearly in reverse AdD2R, with a 2 fold increased expression after treatment with H_2O_2 and the presence of several inducible TF binding sites such as RREB, ATF2 and CREB (Thiagalingam et al. 1996; Trumper et al. 2002; Hess et al. 2004; Chappell et al. 2011; Hönscheid et al. 2011; Lau and Ronai 2012). This inducibility is Neuro-2a cell specific so we can assume AdD2 plays a direct role in neuronal precursor stress protection. An interesting fact observed was that although AdD2R showed a 2 fold increase in expression in Neuro-2a, a 0.5 fold inhibition was observed in α-T3 cells. This difference was only observed in reverse oriented AdD2, this fact might be used to narrow down which TF sites are involved in inducible activity in future studies.

This specific induction effect in Neuro-2a cells is not observed in transfections without H_2O_2 induction as there is no difference in expression Neuro-2a and the other cell lines. So it appears initially AdD2 activity is mainly driven due to H_2O_2 induced stress and shows positive induction in Neuro-2a and negative induction in α-T3 when it is activated. However, it is important to note that although expression showed no difference between cell lines without H_2O_2 induction, reverse orientedAdD2R showed significantly higher levels of expression in all cell lines compared to pGL-3 Basic control. Therefore perhaps there is a role for AdD2 that is not H_2O_2 stress induced this may be supported by the band shifts seen in the EMSA in cells untreated with H_2O_2.

Neuro-2a cells EMSA showed the usual loss of control band and multiple binding observed in most of the EMSA assays. Surprisingly even with nuclear extracts from Neuro-2a cells untreated with H_2O_2.The EMSA assays also showed a band shift in α-T3 nuclear extracts they were very faint and the control band was not lost or reduced. This is better highlighted with the clear dark band shifts observed in Cos-7 cells only in nuclear extracts from cells treated with H_2O_2. So the negative hydrogen peroxide induced expression seen in α-T3 cells taken together with EMSA results, indicate there might be some AdD2 transcriptional activity in α-T3 gonadotroph models. Also a possible role without H_2O_2 induction may still be viable.

7.5 Transfection considerations

A problem encountered in our transfection experiments was the high basal expression of the pGL-3 Promoter plasmid used for the enhancer analysis. This was done in the later stages of the study as an attempt to amplify the expression of the upstream and downstream promoter regions to better identify inhibition after H_2O_2 insult. All the pGL-3 Promoter clones did show significantly higher expression than pGL-3 Promoter control in Neuro-2a cells. So it seems it pGL-3 promoter was successful in amplifying the Neuro-2a specific effect seen in the upstream and downstream promoters. The main difference in expression pattern between pGL-3 Basic and pGL-3 Promoter clones was the higher expression in Cos-7 cells in all pGL-3 Promoter constructs except pGP-AdD1F. A good way to see this is to contrast

Figure 5.7 b, c and Figure 5.12 which show the expression in all cell lines of the pGL-3 Basic and pGL-3 Promoter constructs, respectively. This is because Cos-7 cells have been immortalized with the SV40 virus, that produces large T antigen. Large T antigen can act in a similar way to TATA binding protein(TBP)-associated factors to enhance expression from basal promoters, In addition, there is an SV40 origin of replication within the SV40 promoter region and this leads to replication of the plasmid by the Large T antigen in Cos-7 cells leading to very high levels of expression (Kelly et al. 1987; Chittenden et al. 1991; Damania and Alwine 1996). A way around this would be the selection of a new control cell line that doesn't express PAC1 receptor and is not strongly activated by SV40. A way to resolve this issue is to redo the clones in a plasmid with a different strong constitutive promoter such as the CMV promoter obtained from Promega for example and is used for strong transient expression (Nicklin and Baker 2008).

The Cos-7 selectivity does not explain the loss of inducibility in some of the promoter constructs after H_2O_2 insult. An example would be AdU2F, which showed a 2 fold induction in Cos-7 cells when in pGL-3 Basic, the induction is lost in pGP-AdU2F which shows no difference in expression after H_2O_2 insult in Cos-7 cells. The SV40 promoter is known to interact with P53 and inhibit its effects (Bocchetta et al. 2008). P53 is upregulated after stress response situations and induce apoptosis and DNA repair after insult (Gurley and Kemp 1996; Goh and Lane 2012), it can also can induce PAC1 receptor expression (Hoffmann et al. 1998; Ciani et al. 1999). P53's interaction with SV40 may account for this difference in induction of expression observed which was far larger than we anticipated.

A repeat of this secondary transfection experiment would involve several changes a change of plasmid or simply a repeat of the pGL-3 Basic and Promoter above with more cell lines to see if the results are consistent. For example, the additions of a second neuronal development cell line like SH-SY5Y cells and check if selectivity seen in Neuro-2a is retained and inducibility of AdD2 in Neuro-2a is also retained. As well as the addition of negative control cells, that don't interact with SV40 and don't express PAC1 receptor.

The type of insults/inducers/conditions used to stress the cells can also be changed. Many studies have used various insults to stress the cells to test anti-apoptotic PAC1 receptor effects such as Ethanol, Hydrogen peroxide and TNF (Vaudry et al. 2002; Monaghan et al. 2008b). That is why it was deemed necessary to use hydrogen peroxide or a similar substance to stress cells which was mainly to test one of its main functions cell protection.

Some studies however have tested PAC1 receptor induction beyond its anti-apoptotic functions such as its induction by NGF, IGF and progesterone (Ha et al. 2000; Jamen et al. 2004). It also has well established immune modulatory effects modulating cytokine production (Martinez et al. 1998; Delgado et al. 1999; Martinez et al. 2002; Ganea and Delgado 2002; Vaudry et al. 2009). Some studies tested PAC1 receptor role in immune system *in vivo* such as DSS induced colitis and collagen induced arthritis and septic shock (Abad et al. 2001; Martinez et al. 2002; Martínez et al. 2005; Azuma et al. 2008). The investigation of non-apoptotic related TF is very relevant in view of the large amount of TF binding sites directly involved with immune cell maturation and activations such as BCL-6, SPL1. There was also a large amount of TF binding sites involved in immune system activation such as binding sites like AP-1, AP-2, IRF7 and STAT5. This is demonstrated very well in AdU2 where its transfection into an immune cell model or induction by a different immune related 'insult' might yield interesting data.

Other induced expression that should be investigated are the steroidal hormone family, this study showed a very large cluster of steroidal hormone related TF binding sites in AdD1. So the progesterone induction of PAC1 receptor might be due to the TF binding site observed in AdD1.

7.6 Transcription regulation interactions

The data observed in this study show a rather complex transcription control pattern with a substantial amount yet to be fully determined. What is evidently clear thus far is that most of the promoter regions we tested are geared specifically for neuronal developmental expression. This is shown in the high levels of selectivity shown by most clones in Neuro-2a cells. In this study we showed TF binding sites for 176 different TF, a total of 279 binding sites, most of which were previously unobserved or reported. Very stringent criteria were used to exclude false positive binding sites with a <0.85 optimised matrix threshold.

7.6.1 Site overlap

The TF binding sites shown and their large variety, fit in nicely with the multi-faceted temporal, spatial and functional expression pattern and functions of the PAC1 receptor. Many of the TF binding sites show overlapping binding sites which would allow for a conserved region to have multiple functions based on what is required of PAC1 receptor at the time. This would allow a singly conserved region to have several effects on expression in different conditions. An example would be AdD1 which has several E2F sites involved in development overlapping with cell cycle arrest. So for example the E2F3 TF which induces angiogenesis will compete with ZF5 which supresses cell growth (Numoto et al. 1999; Zhou et al. 2013). This potential competition might be part of a growth regulator system controlling cell growth effect of PAC1 receptor my modulating its expression. As to how it might specifically affect the expression of PAC1 receptor that will have to be determined experimentally via direct induction experiments.

7.6.2 Multiple binding to one site

Another level of complexity is that several TF binding sites for example bind to multiple TFs such as CCAAT which can be bound by NFY, NF-1 and several C/EBP members (Latchman 1998; Ramji and Foka 2002; Dolfini et al. 2012; Kilpatrick et al. 2012). Another example is AP-1 which is bound by different dimers of TF like

Jun, Fos, ATF and CREB (Hess et al. 2004). This would allow 1 TF to serve multiple purposes by responding to varied TF stimuli from several cell signalling pathways. For example AP-1 binding site can respond to dimers of apoptotic pathways such as c-fos and jun which can dimerise with ATF-2 which plays a role in cellular development (Lopez-Bergami et al. 2010; Ackermann et al. 2011; Lau and Ronai 2012). So potentially a developmentally available TF can dimerise with a stress induced TF and still bind to AP-1 binding site, although they TF are activated by different conditions. Also AP-1 binding site can still be activated without ATF-2 by different dimer combinations. CCAAT box also shows this variability, members of C/EBP show a range of temporal and tissue expression patterns. The expression and therefore availability would allow them to bind and activate CCAAT, for a specific developmental context such as in myeloid cells or in a tissue specific context based on type of C/EBP. For example C/EBP-β protects cortical cells from apoptotic death due to hypoxia, and its expression in the cells via herpes virus delivery resulted in 4 fold cell protection (Halterman et al. 2008). C/EBP-β can bind to a specific CCAAT site like that found in AdU3 for example, in a neuroprotective role, while that same CCAAT site can have NF-1, NFY or a different C/EBP in a different developmental or inducible context. Such as C/EBPε which regulates maturation of granulocytes and can bind and in this context may regulate PAC1 receptor immune functions (Halene et al. 2010).

7.6.3 Multiple Functions of TF single binding site

The TF classifications we used here constitutive, developmental, tissue specific and inducible are for the sake of simplicity and don't usually do justice to complexity of a TFs functions. This is due to the face that a single TF with its binding site can still play different roles, so a developmental TF like OCT-1 still plays a role in stress response via its direct activation of hiNOS in synergy with cytokines (Park et al. 2009) or indirectly by its regulation by STAT3 for example (Wang et al. 2013). While AP-1 TF can sometimes play a role in development and still be induced in response to stress stimuli. TGIF1 in addition to its role in brain development (Taniguchi et al. 2012) has an role in the immune system regulating necrosis via

TNF-α. Modified Madin-Darby Canine Kidney Epithelial Cells (MDCK) overexpressing TGIF1, had increased sensitivity to TNF-α apoptotic inducing effect and reducing TGIF1 with short hairpin RNA resulted in decreased TNF-α induced apoptosis (Demange et al. 2009). These examples illustrate that TF can have multiple roles and the presence of a TF may not confer a specific classification such as constitutive etc.

So in summary TF sites can have multiple binding TFs, multiple effect TFs can interact with one another leading to different functions for the TF like the example of TGIF1 and OCT1. Also different TF binding sites can interact with one another such as the synergy shown with OCT-1 and cytokine binding sites for example. The following Figure 7.1 summarises the interactions one would expect.

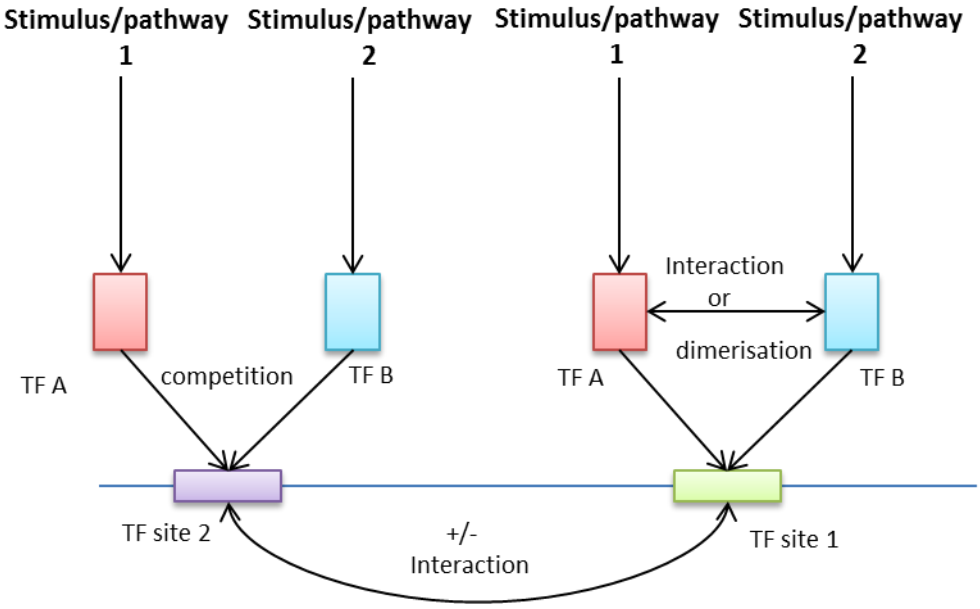

Figure 7.1:

Diagram summarising the various interactions expected between TF binding sites and the TF themselves. The stimulus or signal transduction pathway at the top activates a TF via direct expression or reaction such as phosphorylation. TF interact with TF sites and one another while the TF sites work together and interacts such as in the initiation of transcription. Shaded boxes on the bottom line represent TF binding sites.

7.7 Further investigation directions

Future work should focus on expanding the transfection experiments into a wider range of cell lines. This is to investigate possible endocrine activity of AdD1 using chromaffin cells or, Chinese hamster ovary cells for example (McCulloch et al. 2000; Mustafa et al. 2007), and immune cell expression of AdU2 using macrophages and lymphocytes from primary cultures for example (Martinez et al. 1998). As well as give a better picture of neuronal expression using several other neuronal precursor models such as SH-SY5Y or NB-100 neuroblastoma cells (Lutz et al. 2006).

It would also be worth studying the interactions of the promoter regions with each other which can be done with ease using cloning and transfection experiments. Constructs with the upstream promoter regions for example would be cloned with basal Ad1 promoter with different combinations and transfected to investigate their neuronal role. This can be taken a step further and cell line with a combination of promoter regions deleted from the PAC1 receptor gene can also tested. For example will SH-SY5Y cells still differentiate after PACAP-38 treatment with AdU1 deleted? As seen in two Monaghan et al 2008 SH-SY5Y differentiation induction studies (Monaghan et al. 2008a; Monaghan et al. 2008b). Will the PACAP rescue of cells treated with a sub lethal insult be functional with AdD2 deleted from the PAC1 receptor gene? Such as the PACAP protection studies on rat astrocytes after Hydrogen peroxide treatment by Masmoudi-kouki et al 2011 (Masmoudi-Kouki et al. 2011).

Naturally an important step would be to investigate which TF specifically bind to and activate the promoter regions, as we did not have the means to investigate specific TFs in this study. This can be done with mutating the binding site like shown with Rodriguez-Henche et al 2002 and the ZAC1 binding site (Rodríguez-Henche et al. 2002). However several TF binding sites overlap so mutation can delete multiple TF binding sites, a probably faster convenient and accurate way to investigate the TF would be their inhibition with siRNA. A large number of TF can be investigated in cells transfected with the same clone and the binding investigated using EMSAs or Chromatin immunoprecipitation (ChIP) (Laajala et al. 2009).

It would also be very informative to take these approaches in promoter region functions and their interactions to *in vivo* studies. An example would be PAC1 receptor -/- mice investigated by Falluel-Morel et al 2008 (Falluel-Morel et al. 2008) where the knock-out mice showed decreased survival of cells migrating from EGL to IGL. Rather than knock out the whole gene, conserved region AdU3 for example would be mutated or deleted. Another example would be the septic shock experiments conducted on $PAC1^{-/-}$ mice by Martinez et al 2002 using LPS (Martinez et al. 2002) or collagen induced arthritis (Abad et al. 2001) with a conserved region deleted like AdD1 for example which has TF binding sites for immune related TFs. We can also investigate the survival and protection PACAP-38 on mice with AdD2 deleted in stroke models. The data if valid can provide possible therapeutic targets for improved ischaemic stroke therapies. This can be in the form of a direct TF site stimulating agent in AdD2 for example or in gene therapy in an approach similar to Park et al 2009, where the insertion of additional OCT-1 sites improved its hiNOS gene induction (Park et al. 2009).

The promoter regions can be used in a similar manner in a therapeutic gene therapy setting to drive therapeutic genes not necessarily PAC1, or in *in vitro* studies in nerve growth/repair from stem cells for example. This would be rather than attempting to use artificial promoter constructs, we use a natural promoter elements complexity, this approach has been used with simple viral promoters like SV40 used in pGL-3 Promoter plasmids. More complex artificial promoter constructs have been used such as the unsuccessful cardiomyoblast selective, stress reactive promoter constructs made by Dr S Nicklin that I worked on during my MSc (unpublished work). A published example would be the modified murine pre-proendothelin promoter PPEx3 was used to selectively express green fluorescent protein in endothelial cells of skeletal vasculature in a limb ischaemic model (Nicklin and Baker 2008). Importantly in this example it was the promoter that conferred selectivity as the viral delivery system showed non-specific binding to other tissue.

Looking at the functions in a biomolecular cellular level may not give the full picture and bringing in different disciplines can be of great relevance. This has relevance with the PAC1 receptor gene, as demonstrated by several studies that showing an association with post-traumatic stress disorder (PTSD) in African American females and a single nucleotide polymorphism (SNP) in a potential oestrogen response element site in the PAC1 receptor gene intron 15 (Ressler et al. 2011). Using the BLAT function in the university of California Santa Cruz (UCSC) genome browser (http://genome.ucsc.edu/), we observed several SNPs in the conserved regions of both the human and mouse databases. We are not aware of other association studies apart from the PTSD study, which investigated SNPs in PAC1 receptor gene and disease. It would worthwhile investigating such an association for example in Alzheimer's or Parkinson's. There are several studies investigating the role of PAC1 receptor ligand PACAP-38 and PACAP-27 as a neuroprotective agent and its role in Parkinson's and Alzheimer's and neurodegenerative disease (Reglódi et al. 2006; Wang et al. 2008; Du et al. 2011; Waschek 2013). Since here we report several TF binding sites for TF involved in dopaminergic and serotonergic neuron differentiation and proliferation such as LMX1B (Lin et al. 2009; Song et al. 2011; Yan et al. 2013) and DLX1 which plays a role in the hippocampal GABAergic neuron development both found in AdU1 for example (Long et al. 2009; Jones et al. 2011). It would be interesting to investigate any potential associations with SNPs in promoter regions and prevalence or prognosis of neuronal pathological conditions, as this approach hasn't been frequently investigated.

7.8 PAC1 receptor Transcription Overview

Taking a step back and considering the complex TF and TF binding site interactions mentioned in the previous paragraphs, we can predict some further potential roles of the promoter regions. This is to try and get an overview and focus future studies on some of the potential regulatory functions of the promoter regions. Some regulatory functions were established with experimental data while some transcriptional sites/functions have had some light shed on them.

This study reports that the basal promoter region, the main 'On switch' starts at -80 and includes most of exon1 (+389) ending at +353 and it shows very strong neural precursor activity. Exclusion of the TF2B binding site at 310 results in a 4 fold decrease in expression in Neuro-2a. Including TF binding sites upstream of -80 up to -180 shows a strong inhibitory effect in Neuro-2a expression, while inverting the same region shows a 3 fold increase in Neuro-2a expression.

This basal promoter is supplemented with 3 upstream promoter regions AdU1,2,3 that largely show selectivity and TF binding sites for Neuronal development with some specialisations such as AdU2 which may play a role in immune modulation due to the higher number of immune related TF binding sites. Furthermore, AdU3 also has several constitutive TF binding sites which may potentially play a strong enhancer role for the basal promoter; this is also supported by the expression levels of AdU3 in Neuro-2a, which was the highest in the non-basal promoter regions.

The downstream promoter region AdD2 appears to be the main response element for cellular stress/apoptotic stimuli. The cell stress/apoptotic response of AdD2 was well established in the transfection experiments. AdD1 however, might potentially play a role in development, modulation of steroidogenic endocrine stimuli/tissue though its functionality has to definitely be resolved with further experiments.

Several common factors were most of the conserved regions, most had large numbers of TF binding sites for TFs involved in neuronal development. The exception was AdD1 which showed 1 neuronal developmental TF binding site. This is supported by

its expression which did not show Neuro-2a specificity. The promoter regions also had a large number of TF binding sites for TFs involved in cell cycle control and apoptosis the exception again, was AdD1. Interestingly these cell cycle and in some cases oncogenic TFs were expressed in conjunction with the developmental TF sites, both neuronal and non-neuronal such as the immune system developmental TF sites in AdU2.

There were some unique patterns in some promoter regions, naturally the transcriptional start machinery and constitutive TF sites in Ad1 and AdU3. Some of the specialisations seen in the promoter regions were the large number of TF binding sites for TF involved in immune system development in AdU2 and steroidogenic/sex hormone TF binding sites on AdD1. The figure below shows a summary of the TF types observed in the promoter regions (*Figure 7.2*).

Classification	AdU1	AdU2	AdU3	Ad1	AdD1	AdD2
Constitutive/basal	-	-	+	+++	+	-
Development						
Neuronal	+++	++	+++	+++	-	+++
steroidal	-	-	-	-	+++	-
Haematopoiesis	+	+	++	+	+	+
Immune	+	+++	+	-	-	-
Cell cycle	++	+	++	+++	-	+++
Inducible						
Apoptotic stress	+	++	++	+	+	+++
Immune response	+	+++	+	+	+	+

Figure 7.2:

A summary of the TF binding sites found in the promoter regions classified based on functions on the left hand side. Prevalence of TF sites shown by + signs, - sign indicates very low numbers or none.

Bibliography

Abad C, Martinez C, Leceta J, et al. (2001) Pituitary adenylate cyclase-activating polypeptide inhibits collagen-induced arthritis: an experimental immunomodulatory therapy. J Immunol 167:3182–9.

Ackermann J, Ashton G, Lyons S, et al. (2011) Loss of ATF2 function leads to cranial motoneuron degeneration during embryonic mouse development. PLoS One 6:e19090.

Adams B a, Gray SL, Isaac ER, et al. (2008) Feeding and metabolism in mice lacking pituitary adenylate cyclase-activating polypeptide. Endocrinology 149:1571–80.

Aggarwal A, Hunter WJ, Aggarwal H, et al. (2010) Expression of leukemia/lymphoma-related factor (LRF/POKEMON) in human breast carcinoma and other cancers. Exp Mol Pathol 89:140–8.

Aino H, Hashimoto H, Ogawa N, et al. (1995) Structure of the gene encoding the mouse pituitary adenylate cyclase-activating polypeptide receptor. Gene 164:301–4.

Akhtar M, Holmgren C, Göndör A, et al. (2012) Cell type and context-specific function of PLAG1 for IGF2 P3 promoter activity. Int J Oncol 41:1959–66.

Allais A, Burel D, Isaac ER, et al. (2007) Altered cerebellar development in mice lacking pituitary adenylate cyclase-activating polypeptide. Eur J Neurosci 25:2604–18.

Antequera F (2003) Structure, function and evolution of CpG island promoters. Cell Mol Life Sci 60:1647–58.

Asada M, Rauch A, Shimizu H (2010) DNA binding-dependent glucocorticoid receptor activity promotes adipogenesis via Krüppel-like factor 15 gene expression. Lab … 91:203–215.

Auld KL, Berasi SP, Liu Y, et al. (2012) Estrogen-related receptor α regulates osteoblast differentiation via Wnt/β-catenin signaling. J Mol Endocrinol 48:177–91.

Azuma Y-T, Hagi K, Shintani N, et al. (2008) PACAP provides colonic protection against dextran sodium sulfate induced colitis. J Cell Physiol 216:111–9.

Bahrami A, Dalton JD, Shivakumar B, Krane JF (2012) PLAG1 alteration in carcinoma ex pleomorphic adenoma: immunohistochemical and fluorescence in situ hybridization studies of 22 cases. Head Neck Pathol 6:328–35.

Barber B a, Liyanage VRB, Zachariah RM, et al. (2013) Dynamic expression of MEIS1 homeoprotein in E14.5 forebrain and differentiated forebrain-derived neural stem cells. Ann Anat 1–10.

Basille M, Cartier D, Vaudry D, et al. (2006) Localization and characterization of pituitary adenylate cyclase-activating polypeptide receptors in the human cerebellum during development. J Comp Neurol 496:468–78.

Basille M, Vaudry D, Coulouarn Y, et al. (2000) Comparative Distribution of Pituitary Polypeptide (PACAP) Binding Sites and PACAP Receptor mRNAs in the Rat Brain During Development. J Comp Neurol 509:495–509.

Basso K, Dalla-Favera R (2012) Roles of BCL6 in normal and transformed germinal center B cells. Immunol Rev 247:172–83.

Bel-Vialar S, Medevielle F, Pituello F (2007) The on/off of Pax6 controls the tempo of neuronal differentiation in the developing spinal cord. Dev Biol 305:659–73.

Berridge MJ (1993) Inositol trisphosphate and calcium signalling. Nature 361:315–25.

Bird a P, Wolffe a P (1999) Methylation-induced repression--belts, braces, and chromatin. Cell 99:451–4.

Bocchetta M, Eliasz S, De Marco MA, et al. (2008) The SV40 large T antigen-p53 complexes bind and activate the insulin-like growth factor-I promoter stimulating cell growth. Cancer Res 68:1022–9.

Botia B, Seyer D, Ravni A, et al. (2008) Peroxiredoxin 2 is involved in the neuroprotective effects of PACAP in cultured cerebellar granule neurons. J Mol Neurosci 36:61–72.

Boudreau HE, Casterline BW, Rada B, et al. (2012) Nox4 involvement in TGF-beta and SMAD3-driven induction of the epithelial-to-mesenchymal transition and migration of breast epithelial cells. Free Radic Biol Med 53:1489–99.

Boultwood J (2013) CUX1 in leukemia: dosage matters. Blood 121:869–71.

Brenneman DE (2007) Neuroprotection: a comparative view of vasoactive intestinal peptide and pituitary adenylate cyclase-activating polypeptide. Peptides 28:1720–6.

Brenneman DE, Nicol T, Warren D, Bowers LM (1990) Vasoactive intestinal peptide: a neurotrophic releasing agent and an astroglial mitogen. J Neurosci Res 25:386–94.

Brown T. (1999) Genomes, First edit. Bios Scientific Publishers

Calafat M, Larocca L, Roca V, et al. (2009) Vasoactive intestinal peptide inhibits TNF-alpha-induced apoptotic events in acinar cells from nonobese diabetic mice submandibular glands. Arthritis Res Ther 11:R53.

Carney RSE, Cocas L a, Hirata T, et al. (2009) Differential regulation of telencephalic pallial-subpallial boundary patterning by Pax6 and Gsh2. Cereb Cortex 19:745–59.

Cartharius K, Frech K, Grote K, et al. (2005) MatInspector and beyond: promoter analysis based on transcription factor binding sites. Bioinformatics 21:2933–42.

Catalano RD, Kyriakou T, Chen J, et al. (2003) Regulation of corticotropin-releasing hormone type 2 receptors by multiple promoters and alternative splicing: identification of multiple splice variants. Mol Endocrinol 17:395–410.

Cazillis M, Gonzalez BJ, Billardon C, et al. (2004) VIP and PACAP induce selective neuronal differentiation of mouse embryonic stem cells. Eur J Neurosci 19:798–808.

Chappell W, Steelman L, Long J (2011) Ras/Raf/MEK/ERK and PI3K/PTEN/Akt/mTOR inhibitors: rationale and importance to inhibiting these pathways in human health. Oncotarget 2:135–164.

Chaudhury D, Loh DH, Dragich JM, et al. (2008) Select cognitive deficits in vasoactive intestinal peptide deficient mice. BMC Neurosci 9:63.

Chittenden T, Frey a, Levine a J (1991) Regulated replication of an episomal simian virus 40 origin plasmid in COS7 cells. J Virol 65:5944–51.

Cianfrocco M a, Kassavetis G a, Grob P, et al. (2013) Human TFIID binds to core promoter DNA in a reorganized structural state. Cell 152:120–31.

Ciani E, Hoffmann a, Schmidt P, et al. (1999) Induction of the PAC1-R (PACAP-type I receptor) gene by p53 and Zac. Brain Res Mol Brain Res 69:290–4.

Cillo C, Cantile M, Faiella a, Boncinelli E (2001) Homeobox genes in normal and malignant cells. J Cell Physiol 188:161–9.

Clement TM, Bhandari RK, Sadler-Riggleman I, Skinner MK (2011) SRY directly regulates the neurotrophin 3 promoter during male sex determination and testis development in rats. Biol Reprod 85:277–84.

Colot V, Rossignol JL (1999) Eukaryotic DNA methylation as an evolutionary device. Bioessays 21:402–11.

Damania B, Alwine JC (1996) TAF-like function of SV40 large T antigen. Genes Dev 10:1369–81.

Darr H, Mayshar Y, Benvenisty N (2006) Overexpression of NANOG in human ES cells enables feeder-free growth while inducing primitive ectoderm features. Development 133:1193–201.

Delgado M, Ganea D (1999) Vasoactive intestinal peptide and pituitary adenylate cyclase-activating polypeptide inhibit interleukin-12 transcription by regulating nuclear factor kappaB and Ets activation. J Biol Chem 274:31930–40.

Delgado M, Pozo D, Ganea D (2004) The significance of vasoactive intestinal peptide in immunomodulation. Pharmacol Rev 56:249.

Delgado M, Pozo D, Martinez C, et al. (1999) Vasoactive intestinal peptide and pituitary adenylate cyclase-activating polypeptide inhibit endotoxin-induced TNF-alpha production by macrophages: in vitro and in vivo studies. J immunol 162:2358–67.

Demange C, Ferrand N, Prunier C, et al. (2009) A model of partnership co-opted by the homeodomain protein TGIF and the Itch/AIP4 ubiquitin ligase for effective execution of TNF-alpha cytotoxicity. Mol Cell 36:1073–85.

Dickson L, Finlayson K (2009) VPAC and PAC receptors: From ligands to function. Pharmacol Ther 121:294–316.

Dolfini D, Gatta R, Mantovani R (2012) NF-Y and the transcriptional activation of CCAAT promoters. Crit Rev Biochem Mol Biol 47:29–49.

Dominguez MH, Ayoub AE, Rakic P (2012) POU-III Transcription Factors (Brn1, Brn2, and Oct6) Influence Neurogenesis, Molecular Identity, and Migratory Destination of Upper-Layer Cells of the Cerebral Cortex. Cereb Cortex 1–12.

Dong Y, Yang H, Elliott M, McMasters K (2002) Adenovirus-mediated E2F-1 gene transfer sensitizes melanoma cells to apoptosis induced by topoisomerase II inhibitors. Cancer Res 1776–1783.

Du P, Lee CH, Choi JH, et al. (2011) Pituitary Adenylate Cyclase-Activating Polypeptide-Immunoreactive Cells in the Ageing Gerbil Hippocampus. Anat Histol Embryol 1–8.

Ersing I, Bernhardt K, Gewurz BE (2013) NF-κB and IRF7 Pathway Activation by Epstein-Barr Virus Latent Membrane Protein 1. Viruses 5:1587–606.

Fahrenkrug J, Buhl T, Hannibal J (1995) PreproPACAP-derived peptides occur in VIP-producing tumours and co-exist with VIP. Regul Pept 58:89–98.

Fahrenkrug J, Emson PC (1982) Vasoactive intestinal polypeptide: functional aspects. Br Med Bull 38:265–70.

Fahrenkrug J, Hannibal J (2004) Neurotransmitters co-existing with VIP or PACAP. Peptides 25:393–401.

Fahrenkrug J, Hannibal J, Honoré B, Vorum H (2005) Altered calmodulin response to light in the suprachiasmatic nucleus of PAC1 receptor knockout mice revealed by proteomic analysis. J Mol Neurosci 25:251–8.

Falktoft B, Georg B, Fahrenkrug J (2009) Signaling pathways in PACAP regulation of VIP gene expression in human neuroblastoma cells. Neuropeptides 43:387–96.

Falluel-Morel A, Tascau LI, Sokolowski K, et al. (2008) Granule cell survival is deficient in PAC1-/- mutant cerebellum. J Mol Neurosci 36:38–44.

Felizola SJ a, Nakamura Y, Hui X-G, et al. (2013) Estrogen-related receptor α in normal adrenal cortex and adrenocortical tumors: involvement in development and oncogenesis. Mol Cell Endocrinol 365:207–11.

Feng C, Xu W, Zuo Z (2009) Knockout of the regulatory factor X1 gene leads to early embryonic lethality. Biochem Biophys Res Commun 386:715–7.

Ferraz-de-Souza B, Lin L, Achermann JC (2011) Steroidogenic factor-1 (SF-1, NR5A1) and human disease. Mol Cell Endocrinol 336:198–205.

Fila T, Trazzi S, Crochemore C, et al. (2009) Lot1 is a key element of the pituitary adenylate cyclase-activating polypeptide (PACAP)/cyclic AMP pathway that negatively regulates neuronal precursor proliferation. J Biol Chem 284:15325–38.

Filipsson K, Kvist-Reimer M, Ahrén B (2001) The Neuropeptide Pituitary Adenylate Cyclase–Activating Polypeptide and Islet Function. Diabetes 50:1959.

Franco CB, Scripture-Adams DD, Proekt I, et al. (2006) Notch/Delta signaling constrains reengineering of pro-T cells by PU.1. Proc Natl Acad Sci U S A 103:11993–8.

Fujiwara Y, Browne CP, Cunniff K, et al. (1996) Arrested development of embryonic red cell precursors in mouse embryos lacking transcription factor GATA-1. Proc Natl Acad Sci U S A 93:12355–8.

Gallia GL, Johnson EM, Khalili K (2000) Puralpha: a multifunctional single-stranded DNA- and RNA-binding protein. Nucleic Acids Res 28:3197–205.

Le Gallou S, Caron G, Delaloy C, et al. (2012) IL-2 requirement for human plasma cell generation: coupling differentiation and proliferation by enhancing MAPK-ERK signaling. J Immunol 189:161–73.

Ganea D, Delgado M (2002) Vasoactive Intestinal Peptide (Vip) and Pituitary Adenylate Cyclase-Activating Polypeptide (Pacap) As Modulators of Both Innate and Adaptive Immunity. Crit Rev Oral Biol Med 13:229–237.

Gillardon F, Hata R, Hossmann K a (1998) Delayed up-regulation of Zac1 and PACAP type I receptor after transient focal cerebral ischemia in mice. Brain Res Mol Brain Res 61:207–10.

Girard B a, Lelievre V, Braas KM, et al. (2006) Noncompensation in peptide/receptor gene expression and distinct behavioral phenotypes in VIP- and PACAP-deficient mice. J Neurochem 99:499–513.

Glowa JR, Panlilio L V, Brenneman DE, et al. (1992) Learning impairment following intracerebral administration of the HIV envelope protein gp120 or a VIP antagonist. Brain Res 570:49–53.

Gluzman Y (1981) SV40-transformed simian cells support the replication of early SV40 mutants. Cell 23:175–82.

Goh AM, Lane DP (2012) How p53 wields the scales of fate. 3:240–244.

Gomariz RP, Juarranz Y, Abad C, et al. (2006) VIP-PACAP system in immunity: new insights for multitarget therapy. Ann N Y Acad Sci 1070:51–74.

Gurley KE, Kemp CJ (1996) p53 induction, cell cycle checkpoints, and apoptosis in DNAPK-deficient scid mice. Carcinogenesis 17:2537–42.

Gutiérrez-Cañas I, Rodríguez-Henche N, Bolaños O, et al. (2003) VIP and PACAP are autocrine factors that protect the androgen-independent prostate cancer cell line PC-3 from apoptosis induced by serum withdrawal. Br J Pharmacol 139:1050–8.

Ha CM, Kang JH, Choi EJ, et al. (2000) Progesterone increases mRNA levels of pituitary adenylate cyclase-activating polypeptide (PACAP) and type I PACAP receptor (PAC(1)) in the rat hypothalamus. Brain Res Mol Brain Res 78:59–68.

Halene S, Gaines P, Sun H, et al. (2010) C/EBPepsilon directs granulocytic-vs-monocytic lineage determination and confers chemotactic function via Hlx. Exp Hematol 38:90–103.

Halterman M, De Jesus C, Rempe D, et al. (2008) Loss of c/EBP-β activity promotes the adaptive to apoptotic switch in hypoxic cortical neurons. Mol Cell Neurosci 38:125–137.

Hannibal J, Hindersson P, Knudsen SM, et al. (2002) The photopigment melanopsin is exclusively present in pituitary adenylate cyclase-activating polypeptide-containing retinal ganglion cells of the retinohypothalamic tract. J Neurosci 22:RC191.

Hannibal J, Vrang N, Card JP, Fahrenkrug J (2001) Light-Dependent Induction of cFos during Subjective Day and Night in PACAP-Containing Ganglion Cells of the Retinohypothalamic Tract. J Biol Rhythms 16:457–470.

Harmar a J (2003) An essential role for peptidergic signalling in the control of circadian rhythms in the suprachiasmatic nuclei. J Neuroendocrinol 15:335–8.

Harmar AJ (2001) Family-B G-protein-coupled receptors. Genome Biol 2:reviews3013.1–reviews3013.10.

Hashimoto H, Shintani N, Tanaka K, et al. (2001) Altered psychomotor behaviors in mice lacking pituitary adenylate cyclase-activating polypeptide (PACAP). Proc Natl Acad Sci U S A 98:13355–60.

Haussler, M RHaussler CA, Jurutka PW, Thompson PD, et al. (1997) The vitamin D hormone and its nuclear receptor: molecular actions and disease states. J Endocrinol 154:S57–S73.

Hautmann M, Friis UG, Desch M, et al. (2007) Pituitary adenylate cyclase-activating polypeptide stimulates renin secretion via activation of PAC1 receptors. J Am Soc Nephrol 18:1150–6.

Hess J, Angel P, Schorpp-Kistner M (2004) AP-1 subunits: quarrel and harmony among siblings. J Cell Sci 117:5965–73.

Hilger-Eversheim K, Moser M, Schorle H, Buettner R (2000) Regulatory roles of AP-2 transcription factors in vertebrate development, apoptosis and cell-cycle control. Gene 260:1–12.

Hirose M, Hashimoto H, Shintani N, et al. (2005) Differential expression of mRNAs for PACAP and its receptors during neural differentiation of embryonic stem cells. Regul Pept 126:109–13.

Hoffmann a, Ciani E, Houssami S, et al. (1998) Induction of type I PACAP receptor expression by the new zinc finger protein Zac1 and p53. Ann N Y Acad Sci 865:49–58.

Hönscheid A, Dubben S, Rink L, Haase H (2011) Zinc differentially regulates mitogen-activated protein kinases in human T cells. J Nutr Biochem.

Icardi L, Lievens S, Mori R, et al. (2012) Opposed regulation of type I IFN-induced STAT3 and ISGF3 transcriptional activities by histone deacetylases (HDACS) 1 and 2. FASEB J 26:240–9.

Ishihara T, Shigemoto R, Mori K, et al. (1992) Functional expression and tissue distribution of a novel receptor for vasoactive intestinal polypeptide. Neuron 8:811–819.

Jamen F, Bouschet T, Laden J-C, et al. (2004) Up-regulation of the PACAP type-1 receptor (PAC1) promoter by neurotrophins in rat PC12 cells and mouse cerebellar granule cells via the Ras/mitogen-activated protein kinase cascade. J Neurochem 82:1199–1207.

Jamen F, Persson K, Bertrand G, et al. (2000) PAC1 receptor-deficient mice display impaired insulinotropic response to glucose and reduced glucose tolerance. J Clin Invest 105:1307–15.

Jeon HM, Lee SY, Ju MK, et al. (2013) Early growth response 1 regulates glucose deprivation-induced necrosis. Oncol Rep 29:669–75.

Jolivel V, Basille M, Aubert N, et al. (2009) Distribution and functional characterization of pituitary adenylate cyclase-activating polypeptide receptors in the brain of non-human primates. Neuroscience 160:434–51.

Jones DL, Howard M a, Stanco A, et al. (2011) Deletion of Dlx1 results in reduced glutamatergic input to hippocampal interneurons. J Neurophysiol 105:1984–91.

Joulin V, Bories D, Eléouet JF, et al. (1991) A T-cell specific TCR delta DNA binding protein is a member of the human GATA family. EMBO J 10:1809–16.

Jung JH, Kwon T-R, Jeong S-J, et al. (2013) Apoptosis Induced by Tanshinone IIA and Cryptotanshinone Is Mediated by Distinct JAK/STAT3/5 and SHP1/2 Signaling in Chronic Myeloid Leukemia K562 Cells. Evid Based Complement Alternat Med 2013:805639.

Juven-Gershon T, Kadonaga JT (2010) Regulation of gene expression via the core promoter and the basal transcriptional machinery. Dev Biol 339:225–9.

Kang H-S, Ock J, Lee H-J, et al. (2013) Early growth response protein 1 upregulation and nuclear translocation by 2'-benzoyloxycinnamaldehyde induces prostate cancer cell death. Cancer Lett 329:217–27.

Kastner P, Mark M, Ghyselinck N, et al. (1997) Genetic evidence that the retinoid signal is transduced by heterodimeric RXR/RAR functional units during mouse development. Development 124:313–26.

Kelly TJ, Rosenfeld PJ, Wides RJ, et al. (1987) Replication of adenovirus and SV40 chromosomes in vitro. Philos Trans R Soc Lond B Biol Sci 317:429–38.

Kiiveri S, Liu J, Westerholm-Ormio M, et al. (2002) Differential expression of GATA-4 and GATA-6 in fetal and adult mouse and human adrenal tissue. Endocrinology 143:3136–43.

Kilpatrick D, Wang W, Gronostajski R, Litwack E (2012) Nuclear factor I and cerebellar granule neuron development: an intrinsic–extrinsic interplay. The Cerebellum 11:41–49.

Kim TE, Seo JS, Yang JW, et al. (2013) Nurr1 Represses Tyrosine Hydroxylase Expression via SIRT1 in Human Neural Stem Cells. PLoS One 8:e71469.

Kiyota T, Kato A, Altmann CR, Kato Y (2008) The POU homeobox protein Oct-1 regulates radial glia formation downstream of Notch signaling. Dev Biol 315:579–92.

Ko C, Park-Sarge OK (2000) Progesterone receptor activation mediates LH-induced type-I pituitary adenylate cyclase activating polypeptide receptor (PAC(1)) gene expression in rat granulosa cells. Biochem Biophys Res Commun 277:270–9.

Koh SWM, Cheng J, Dodson RM, et al. (2009) VIP down-regulates the inflammatory potential and promotes survival of dying (neural crest-derived) corneal endothelial cells ex vivo: necrosis to apoptosis switch and up-regulation of Bcl-2 and N-cadherin. J Neurochem 109:792–806.

Kurosaka M, Machida S (2013) Interleukin-6-induced satellite cell proliferation is regulated by induction of the JAK2/STAT3 signalling pathway through cyclin D1 targeting. Cell Prolif 46:365–73.

Laajala TD, Raghav S, Tuomela S, et al. (2009) A practical comparison of methods for detecting transcription factor binding sites in ChIP-seq experiments. BMC Genomics 10:618.

Latchman D (1999) POU family transcription factors in the nervous system. J Cell Physiol 133:126–133.

Latchman DS (1998) Eukaryotic Transcription Factors, Third Edit. Academic Press

Lau E, Ronai Z a (2012) ATF2 - at the crossroad of nuclear and cytosolic functions. J Cell Sci 125:2815–24.

Lee LTO, Tam JK V, Chan DW, Chow BKC (2009) Molecular cloning and mRNA distribution of pituitary adenylate cyclase-activating polypeptide (PACAP)/PACAP-related peptide in the lungfish. Ann N Y Acad Sci 1163:209–14.

Lee LT-O, Tan-Un K-C, Pang RT-K, et al. (2004) Regulation of the human secretin gene is controlled by the combined effects of CpG methylation, Sp1/Sp3 ratio, and the E-box element. Mol Endocrinol 18:1740–55.

Lee S, Maeda T (2012) POK/ZBTB proteins: an emerging family of proteins that regulate lymphoid development and function. Immunol Rev 247:107–119.

Leone G, Sears R, Huang E, et al. (2001) Myc requires distinct E2F activities to induce S phase and apoptosis. Mol Cell 8:105–13.

Li Y, Chopp M, Powers C, Jiang N (1997) Apoptosis and protein expression after focal cerebral ischemia in rat. Brain Res 765:301–12.

Li Y, Shaw C a, Sheffer I, et al. (2012) Integrated copy number and gene expression analysis detects a CREB1 association with Alzheimer's disease. Transl Psychiatry 2:e192.

Lim CY, Santoso B, Boulay T, et al. (2004) The MTE, a new core promoter element for transcription by RNA polymerase II. Genes Dev 18:1606–17.

Lin W, Metzakopian E, Mavromatakis YE, et al. (2009) Foxa1 and Foxa2 function both upstream of and cooperatively with Lmx1a and Lmx1b in a feedforward loop promoting mesodiencephalic dopaminergic neuron development. Dev Biol 333:386–96.

Liu W, Khare SL, Liang X, et al. (2000) All Brn3 genes can promote retinal ganglion cell differentiation in the chick. Development 127:3237–47.

Long J, Swan C, Liang W (2009) Dlx1&2 and Mash1 transcription factors control striatal patterning and differentiation through parallel and overlapping pathways. J … 512:556–572.

Lopez-Bergami P, Lau E, Ronai Z (2010) Emerging roles of ATF2 and the dynamic AP1 network in cancer. Nat Rev Cancer 10:65–76.

Lutz EM, Ronaldson E, Shaw P, et al. (2006) Characterization of novel splice variants of the PAC1 receptor in human neuroblastoma cells: consequences for signaling by VIP and PACAP. Mol Cell Neurosci 31:193–209.

Lutz EM, Sheward WJ, West KM, et al. (1993) The VIP2 receptor: molecular characterisation of a cDNA encoding a novel receptor for vasoactive intestinal peptide. FEBS Lett 334:3–8.

MacKenzie CJ, Lutz EM, Johnson MS, et al. (2001) Mechanisms of phospholipase C activation by the vasoactive intestinal polypeptide/pituitary adenylate cyclase-activating polypeptide type 2 receptor. Endocrinology 142:1209–17.

Macleod D, Charlton J, Mullins J, Bird a P (1994) Sp1 sites in the mouse aprt gene promoter are required to prevent methylation of the CpG island. Genes Dev 8:2282–2292.

Mahdipour E, Charnock JC, Mace K a (2011) Hoxa3 promotes the differentiation of hematopoietic progenitor cells into proangiogenic Gr-1+CD11b+ myeloid cells. Blood 117:815–26.

Maia A-T, Antoniou AC, O'Reilly M, et al. (2012) Effects of BRCA2 cis-regulation in normal breast and cancer risk amongst BRCA2 mutation carriers. Breast Cancer Res 14:R63.

Maity SN, de Crombrugghe B (1998) Role of the CCAAT-binding protein CBF/NF-Y in transcription. Trends Biochem Sci 23:174–8.

Mallipattu SK, Liu R, Zheng F, et al. (2012) Kruppel-like factor 15 (KLF15) is a key regulator of podocyte differentiation. J Biol Chem 287:19122–35.

Mao C, Byers S (2011) Cell-context dependent TCF/LEF expression and function: alternative tales of repression, de-repression and activation potentials. Rev Eukaryot Gene Expr 21:207–236.

Marin M, Karis a, Visser P, et al. (1997) Transcription factor Sp1 is essential for early embryonic development but dispensable for cell growth and differentiation. Cell 89:619–28.

Martinez C, Abad C, Delgado M, et al. (2002) Anti-inflammatory role in septic shock of pituitary adenylate cyclase-activating polypeptide receptor. Proc Natl Acad Sci U S A 99:1053–8.

Martinez C, Delgado M, Pozo D, et al. (1998) VIP and PACAP enhance IL-6 release and mRNA levels in resting peritoneal macrophages: in vitro and in vivo studies. J Neuroimmunol 85:155–67.

Martínez C, Delgado M, Pozo D, et al. (1998) Vasoactive intestinal peptide and pituitary adenylate cyclase-activating polypeptide modulate endotoxin-induced IL-6 production by murine peritoneal macrophages. J Leukoc Biol 63:591–601.

Martínez C, Juarranz Y, Abad C, et al. (2005) Analysis of the role of the PAC1 receptor in neutrophil recruitment, acute-phase response, and nitric oxide production in septic shock. J Leukoc Biol 77:729–38.

Masmoudi-Kouki O, Douiri S, Hamdi Y, et al. (2011) Pituitary adenylate cyclase-activating polypeptide protects astroglial cells against oxidative stress-induced apoptosis. J Neurochem 117:403–411.

Masmoudi-Kouki O, Gandolfo P, Castel H, et al. (2007) Role of PACAP and VIP in astroglial functions. Peptides 28:1753–60.

Mazzocchi G, Malendowicz LK, Rebuffat P, et al. (2002) Expression and function of vasoactive intestinal peptide, pituitary adenylate cyclase-activating polypeptide, and their receptors in the human adrenal gland. J Clin Endocrinol Metab 87:2575–80.

McCulloch D a, Lutz EM, Johnson MS, et al. (2000) Differential activation of phospholipase D by VPAC and PAC1 receptors. Ann N Y Acad Sci 921:175–85.

McCulloch D a, Lutz EM, Johnson MS, et al. (2001) ADP-ribosylation factor-dependent phospholipase D activation by VPAC receptors and a PAC(1) receptor splice variant. Mol Pharmacol 59:1523–32.

McCulloch D, MacKenzie C, Johnson M, et al. (2002) Additional signals from VPAC/PAC family receptors. Biochem Soc Trans 30:441.

McRory J (1997) Two Protochordate Genes Encode Pituitary Adenylate Cyclase-Activating Polypeptide and Related Family Members. Endocrinology 138:2380–2390.

Mitchell PJ, Timmons PM, Hebert JM, et al. (1991) Transcription factor AP-2 is expressed in neural crest cell lineages during mouse embryogenesis. Genes Dev 5:105–119.

Miura A, Kambe Y, Inoue K, et al. (2013) Pituitary adenylate cyclase-activating polypeptide type 1 receptor (PAC1) gene is suppressed by transglutaminase 2 activation. J Biol Chem 1–19.

Miyata A, Arimura A, Dahl RR, et al. (1989) Isolation of a novel 38 residue-hypothalamic polypeptide which stimulates adenylate cyclase in pituitary cells. Biochem Biophys Res Commun 164:567–574.

Miyata A, Jiang L, Dahl RD, et al. (1990) Isolation of a neuropeptide corresponding to the N-terminal 27 residues of the pituitary adenylate cyclase activating polypeptide with 38 residues (PACAP38). Biochem Biophys Res Commun 170:643–648.

Monaghan TK, Mackenzie CJ, Plevin R, Lutz EM (2008a) PACAP-38 induces neuronal differentiation of human SH-SY5Y neuroblastoma cells via cAMP-mediated activation of ERK and p38 MAP kinases. J Neurochem 104:74–88.

Monaghan TK, Pou C, MacKenzie CJ, et al. (2008b) Neurotrophic actions of PACAP-38 and LIF on human neuroblastoma SH-SY5Y cells. J Mol Neurosci 36:45–56.

Moroo I, Tatsuno I, Uchida D, et al. (1998) Pituitary adenylate cyclase activating polypeptide (PACAP) stimulates mitogen-activated protein kinase (MAPK) in cultured rat astrocytes. Brain Res 795:191–6.

Morrow J a, Lutz EM, West KM, et al. (1993) Molecular cloning and expression of a cDNA encoding a receptor for pituitary adenylate cyclase activating polypeptide (PACAP). FEBS Lett 329:99–105.

Müller G a, Engeland K (2010) The central role of CDE/CHR promoter elements in the regulation of cell cycle-dependent gene transcription. FEBS J 277:877–93.

Mustafa T, Grimaldi M, Eiden LE (2007) The hop cassette of the PAC1 receptor confers coupling to Ca2+ elevation required for pituitary adenylate cyclase-activating polypeptide-evoked neurosecretion. J Biol Chem 282:8079–91.

Nicklin S a, Baker AH (2008) Efficient vascular endothelial gene transfer following intravenous adenovirus delivery. Mol Ther 16:1904–5.

Nicot A, Otto T, Brabet P, Dicicco-Bloom EM (2004) Altered social behavior in pituitary adenylate cyclase-activating polypeptide type I receptor-deficient mice. J Neurosci 24:8786–95.

Nishizuka Y (1992) Intracellular signaling by hydrolysis of phospholipids and activation of protein kinase C. Science 258:607–14.

Nogueira TC, Paula FM, Villate O, et al. (2013) GLIS3, a Susceptibility Gene for Type 1 and Type 2 Diabetes, Modulates Pancreatic Beta Cell Apoptosis via Regulation of a Splice Variant of the BH3-Only Protein Bim. PLoS Genet 9:e1003532.

Numoto M, Yokoro K, Koshi J (1999) ZF5, which is a Kruppel-type transcriptional repressor, requires the zinc finger domain for self-association. Biochem Biophys Res Commun 256:573–8.

Numoto M, Yokoro K, Yanagihara K (1995) Over-expressed ZF5 Gene Product, a c-myc-binding Protein Related to GL1-Kruppel Protein, Has a Growth-suppressive Activity in Mouse Cell Lines. Cancer Sci. 86:227-283.

Nussdorfer GG, Bahcelioglu M, Neri G, Malendowicz LK (2000) Secretin, glucagon, gastric inhibitory polypeptide, parathyroid hormone, and related peptides in the regulation of the hypothalamus-pituitary-adrenal axis. Peptides 21:309–324.

Nussdorfer GG, Malendowicz LK (1998) Role of VIP, PACAP, and related peptides in the regulation of the hypothalamo-pituitary-adrenal axis. Peptides 19:1443–67.

Okada T, Moriyama S, Kitano M (2012) Differentiation of germinal center B cells and follicular helper T cells as viewed by tracking Bcl6 expression dynamics. Immunol Rev 247:120–32.

Okazaki K, Itoh Y, Ogi K, et al. (1995) Characterization of murine PACAP mRNA. Peptides 16:1295–1299.

Ola a, Kerkelä R, Tokola H, et al. (2010) The mixed-lineage kinase 1-3 signalling pathway regulates stress response in cardiac myocytes via GATA-4 and AP-1 transcription factors. Br J Pharmacol 159:717–25.

Olmsted JB, Carlson K, Klebe R, et al. (1970) Isolation of microtubule protein from cultured mouse neuroblastoma cells. Proc Natl Acad Sci U S A 65:129–36.

Orlov I, Rochel N, Moras D, Klaholz BP (2012) Structure of the full human RXR/VDR nuclear receptor heterodimer complex with its DR3 target DNA. EMBO J 31:291–300.

Otto C, Hein L, Brede M, et al. (2004) Pulmonary hypertension and right heart failure in pituitary adenylate cyclase-activating polypeptide type I receptor-deficient mice. Circulation 110:3245–51.

Otto C, Kovalchuk Y, Wolfer DP, et al. (2001a) Impairment of mossy fiber long-term potentiation and associative learning in pituitary adenylate cyclase activating polypeptide type I receptor-deficient mice. J Neurosci 21:5520–7.

Otto C, Martin M, Wolfer DP, et al. (2001b) Altered emotional behavior in PACAP-type-I-receptor-deficient mice. Brain Res Mol Brain Res 92:78–84.

Park H, Choi H-J, Kim J, et al. (2011) Homeobox D1 regulates angiogenic functions of endothelial cells via integrin β1 expression. Biochem Biophys Res Commun 408:186–92.

Park KS, Guo Z, Shao L, et al. (2009) A far-upstream Oct-1 motif regulates cytokine-induced transcription of the human inducible nitric oxide synthase gene. J Mol Biol 390:595–603.

Parker DB, Power ME, Swanson P, et al. (1997) Exon skipping in the gene encoding pituitary adenylate cyclase-activating polypeptide in salmon alters the expression of two hormones that stimulate growth hormone release. Endocrinology 138:414–23.

Pearson RCM, Funnell APW, Crossley M (2011) The mammalian zinc finger transcription factor Krüppel-like factor 3 (KLF3/BKLF). IUBMB Life 63:86–93.

Persson K, Ahrén B (2002) The neuropeptide PACAP contributes to the glucagon response to insulin-induced hypoglycaemia in mice. Acta Physiol Scand 175:25–8.

Petrovic I, Kovacevic-Grujicic N, Stevanovic M (2009) ZBP-89 and Sp3 down-regulate while NF-Y up-regulates SOX18 promoter activity in HeLa cells. Mol Biol Rep 36:993–1000.

Pons G, O'Dea R, Mirkin B (1982) Biological characterization of the C-1300 murine neuroblastoma: an in vivo neural crest tumor model. Cancer Res 3719–3723.

Pope NJ, Bresnick EH (2010) Differential coregulator requirements for function of the hematopoietic transcription factor GATA-1 at endogenous loci. Nucleic Acids Res 38:2190–200.

Raff MC, Barres BA, Burne JF, et al. (1993) Programmed cell death and the control of cell survival: lessons from the nervous system. Science (80-) 262:695.

Raivich G, Behrens A (2006) Role of the AP-1 transcription factor c-Jun in developing, adult and injured brain. Prog Neurobiol 78:347–63.

Ramji DP, Foka P (2002) CCAAT/enhancer-binding proteins: structure, function and regulation. Biochem J 365:561–75.

Ravni A, Vaudry D, Gerdin MJ, et al. (2008) A cAMP-dependent, protein kinase A-independent signaling pathway mediating neuritogenesis through Egr1 in PC12 cells. Mol Pharmacol 73:1688–708.

Rawlings SR, Demaurex N, Schlegel W (1994) Pituitary adenylate cyclase-activating polypeptide increases [Ca2]i in rat gonadotrophs through an inositol trisphosphate-dependent mechanism. J Biol Chem 269:5680–6.

Rawlings SR, Piuz I, Schlegel W, et al. (1995) Differential expression of pituitary adenylate cyclase-activating polypeptide/vasoactive intestinal polypeptide receptor subtypes in clonal pituitary somatotrophs and gonadotrophs. Endocrinology 136:2088.

Reglódi D, Tamás a, Lengvári I, et al. (2006) Comparative study of the effects of PACAP in young, aging, and castrated males in a rat model of Parkinson's disease. Ann N Y Acad Sci 1070:518–24.

Ressler KJ, Mercer KB, Bradley B, et al. (2011) Post-traumatic stress disorder is associated with PACAP and the PAC1 receptor. Nature 470:492–497.

Revilla-I-Domingo R, Bilic I, Vilagos B, et al. (2012) The B-cell identity factor Pax5 regulates distinct transcriptional programmes in early and late B lymphopoiesis. EMBO J 31:3130–46. d

Rodda DJ, Chew J-L, Lim L-H, et al. (2005) Transcriptional regulation of nanog by OCT4 and SOX2. J Biol Chem 280:24731–7.

Rodríguez-Henche N, Jamen F, Leroy C, et al. (2002) Transcription of the mouse PAC1 receptor gene: cell-specific expression and regulation by Zac1. Biochim Biophys Acta 1576:157–62.

Romano R, Palamaro L, Fusco A, et al. (2013) FOXN1: A Master Regulator Gene of Thymic Epithelial Development Program. Front Immunol 4:187.

Ronaldson E, Robertson DN, Johnson MS, et al. (2002) Specific interaction between the hop1 intracellular loop 3 domain of the human PAC(1) receptor and ARF. Regul Pept 109:193–8.

Rong L, Liu J, Qi Y, et al. (2012) GATA-6 promotes cell survival by up-regulating BMP-2 expression during embryonic stem cell differentiation. Mol Biol Cell 23:3754–63.

Rowe a, Eager NS, Brickell PM (1991) A member of the RXR nuclear receptor family is expressed in neural-crest-derived cells of the developing chick peripheral nervous system. Development 111:771–8.

Ruiz i Altaba a (1996) Coexpression of HNF-3 beta and Isl-1/2 and mixed distribution of ventral cell types in the early neural tube. Int J Dev Biol 40:1081–8.

Sakai T, Hino K, Wada S, Maeda H (2003) Identification of the DNA binding specificity of the human ZNF219 protein and its function as a transcriptional repressor. DNA Res 10:155–65.

Sampson EM, Haque ZK, Ku MC, et al. (2001) Negative regulation of the Wnt-beta-catenin pathway by the transcriptional repressor HBP1. EMBO J 20:4500–11.

Samson SL, Wong NCW (2002) Role of Sp1 in insulin regulation of gene expression. J Mol Endocrinol 29:265–79.

Sauvage M, Brabet P, Holsboer F, et al. (2000) Mild deficits in mice lacking pituitary adenylate cyclase-activating polypeptide receptor type 1 (PAC1) performing on memory tasks. Brain Res Mol Brain Res 84:79–89.

Schorle H, Meier P, Buchert M, et al. (1996) Transcription factor AP-2 essential for cranial closure and craniofacial development. Nature 381:235–8.

Sherwood NM, Krueckl SL, McRory JE (2000) The origin and function of the pituitary adenylate cyclase-activating polypeptide (PACAP)/glucagon superfamily. Endocr Rev 21:619–70.

Sheward WJ, Lutz EM, Copp a J, Harmar a J (1998) Expression of PACAP, and PACAP type 1 (PAC1) receptor mRNA during development of the mouse embryo. Brain Res Dev Brain Res 109:245–53.

Shintani N, Suetake S, Hashimoto H, et al. (2005) Neuroprotective action of endogenous PACAP in cultured rat cortical neurons. Regul Pept 126:123–8.

Silva a J, Kogan JH, Frankland PW, Kida S (1998) CREB and memory. Annu Rev Neurosci 21:127–48.

Song B, Young CS (1998) Functional analysis of the CAAT box in the major late promoter of the subgroup C human adenoviruses. J Virol 72:3213–20.

Song N-N, Xiu J-B, Huang Y, et al. (2011) Adult raphe-specific deletion of Lmx1b leads to central serotonin deficiency. PLoS One 6:e15998.

Sorrell MRJ, Dohn TE, D'Aniello E, Waxman JS (2013) Tcf7l1 proteins cell autonomously restrict cardiomyocyte and promote endothelial specification in zebrafish. Dev Biol 380:199–210.

Spengler D, Villalba M, Hoffmann a, et al. (1997) Regulation of apoptosis and cell cycle arrest by Zac1, a novel zinc finger protein expressed in the pituitary gland and the brain. EMBO J 16:2814–25.

Spengler D, Waeber C, Pantaloni C, et al. (1993) Differential signal transduction by five splice variants of the PACAP receptor. Nature 365:170–5.

Steinbrunn T, Stühmer T, Sayehli C, et al. (2012) Combined targeting of MEK/MAPK and PI3K/Akt signalling in multiple myeloma. Br J Haematol 159:430–40.

Stern JL, Cao JZ, Xu J, et al. (2008) Repression of human cytomegalovirus major immediate early gene expression by the cellular transcription factor CCAAT displacement protein. Virology 378:214–25.

Sugiyama Y, Kakoi K, Kimura A, et al. (2012) Smad2 and Smad3 are redundantly essential for the suppression of iNOS synthesis in macrophages by regulating IRF3 and STAT1 pathways. Int Immunol 24:253–65.

Sun G, Liu X, Mercado P, et al. (2005) The zinc finger protein cKrox directs CD4 lineage differentiation during intrathymic T cell positive selection. Nat Immunol 6:373–81.

Takashima A, Maeda Y, Itoh S (1993a) Influence of chronic intracerebroventricular infusion of vasoactive intestinal peptide (VIP) on memory processes in Morris water pool test in the rat. Peptides 14:1073–8.

Takashima A, Maeda Y, Itoh S (1993b) Vasoactive intestinal peptide (VIP) causes memory impairment in passive avoidance responding of the rat. Peptides 14:1067–71.

Takigawa Y, Hata K, Muramatsu S, et al. (2010) The transcription factor Znf219 regulates chondrocyte differentiation by assembling a transcription factory with Sox9. J Cell Sci 123:3780–3788.

Tan X, Zhang L, Qin J, et al. (2013) Transplantation of neural stem cells co-transfected with Nurr1 and Brn4 for treatment of Parkinsonian rats. Int J Dev Neurosci 31:82–7.

Tan X-F, Qin J-B, Jin G-H, et al. (2010) Effects of Brn-4 on the neuronal differentiation of neural stem cells derived from rat midbrain. Cell Biol Int 34:877–82.

Taniguchi K, Anderson AE, Sutherland AE, Wotton D (2012) Loss of Tgif function causes holoprosencephaly by disrupting the SHH signaling pathway. PLoS Genet 8:e1002524.

Tao X, West AE, Chen WG, et al. (2002) A calcium-responsive transcription factor, CaRF, that regulates neuronal activity-dependent expression of BDNF. Neuron 33:383–95.

Thiagalingam A, De Bustros A, Borges M, et al. (1996) RREB-1, a novel zinc finger protein, is involved in the differentiation response to Ras in human medullary thyroid carcinomas. Mol Cell Biol 16:5335–45.

Thomas M, Sukhai M a, Kamel-Reid S (2012) An emerging role for retinoid X receptor α in malignant hematopoiesis. Leuk Res 36:1075–81.

Thomas MC, Chiang C-M (2006) The general transcription machinery and general cofactors. Crit Rev Biochem Mol Biol 41:105–78.

Tokuda N, Arudchelvan Y, Sawada T, et al. (2006) PACAP receptor (PAC1-R) expression in rat and rhesus monkey thymus. Ann N Y Acad Sci 1070:581–5.

Tokuda N, Hamasaki K, Mizutani N, et al. (2004) Expression of PAC1 receptor in rat thymus after irradiation. Regul Pept 123:167–72.

Toresson H, Mata de Urquiza a, Fagerström C, et al. (1999) Retinoids are produced by glia in the lateral ganglionic eminence and regulate striatal neuron differentiation. Development 126:1317–26.

Trumper A, Trumper K, Horsch D (2002) Mechanisms of mitogenic and anti-apoptotic signaling by glucose-dependent insulinotropic polypeptide in beta (INS-1)-cells. J Endocrinol 174:233.

Tsantoulis PK, Gorgoulis VG (2005) Involvement of E2F transcription factor family in cancer. Eur J Cancer 41:2403–14.

Tsuchida T, Ensini M, Morton SB, et al. (1994) Topographic organization of embryonic motor neurons defined by expression of LIM homeobox genes. Cell 79:957–970.

Tsukiyama N, Saida Y, Kakuda M, et al. (2011) PACAP centrally mediates emotional stress-induced corticosterone responses in mice. Stress 14:368–75.

Tsukumo S-I, Unno M, Muto A, et al. (2013) Bach2 maintains T cells in a naive state by suppressing effector memory-related genes. Proc Natl Acad Sci U S A 110:10735–40.

Ushiyama M, Ikeda R, Sugawara H, et al. (2007) Differential intracellular signaling through PAC1 isoforms as a result of alternative splicing in the first extracellular domain and the third intracellular loop. Mol Pharmacol 72:103–111.

Vana A, Lucchinetti C, Le T, Armstrong R (2007) Myelin transcription factor 1 (Myt1) expression in demyelinated lesions of rodent and human CNS. Glia 55:687–697.

Vaudry D, Falluel-Morel A, Bourgault S, et al. (2009) Pituitary adenylate cyclase-activating polypeptide and its receptors: 20 years after the discovery. Pharmacol Rev 61:283.

Vaudry D, Gonzalez B, Basille M, et al. (1998) Pituitary adenylate cyclase-activating polypeptide stimulates both c-fos gene expression and cell survival in rat cerebellar granule neurons through activation of the protein kinase A pathway. Neuroscience 84:801–812.

Vaudry D, Gonzalez BJ, Basille M, et al. (2000a) The neuroprotective effect of pituitary adenylate cyclase-activating polypeptide on cerebellar granule cells is mediated through inhibition of the CED3-related cysteine protease caspase-3/CPP32. Proc Natl Acad Sci U S A 97:13390–5.

Vaudry D, Gonzalez BJ, Basille M, et al. (2000b) PACAP acts as a neurotrophic factor during histogenesis of the rat cerebellar cortex. Ann N Y Acad Sci 921:293–9.

Vaudry D, Rousselle C, Basille M, et al. (2002) Pituitary adenylate cyclase-activating polypeptide protects rat cerebellar granule neurons against ethanol-induced apoptotic cell death. Proc Natl Acad Sci U S A 99:6398–403.

Van de Ven C, Bialecka M, Neijts R, et al. (2011) Concerted involvement of Cdx/Hox genes and Wnt signaling in morphogenesis of the caudal neural tube and cloacal derivatives from the posterior growth zone. Development 138:3859–3859.

Wagner EF (2010) Bone development and inflammatory disease is regulated by AP-1 (Fos/Jun). Ann Rheum Dis 69 Suppl 1:i86–88.

Wang G, Pan J, Tan Y-Y, et al. (2008) Neuroprotective effects of PACAP27 in mice model of Parkinson's disease involved in the modulation of K(ATP) subunits and D2 receptors in the striatum. Neuropeptides 42:267–76.

Wang SW, Mu X, Bowers WJ, et al. (2002) Brn3b/Brn3c double knockout mice reveal an unsuspected role for Brn3c in retinal ganglion cell axon outgrowth. Development 129:467–77.

Wang X, Liu Q, Ihsan A, et al. (2012) JAK/STAT pathway plays a critical role in the proinflammatory gene expression and apoptosis of RAW264.7 cells induced by trichothecenes as DON and T-2 toxin. Toxicol Sci 127:412–24.

Wang Z, Zhu S, Shen M, et al. (2013) STAT3 is involved in esophageal carcinogenesis through regulation of Oct-1. Carcinogenesis 34:678–88.

Waschek J A (2013) VIP and PACAP: neuropeptide modulators of CNS inflammation, injury, and repair. Br J Pharmacol 169:512–23.

Watanabe J, Nakamachi T, Matsuno R, et al. (2007) Localization, characterization and function of pituitary adenylate cyclase-activating polypeptide during brain development. Peptides 28:1713–9.

Watanabe J, Ohba M, Ohno F, et al. (2006) Pituitary adenylate cyclase-activating polypeptide-induced differentiation of embryonic neural stem cells into astrocytes is mediated via the β isoform of protein kinase C. J Neurosci Res 84:1645–1655.

West A E (2011) Biological functions and transcriptional targets of CaRF in neurons. Cell Calcium 49:290–5.

White MK, Johnson EM, Khalili K (2009) Multiple roles for Pur-α in cellular and viral regulation. Cell Cycle 8:414–420.

Wierstra I (2008) Sp1: emerging roles--beyond constitutive activation of TATA-less housekeeping genes. Biochem Biophys Res Commun 372:1–13.

Windle JJ, Weiner RI, Mellon PL (1990) Cell lines of the pituitary gonadotrope lineage derived by targeted oncogenesis in transgenic mice. Mol Endocrinol 4:597–603.

Xanthoulis A, Tiniakos DG (2013) E2F transcription factors and digestive system malignancies: How much do we know? World J Gastroenterol 19:3189–98.

Xia Z, Storm D (2002) CaRF: a neuronal transcription factor that CaREs. Neuron 33:315–316.

Xiu M, Kim J, Sampson E, et al. (2003) The Transcriptional Repressor HBP1 Is a Target of the p38 Mitogen-Activated Protein Kinase Pathway in Cell Cycle Regulation. Mol Cell Biol 23:8890–8901.

Yadav M, Goetzl EJ (2008) Vasoactive intestinal peptide-mediated Th17 differentiation: an expanding spectrum of vasoactive intestinal peptide effects in immunity and autoimmunity. Ann N Y Acad Sci 1144:83–9.

Yamaguchi N (2001) Pituitary adenylate cyclase activating polypeptide enhances glucose-evoked insulin secretion in the canine pancreas in vivo. JOP 2:306–16.

Yamashita M, Ukai-Tadenuma M, Miyamoto T, et al. (2004) Essential role of GATA3 for the maintenance of type 2 helper T (Th2) cytokine production and chromatin remodeling at the Th2 cytokine gene loci. J Biol Chem 279:26983–90.

Yan R, Huang T, Xie Z, et al. (2013) Lmx1b controls peptide phenotypes in serotonergic and dopaminergic neurons. Acta Biochim Biophys Sin (Shanghai) 45:345–52.

Yang MQ, Elnitski LL (2008) Diversity of core promoter elements comprising human bidirectional promoters. BMC Genomics 9 Suppl 2:S3.

Yun K, Potter S, Rubenstein JL (2001) Gsh2 and Pax6 play complementary roles in dorsoventral patterning of the mammalian telencephalon. Development 128:193–205.

Zaehres H, Lensch MW, Daheron L, et al. (2005) High-efficiency RNA interference in human embryonic stem cells. Stem Cells 23:299–305.

Zhang CZY, Chen GG, Lai PBS (2010) Transcription factor ZBP-89 in cancer growth and apoptosis. Biochim Biophys Acta 1806:36–41.

Zhang CZY, Chen GG, Merchant JL, Lai PBS (2012) Interaction between ZBP-89 and p53 mutants and its contribution to effects of HDACi on hepatocellular carcinoma. Cell Cycle 11:322–34.

Zhao M, Sun Y, Gao F, et al. (2010a) Epigenetics and SLE: RFX1 downregulation causes CD11a and CD70 overexpression by altering epigenetic modifications in lupus CD4+ T cells. J Autoimmun 35:58–69.

Zhao M, Wu X, Zhang Q, et al. (2010b) RFX1 regulates CD70 and CD11a expression in lupus T cells by recruiting the histone methyltransferase SUV39H1. Arthritis Res Ther 12:R227.

Zheng XL, Matsubara S, Diao C, et al. (2001) Epidermal growth factor induction of apolipoprotein A-I is mediated by the Ras-MAP kinase cascade and Sp1. J Biol Chem 276:13822–9.

Zhou CJ, Shioda S, Shibanuma M, et al. (1999) Pituitary adenylate cyclase-activating polypeptide receptors during development: expression in the rat embryo at primitive streak stage. Neuroscience 93:375–91.

Zhou J, Cheng M, Wu M, et al. (2013) Contrasting roles of E2F2 and E2F3 in endothelial cell growth and ischemic angiogenesis. J Mol Cell Cardiol 60:68–71.

Zhu X, Wang Y, Pi W, et al. (2012) NF-Y recruits both transcription activator and repressor to modulate tissue- and developmental stage-specific expression of human γ-globin gene. PLoS One 7:e47175.

Zolnierowicz S, Cron P, Solinas-Toldo S, et al. (1994) Isolation, characterization, and chromosomal localization of the porcine calcitonin receptor gene. Identification of two variants of the receptor generated by alternative splicing. J Biol Chem 269:19530–8.